



UNIVERSIDAD NACIONAL AUTÓNOMA DE MÉXICO

Posgrado en Ciencias de la Tierra

Papel de los Sistemas Hidrotermales en Evolución Química: Ensayos de
Química Prebiótica

TESIS

QUE PARA OPTAR POR EL GRADO DE:

DOCTOR EN CIENCIAS

Presenta

Saúl Alberto Villafañe-Barajas

Asesor

Dra. María Colín García

Instituto de Geología

Cd. de México, Agosto, 2021



Universidad Nacional
Autónoma de México



UNAM – Dirección General de Bibliotecas
Tesis Digitales
Restricciones de uso

DERECHOS RESERVADOS ©
PROHIBIDA SU REPRODUCCIÓN TOTAL O PARCIAL

Todo el material contenido en esta tesis esta protegido por la Ley Federal del Derecho de Autor (LFDA) de los Estados Unidos Mexicanos (México).

El uso de imágenes, fragmentos de videos, y demás material que sea objeto de protección de los derechos de autor, será exclusivamente para fines educativos e informativos y deberá citar la fuente donde la obtuvo mencionando el autor o autores. Cualquier uso distinto como el lucro, reproducción, edición o modificación, será perseguido y sancionado por el respectivo titular de los Derechos de Autor.

“Declaro conocer el Código de Ética de la Universidad Nacional Autónoma de México, plasmado en la Legislación Universitaria. Con base en las definiciones de integridad y honestidad ahí especificadas, aseguro mediante mi firma al calce que el presente trabajo es original y enteramente de mi autoría. Todas las citas de, o referencias a, las obras de otros autores aparecen debida y adecuadamente señaladas, así como acreditadas mediante los recursos editoriales convencionales”.



Maestro en Ciencias

Saúl Alberto Villafañe Barajas

Agradecimientos Institucionales

Al CONACyT por el apoyo económico otorgado a través de la beca 697442 durante la realización de mis estudios de posgrado. De igual manera, por el apoyo económico complementario para la realización de las estancias de investigación y el financiamiento a través de proyecto A1-S-25341 e IN110919.

Al Posgrado en Ciencias de la Tierra de la Universidad Nacional Autónoma de México por permitirme continuar con mi formación académica y las oportunidades brindadas a lo largo de ella.

Al Instituto de Ciencias Nucleares, UNAM, por permitirme realizar gran parte de los experimentos dentro de sus instalaciones así como el apoyo financiero a lo largos de mis estudios de posgrado para asistir a congresos y estancias de investigación.

Al Programa de Apoyo a Proyectos de investigación e innovación tecnológica (DGAPA-PAPIIT) por financiar parte de este trabajo a través del proyecto IA203217.

A la UNAM Extranjero y Beca de Excelencia Lomnitz-Castaños por el apoyo económico para realizar mis estancias de investigación.

Al Dr. Jean François Lambert y al Laboratoire de Réactivité de Surface, Sorbonne Université Paris VI, por abrirme sus puertas, permitirme complementar los experimentos y crecer académica y personalmente. A Hagop y Lise, por su paciencia y ayuda en cada momento. A la Dra. Maguy Jaber, por compartirme su conocimiento, tiempo y ayuda.

A la Dra. Marta Ruiz Bermejo, al técnico Pedro Rayo Pizarroso y al Centro de Astrobiología, CAB-CSIC-INTA, por abrirme sus puertas, permitirme complementar los experimentos y concluir gran parte de este trabajo.

A la Fondation de la maison du Mexique por todo el apoyo brindado. A la directora, Claudia Saucedo. Por todo.

Al Laboratorio de Evolución Química y Radioquímica, a la Dra. Alicia Negrón Mendoza y a la QFB. Claudia Camargo Raya por todo el apoyo, la ayuda y las oportunidades brindadas a lo largo de mis estudios de posgrado.

A mi comité tutor, conformado por la Dra. Alicia Negrón Mendoza, el Dr. Arturo Becerra Bracho y la Dra. María Colín García por apoyarme y ayudarme a crecer como persona y estudiante a lo largo de mi posgrado.

A todas esas personas que hacen posibles los trámites y siempre me orientaron de la mejor manera. Mil gracias.

Agradecimientos Personales

A los miembros del jurado: el Dr. Fernando Ortega Gutiérrez, el Dr. Arturo Becerra Bracho, la Dra. Sandra Ramírez Jiménez, la Dra. Marta Ruiz Bermejo y la Dra. María Colín García por el tiempo que destinaron a evaluar este trabajo, por su paciencia, por sus atinados comentarios y sugerencias y la disponibilidad para ayudarme a mejorar este trabajo en todos los aspectos.

A la Dra. María Colín García, mi tutora. Por creer en mí y ayudarme a crecer académica y personalmente. Por ayudarme a enfrentar mis miedos y cruzar fronteras.

A Checo, Coco, Gis y Wifi. Sin ustedes jamás lo hubiera podido lograr. A mi segunda familia, por su apoyo incondicional y siempre estar ahí. Donde quiera que estén... ¡lo logramos!

A la Dra. Alicia Negrón Mendoza, el Dr. Sergio Ramos Bernal y a la QFB. Claudia Camargo Raya. Por todo. A mis amigos del laboratorio. Este trabajo es de todos y sin ustedes no lo hubiera podido lograr.

Gracias a Aztecas Paris. Por darme la oportunidad de pertenecer a una familia aun estando lejos de casa. Por ayudarme a cumplir mi sueño de gritar ¡gol! A Adán y todos ustedes, gracias por tanto.

A la Maison du Mexique. A todos mis amigos. Gracias por las experiencias, las risas, las lágrimas, los viajes y por ayudarme a crecer en todos los aspectos.

A la Ferme du Bonheur. Por permitirme vivir la experiencia de mi vida y no perderme.

A Eugenia, Susana y Josefa. Gracias por ayudarme a entender lo que me pasa y cómo superarlo.

Al Dr. Zaia y a Joao, por siempre darse el tiempo para aportar su conocimiento al trabajo. Gracias por todo.

A todos los que siempre han estado ahí, a los que la vida me dio la oportunidad de conocer, a los que se fueron y a los que vendrán. Gracias por darle sentido a mi vida.

A todos esas personas que han aparecido en mi camino y me cambiaron la vida. La lista es inmensa. Siempre los voy a llevar en mis pensamientos. Gracias por estar ahí en los peores momentos y darme ánimos para seguir y crecer como persona. Esto es para ustedes. De corazón, mil gracias por tanto.

Dedicatoria

Si vas a intentarlo, ve hasta el final...

Roll the Dice, Bukowski

A mi familia y mis amigos.

Artículos obtenidos y participación en congresos

- *Capítulo de libro*

Colin Garcia M., **Villafañe-Barajas**, S. A., Camprubí, A., Ortega-Gutierrez, F., Colás V. and Negrón- Mendoza Alicia. (2018) Prebiotic Chemistry in hydrothermal vent systems (In book: Handbook of Astrobiology, Chapter: 5.4, Publisher: CRC Press, pp.297-329

- *Artículo de revisión*

Villafañe-Barajas, S. A. y Colin-Garcia M. Submarine Hydrothermal Vents Systems: The relevance of dynamic systems in chemical evolution, and aftermath in prebiotic chemistry (Enviado IJA)

- *Divulgación*

González, L., **Villafañe-Barajas**, S. A., y Colín García, M. (2018) Los manantiales hidrotermales submarinos y la evolución química (Nuestra Tierra, ISSN 1665-935X).

Podcast. Estudios Planeteando “Del laboratorio al origen de la vida” **Villafañe-Barajas**, S.

- *Artículos de investigación*

Villafañe-Barajas, S. A., Colín-García, M., Negrón-Mendoza, A., & Ruiz-Bermejo, M. (2020). An experimental study of the thermolysis of hydrogen cyanide: The role of hydrothermal systems in chemical evolution. *International Journal of Astrobiology*, 1-10.

Villafañe-Barajas, S. A., Ruiz-Bermejo, M., Rayo-Pizarroso, P., & Colín-García, M. (2020). Characterization of HCN-Derived Thermal Polymer: Implications for Chemical Evolution. *Processes*, 8(8), 968.

Villafañe-Barajas, S. A., Ruiz-Bermejo, M., Rayo-Pizarroso, P., Gálvez-Martínez, S., Mateo-Martí, E., & Colín-García, M. (2021). A Lizardite–HCN Interaction Leading the Increasing of Molecular Complexity in an Alkaline Hydrothermal Scenario: Implications for Origin of Life Studies. *Life*, 11(7), 661.

- *Congresos y escuelas de verano*

Cartel Studies on the stability of nucleic acids precursors at high temperatures: Implications in Prebiotic Chemistry *Gordon Conferences- Origin of life*, 2018.

Conferencia “Hydrothermal vents and chemical evolution” II Latin American Congress of Astrobiology *UNC*, 2018.

Conferencia y cartel “The thermolysis of HCN from a prebiotic chemistry perspective” 18th EANA Conference European Astrobiology Network Association *FUB*, 2018.

Conferencia Sistemas hidrotermales: evolución química y el origen de la vida *Sociedad Geológica Mexicana*, 2019.

Asistencia FMASOEL: French-Mexican Advanced School on the Origins and Evolution of Life July, Paris, 2019.

Conferencia Sistemas hidrotermales: evolución química y el origen de la vida *Sociedad Geológica Mexicana*, 2019.

Cartel Role of hydrogen cyanide on hydrothermal scenarios: Implications in Chemical Evolution *Origins Conferences*, 2021.

Conferencia Role of serpentinite in HCN-polymerization: molecular complexity under alkaline scenarios *NORCEL*, 2021.

- *Estancias de Investigación*

Study of amino acids polymerization under HV conditions scenario: A prebiotic chemistry experiment. Asesor, Dr. Jean-François Lambert. Sorbonne Universités, UPMC Univ Paris VI 2018-2020.

Caracterización de polímeros de HCN: Ensayos de Química Prebiótica. Asesor, Marta Ruiz Bermejo. Centro de Astrobiología (Consejo Superior de Investigaciones Científicas-Instituto Nacional de Técnica Aeroespacial “Esteban Terradas” (CSIC-INTA) 2019.

RESUMEN

En los últimos años, los sistemas hidrotermales, tanto los submarinos como los subaéreos, han sido reconocidos como posibles nichos para el desarrollo de la evolución química y eventualmente, como escenarios para el surgimiento de las componentes básicas de la vida. Sin embargo, debido al dinamismo y la complejidad de estos ambientes, los experimentos de química prebiótica han estado limitados respecto a las variables geoquímicas utilizadas en los mismos, por ejemplo: considerando sólo altas presiones y altas temperaturas.

Recientemente, dentro del contexto de química prebiótica, se ha sugerido que los experimentos deben considerar el papel de diversas variables geoquímicas en el mismo ambiente primitivo. De esta forma, es necesario considerar otras variables principales, como la mineralogía, los gradientes de pH/temperatura, la salinidad y/o la interacción entre diversas moléculas orgánicas.

En este trabajo, se realizó un estudio sistemático sobre el papel de los sistemas hidrotermales en la evolución química a partir de diversos experimentos de química prebiótica. Este carácter sistemático consistió en estudiar:

- 1) un escenario geoquímico plausible (*i.e.*, sistemas hidrotermales);
- 2) evaluar la estabilidad, la reactividad y el destino de la materia prima disponible para llevar a cabo reacciones químicas (*i.e.*, ácido cianhídrico, HCN);
- 3) determinar las propiedades fisicoquímicas de los polímeros sintetizados (*i.e.*, HCN-DTP);
- 4) evaluar el papel de diversos minerales en la estabilidad y reactividad de diversas moléculas orgánicas (*i.e.*, Mg-Mont, sílica y serpentinita/HCN, aminoácidos) y
- 5) establecer cuál es el destino de las moléculas orgánicas en ese entorno (*i.e.*, modelo de agua hidrotermal).

Nuestros resultados sugieren: **1)** las condiciones geoquímicas del medio definen la reactividad y estabilidad de las moléculas orgánicas utilizadas; **2)** la presencia de algunos minerales afecta directamente el proceso de polimerización y las propiedades fisicoquímicas de los polímeros sintetizados y **3)** los cationes presentes en un modelo de agua hidrotermal pueden favorecer la sorción de algunos aminoácidos.

Es posible concluir que los sistemas hidrotermales pudieron ser ambientes primitivos cruciales para el desarrollo de la complejidad química durante las primeras etapas de la evolución química en la Tierra. El desarrollo de simulaciones de laboratorio que consideren diversas variables geoquímicas en el mismo experimento, como las expuestas aquí, son un buen punto de partida para entender el dinamismo geoquímico presente en estos ambientes así como sus repercusiones en los procesos que precedieron el origen de la vida. Por ende, esta tesis está enfocada en estudiar algunos de los procesos fisicoquímicos que pudieron haber tenido lugar en los sistemas hidrotermales a lo largo de la evolución química y las repercusiones de estos.

ABSTRACT

Currently, hydrothermal systems, both submarines and sub-aerials, have been recognized as possible niches for the development of chemical evolution and eventually, as scenarios for the emergence of the basic components of life. However, due to the dynamism and complexity of these environments, prebiotic chemistry experiments have been limited and they only consider few geochemical variables, for example: high pressures and high temperatures.

Since of point of view of prebiotic chemistry, it has been suggested that experiments should consider the role of several geochemical variables in the same environment. Hence, it is necessary to consider other main variables, such as mineralogy, pH / temperature gradients, salinity, and / or the interaction between various organic molecules.

In this work, a systematic study was carried out on the role of hydrothermal systems in chemical evolution. This systematic character consisted in perform prebiotic experiments which consist in studying:

- 1) a plausible geochemical scenario (*i.e.*, hydrothermal systems);
- 2) evaluate the stability, reactivity and fate of the raw material available to carry out chemical reactions (*i.e.*, hydrogen cyanide, HCN);
- 3) determine the physicochemical properties of the synthesized polymers (*i.e.*, HCN-DTP);
- 4) study the role of some minerals in the stability and reactivity of organic molecules (*i.e.*, Mg-Mont, silica and serpentinite/ HCN, amino acids) and
- 5) study the fate of organic molecules in these environments (*i.e.*, hydrothermal water model).

Our results suggest: **1)** the geochemical conditions of the environment define the reactivity and stability of the organic molecules; **2)** the presence of some minerals affects the polymerization process and the physicochemical properties of the synthesized polymers and **3)** the cations present in a hydrothermal water model can favor the sorption of some amino acids.

It is possible to conclude that hydrothermal systems could be crucial primitive environments for the development of chemical complexity during the early stages of chemical evolution on Earth. The development of laboratory simulations that consider different geochemical variables in the same experiment, such as those set out here, are a good starting point to understand the geochemical dynamism present in these environments as well as their repercussions on the processes that could be involved in the antechamber of the origin of life. Therefore, this thesis is focused on studying some of the physicochemical processes that may have taken place in hydrothermal systems throughout chemical evolution and their repercussions.

ÍNDICE

Capítulo I.....	1
Introducción general	1
Hipótesis	9
Objetivo general	9
Objetivos particulares	10
Artículo de divulgación científica. Los manantiales hidrotermales submarinos y la evolución química	16
Capítulo II	21
Definición de un escenario geoquímico plausible	21
Artículo de revisión. Química Prebiótica en Sistemas Hidrotermales	27
Capítulo III.....	61
Metodología General	61
Capítulo IV	71
Disponibilidad de materia prima para llevar a cabo reacciones	71
Artículo de investigación. Estudio experimental de la termólisis del ácido cianhídrico: El papel de los sistemas hidrotermales en la Evolución Química	72
Capítulo V	82
Síntesis de moléculas orgánicas	82
Artículo de investigación. Caracterización del polímero térmico derivado de HCN: Implicaciones para la Evolución Química	83
Artículo de investigación. Efecto de la lizardita en la polimerización del HCN: Efecto en la síntesis de moléculas orgánicas	102
Capítulo VI.....	126
Estabilidad y reactividad de las moléculas orgánicas.....	126
Polimerización de aminoácidos en sistemas hidrotermales	127

Capítulo VII	159
Destino de las moléculas orgánicas	160
Papel de los iones en la sorción de aminoácidos en serpentinita: Ensayos de Química Prebiótica	160
Capítulo VIII	176
Conclusiones generales.....	176
ANEXO I	179
Artículo de revisión (enviado). Sistemas Hidrotermales Submarinos: La relevancia de los sistemas dinámicos en la Evolución Química y sus consecuencias en la Química Prebiótica	180
ANEXO II	201

ÍNDICE DE ABREVIATURAS

Ácido cianhídrico	HCN
Aminoácidos	AAs
Análisis elemental	EA
Análisis termogravimétrico	TGA
Análisis termogravimétrico acoplado a espectrometría de masas	TG-MS
Análisis térmico diferencial	DTG
Calorimetría diferencial de barrido	DSC
Cromatografía de gases	GC
Cromatografía de gases acoplada a espectrometría de masas	GC-MS
Cromatografía líquida de ultra alta eficiencia	UHPLC
Difracción de rayos X	XRD
Espectrometría de masas por resonancia ion-ciclotrón con transformada de Fourier	FT-ICR MS
Espectroscopía fotoelectrónica de rayos X	XPS
Espectroscopía infrarrojo con transformada de Fourier	FT-IR
Espectroscopía UV-Visible	UV-Vis Spectroscopy
Glicina	Gly, G
L-alanina	Ala, A
L- ácido aspártico	Asp, D
L- ácido glutámico	Glu, E
Modelo de agua hidrotermal	HWM
Montmorillonita de magnesio	Mg-Mont
Polímero térmico de HCN	HCN-DTP
Punto de carga cero	pHpzc
Resonancia magnética nuclear	NMR
Sílice pirogénica	SiO₂, Aerosil 380
Tratamiento de activación en seco	DA
Tratamiento hidrotermal submarino (alta temperatura-presión)	HT

ÍNDICE DE FIGURAS

Capítulo I

Figura 1.1 Concepción artística de las condiciones geológicas durante el Hadeano	2
Figura 1.2 Química prebiótica y química de sistemas.....	5
Figura 1.3 Probable destino del HCN y su polímero térmico en sistemas hidrotermales primitivos	9

Capítulo II

Figura 2.1 Probables eventos geoquímicos durante el Hadeano-Arqueano temprano	23
---	----

Capítulo III

Figura 3.1 Resumen de metodología	61
Figura 3.2 Síntesis de HCN	63
Figura 3.3 Difractograma de las muestras de Mg-Mont y Na-Mont	63
Figura 3.4 Termólisis de HCN	65
Figura 3.5 Experimentos enfocados en la simulación de condiciones hidrotermales	66

Capítulo VI

Figura 6.1 Procedimiento experimental general.....	131
Figura 6.2 Difractogramas de diferentes porcentajes de carga de (A + E)/SiO ₂	133
Figura 6.3 Termogramas (DTG) de diferentes porcentajes de carga de (A + E)/SiO ₂	134
Figura 6.4 Termogramas (DTG) de sistema mixto y sistema con un solo aminoácido	135
Figura 6.5 Probables reacciones de condensación para la formación de oligómeros y compuestos cíclicos.....	136
Figura 6.6 Espectro de ¹³ C NMR de la disolución A HT comparado con los compuestos de referencia	136
Figura 6.7 Espectro de ¹ H NMR de la disolución A HT comparado con los compuestos de referencia	137
Figura 6.8 Espectros de ¹³ C NMR de las disoluciones A +E HT, (A +E)/SiO ₂ HT, y de (A +E)/SiO ₂ DA, comparados con los compuestos de referencia	139

Figura 6.9 Espectro de ^1H NMR de la muestra (A + E)/SiO₂ DA en la región de protones de amida comparado con los compuestos de referencia.....140

Figura 6.10 Espectros ESI-MS de modo positivo de los productos formados después de los tratamientos DA y HT142

Figura 6.11 Oligómeros detectados para tratamientos HT y DA143

Información Complementaria

Figura 6.1 IC Espectro de ^{13}C NMR de la disolución A/SiO₂ HT comparado con el de A HT 152

Figura 6.2 IC Resumen de especies detectadas por ESI-MS de las muestras DA AA153

Figura 6.3 IC Resumen de especies detectadas por ESI-MS de las muestras HT AA154

Figura 6.4 IC Resumen de especies detectadas por ESI-MS de las muestras HT AA/SiO₂155

Figura 6.5 IC Resumen de especies detectadas por ESI-MS de las muestras DA Ala + Glu. ...156

Figura 6.6 IC Resumen de especies detectadas por ESI-MS de las muestras HT Ala + Glu y HT Ala + Glu/SiO₂ 157-158

Capítulo VII

Figura 7.1 Estructura química y valores de constantes de disociación de los de los aminoácidos utilizados.....162

Figura 7.2 Procedimiento experimental general.....163

Figura 7.3 Porcentaje de sorción de aminoácidos a pH ácido, natural de la disolución, básico y en presencia de iones disueltos.....166

Figura 7.4 Diagrama de distribución de especies de los aminoácidos utilizados respecto a la carga superficial de la serpentinita.....167

Figura 7.5 Porcentaje de sorción de aminoácidos a pH básico y usando CaCl₂168

Figura 7.6 Patrón de difracción de rayos X de la muestra de serpentinita169

ÍNDICE DE TABLAS

Capítulo III

Tabla 3.1 Preparación de muestras para la deposición de diferentes cargas de (A+E)/SiO₂65

Capítulo VI

Tabla 6.1 Resumen de estudios experimentales en condiciones hidrotermales submarinas (HT) y subaéreas (DA) respecto a los aminoácidos alanina y ácido glutámico129

Capítulo VII

Tabla 7.1 Composición del modelo de agua hidrotermal (HWM) y de los fluidos hidrotermales naturales.....164

Capítulo I

Introducción General

“Wait a minute. What is that?” *Robert Ballard, 1977*

"Rarely does something like this come along that drives home how much we still have to learn about our own planet" *Deborah Kelley, 2001*

"This gives our first glimpses of what the Earth was like shortly after it formed" *John W. Valley, 2001*

Si bien, desde la década de 1950, había suposiciones del escenario geológico que pudo imperar durante los eones Hadeano y Arqueano¹ (Fig. 1.1.) nuestra concepción de las condiciones que pudieron estar presentes durante los primeros millones de años de la historia de la Tierra ha cambiado radicalmente en las últimas décadas. Notablemente, el descubrimiento de los sistemas hidrotermales submarinos (Corliss *et al.*, 1979)², el descubrimiento del Sistema Hidrotermal *Lost City* (Kelley *et al.*, 2001)³ y la datación y composición isotópica (*i.e.*, $\delta^{18}\text{O}/^{16}\text{O}$) de la muestra

¹ Existe una ausencia de registro geológico desde la formación de la Tierra (*i.e.*, 4,566 Ga, análisis isotópico del sistema U-Pb en inclusiones refractarias de Ca-Al en meteoritas condriticas (Allegre *et al.*, 1995) hasta 4,031 Ga (*i.e.*, análisis isotópico de sistema U-Th-Pb en rocas ígneas del complejo de gneis Acasta, Canadá (Bowring & Williams, 1999)), el cual es llamado eón Hadeano. El eón Arqueano comprende desde 4,031 Ga hasta el comienzo del Proterozoico (*i.e.*, 2,5 Ga, basado en la sucesión estratigráfica de lutitas y formaciones de Hierro Bandeadas (*BIF* por *Banded Iron Formation*) de la cuenca Hamersley, Australia (Eriksson *et al.*, 2006)). No hay total acuerdo en la definición de los límites temporales antes mencionados. Para más información consultar: Altermann *et al.* 2012; Ogg *et al.* 2016.

² La expedición del Rift Galápagos, la cual fue parte de los trabajos de exploración del fondo oceánico por la *International Decade of Ocean Exploration* (1971-1980), estaba enfocada en el estudio detallado de las emisiones de fluidos hidrotermales provenientes del fondo del océano al noreste de las Islas Galápagos. En esta época, se deducía que las anomalías térmicas eran producto de la interacción del agua oceánica y la lava emitida a través de las fracturas producidas por la separación de la corteza. Las primeras fotos de esta zona mostraron al fondo oceánico como un terreno árido, cubierto de *pillow* lavas, fracturas y fluidos *pahoe-pahoe*. Sin embargo, después de avanzar algunos metros y revisar más de 10, 000 fotografías, los flujos de lava próximos a fracturas ¡estaban cubiertos de cientos de almejas y mejillones! Algo nunca antes visto en el fondo oceánico. En febrero de 1977, a 2700 metros debajo de la superficie, una explosión de una comunidad biológica rodeando una fumarola hidrotermal activa, *Clambake I*, fue descubierta (Ballard, 1977).

³ El crucero de la *National Science Foundation* inició con el objetivo de estudiar la estructura, composición e historia geológica del Macizo Atlantis y así, entender cómo se forman los complejos oceánicos centrales. La mañana del 4 de diciembre del 2000, en el océano Atlántico Norte, en la cabina de control *Argo-II*, Barbara John y Gretchen Frueh-Greem observaron las primeras imágenes de estructuras hidrotermales blancas. Para más detalles ver: <http://earthguide.ucsd.edu/mar/dec12.html>.

W74 colectada en *Jack Hills*, Australia (Wilde *et al.*, 2001)⁴, cambiaron la imagen de lo que podemos entender como Tierra primitiva (ver Capítulo II).



Figura 1.1. Concepción artística de las posibles condiciones geológicas durante en Hadeano.
Crédito: Chesley Bonestell, *Beginning of the World (The Earth is Born)*.
Tomado de: *LIFE* magazine cover, December 8, 1952.

Estos hallazgos han modificado las hipótesis y el planteamiento de los experimentos de laboratorio que intentan simular algunas de las condiciones que prevalecieron durante las primeras etapas de la evolución de la Tierra. En consecuencia, aún hay grandes vacíos en el entendimiento del papel y las repercusiones que pudieron tener diversas variables fisicoquímicas en la formación de las tres componentes fundamentales de la vida⁵ y eventualmente, en el origen de ésta⁶.

⁴ En mayo de 1999, después de un exhaustivo análisis de una muestra de más de cien zircones procedentes del conglomerado de Jack Hills perteneciente al cratón *Yilgarn*, Australia; William Peck, John Valley y Simon Wilde dataron un pequeño cristal en 4,404 Ga (Kerr, 2000). Investigaciones posteriores, resolvieron que se trata de una muestra de $4,373 \pm 0,006$ Ga (Valley *et al.*, 2014) la cual pudo provenir de las primeras rocas corticales que cristalizaron a partir de un magma saturado en sílice (*i.e.*, granito) que se fue enriqueciendo en rocas que ya habían interactuado con agua a bajas temperaturas (*e.g.*, suelos, sedimentos y/o corteza oceánica).

⁵ Si bien no existe un consenso respecto a la definición de vida, se ha trabajado bajo la hipótesis que la vida debe contar con, al menos, las siguientes componentes interdependientes: I) la separación del medio a través de membranas (compartimentalización), II) material genético para almacenar y transferir información, y III) la capacidad de realizar reacciones químicas acopladas (metabolismo) (Ruiz-Mirazo *et al.*, 2013).

⁶ Plantear una hipótesis sobre un posible origen de la vida en la Tierra exige considerar transiciones factibles de lo prebiótico (*prae*-antes, *bio*-vida; antes de la vida) a lo biótico. Hoy día, los estudios sobre el origen de la vida se realizan a partir de dos enfoques: de abajo-arriba o de arriba-abajo. Un enfoque de abajo-arriba es el resultado de simular algunos de los procesos fisicoquímicos que pudieron existir en la Tierra primitiva y/o en el medio interplanetario y resultaron en la formación de moléculas orgánicas que pudieron tener un papel importante (*e.g.*, acelerar reacciones, formación de enlaces más estables, interacción con otras moléculas de manera óptima) durante las primeras etapas de la vida en la Tierra. Por otro lado, un enfoque de arriba-abajo implica adquirir información a partir de moléculas informacionales (*e.g.*, ácidos nucleicos), rutas metabólicas, así como estructuras complejas (*e.g.*, ribosoma) presentes en los organismos actuales y que de alguna manera

La **química prebiótica** es el estudio experimental de la síntesis abiótica, la estabilidad y el destino de moléculas orgánicas bajo las distintas condiciones geoquímicas que pudieron estar presentes en la Tierra primitiva (redefinido a partir de Cleaves, 2012). De igual manera, esta área de estudio busca describir las vías que pudieron conducir a la formación espontánea de polímeros así como explicar las relaciones entre las distintas subestructuras químicas presentes en sistemas supramoleculares (Bruylants *et al.* 2011; Mattia y Otto 2015; Islam y Powner 2017). Así mismo, el periodo durante el cual diversas moléculas orgánicas interaccionaron entre sí y con distintos elementos presentes en los entornos primitivos se conoce como **evolución química** (redefinido a partir de Calvin, 1956). Ambas definiciones engloban un campo de investigación que tiene por objetivo dilucidar los mecanismos involucrados en la formación de las tres componentes básicas para la vida (*i.e.*, membranas, material genético y metabolismo) y su eventual interacción, para dar paso al probable Mundo de RNA o sus diversas variantes (Gilbert 1986; Dworkin *et al.* 2003; Robertson y Joyce 2012; Ma 2017).

A pesar de que los primeros experimentos⁷ de química prebiótica no son del todo consistentes con las condiciones que pudieron existir durante los primeros 500 Ma de la historia de la Tierra (ver Capítulo II), sí fueron un parteaguas en la forma de entender qué procesos habrían estado involucrados en la formación de moléculas orgánicas complejas. Es importante mencionar que si bien los términos química prebiótica y origen de la vida han sido usados de manera indistinta y, en ocasiones son términos inseparables⁸, es necesario ser cauteloso en el alcance de los resultados obtenidos experimentalmente en cada simulación. En otras palabras, las extrapolaciones e hipótesis formuladas deben ser prudentes con el papel que esas moléculas orgánicas pudieron tener en cierto ambiente primitivo. Por lo anterior, los alcances que tienen los experimentos de química prebiótica actuales están aún muy alejados de lo que podríamos entender como el origen de la vida. Más bien, en mi consideración, tales experimentos están enfocados en dilucidar los posibles mecanismos que llevaron a la formación de las tres componentes fundamentales para la vida.

Recientemente, el químico Ramanarayanan Krishnamurthy (2017, 2018a, b) enfatizó que la química prebiótica ha estado orientada en la demostración de rutas químicas lineales bajo condiciones específicas y cuestionables respecto a un punto de vista prebiótico. Este enfoque, llamado limpio y aislado⁹, ha considerado a los experimentos como sesgados por centrarse

se les pueden seguir sus caminos evolutivos hasta las características que pudieron estar presentes en el último ancestro común (**LUCA**, *Last Universal Common Ancestor*) (Preiner *et al.*, 2020).

⁷ Alfonso L. Herrera consideró a los minerales como posible base inorgánica del protoplasma (Herrera, 1932; Cleaves *et al.*, 2014). W. Garrison y colaboradores estudiaron el efecto de la radiación ionizante en la reducción de CO₂ en disoluciones y su efecto en la formación de moléculas poliatómicas (Garrison *et al.*, 1951). Stanley Miller y Harold Urey estudiaron la síntesis de compuestos orgánicos a partir de descargas eléctricas en una atmósfera reductora (Miller, 1953).

⁸ Se ha considerado que la química prebiótica es un campo difuso en el sentido de que parte de especulaciones y ausencia de definiciones (*e.g.*, vida). Debido a esto, las hipótesis pueden resultar tendenciosas y no está claro donde deja de ser química prebiótica para dar paso al origen de la vida (Bruylants *et al.*, 2011).

⁹ «Limpios y aislados» hace referencia al hecho de estudiar las componentes fundamentales para la vida de manera separada y están delimitados por el tipo de química que se está estudiando. Por ejemplo, no hay acuerdo en que componente es la más primitiva:

- La **evolución darwiniana** necesita moléculas informativas, así que el **RNA** debe haber sido lo primero.

demasiado en la bioquímica de la vida tal y como la conocemos hoy. Además, se ha cuestionado que los resultados experimentales intentan adaptarse a distintos escenarios primitivos (Cronin y Walker, 2016; Krishnamurthy, 2018b). De igual manera, pese a que ya se había propuesto el desarrollo de experimentos más complejos (en el sentido de tomar en cuenta mezclas de compuestos orgánicos) (Fox *et al.* 1959; Fox y Harada 1960; Eigen 1977) la gran mayoría de los experimentos de química prebiótica han tomado en cuenta moléculas orgánicas específicas y aisladas. Sin embargo, aunque estos experimentos han llegado a considerarse forzados, fueron un excelente punto de partida para sentar las bases de los tres pilares de la química prebiótica¹⁰.

Recientemente, diversos investigadores han propuesto considerar, además de escenarios químicos y geológicos plausibles, nuevos procesos físicos y fuerzas impulsoras (*e.g.*, reacciones favorecidas entre grupos de moléculas que fueron seleccionadas previamente por sus propiedades fisicoquímicas; estas moléculas podrían llevar a cabo reacciones más específicas y con mejores rendimientos) que pudieron tener un papel importante en numerosos escenarios primitivos (Hazen y Sverjensky 2010; Powner y Sutherland 2011; Wagner y Blackmond 2016; Krishnamurthy 2017). Nuevas perspectivas en el área han sugerido que también es necesario considerar las interacciones químicas entre los diferentes ambientes primitivos (*e.g.*, química de interferencia, química prebiótica estocástica) (Stüeken *et al.* 2013; Dass *et al.* 2016; Walton *et al.* 2020; Omran y Pasek 2020).

Actualmente, la propuesta es desarrollar una «**química de sistemas**»¹¹. En general, el objetivo es partir de escenarios que combinen moléculas simples y establecer sistemas autosostenibles. En otras palabras, experimentalmente, la química de sistemas consiste en estudiar el comportamiento y evolución de sistemas compuestos de diversas moléculas orgánicas simples en distintos ambientes geoquímicos. Tales moléculas simples no sólo pueden tener presencia y/o roles en las actuales biomoléculas de la vida sino que también, pudieron ser resultado de un proceso de selección influenciado y dictado por las propiedades fisicoquímicas de las mismas moléculas.

Por ejemplo, J. Sutherland propone que la síntesis de diversos componentes celulares (*e.g.*, nucleótidos, aminoácidos, lípidos) puede darse a partir de materias primas comunes resultado de

-
- No puedes sobrevivir sin **bloques de construcción y energía**, por lo que el **metabolismo** debe ser primero.
 - La genética y el metabolismo sin **catálisis** es difícil de imaginar, por lo que las **proteínas** deben haber sido lo primero.
 - El desarrollo de la selección darwiniana es difícil de imaginar sin **compartimentos**, por lo que las **membranas** deben haber estado allí al principio (Sutherland 2016).

¹⁰ Eschenmoser y Loewenthal (1992) e Islam y Powner (2017) han propuesto como los tres pilares de la química prebiótica a: I) la síntesis de azúcares por la reacción formosa, II) la síntesis de nucleobases a partir de ácido cianhídrico y su oligomerización, y III) la síntesis de aminoácidos por el experimento de descargas eléctricas en una atmósfera reducida.

¹¹ La «química de sistemas» sugiere que las interacciones naturales entre redes moleculares son más efectivas para establecer sistemas autocatalíticos comparados con una sola molécula replicadora. De esta manera, tales interacciones permiten una mayor selección y potencial co-evolutivo químico que, a su vez, establecería la siguiente etapa para selecciones químicas. Además, sugiere que las estructuras supramoleculares que hoy vemos no necesariamente estuvieron presentes desde el comienzo de las vías químicas prebióticas. En otras palabras, pudo haber precursores químicos que se transformaron de manera no lineal en las moléculas orgánicas que son usadas por los organismos actuales (Krishnamurthy, 2017, 2018b).

diversas reacciones semi-independientes. Una vez sintetizados algunos fragmentos reactivos, estos podrían interactuar, bajo condiciones prebióticas todavía muy discutidas, dando paso a estructuras químicas complejas (*e.g.*, ribonucleótidos) (Powner *et al.* 2009; Powner y Sutherland 2011; Patel *et al.* 2015; Sutherland 2016; Islam y Powner 2017). Por otro lado, Krishnamurthy y colaboradores han reportado la formación de oligodepsipéptidos enriquecidos en enlaces peptídicos a partir de una mezcla de α -aminoácidos y α -hidroxiácidos (Forsythe *et al.*, 2015, 2017), la importancia del ácido orótico como punto de partida en las vías químicas hacia el ARN (Kim *et al.*, 2017; Yadav *et al.*, 2020) y la emergencia de polímeros homogéneos a partir de una mezcla de oligómeros heterogéneos (Gavette *et al.* 2016; Efthymiou *et al.* 2018; Bhowmik y Krishnamurthy 2019) (Fig. 1.2.).

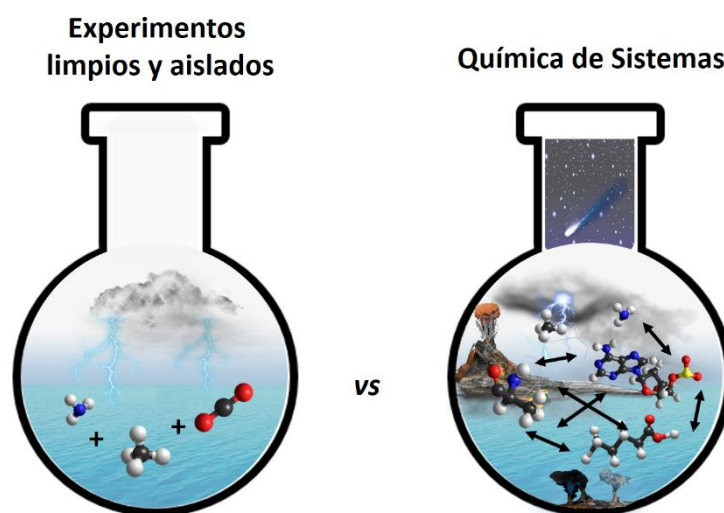


Figura 1.2. Los experimentos en química prebiótica han estado enfocados en la demostración de rutas químicas lineales bajo condiciones potencialmente prebióticas. Sin embargo, es necesario realizar experimentos considerando un amplio espectro de variables geoquímicas y sistemas primitivos dinámicos con el fin de emular entornos más consistentes. De igual manera, aún con el desarrollo de estructuras químicas relativamente complejas (*e.g.*, polímeros, oligómeros de ácidos nucleicos y/o aminoácidos), la formación de las primeras formas de vida aún está fuera del alcance de cualquier experimento de química prebiótica. Por ende, esta tesis está enfocada en estudiar algunos de los procesos fisicoquímicos que pudieron haber tenido lugar en sistemas hidrotermales a lo largo de la evolución química y las repercusiones de estos.

Por otro lado, aunque históricamente se ha asociado la aparición de la vida a partir de algún sistema químico autocatalítico, aún existen un sinnúmero de especulaciones sobre la precisión del camino histórico de lo inanimado a lo animado (Mann 2013; Pross y Pascal 2013). Así mismo, esta ambigüedad puede conducir a proposiciones que resultan de gran interés, aunque con una base científica limitada (Krishnamurthy, 2017). En consecuencia, es necesario ser cauteloso en el uso de términos y extrapolaciones ya que pueden conducir a la sobreestimación de procesos fisicoquímicos en un entorno primitivo. Un claro ejemplo es el caso de las hipótesis que señalan a

los sistemas hidrotermales, en especial a los submarinos, como posibles sitios en que se originó la vida.

Desde el descubrimiento de los sistemas hidrotermales submarinos, Corliss, J. B., Baross, J. A. y Hoffman, S. E (1981) sugirieron que estos entornos proporcionan todas las condiciones necesarias para la creación de vida en la Tierra¹², basándose en la gran disponibilidad de variables geoquímicas presentes en estos sistemas. Años después, Miller y Bada (1988) sugirieron que existen al menos tres requisitos cruciales para considerar una hipótesis del origen de la vida, y difícilmente son consistentes con un ambiente hidrotermal: I) la síntesis de compuestos orgánicos esenciales a través de un gradiente de temperatura ($T_i > 350 \text{ }^\circ\text{C}$ a $\approx 2 \text{ }^\circ\text{C}$); II) la síntesis de oligómeros por deshidratación térmica en condiciones de alta temperatura y III) la síntesis de prototipos o moléculas similares al RNA en alguna etapa del gradiente térmico. Naturalmente, ambas propuestas deben ser puestas a prueba. Por un lado, es necesario tener claro que, la forma de descifrar el posible origen de la vida es mucho más que lograr la síntesis de polímeros orgánicos de alto peso molecular o estructuras similares. Del mismo modo, desde el punto de vista de la química prebiótica, es necesario tener bien definidas las condiciones geoquímicas que se están asumiendo, el enfoque del experimento (*e.g.*, síntesis vs estabilidad vs reactividad), los pasos empleados durante el procedimiento, y la presunta etapa prebiótica del experimento realizado (Richert, 2018). En consecuencia, es imprescindible estudiar a detalle diversos mecanismos fisicoquímicos, respecto al enfoque del experimento, para poder hacer conjeturas sobre el papel que pudo tener un escenario geoquímico primitivo en evolución química, y tal vez, en origen de la vida¹³.

En los últimos años, nuestra comprensión del papel de los escenarios hidrotermales en evolución química se ha enriquecido considerablemente. Actualmente, es bastante claro que los sistemas hidrotermales son más que ambientes de altas presiones y temperaturas. Sin embargo, muchos experimentos de química prebiótica aún permanecen sesgados respecto a las variables de estudio utilizadas así como en las extrapolaciones de los resultados obtenidos. De esta manera, es necesario realizar estudios experimentales sistemáticos que consideren escenarios prebióticos plausibles y analizar cada una de las repercusiones de los mismos en los pasos subsecuentes que llevarían a un aumento de complejidad química. Este carácter sistemático podría ser así: **1)** definir un escenario geoquímico consistente con las condiciones de la Tierra primitiva, **2)** evaluar la disponibilidad de materia prima para llevar a cabo reacciones químicas, **3)** determinar las condiciones de síntesis de compuestos orgánicos y estudiar su estabilidad y reactividad, y **4)** estudiar la disponibilidad y el destino de las moléculas orgánicas en ese entorno geoquímico (Fig. 1.3). En esta tesis se estudia cada uno de los puntos antes mencionados de la siguiente manera:

¹² El hecho de que los sistemas hidrotermales pueden albergar una compleja biota, basada en procesos de quimiosíntesis (*e.g.*, metabolismo de H_2S), planteó la posibilidad de que la vida pudo haberse originado en un sistema oceánico hidrotermal Precámbrico y no como se suponía: resultado de descargas eléctricas y/o fuentes exoplanetarias (Goldie y Bottrill 1981).

¹³ Miller y Bada (1988) sugirieron que es posible la existencia de mecanismos de protección en condiciones hidrotermales que mejorarían la estabilidad de los compuestos aunque no habían sido descubiertos.

- 1) *Definición de un escenario geoquímico consistente con las condiciones de la Tierra primitiva.* Tan pronto comenzó la interacción entre la hidrósfera y la corteza (oceánica/continental), una intensa actividad hidrotermal pudo formar una gran cantidad de sistemas hidrotermales (submarinos y subaéreos) durante el Hadeano-Arqueano (Kelley, 2005; Sleep, 2010; Golding *et al.*, 2011; Arndt y Nisbet, 2012; Westall *et al.*, 2018). Esta actividad hidrotermal produjo grandes cambios en los procesos geoquímicos presentes en la Tierra Primitiva, por ejemplo: 1) grandes depósitos de minerales y nichos de evolución química, 2) síntesis de un amplio espectro de moléculas orgánicas, 3) enriquecimiento de gases y iones disueltos en un océano neutro-alcalino, y 4) la formación de oligómeros y polímeros como antesala de biomoléculas (Sleep *et al.* 2004; Schulte *et al.* 2006; Novoselov y Silantyev 2010; Schrenk *et al.* 2013; Wang *et al.* 2014; Shibuya *et al.* 2015) (Figura 1.3, paso 1). De esta manera, se describió detalladamente el entorno geológico primitivo y las variables fisicoquímicas presentes en sistemas hidrotermales así como sus repercusiones en evolución química (Ver Capítulo II y Anexo I).

- 2) *Evaluar la disponibilidad de materia prima para llevar a cabo reacciones químicas.* Varios mecanismos podrían haber contribuido al inventario del ácido cianhídrico, HCN, en la Tierra primitiva por la acción de diferentes fuentes de energía (*e.g.*, fotólisis, ondas de choque, descargas eléctricas y vulcanismo; Ferris y Hagan 1984; Holm y Neubeck 2009; Tian *et al.* 2011; Parkos *et al.* 2016; Ferus *et al.* 2017; Rimmer y Rugheimer 2019). En particular, se ha propuesto que el HCN pudo desempeñar un papel importante en la formación de moléculas orgánicas complejas en entornos hidrotermales (Mukhin, 1974, 1976; Dowler y Ingmanson, 1979; Corliss, J. B., Baross, J. A., y Hoffman, S. E, 1981; Baross y Hoffman, 1985; Ferris, 1992; Holm *et al.*, 2006; Aubrey *et al.*, 2009; Holm y Neubeck, 2009). En consecuencia, si el HCN estuviera presente en ambientes hidrotermales, las reacciones que experimentaría serían cruciales para comprender su papel en las rutas prebióticas que ocurren en estos sistemas. Por lo tanto, se realizó un estudio de la estabilidad y reactividad (*i.e.*, termólisis vs polimerización) del HCN considerando diversas variables fisicoquímicas que pueden estar presentes en entornos hidrotermales (*i.e.*, pH, temperatura y presencia de minerales). El escenario en donde ocurre una transformación preferencial del HCN en moléculas orgánicas/polímeros es en ambientes alcalinos y en ausencia de mineral (Figura 1.3, paso 2) (Ver Capítulo IV).

- 3) *Determinar las condiciones de síntesis de compuestos orgánicos y estudiar su estabilidad y reactividad.* Una vez que se forman los polímeros térmicos del ácido cianhídrico (*i.e.*, HCN-DTP), experimentarán varios fenómenos. Por ejemplo, los fluidos turbulentos y las corrientes profundas podrían esparcirlos a lo largo del sistema hidrotermal. Como este material es esencialmente insoluble, eventualmente precipitará (Figura 2, paso 3) y podrá interactuar con el basamento mineral del sistema a distintas temperaturas. Del mismo modo, debido a la continua circulación de fluidos hidrotermales, existe una enorme disponibilidad de gradientes de temperatura y pH que podrán favorecer la termólisis (desde 2 hasta 350 ° C) y la hidrólisis (a diversos valores de pH) (Lupton *et al.*, 1985; Little *et al.*, 1987; Holm y Hennet, 1992; Bemis *et al.*, 2012; Mittelstaedt *et al.*, 2012) de los polímeros

formados. En consecuencia, se realizó un estudio detallado de las propiedades fisicoquímicas y térmicas del polímero derivado de la termólisis del HCN, así como el efecto de las condiciones de hidrólisis en la liberación de moléculas orgánicas a partir de este material. Igualmente, se realizaron experimentos en presencia de una superficie mineral disponible en sistemas hidrotermales alcalinos (*e.g.*, serpentinita) con el objetivo de estudiar el efecto de los minerales en la formación de moléculas orgánicas (Ver Capítulo V y Anexo II) (Figura 1.3, paso 4)

- 4) *Estudiar la disponibilidad y el destino de las moléculas orgánicas en ese entorno geoquímico.* Una vez liberadas diversas moléculas orgánicas (*e.g.*, aldehídos, ácidos carboxílicos, aminoácidos, compuestos N-heterocíclicos) a partir de la termólisis e hidrólisis de los polímeros de HCN, el medio circundante estará enriquecido en material orgánico (Figura 1.3, paso 5). Tales moléculas podrían transportarse y experimentar diversos fenómenos fisicoquímicos bajo ciertas condiciones ambientales (*e.g.*, gases, iones, metales y minerales) (Stüeken *et al.*, 2013b). Por ejemplo, procesos de descomposición, oligomerización, dilución, precipitación y/o sorción (Zaia *et al.*, 2008; Zaia, 2012; Bedoin *et al.*, 2020; Damer & Deamer, 2020; Omran & Pasek, 2020) (Figura 1.3, paso 6). Respecto a lo anterior, se analizó el destino de diferentes aminoácidos (moléculas identificadas a partir de la termólisis e hidrólisis de los polímeros térmicos de HCN) en escenarios hidrotermales. Por un lado, se estudió la oligomerización del sistema Ala + Glu en presencia de sílica, SiO₂, tanto en condiciones hidrotermales submarinas (*e.g.*, altas presiones y temperaturas) y subaeras (*e.g.*, ciclos mojado-secado) (Ver Capítulo VI). Por otro lado, se estudió el efecto de iones disueltos en la sorción de aminoácidos en serpentinita considerando un modelo de agua hidrotermal (Ver Capítulo VII).

En conclusión, es necesario delimitar el tiempo y las condiciones geoquímicas que se van a considerar en cualquier experimento de química prebiótica. Por ende, se debe hacer hincapié en que hay un gran número de incógnitas respecto a las investigaciones entre los ensayos de química prebiótica, la formación e interacción entre las tres componentes fundamentales para la vida y el origen de la vida. Con base en lo anterior, en este trabajo se propone a los sistemas hidrotermales como escenarios prebióticos consistentes con las primeras etapas de la Tierra y se estudia detalladamente cada uno de los puntos requeridos para considerar su rol en la evolución química. Por ende, sus repercusiones están fuera del alcance de cualquier hipótesis del origen de la vida y más bien son una conexión entre los experimentos limpios y aislados con la química de sistemas.

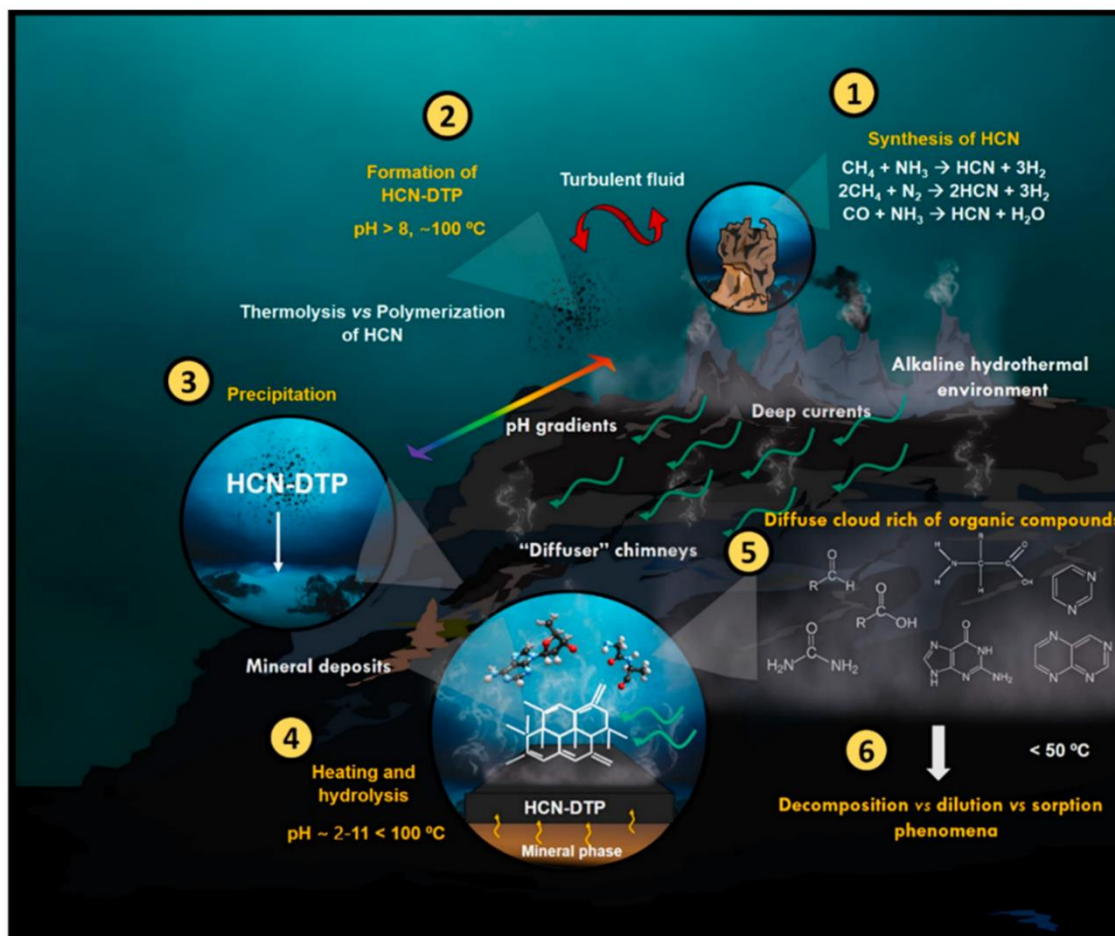


Figura 1.3. Destino probable del HCN y su polímero térmico (HCN-DTP) en un sistema hidrotermal primitivo. Cada punto se describe a detalle en el texto. Crédito: Villafaña-Barajas, Saúl A., *et al.* "Characterization of HCN-derived thermal polymer: implications for chemical evolution." *Processes* 8.8 (2020): 968.

Hipótesis

La disponibilidad de diversas variables geoquímicas en los sistemas hidrotermales, tanto submarinos como subaéreos, puede favorecer la transformación de materia orgánica en componentes más complejos. De esta manera, los sistemas hidrotermales pudieron ser nichos de evolución química en donde ocurrió la formación e interacción de las tres componentes fundamentales para la vida.

Objetivo general

Realizar estudios experimentales sistemáticos sobre el papel de los sistemas hidrotermales, tanto submarinos como subaéreos, en la transformación del ácido cianhídrico considerando escenarios prebióticos plausibles. De igual manera, analizar cada una de las repercusiones de los

experimentos de química prebiótica desarrollados en los pasos subsecuentes que llevarían a un aumento de complejidad química. Por ejemplo, la polimerización y la sorción de aminoácidos.

Objetivos Particulares

- Describir las condiciones geoquímicas que pudieron estar presentes en los sistemas hidrotermales primitivos.
- Evaluar la disponibilidad, la estabilidad y la reactividad del ácido cianhídrico considerando modelos experimentales simples de sistemas hidrotermales.
- Estudiar el papel de diversos minerales en la reactividad del ácido cianhídrico así como en el fenómeno de polimerización y la formación de moléculas orgánicas.
- Realizar un estudio comparativo del efecto de las condiciones presentes en sistemas hidrotermales submarinos y subaéreos en la polimerización de aminoácidos.
- Analizar el efecto de iones disueltos en el fenómeno de sorción de amino ácidos en serpentinita.

Referencias

- Allegre CJ, Manhès G, Göpel C (1995) The age of the Earth. *Geochimica et Cosmochimica Acta* **59**, 1445–1456.
- Altermann W, Beard B, Hoffman P, Johnson C, Kasting J, Melezhik V, Nutman AP, Papineau D, Pirajno F (2012) A chronostratigraphic division of the Precambrian: possibilities and challenges.
- Arndt NT, Nisbet EG (2012) Processes on the young Earth and the habitats of early life. *Annual Review of Earth and Planetary Sciences* **40**, 521–549.
- Aubrey AD, Cleaves HJ, Bada JL (2009) The Role of Submarine Hydrothermal Systems in the Synthesis of Amino Acids. *Origins of Life and Evolution of Biospheres* **39**, 91–108.
- Ballard RD (1977) Notes on a major oceanographic find (marine animals near hot-water vents at ocean bottom). *Oceanus* **20**, 35–44.
- Baross JA, Hoffman SE (1985) Submarine hydrothermal vents and associated gradient environments as sites for the origin and evolution of life. *Origins of Life and Evolution of the Biosphere* **15**, 327–345.
- Bedoin L, Alves S, Lambert J-F (2020) Origins of Life and Molecular Information: Selectivity in Mineral Surface-Induced Prebiotic Amino Acid Polymerization. *ACS Earth and Space Chemistry* **4**, 1802–1812.
- Bemis K, Lowell R, Farough A (2012) Diffuse Flow On and Around Hydrothermal Vents at Mid-Ocean Ridges. *Oceanography* **25**, 182–191.
- Bhowmik S, Krishnamurthy R (2019) The role of sugar-backbone heterogeneity and chimeras in the simultaneous emergence of RNA and DNA. *Nature chemistry* **11**, 1009–1018.

- Bowring SA, Williams IS (1999) Priscoan (4.00–4.03 Ga) orthogneisses from northwestern Canada. *Contributions to Mineralogy and Petrology* **134**, 3–16.
- Bruylants G, Bartik K, Reisse J (2011) Prebiotic chemistry: a fuzzy field. *Comptes Rendus Chimie* **14**, 388–391.
- Calvin M (1956) Chemical evolution and the origin of life. *American Scientist* **44**, 248–263.
- Cleaves HJ (2012) Prebiotic chemistry: what we know, what we don't. *Evolution: Education and Outreach* **5**, 342.
- Cleaves HJ, Lazcano A, Mateos IL, Negrón-Mendoza A, Peretó J, Silva E (2014) *Herrera's' Plasmogenia' and Other Collected Works: Early Writings on the Experimental Study of the Origin of Life*. Springer.
- Corliss, J. B., Baross, J. A., & Hoffman, S. E (1981) An hypothesis concerning the relationships between submarine hot springs and the origin of life on earth.
- Corliss JB, Dymond J, Gordon LI, Edmond JM, Herzen RP von, Ballard RD, Green K, Williams D, Bainbridge A, Crane K, Andel TH van (1979) Submarine Thermal Springs on the Galápagos Rift. *Science* **203**, 1073–1083.
- Cronin L, Walker SI (2016) Beyond prebiotic chemistry. *Science* **352**, 1174–1175.
- Damer B, Deamer D (2020) The Hot Spring Hypothesis for an Origin of Life. *Astrobiology* **20**, 429–452.
- Dass AV, Hickman-Lewis K, Brack A, Kee TP, Westall F (2016) Stochastic Prebiotic Chemistry within Realistic Geological Systems. *ChemistrySelect* **1**, 4906–4926.
- Dowler MJ, Ingmanson DE (1979) Thiocyanate in Red Sea brine and its implications. *Nature* **279**, 51.
- Dworkin JP, Lazcano A, Miller SL (2003) The roads to and from the RNA world. *Journal of Theoretical Biology* **222**, 127–134.
- Efthymiou T, Gavette J, Stoop M, De Riccardis F, Froeyen M, Herdewijn P, Krishnamurthy R (2018) Chimeric XNA: an unconventional design for orthogonal informational systems. *Chemistry—A European Journal* **24**, 12811–12819.
- Eigen M (1977) The hypercycle. A principle of natural self-organization. Part A: Emergence of the hypercycle. *Naturwissenschaften* **64**, 541–565.
- Eriksson PG, Mazumder R, Catuneanu O, Bumby AJ, Ilondo BO (2006) Precambrian continental freeboard and geological evolution: a time perspective. *Earth-Science Reviews* **79**, 165–204.
- Ferris JP (1992) Chemical Markers of Prebiotic Chemistry in Hydrothermal Systems. In: *Marine Hydrothermal Systems and the Origin of Life* (ed. Holm NG). Springer Netherlands, Dordrecht, pp. 109–134.
- Ferris JP, Hagan WJ (1984) HCN and chemical evolution: The possible role of cyano compounds in prebiotic synthesis. *Tetrahedron* **40**, 1093–1120.
- Ferus M, Kubelík P, Knížek A, Pastorek A, Sutherland J, Civiš S (2017) High energy radical chemistry formation of HCN-rich atmospheres on early Earth. *Scientific reports* **7**, 6275.

- Forsythe JG, Petrov AS, Millar WC, Yu S-S, Krishnamurthy R, Grover MA, Hud NV, Fernández FM (2017) Surveying the sequence diversity of model prebiotic peptides by mass spectrometry. *Proceedings of the National Academy of Sciences* **114**, E7652–E7659.
- Forsythe JG, Yu S-S, Mamajanov I, Grover MA, Krishnamurthy R, Fernández FM, Hud NV (2015) Ester-mediated amide bond formation driven by wet–dry cycles: A possible path to polypeptides on the prebiotic Earth. *Angewandte Chemie International Edition* **54**, 9871–9875.
- Fox SW, Harada K (1960) The thermal copolymerization of amino acids common to protein1. *Journal of the American Chemical Society* **82**, 3745–3751.
- Fox SW, Harada K, Vegotsky A (1959) Thermal polymerization of amino acids and a theory of biochemical origins. *Cellular and Molecular Life Sciences* **15**, 81–84.
- Garrison WM, Morrison DC, Hamilton JG, Benson AA, Calvin M (1951) *Reduction of Carbon Dioxide in Aqueous Solutions by Ionizing Radiation*. Ernest Orlando Lawrence Berkeley National Laboratory, Berkeley, CA (US).
- Gavette JV, Stoop M, Hud NV, Krishnamurthy R (2016) RNA–DNA chimeras in the context of an RNA world transition to an RNA/DNA world. *Angewandte Chemie International Edition* **55**, 13204–13209.
- Gilbert W (1986) Origin of life: The RNA world. *nature* **319**, 618–618.
- Goldie R, Bottrill TJ (1981) Seminar on sea-floor hydrothermal systems. *Geoscience Canada* **8**.
- Golding SD, Duck LJ, Young E, Baublys KA, Glikson M, Kamber BS (2011) Earliest Seafloor Hydrothermal Systems on Earth: Comparison with Modern Analogues. In: *Earliest Life on Earth: Habitats, Environments and Methods of Detection* (eds. Golding SD, Glikson M). Springer Netherlands, Dordrecht, pp. 15–49.
- Hazen RM, Sverjensky DA (2010) Mineral Surfaces, Geochemical Complexities, and the Origins of Life. *Cold Spring Harbor Perspectives in Biology* **2**, a002162–a002162.
- Herrera AL (1932) *La Plasmogenia: Nueva ciencia del origen de la vida...*
- Holm NG, Dumont M, Ivarsson M, Konn C (2006) Alkaline fluid circulation in ultramafic rocks and formation of nucleotide constituents: a hypothesis. *Geochemical Transactions* **7**, 7.
- Holm NG, Hennem RJ-C (1992) Hydrothermal systems: their varieties, dynamics, and suitability for prebiotic chemistry. In: *Marine Hydrothermal Systems and the Origin of Life*. Springer, pp. 15–31.
- Holm NG, Neubeck A (2009) Reduction of nitrogen compounds in oceanic basement and its implications for HCN formation and abiotic organic synthesis. *Geochemical Transactions* **10**, 9.
- Islam S, Powner MW (2017a) Prebiotic Systems Chemistry: Complexity Overcoming Clutter. *Chem* **2**, 470–501.
- Islam S, Powner MW (2017b) Prebiotic systems chemistry: Complexity overcoming clutter. *Chem* **2**, 470–501.
- Kelley DS (2005) A Serpentinite-Hosted Ecosystem: The Lost City Hydrothermal Field. *Science* **307**, 1428–1434.

- Kelley DS, Karson JA, Blackman DK, FruÈh-Green GL, Butterfield DA, Lilley MD, Olson EJ, Schrenk MO, Roe KK, Lebon GT (2001) An off-axis hydrothermal vent field near the Mid-Atlantic Ridge at 30 N. *Nature* **412**, 145.
- Kerr RA (2000) *Geologists pursue solar system's oldest relics*. American Association for the Advancement of Science.
- Kim E-K, Martin V, Krishnamurthy R (2017) Orotidine-Containing RNA: Implications for the Hierarchical Selection (Systems Chemistry Emergence) of RNA. *Chemistry - A European Journal* **23**, 12668–12675.
- Krishnamurthy R (2017) Giving rise to life: Transition from prebiotic chemistry to protobiology. *Accounts of chemical research* **50**, 455–459.
- Krishnamurthy R (2018a) Experimentally investigating the origin of DNA/RNA on early Earth. *Nature communications* **9**, 5175.
- Krishnamurthy R (2018b) Life's Biological Chemistry: A Destiny or Destination Starting from Prebiotic Chemistry? *Chemistry—A European Journal* **24**, 16708–16715.
- Little SA, Stolzenbach KD, Von Herzen RP (1987) Measurements of plume flow from a hydrothermal vent field. *Journal of Geophysical Research: Solid Earth* **92**, 2587–2596.
- Lupton JE, Delaney JR, Johnson HP, Tivey MK (1985) Entrainment and vertical transport of deep-ocean water by buoyant hydrothermal plumes. *Nature* **316**, 621–623.
- Ma W (2017) What does “the RNA world” mean to “the origin of life”? *Life* **7**, 49.
- Mann S (2013) The origins of life: old problems, new chemistries. *Angewandte Chemie International Edition* **52**, 155–162.
- Mattia E, Otto S (2015) Supramolecular systems chemistry. *Nature nanotechnology* **10**, 111–119.
- Miller SL (1953) A production of amino acids under possible primitive earth conditions. *Science* **117**, 528–529.
- Miller SL, Bada JL (1988) Submarine hot springs and the origin of life. *Nature* **334**, 609–611.
- Mittelstaedt E, Escartín J, Gracias N, Olive J-A, Barreyre T, Davaille A, Cannat M, Garcia R (2012) Quantifying diffuse and discrete venting at the Tour Eiffel vent site, Lucky Strike hydrothermal field: HEAT FLUX TOUR EIFFEL. *Geochemistry, Geophysics, Geosystems* **13**, n/a-n/a.
- Mukhin L (1976) Volcanic processes and synthesis of simple organic compounds on primitive earth. *Origins of life* **7**, 355–368.
- Mukhin LEV (1974) Evolution of organic compounds in volcanic regions. *Nature* **251**, 50–51.
- Novoselov AA, Silantyev SA (2010) Hydrothermal systems of the hadean ocean and their influence on the matter balance in the crust-hydrosphere-atmosphere system of the early earth. *Geochemistry International* **48**, 643–654.
- Ogg JG, Ogg G, Gradstein FM (2016) *A concise geologic time scale: 2016*. Elsevier.
- Omran A, Pasek M (2020) A Constructive Way to Think about Different Hydrothermal Environments for the Origins of Life. *Life* **10**, 36.

- Parkos D, Pikus A, Alexeenko A, Melosh HJ (2016) HCN production from impact ejecta on the early Earth. In: *AIP Conference Proceedings*. AIP Publishing, p. 170001.
- Patel BH, Percivalle C, Ritson DJ, Duffy CD, Sutherland JD (2015) Common origins of RNA, protein and lipid precursors in a cyanosulfidic protometabolism. *Nature Chemistry* **7**, 301–307.
- Powner MW, Gerland B, Sutherland JD (2009) Synthesis of activated pyrimidine ribonucleotides in prebiotically plausible conditions. *Nature* **459**, 239.
- Powner MW, Sutherland JD (2011) Prebiotic chemistry: a new *modus operandi*. *Philosophical Transactions of the Royal Society B: Biological Sciences* **366**, 2870–2877.
- Preiner M, Asche S, Becker S, Betts HC, Boniface A, Camprubi E, Chandru K, Erastova V, Garg SG, Khawaja N (2020) The future of origin of life research: bridging decades-old divisions. *Life* **10**, 20.
- Pross A, Pascal R (2013) The origin of life: what we know, what we can know and what we will never know. *Open biology* **3**, 120190.
- Richert C (2018) Prebiotic chemistry and human intervention. *Nature Communications* **9**, 5177.
- Rimmer PB, Rugheimer S (2019) Hydrogen cyanide in nitrogen-rich atmospheres of rocky exoplanets. *Icarus* **329**, 124–131.
- Robertson MP, Joyce GF (2012) The origins of the RNA world. *Cold Spring Harbor perspectives in biology* **4**, a003608.
- Ruiz-Mirazo K, Briones C, Escosura A de la (2013) Prebiotic systems chemistry: new perspectives for the origins of life. *Chemical Reviews* **114**, 285–366.
- Schrenk MO, Brazelton WJ, Lang SQ (2013) Serpentinization, carbon, and deep life. *Reviews in Mineralogy and Geochemistry* **75**, 575–606.
- Schulte M, Blake D, Hoehler T, McCollom T (2006) Serpentinization and Its Implications for Life on the Early Earth and Mars. *Astrobiology* **6**, 364–376.
- Shibuya T, Yoshizaki M, Sato M, Shimizu K, Nakamura K, Omori S, Suzuki K, Takai K, Tsunakawa H, Maruyama S (2015) Hydrogen-rich hydrothermal environments in the Hadean ocean inferred from serpentinization of komatiites at 300 C and 500 bar. *Progress in Earth and Planetary Science* **2**, 46.
- Sleep NH (2010) The hadean-archaeon environment. *Cold spring harbor perspectives in biology* **2**, a002527.
- Sleep NH, Meibom A, Fridriksson T, Coleman RG, Bird DK (2004) H₂-rich fluids from serpentinization: geochemical and biotic implications. *Proceedings of the National Academy of Sciences* **101**, 12818–12823.
- Stüeken EE, Anderson RE, Bowman JS, Brazelton WJ, Colangelo-Lillis J, Goldman AD, Som SM, Baross JA (2013a) Did life originate from a global chemical reactor? *Geobiology* **11**, 101–126.
- Stüeken EE, Anderson RE, Bowman JS, Brazelton WJ, Colangelo-Lillis J, Goldman AD, Som SM, Baross JA (2013b) Did life originate from a global chemical reactor? *Geobiology* **11**, 101–126.

- Sutherland JD (2016a) The origin of life—out of the blue. *Angewandte Chemie International Edition* **55**, 104–121.
- Sutherland JD (2016b) The Origin of Life-Out of the Blue. *Angewandte Chemie International Edition* **55**, 104–121.
- Tian F, Kasting JF, Zahnle K (2011) Revisiting HCN formation in Earth’s early atmosphere. *Earth and Planetary Science Letters* **308**, 417–423.
- Valley JW, Cavosie AJ, Ushikubo T, Reinhard DA, Lawrence DF, Larson DJ, Clifton PH, Kelly TF, Wilde SA, Moser DE (2014) Hadean age for a post-magma-ocean zircon confirmed by atom-probe tomography. *Nature Geoscience* **7**, 219.
- Wagner AJ, Blackmond DG (2016) *The future of prebiotic chemistry*. ACS Publications.
- Walton C, Rimmer PB, Williams H, Shorttle O (2020) Prebiotic chemistry in the wild: How geology interferes with the origins of life.
- Wang X, Ouyang Z, Zhuo S, Zhang M, Zheng G, Wang Y (2014) Serpentinization, abiogenic organic compounds, and deep life. *Science China Earth Sciences* **57**, 878–887.
- Westall F, Hickman-Lewis K, Hinman N, Gautret P, Campbell KA, Bréhéret JG, Foucher F, Hubert A, Sorieul S, Dass AV, Kee TP, Georgelin T, Brack A (2018) A Hydrothermal-Sedimentary Context for the Origin of Life. *Astrobiology* **18**, 259–293.
- Wilde SA, Valley JW, Peck WH, Graham CM (2001) Evidence from detrital zircons for the existence of continental crust and oceans on the Earth 4.4 Gyr ago. *Nature* **409**, 175.
- Yadav M, Kumar R, Krishnamurthy R (2020) Chemistry of Abiotic Nucleotide Synthesis. *Chemical Reviews* **120**, 4766–4805.
- Zaia DAM (2012) Adsorption of amino acids and nucleic acid bases onto minerals: a few suggestions for prebiotic chemistry experiments. *International Journal of Astrobiology* **11**, 229–234.
- Zaia DAM, Zaia CTBV, De Santana H (2008) Which Amino Acids Should Be Used in Prebiotic Chemistry Studies? *Origins of Life and Evolution of Biospheres* **38**, 469–488.

Artículos complementarios a este capítulo

- González, L., **Villafañe-Barajas, S.**, y Colín García, M. (2018) Los manantiales hidrotermales submarinos y la evolución química (Nuestra Tierra, ISSN 1665-935X).

Los manantiales hidrotermales submarinos y la evolución química

Artículo de divulgación científica

González, L., **Villafañe-Barajas, S.**, y Colín García, M. (2018) Los manantiales hidrotermales submarinos y la evolución química (Nuestra Tierra, ISSN 1665-935X).

LOS MANANTIALES HIDROTERMALES SUBMARINOS Y LA EVOLUCIÓN QUÍMICA

Lucía González-López¹, Saúl Villafañe Barajas¹, María Colín-García^{2*}

¹Posgrado en Ciencias de la Tierra, Universidad Nacional Autónoma de México, Ciudad Universitaria, Coyoacán, Ciudad de México, C.P. 04510

²Instituto de Geología, Universidad Nacional Autónoma de México, Circuito de la Investigación Científica, Ciudad Universitaria, Coyoacán, Ciudad de México, C.P. 04510

*mcolin@geologia.unam.mx



Figura 1. El sumergible Alvin es un submarino tripulado que permite la recolección de datos en el fondo oceánico. Su alcance es de hasta 4500 metros de profundidad en inmersiones que pueden durar hasta 10 horas. Este sumergible es propiedad de la Marina de los Estados Unidos, fue puesto en servicio el 5 de junio de 1964 y es operado por la Institución Oceanográfica Woods Hole.

El 15 de febrero de 1977, cruzando las aguas sobre la cordillera submarina de las Islas Galápagos, el sumergible *ANGUS* detectó algunas variaciones de temperatura en las profundidades del océano y una densa acumulación de organismos nunca antes vista. Dos días después, los científicos J. B. Corliss, T. van Andel y J. Donnelly, a bordo del mítico sumergible *Alvin* (Figura 1), observaron por primera vez y de manera directa, a más de dos kilómetros de profundidad, el primer manantial hidrotermal submarino: había sido descubierto el llamado “Clambake 1”. De esta manera, la frase que

Conceptos básicos

La **evolución química** comprende los diversos procesos físico-químicos que llevaron a la formación de las primeras moléculas importantes, los “bloques de la vida”. Se supone que estos procesos tuvieron lugar durante las primeras etapas de formación de la Tierra.

La **química prebiótica** es el estudio experimental de la síntesis de los bloques de la vida. Entre otros compuestos se estudia la formación de ácidos carboxílicos, aminoácidos y bases nitrogenadas. En esta área es muy importante incluir diversas variables geoquímicas que pudieron contribuir al surgimiento de la vida con sus características imprescindibles: el metabolismo, la división por membranas (compartimentación) y el almacenamiento de información genética.

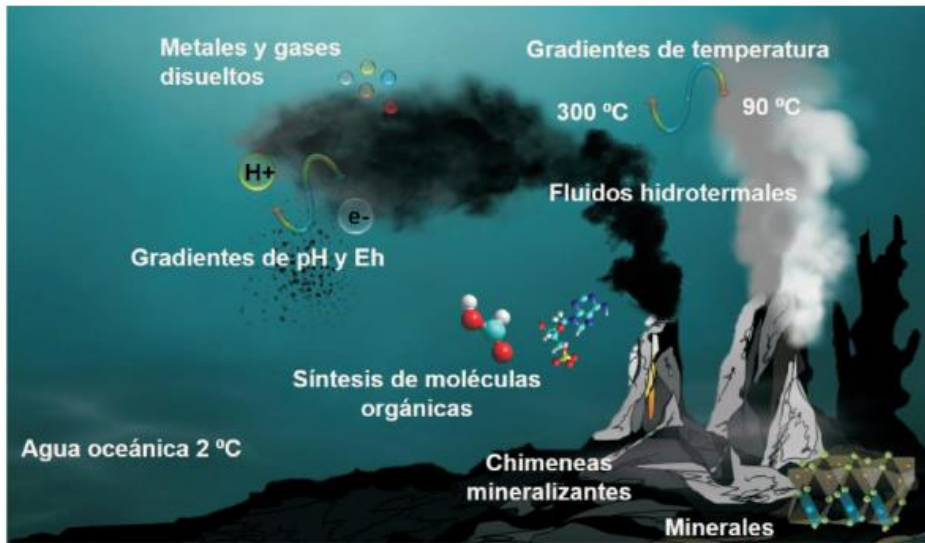


Figura 2. Esquema general de un sistema hidrotermal submarino. En estos sistemas geológicos existe una gran cantidad de variables geoquímicas como son: diferentes metales y gases disueltos, gradientes de temperatura, pH y presencia de minerales.

en la litósfera o en la superficie de ésta, que se encuentre a una temperatura superior a la ambiental. Esta agua, procedente de la lluvia, del océano o incluso del magma, puede filtrarse a través de fracturas y/o rocas porosas a distintas presiones y temperaturas y reaccionar químicamente con dichas rocas. En el caso de los sistemas hidrotermales submarinos, los fluidos pueden brotar del fondo oceánico y producir chimeneas mineralizantes. Existen muchos factores geoquímicos en estos

plasmó H. G. Wells en su historia corta *In the Abyss* en 1896, "Pensaste que no encontraría nada más que lodo, y he descubierto un mundo nuevo", adquirió un verdadero significado.

En los años siguientes, la participación de científicos de diversas áreas provocó un alud de cuestiones sobre el océano profundo, hasta entonces desconocido. Se plantearon preguntas como: ¿cuál es el motor que mueve la corteza terrestre?, ¿cómo puede existir la vida en ambientes sin luz solar y en condiciones de altas presiones y temperaturas? Incluso se llegó a proponer que en los ambientes hidrotermales se podría haber originado la vida. Pero, ¿qué son los sistemas hidrotermales? y en particular ¿por qué son tan importantes para la evolución química? (Figura 1).

¿Qué son los sistemas hidrotermales?

Un sistema hidrotermal tiene dos componentes esenciales: una fuente de energía térmica y la presencia de fluidos, casi siempre acuosos. Los sistemas hidrotermales pueden ser submarinos (se ubican en el fondo del océano) o sub-aéreos (se encuentran en la superficie de los continentes), como es el caso de los géiseres del conocido Parque Nacional de Yellowstone en los Estados Unidos de América.

Los ambientes hidrotermales se forman cuando existe un flujo de agua,

sistemas (temperatura, presión, profundidad, tipo de rocas, etc.) que dan características únicas a cada fluido y a cada ambiente (Figura 2).

En los sistemas hidrotermales submarinos existen, en términos generales, dos tipos de chimeneas mineralizantes: las "fumarolas negras" y las "fumarolas blancas" (Figura 3). Se llaman "fumarolas" (*smokers* en inglés) porque parecen humo, pero no se deben confundir con las fumarolas verdaderas, que se encuentran en los volcanes. Las fumarolas de los ambientes hidrotermales



Figura 3. Esquema comparativo entre las características de las fumarolas negras y las blancas. Como se observa, las fumarolas negras se encuentran más cerca de la fuente de calor (foco hidrotermal), mientras que las blancas se encuentran más alejadas de ésta. Otras diferencias incluyen la temperatura, que es más baja en las fumarolas blancas y los valores diferentes del pH.

son emanaciones de agua caliente con cierta coloración, que depende de los minerales que lleva en suspensión.

Las fumarolas negras más conocidas están cerca de zonas donde se genera el piso oceánico, las cordilleras a la mitad de los océanos o dorsales meso-oceánicas, así como en otros ambientes geológicos con actividad volcánica submarina. En estos sitios, los fluidos acuosos alcanzan temperaturas superiores a los 300 °C. Bajo el océano, el agua sigue en estado líquido, aún a temperaturas mayores a 100 °C, debido a las grandes presiones que existen en estos ambientes. La coloración oscura de estas fumarolas se debe a que los fluidos tienen abundantes minerales metálicos en suspensión, que incluyen elementos como Fe, Cu, Pb, Zn, Ba, Au y Ag. Al entrar en contacto con el agua fría del océano (que se encuentra a unos 2 °C) los minerales precipitan y se depositan.

Las fumarolas blancas suelen encontrarse alrededor de las fumarolas negras aunque más lejos de la fuente de calor, y también se forman durante las etapas finales de la vida del sistema hidrotermal. Una diferencia importante entre los dos tipos de fumarolas es que en las negras precipitan mayoritariamente sulfuros, mientras que en las blancas precipitan sulfatos (especialmente de Ba y Ca). Además, las fumarolas blancas son de temperatura más baja, más alcalinas y más oxidadas que las negras.

El estudio de los sistemas hidrotermales es relevante para áreas de conocimiento como la mineralogía, la metalurgia, la biología molecular, pero también para entender cómo se sintetizaron las moléculas, durante el período de evolución química.

Relevancia en evolución química

Nuestro planeta se ha mantenido en constante actividad desde su formación; cada paso en su evolución ha tenido diversas manifestaciones. Una de estas expresiones es la variada gama de sistemas hidrotermales que existen. Desde su descubrimiento, los sistemas hidrotermales submarinos fueron propuestos como ambientes en los que pudo haber ocurrido la evolución química en los primeros períodos de la Tierra. En estos ambientes convergen factores para que ocurran reacciones químicas: hay abundante energía, moléculas orgánicas y agua líquida (un medio donde se pudieron llevar a cabo las reacciones químicas). A la par, algunos científicos propusieron que hay una relación directa entre algunos procesos geoquímicos que ocurren en

estos sistemas y los procesos biológicos, lo que condujo a que fueran considerados como los ambientes donde se originó la vida en nuestro planeta; actualmente esta idea es muy cuestionada.

Para entender el papel de los sistemas hidrotermales submarinos en la evolución química, actualmente se realizan experimentos, en los que se simulan algunas de las condiciones que persisten en estos ambientes. Típicamente se estudia la producción de compuestos químicos con importancia biológica, así como su descomposición a altas temperaturas y presiones. Estos estudios se realizan para determinar si las moléculas orgánicas son capaces de permanecer en estos ambientes y por cuánto tiempo y, si llegan a descomponerse, determinar los productos que se forman.

Los resultados que se han obtenido hasta ahora son muy variados. Por un lado, se ha demostrado que es posible sintetizar^a moléculas de distintos tipos, como hidrocarburos e incluso moléculas con relevancia biológica -como los aminoácidos (partes fundamentales de las proteínas) o los ácidos carboxílicos (moléculas fundamentales en el metabolismo), a partir de elementos y compuestos tan simples como el hidrógeno, el monóxido de carbono y algunos aldehídos y cetonas. Por otro lado, sabemos que los compuestos orgánicos son muy sensibles a altas temperaturas y presiones, como las presentes en los sistemas hidrotermales submarinos; en estas condiciones y en algunos casos, moléculas como los azúcares, sólo son estables por unos cuantos minutos antes de descomponerse.

Sin embargo, los sistemas geológicos son muy complejos y en ellos existen muchas variables además de la temperatura y la presión. Para determinar la estabilidad y la reactividad de las moléculas orgánicas en estos sitios, también es necesario considerar la gran variedad de minerales, la existencia de gradientes de temperatura, la acidez, las condiciones de oxidación-reducción, la presencia de todo tipo gases y los elementos disueltos.

Por si fuera poco, en estos ambientes las condiciones cambian en unos cuantos centímetros. Por ejemplo, la temperatura de los fluidos hidrotermales cambia muy rápidamente debido al fuerte contraste que existe con los alrededores: en distancias de sólo 15 cm hay diferencias de hasta 30 °C. Se ha demostrado que los aminoácidos se pueden unir para formar cadenas: cuando se forman cadenas cortas y se unen entre dos y diez aminoácidos, estas cadenas se llaman oligopéptidos; pero eso no es

^aSíntesis: proceso de obtención de un compuesto a partir de sustancias más sencillas.

todo, pues los aminoácidos pueden llegar a formar cadenas más largas (llamadas polipéptidos) cuando se simulan ambientes hidrotermales con gradientes de temperatura.

Una de las variables más relevantes en los ambientes hidrotermales es la composición mineral. Los minerales disponibles en estos ambientes pueden servir para que las moléculas se concentren, o bien, reaccionen. Se ha demostrado que los elementos disueltos en los fluidos pueden favorecer la estabilidad de los compuestos orgánicos y afectar sus mecanismos de reacción. Las sales disueltas, por ejemplo, pueden unirse a las moléculas, formar complejos y favorecer que las moléculas orgánicas y los minerales interactúen.

Un ejemplo de lo anterior es la reacción que tiene lugar entre el agua marina y la roca predominante en el lecho oceánico, que es el basalto: a este proceso se le llama serpentinización y consiste en la transformación de minerales de silicio ricos en hierro y magnesio (como el olivino) en minerales hidratados, llamados serpentinas. Este proceso genera hidrógeno (H_2), un elemento muy reactivo, que si se encuentra con alguna molécula que contenga carbono (p. ej. CO_2) forma metano (CH_4). Esta interacción es crucial en evolución química, ya que se producen gases muy reactivos y se liberan enormes cantidades de energía. El metano y el dióxido de carbono son una fuente natural de energía y actualmente proveen el “combustible” del que se alimentan las comunidades microbianas en estos ambientes.

En resumen, en este tipo de ambientes, la interacción de las moléculas orgánicas que forman compuestos más complejos, ofrecen la posibilidad del estudio de la formación y destino de los “bloques de la vida” en las primeras etapas de la historia del planeta.

Hasta hace cuatro décadas, la hipótesis de la “sopa primitiva” sugerida por Charles Darwin y detallada por los iniciadores de las investigaciones relacionadas con el origen de la vida, Aleksandr Oparin y John Haldane, era la propuesta que dominaba la explicación de los pasos físico-químicos que llevaron al origen de la vida. Sin embargo, el descubrimiento de los sistemas hidrotermales planteó el surgimiento de nuevas ideas y otros tipos de mecanismos que también pudieron contribuir de manera importante en la

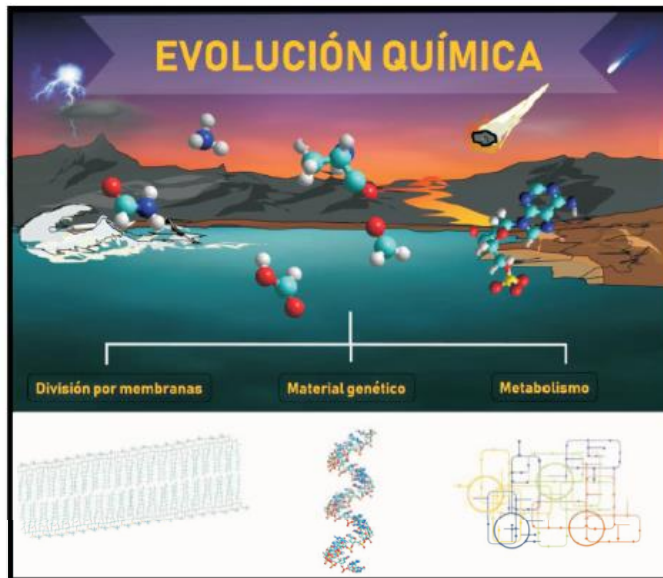


Figura 4. Las características básicas de la vida incluyen: (i) la separación del medio a través de membranas (compartimentación), generalmente compuestas por lípidos o sus derivados; (ii) la capacidad de almacenar información, en este caso del material genético en moléculas especiales, los ácidos nucleicos como el DNA y el RNA (éstos se encuentran formados por bases nitrogenadas y azúcares) y el metabolismo, es decir, la capacidad que tienen las células para aprovechar los compuestos orgánicos, transformarlos y de este modo crecer, reproducirse y responder a estímulos. Los sistemas hidrotermales cuentan con las condiciones necesarias, compuestos orgánicos y energía, para que se formen muchas de las moléculas orgánicas relevantes para la vida. Entre las moléculas que se han logrado formar, se encuentran los aminoácidos (que al unirse forman proteínas) y los ácidos carboxílicos (parte fundamental del metabolismo celular).

síntesis de las piezas necesarias para la vida. El primer paso en los estudios de química prebiótica es sintetizar las moléculas básicas que forman a los seres vivos actuales, es decir, aminoácidos, bases nitrogenadas, azúcares y lípidos. Estas moléculas, posteriormente, al polimerizarse formarán macromoléculas tales como proteínas, ácidos nucleicos^b o polisacáridos^c. Tanto las moléculas sencillas como sus polímeros, realizan funciones muy complejas en las células de los organismos actuales (Figura 4).

Por ello, es necesario continuar el estudio de los ambientes hidrotermales, pero considerándolos como sistemas complejos llenos de variables: este es un reto para la química prebiótica. Sin embargo, la inclusión de las variables geoquímicas permitirá entender con mayor precisión cómo ocurrió la evolución química en nuestro planeta.

^b Ácidos nucleicos: moléculas que constituyen el material genético de los organismos vivos.

^c Polisacáridos: cadenas de moléculas compuestas por hidrógeno y carbono, las cuales cumplen funciones energéticas y estructurales.

Ilustraciones originales de Saúl Villafaña Barajas.

Capítulo II

Definición de un escenario geoquímico plausible

“Finding these rocks is like having a jewel dropped in my lap” Ross Stevenson

¿Cuáles fueron las condiciones geoquímicas en la Tierra primitiva durante la evolución química?

Pese a la falta de registro geológico, debido al continuo reciclamiento de la corteza por acción de la tectónica de placas y los distintos procesos de erosión, meteorización y/o impactos meteóricos (Ogg *et al.* 2016), existe información valiosa acerca de la mineralogía y petrología de la Tierra primitiva.

Océano-Atmósfera

Se ha sugerido que la atmósfera del Hadeano-Arqueano temprano estuvo compuesta predominantemente por CO₂, N₂, SO₂ and H₂O (con trazas de CH₄, CO, H₂, H₂S, NH₃) y fue producto de la actividad volcánica, la actividad hidrotermal, la contribución de cometas y meteoritas así como de la fotólisis de diversas especies químicas por radiación ultravioleta (Kasting 2014). Por otro lado, el estudio de zircones detríticos sugiere que la Tierra contaba con una hidrósfera estable y estaba enriquecida en iones disueltos (*e.g.*, Cl⁻, Ca²⁺, Mg²⁺, SO₄²⁻ >> K⁺, Na⁺) (Lahav y Chang 1982; De Ronde *et al.* 1997; Knauth 1998; Pinti 2005; Zaia 2012). Adicionalmente, los fluidos hidrotermales pudieron contribuir de manera importante en la composición global del océano (ver Capítulo VII). Por otro lado, algunos estudios sugieren que la temperatura global de los océanos no superó los 100 °C (Marin-Carbonne *et al.* 2014; Tartèse *et al.* 2017) y aún después de eventos como el gran bombardeo tardío, algunas regiones, *Goldilocks*, pudieron permanecer estables (Sleep 2010). Con base en lo anterior, algunos modelos proponen que, tan pronto se formó el primer sistema océano/atmósfera y la parte más superficial del océano de magma, su dinámica fue gobernada por el ciclo del CO₂ (Sleep y Zahnle 2001; Sleep *et al.* 2001)

Una atmósfera gobernada por CO₂ pudo haber tenido grandes repercusiones en la historia de la Tierra. Bajo estas condiciones, el CO₂ presente en los océanos reaccionó con la corteza resultando en la formación de carbonatos. Del mismo modo, la paulatina formación y meteorización de magmas graníticos hidratados formó sedimentos ricos en arcillas y otros minerales (ver Anexo). De esta manera, se estableció un equilibrio entre la continua formación de carbonatos en la corteza oceánica, el intemperismo de la superficie y la eventual subducción (Sleep 2010; Arndt y Nisbet 2012). Algunos modelos sugieren que el secuestro de CO₂ pudo haber llevado a una “era de hielo” parcial o total, que duró millones de años y pudo dejar océanos relativamente fríos (Nisbet y Sleep 2001). Tal fenómeno pudo estar reforzado por la baja luminosidad del Sol (Valley 2005).

Corteza

Es comúnmente aceptado que la primera corteza (> 4.2 Ga) se formó a partir de rocas que derivaron de magmas con composición máfica (*e.g.*, basalto, gabro) y ultramáfica (*e.g.*, komatiita, peridotita). Eventualmente, la continua interacción atmósfera-océano-corteza en los primeros Ma de la Tierra llevó a la formación de una corteza continental formada por la fusión de rocas de corteza máfica/ultramáfica hidratadas (Kemp *et al.* 2010; Boehnke *et al.* 2018). Así mismo, dejó un incremento de depósitos de carbonatos, evaporíticos, arcillas, esquistos, hidrotermales y sedimentos ricos en hierro (Papineau 2010).

Existen al menos cinco muestras asociadas a restos de la corteza continental más antigua, con edades entre 4.031 – 3.825 Ga (ver Anexo III). No obstante, algunas muestras de zircones, con edades > 4 Ga y provenientes de distintas regiones, han cambiado nuestra concepción sobre las condiciones físicoquímicas en la Tierra primitiva y la evolución del planeta durante los primeros 500 Ma (Cavosie *et al.* 2007; Harrison 2009). En general, la evidencia sugiere: 1) la posible presencia de agua líquida en la superficie; 2) la existencia de una proto-corteza continental compuesta predominantemente por rocas graníticas tipo tonalita-trondhjemitita-granodiorita (TTG); 3) la presencia de procesos de erosión fluvial; y 4) procesos de reciclamiento de corteza continental durante eventos de subducción (Harrison 2009; Sleep 2010; Arndt y Nisbet 2012; Trail *et al.* 2013; Harrison *et al.* 2017).

Tectónica de placas y sistemas hidrotermales

El registro geológico (Condie y Kröner 2008), los sistemas isotópicos en rocas máficas y ultramáficas (*i.e.*, Nb-Th, Sm-Nd) (Shirey *et al.* 2008), las aproximaciones teóricas (Stern 2007), los estudios basados en registro orogénico (Pease *et al.* 2008) y los modelos de composición cortical (*i.e.*, anortosítica) (Santosh *et al.* 2017) sugieren que los procesos de subducción ya estaban presentes durante el Hadeano. Notablemente, la amplia presencia de zircones entre 4.4 – 4 Ga, sugiere varias fases de reciclado de la corteza continental en este período (Cavosie *et al.* 2007; Korenaga 2013). Sin embargo, otras líneas de evidencia sugieren que, si la subducción estuvo presente fue a finales del Hadeano y más bien episódica y puntual (Van Hunen y Moyen 2012). Por tanto, se ha propuesto que la primera corteza estuvo más bien estancada con subducciones episódicas (O’Neill y Debaille 2014) y/o con pulsos de actividad magmática durante 4.5-2.4 Ga. (Griffin *et al.* 2014; Van Kranendonk *et al.* 2015).

El dinamismo de los primeros 500 millones de la historia de la Tierra favoreció una intensa actividad hidrotermal evidenciándose en una gran cantidad de sistemas hidrotermales (submarino y subaéreos) durante el Hadeano-Arqueano (Kelley 2005; Sleep 2010; Golding *et al.* 2011; Arndt y Nisbet 2012). Esta actividad pudo tener grandes repercusiones en la formación de moléculas orgánicas así como el desarrollo de estructuras químicas complejas. De esta manera, es necesario tomar en consideración estos ambientes ya que pudieron ser cruciales en el establecimiento de nichos de evolución química durante la Tierra primitiva (Sleep *et al.* 2004; Schulte *et al.* 2006; Novoselov y Silantyev 2010; Schrenk *et al.* 2013; Wang *et al.* 2014; Shibuya *et al.* 2015) (Fig. 2.1.) En la siguiente sección se detalla la metodología general utilizada para desarrollar el trabajo experimental desde el punto de vista de la química prebiótica.

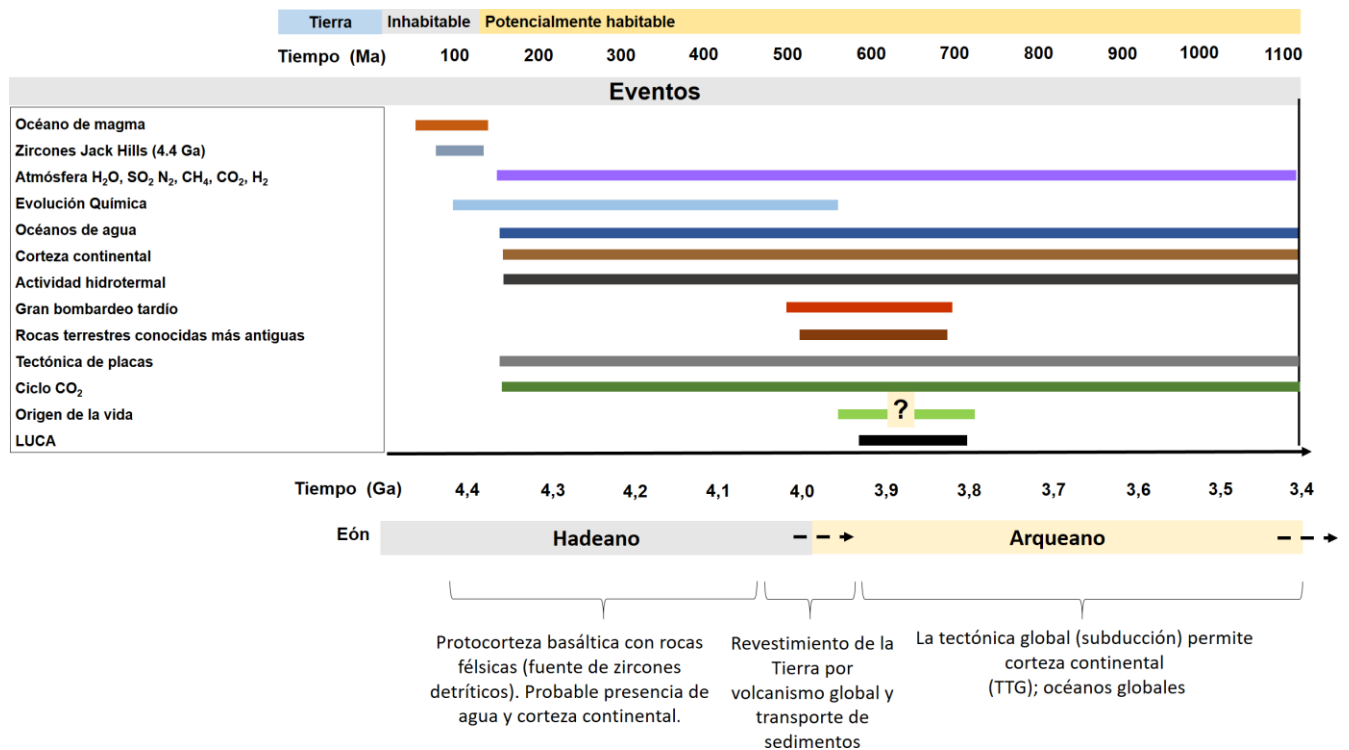


Figura 2.1. Posibles eventos geoquímicos que tuvieron lugar durante el Hadeano y el Arqueano temprano.

Referencias

- Arndt NT, Nisbet EG (2012) Processes on the young Earth and the habitats of early life. *Annual Review of Earth and Planetary Sciences* 40:521–549
- Boehnke P, Bell EA, Stephan T, et al (2018) Potassic, high-silica Hadean crust. *Proc Natl Acad Sci USA* 115:6353–6356. <https://doi.org/10.1073/pnas.1720880115>
- Cavosie AJ, Valley JW, Wilde SA (2007) .5 The Oldest Terrestrial Mineral Record: A Review of 4400 to 4000 Ma Detrital Zircones from Jack Hills, Western Australia. *Developments in Precambrian Geology* 15:91–111
- Condie KC, Kröner A (2008) When did plate tectonics begin? Evidence from the geologic record. In: *When did plate tectonics begin on planet Earth*. Geological Society of America Special Papers, pp 281–294
- De Ronde CEJ, Channer DM deR., Faure K, et al (1997) Fluid chemistry of Archean seafloor hydrothermal vents: Implications for the composition of circa 3.2 Ga seawater. *Geochimica et Cosmochimica Acta* 61:4025–4042. [https://doi.org/10.1016/S0016-7037\(97\)00205-6](https://doi.org/10.1016/S0016-7037(97)00205-6)

- Golding SD, Duck LJ, Young E, et al (2011) Earliest Seafloor Hydrothermal Systems on Earth: Comparison with Modern Analogues. In: Golding SD, Glikson M (eds) Earliest Life on Earth: Habitats, Environments and Methods of Detection. Springer Netherlands, Dordrecht, pp 15–49
- Griffin WL, Belousova EA, O'Neill C, et al (2014) The world turns over: Hadean–Archean crust–mantle evolution. *Lithos* 189:2–15
- Harrison TM (2009) The Hadean crust: evidence from > 4 Ga zircons. *Annual Review of Earth and Planetary Sciences* 37:479–505
- Harrison TM, Bell EA, Boehnke P (2017) Hadean Zircon Petrochronology. *Reviews in Mineralogy and Geochemistry* 83:329–363. <https://doi.org/10.2138/rmg.2017.83.11>
- Kasting JF (2014) Atmospheric composition of Hadean–early Archean Earth: the importance of CO₂. *Geological Society of America Special Papers* 504:19–28
- Kelley DS (2005) A Serpentinite-Hosted Ecosystem: The Lost City Hydrothermal Field. *Science* 307:1428–1434. <https://doi.org/10.1126/science.1102556>
- Kemp AIS, Wilde SA, Hawkesworth CJ, et al (2010) Hadean crustal evolution revisited: New constraints from Pb–Hf isotope systematics of the Jack Hills zircons. *Earth and Planetary Science Letters* 296:45–56. <https://doi.org/10.1016/j.epsl.2010.04.043>
- Knauth LP (1998) Salinity history of the Earth's early ocean. *Nature* 395:554–555
- Korenaga J (2013) Initiation and Evolution of Plate Tectonics on Earth: Theories and Observations. *Annu Rev Earth Planet Sci* 41:117–151. <https://doi.org/10.1146/annurev-earth-050212-124208>
- Lahav N, Chang S (1982) The possible role of soluble salts in chemical evolution. *Journal of molecular evolution* 19:36–46
- Marin-Carbonne J, Robert F, Chaussidon M (2014) The silicon and oxygen isotope compositions of Precambrian cherts: A record of oceanic paleo-temperatures? *Precambrian Research* 247:223–234
- Nisbet EG, Sleep NH (2001) The habitat and nature of early life. *Nature* 409:1083–1091
- Novoselov AA, Silantyev SA (2010) Hydrothermal systems of the hadean ocean and their influence on the matter balance in the crust-hydrosphere-atmosphere system of the early earth. *Geochemistry International* 48:643–654
- Ogg JG, Ogg G, Gradstein FM (2016) A concise geologic time scale: 2016. Elsevier
- O'Neill C, Debaille V (2014) The evolution of Hadean–Eoarchean geodynamics. *Earth and Planetary Science Letters* 406:49–58
- Papineau D (2010) Mineral Environments on the Earliest Earth. *Elements* 6:25–30. <https://doi.org/10.2113/gselements.6.1.25>
- Pease V, Percival J, Smithies H, et al (2008) When did plate tectonics begin? Evidence from the orogenic record. *When did plate tectonics begin on planet Earth* 440:199–228
- Pinti DL (2005) The origin and evolution of the oceans. In: *Lectures in astrobiology*. Springer, pp 83–112

- Santosh M, Arai T, Maruyama S (2017) Hadean Earth and primordial continents: the cradle of prebiotic life. *Geoscience Frontiers* 8:309–327
- Schrenk MO, Brazelton WJ, Lang SQ (2013) Serpentinization, carbon, and deep life. *Reviews in Mineralogy and Geochemistry* 75:575–606
- Schulte M, Blake D, Hoehler T, McCollom T (2006) Serpentinization and Its Implications for Life on the Early Earth and Mars. *Astrobiology* 6:364–376. <https://doi.org/10.1089/ast.2006.6.364>
- Shibuya T, Yoshizaki M, Sato M, et al (2015) Hydrogen-rich hydrothermal environments in the Hadean ocean inferred from serpentinization of komatiites at 300 C and 500 bar. *Progress in Earth and Planetary Science* 2:46
- Shirey SB, Kamber BS, Whitehouse MJ, et al (2008) A review of the isotopic and trace element evidence for mantle and crustal processes in the Hadean and Archean: Implications for the onset of plate tectonic subduction. When did plate tectonics begin on planet Earth? 440:1
- Sleep NH (2010) The hadean-archaeon environment. *Cold spring harbor perspectives in biology* 2:a002527
- Sleep NH, Meibom A, Fridriksson T, et al (2004) H₂-rich fluids from serpentinization: geochemical and biotic implications. *Proceedings of the National Academy of Sciences* 101:12818–12823
- Sleep NH, Zahnle K (2001) Carbon dioxide cycling and implications for climate on ancient Earth. *Journal of Geophysical Research: Planets* 106:1373–1399
- Sleep NH, Zahnle K, Neuhoff PS (2001) Initiation of clement surface conditions on the earliest Earth. *Proceedings of the National Academy of Sciences* 98:3666–3672
- Stern RJ (2007) When and how did plate tectonics begin? Theoretical and empirical considerations. *Chinese Science Bulletin* 52:578–591
- Tartèse R, Chaussidon M, Gurenko A, et al (2017) Warm Archean oceans reconstructed from oxygen isotope composition of early-life remnants. *Geochem Persp Let* 55–65. <https://doi.org/10.7185/geochemlet.1706>
- Trail D, Watson EB, Tailby ND (2013) Insights into the Hadean Earth from experimental studies of zircon. *Journal of the geological Society of India* 81:605–636
- Valley JW (2005) A cool early Earth? *Scientific American* 293:58–65
- Van Hunen J, Moya J-F (2012) Archean subduction: fact or fiction? *Annual Review of Earth and Planetary Sciences* 40:195–219
- Van Kranendonk MJ, Kirkland CL, Cliff J (2015) Oxygen isotopes in Pilbara Craton zircons support a global increase in crustal recycling at 3.2Ga. *Lithos* 228–229:90–98. <https://doi.org/10.1016/j.lithos.2015.04.011>
- Wang X, Ouyang Z, Zhuo S, et al (2014) Serpentinization, abiogenic organic compounds, and deep life. *Science China Earth Sciences* 57:878–887

Zaia DAM (2012) Adsorption of amino acids and nucleic acid bases onto minerals: a few suggestions for prebiotic chemistry experiments. *International Journal of Astrobiology* 11:229–234. <https://doi.org/10.1017/S1473550412000195>

Artículos complementarios a este capítulo

Colín-García, M., **Villafañe-Barajas, S.**, Camprubí, A., Ortega-Gutiérrez, F., Colás, V., & Negrón-Mendoza, A. (2018). 5.4 Prebiotic Chemistry in Hydrothermal Vent Systems. *Handbook of Astrobiology*, 297.

Villafañe-Barajas, S. A. y Colin-Garcia M. Submarine Hydrothermal Vents Systems: The relevance of dynamic systems in chemical evolution, and aftermath in prebiotic chemistry (Enviado). Ver Anexo I.

Química Prebiótica en Sistemas Hidrotermales

Artículo de revisión

Colín-García, M., **Villafañe-Barajas, S.**, Camprubí, A., Ortega-Gutiérrez, F., Colás, V., & Negrón-Mendoza, A. (2018). 5.4 Prebiotic Chemistry in Hydrothermal Vent Systems. *Handbook of Astrobiology*, 297.

Resumen En las últimas décadas, los sistemas hidrotermales, tanto submarinos como subaéreos, han tomado relevancia como ambientes primitivos ideales para el desarrollo de complejidad molecular. El amplio espectro de variables geoquímicas presentes en estos ambientes, así como la continua interacción entre ellas, permite un sinnúmero de nichos fisicoquímicos que podrían repercutir en la formación de estructuras orgánicas complejas. En esta revisión nos enfocamos en la parte geoquímica de tales sistemas, así como en los resultados y conclusiones de los experimentos de química prebiótica que han considerado alguna de las variables fisicoquímicas disponibles en los ambientes hidrotermales.

5.4 Prebiotic Chemistry in Hydrothermal Vent Systems

*María Colín-García, Saúl Villafañe-Barajas, Antoni Camprubí,
Fernando Ortega-Gutiérrez, Vanessa Colás, and Alicia Negrón-Mendoza*

CONTENTS

5.4.1	Introduction.....	297
5.4.2	The Link Between the Origin of Life and Hydrothermal Systems	298
5.4.2.1	Prebiotic Chemistry.....	298
5.4.2.2	The Relevance of Oceans and Hydrothermal Vents for Prebiotic Chemistry.....	299
5.4.3	Geological Settings for Hydrothermal Systems.....	300
5.4.3.1	Subaqueous Hydrothermal Systems.....	304
5.4.3.1.1	Volcanogenic Massive Sulfide-Type Systems	304
5.4.3.1.2	Sedimentary-Exhalative-Type Systems.....	307
5.4.3.1.3	Shallow Subaqueous Hydrothermal Systems.....	307
5.4.3.1.4	Seafloor Serpentinization Systems.....	308
5.4.3.2	Subaerial Hydrothermal Systems	309
5.4.4	Prebiotic Experiments Related to Hydrothermal Vents.....	310
5.4.4.1	Stability of Organics at High Temperatures and Pressures	311
5.4.4.2	Temperature Gradients	311
5.4.4.3	Redox State and Dissolved Gases	318
5.4.4.4	pH Gradients	318
5.4.4.5	Experiments That Include Minerals.....	318
5.4.5	Summary of Relevant Geological and Mineralogical Aspects for Experimental Studies with Regard to Prebiotic Synthesis.....	319
5.4.6	Final Considerations	322
	Acknowledgments.....	323
	References.....	323

5.4.1 INTRODUCTION

In this chapter, the role of hydrothermal systems in prebiotic evolution is exposed. When Oparin and Haldane presented the first scientific explanation about the origin of life in the late 1920 decade, neither the Earth's structure nor its dynamics were understood. Oparin started exposing his ideas about the origin of life at a time when plate tectonics was not an existing theory, and yet, he considered a possible relationship between igneous processes and chemical evolution (Oparin 1936 in Holm 1992). Later, the first experiments performed by Miller and Urey in 1953 highlighted the role of the atmosphere and ultraviolet (UV) radiation in chemical evolution (Miller 1953). Such experiments considered some of the geological variables known at the time, which were only a promising start in comparison with the present wealth of knowledge about the Earth's dynamics and history. However, the arrival of new knowledge led to new paradigms.

Little is known about the first stages of the Earth, since geological evidence has been wiped out by erosion, modified by metamorphism, or concealed by later rocks. The oldest geological records the poorest its preservation. Step by step, geologists have contributed to solve the puzzle and new evidence is still coming to better understand those epochs. Even so, the study of the origin of life has matured based in part on the growing geological evidence. One amazing breakthrough that brought with it a completely new wealth of knowledge was the discovery of submarine hydrothermal vents in the 1980 decade. Among other side effects, such discovery promoted many attempts in order to connect these systems with the origin of life on Earth.

Hydrothermal vents are environments that could have been important for chemical evolution since they harbor a great combination of physical, chemical and geological conditions that probably conditioned prebiotic synthesis. In this chapter, the role of such systems in prebiotic chemistry will be

discussed. With this aim, we focus on (1) characterizing the link between the origin of life and hydrothermal systems, (2) the variety of geological settings that could have accounted for chemical evolution, by describing the main geological variables that could have contributed to chemical evolution, and (3) presenting a review of the types of experiments that have been performed in order to model prebiotic reactions in hydrothermal systems.

5.4.2 THE LINK BETWEEN THE ORIGIN OF LIFE AND HYDROTHERMAL SYSTEMS

The study of the origin of life is a very complex matter, provided that the emergence of life depended largely on variables and events that cannot be observed in the meantime. In fact, many of them have left little or absolutely no trace in the geological record (Cleaves 2013). Some facts await more evidence for their fully understanding; among them are (1) the nature of the atmosphere, (2) the amount and action of different types of energy, and, most importantly, the available amount of them for organic synthesis, (3) the temperature at the planet's surface, and (4) the pH of the oceans and their salinity, to name some of the most relevant unknowns (Delaye and Lazcano 2005). All these variables certainly conditioned the reaction of molecules on Earth and other bodies in the solar system; of course, they determined the emergence of life and its evolution in our planet. In fact, even if the time, place and mode in the origin of life are not fully understood (Walker 2017), life in this planet came out from the fortunate convergence of physical, chemical and geological processes.

As emphasized by Walker (2017), the research on origin of life started historically as a chemical problem. This was a natural consequence of the development of organic chemistry and biochemistry on the twentieth century that made possible the understanding of the metabolic pathways and the genetic coding of living beings (Schwille 2017). The main attributes of life are known, although life itself is not fully understood. The incomplete knowledge of the rules that underlie the biological processes has not thwarted the research nonetheless. The first experiments were thus designed to synthesize organic molecules known to be relevant for living beings: amino acids, nucleic bases, sugars, and carboxylic acids, among the most important ones.

The geologic time scale on Earth defined the Hadean Eon, as the time running from the origin of the Earth as a planet ~4.65 to 4.0 Ga (International Commission on Stratigraphy 2017), when the oldest vestiges of continental crust had been found. If the planet is as old as 4.6 Ga (Jacobsen 2003) and the oldest true fossils were dated at 3.4 Ga (Wacey et al. 2011a, 2011b), life must have appeared and evolved much earlier than the latter. The inclusion trails in sandstones of the Strelley Pool in Australia (dated at 3.4 Ga) when analyzed by nanoscale secondary ion mass spectrometry (NanoSIMS) indicate that their formation is the result of biological activity (Wacey et al. 2008). Evidence suggests that life emerged in a relatively short geological time in our planet (Bada and

Lazcano 2009). If the available geochemical evidence is analyzed, there is a gap of 1 Ga during which the chemical reactions that preceded the life must have occurred. However, there is not much information about the rhythm or rate of chemical evolution (Cleaves 2013).

Lazcano and Miller (1994) suggested that it took a few million years for life to originate from a completely inert world. The precedent hypothetical period before the origin of life has been called "*chemical evolution*." This term includes all the chemical processes that led to the formation of relevant organic compounds, those that structurally, genetically, or metabolically constitute present living beings. This is a fundamental point, provided that life is crucially organized along these three axes: structure, metabolism, and genetics (Ruiz-Mirazo et al. 2014).

5.4.2.1 PREBIOTIC CHEMISTRY

The synthesis of complex molecules must have required simpler molecules as raw material and the action of one or more energy sources to induce reactions. If those conditions were fulfilled then the synthesis of more complex organics would have been possible. An energy source could be considered as any physical or chemical process that triggered chemical prebiotic reactions (Stüeken et al. 2013). The relevance of a source was directly related to its availability, abundance, and its ability to promote reactions in specific environments on prebiotic Earth. In chemical evolution studies, to determine the best suitable location for chemical reactions to occur constitutes a major question. Different environments were subjected to diverse energy sources.

Undoubtedly, the most abundant energy source on primitive Earth by far was cosmic rays; these are charged particles (electrons, neutrons, and atomic nuclei) accelerated by astrophysical sources and that originate beyond the Earth's atmosphere, and they constituted the main source of ionizing radiation (Ferrari and Szuszkiewicz 2009). The advantage of ionizing radiation is their ability to form free radicals that quickly react to form more stable species. This energy source was effective for promoting reactions in almost every environment due to its penetrating power.

For a long time, UV radiation, emitted by the Sun, was considered the most important energy source for the early Earth. It was capable to generate photolytic reactions in the atmosphere; this kind of reactions is still important on the planet and determines the atmospheric chemistry. Another energy source is shock energy originated by the impacts of different objects, such as meteorites and comets, and it was very important during the early stages of the planet, when the planetesimals that did not accrete impacted the inner planets, including Earth (Chyba and Sagan 1992).

Radioactivity due to the decay of radionuclides was also relevant, even if it was undervalued for many years, since it was thought that its main effects were confined to the lithosphere (Miller 1993). However, it is now known that radiogenic atoms were also abundantly produced in the atmosphere, and some of them (*i.e.*, ^{40}K) might have also been present in water

bodies in which they could have promoted many chemical reactions (Draganić et al. 1991). Geothermal energy, responsible for processes such as mantle convection, plate tectonics, and hydrothermal circulation (Stüeken et al. 2013), has been traditionally underestimated as well. Geothermal energy generated by volcanoes and hydrothermal springs was capable of promoting the synthesis by pyrolysis of organic compounds; even so, besides its direct contribution as heat, this energy also can result in electrochemical energy (Stüeken et al. 2013).

Nature itself is a continuum and environments are not isolated but connected, which must also have been the case in primitive environments. Accordingly, energy sources must have acted simultaneously to promote chemical reactions. This means that some specific environment must have been under the influence of different energy sources, and that the products that were synthesized by a sole energy source could be modified later by another one.

Some environments have been considered as the most plausible for chemical synthesis on prebiotic Earth. The supply of organics and the presence of energy must be a requisite in them. The atmosphere, the water bodies, the interfaces, and the hydrothermal environments (Cleaves 2013) all meet the requisites of holding organics and energy. They also represent the main plausible scenarios in which chemical reactions could have occurred on early Earth. For instance, the composition of the atmosphere determined the nature of the chemical reactions that could have taken place in it. The atmospheric composition was very important not only for the synthesis, but it also affected the amount of radiation that reached the surface (Cnossen et al. 2007) and determined its density. Consequently, it also determined the erosion that experienced bodies (such as comets, asteroids, and dust) when entering the atmosphere (Chyba and Sagan 1992). As a result, the atmosphere composition also affected the type and flow of organic compounds that reached the surface of early Earth (Cleaves 2013). Another relevant factor was the availability of continental areas, which allowed the concentration of some organics by evaporation. In those environments, the action of solar radiation was also combined with the presence of minerals that could have acted as surface concentrators or catalyst of reactions.

However, depending on the aggregation state, the type and abundance of molecules, and the availability of energy, some places surely were more efficient in promoting synthesis than others. In chemical evolution, to determine the best suitable location for chemical reactions to occur constitutes a major question, and here relies the importance of analyzing contemporary natural environments. Just by understanding the variables present in such places, more realistic experiments can be designed in prebiotic chemistry studies. Hydrothermal vents constitute natural complex environments in which many variables interact and can be characterized in active systems. Some environmental variables in such systems would have contributed to the increase in complexity of molecules on primitive Earth, whereas others would have inhibited it (Cleaves 2013), even in association within a single hydrothermal manifestation. As explained in the next section, several

types of hydrothermal systems may meet the physicochemical requirements for hosting and promoting prebiotic reactions.

5.4.2.2 THE RELEVANCE OF OCEANS AND HYDROTHERMAL VENTS FOR PREBIOTIC CHEMISTRY

The primitive hydrosphere must have played a fundamental role in chemical evolution. In fact, the presence of liquid water on the surface for long periods of time is a necessary condition for life to emerge and evolve (Komiya et al. 2008). Some hydrothermal processes would have occurred on primitive oceans, and many organic compounds could have formed, diffused, and eventually reacted to form more complex molecules in oceans. The composition and physicochemical properties of oceans (including, but not restricted to, pH, salinity, temperature, etc.) surely inhibited some reactions and favored others.

Oceans were formed very soon (Kasting 1993a). Direct evidence, such as turbiditic sandstone beds, shales, conglomerates, silica sediments, and banded iron formations (BIFs), indicates the unequivocal presence of water at about 3.8 Ga (Nutman et al. 1984). However, there is evidence for the presence of liquid water during the Hadean time at 4.4 Ga: $\delta^{18}\text{O}$ positive anomalies in zircons can be explained by the presence of liquid water (Wilde et al. 2001; Valley et al. 2002; Cavosie et al. 2005). The formation of the oceans began shortly after the planetary accretion period ended. As stated above, isotopic evidence of liquid water and oceans on the surface of the Earth goes back to a little more than 4.4 Ga (Wilde et al. 2001), but what happened between this time and the first geologic (not isotopic) record of sediments deposited in the ~3.8 Ga ancient seas of the Isua Greenstone Belt in southwest Greenland (Mojzsis et al. 1996) is not known and probably will never be known; the oldest continental crust and hence the first possible evidence of plate tectonics processes and deep recycling of materials, which constitute the life engine of the modern Earth, goes back only to the 4.03 Ga metamorphic rocks that constitute the Acasta Gneiss of northern Canada (Bowring and Williams 1999).

Probably, one of the latest catastrophic events that contributed most to the destruction of the oldest continents was the so-called Late Heavy Bombardment (LHB), variously estimated to have occurred between 4.1 billion and 3.9 billion years based on a time scale calibrated for the Moon, where the record was not erased by subsequent geological evolution as happened on the Earth. Models associated to the effects of LHB on the environmental conditions of the epoch are divided between those that (a) consider a fortunate cosmic event that may have triggered the first emergence of life because of some massive contribution of biogenic compounds, such as methane and water, to the outer layers of the primitive Earth, as well as by the building of ideal environmental niches where chemical evolution eventually originated life (*e.g.*, Gladman et al. 2005; Cockell 2006), or (b) those that blame such event for having caused the total extinction of former living matter that possibly evolved in the preceding 500 million years elapsed between the emplacement of the

earliest oceans (4.4 Ga) and the peak of the LHB (~3.9 Ga) (Ryder 2003). Continuous bombardments must have generated a highly dense vapor atmosphere; when the temperature changed, the dispersed water (in the form of vapor) condensed to form the oceans (Kasting 1993b).

Geological evidence indicates that both plate tectonics and liquid water on the surface would have been present at 4.0 Ga (Bowring et al. 1990; Bowring and Williams 1999; Iizuka et al. 2006, 2007). There is sound evidence for plate tectonics and the presence of an open sea at 3.8 Ga (Komiya et al. 1999). One direct consequence of plate tectonics was the formation of hydrothermal systems.

Due to the lack of geological evidence, the physicochemical conditions of the primitive oceans (pH, temperature, ionic strength, etc.) are ill defined. However, some inferences can be made from the available wealth of data. The oceanic pH depended strongly, as ever, on the chemical composition of the atmosphere and the lithosphere. When examining sedimentary deposits, Holland (2003) found that the most abundant minerals in Archean oceans were calcite [CaCO₃], aragonite [CaCO₃], and dolomite [CaMg(CO₃)₂], which means that the ocean must have been saturated with salts containing high amounts of calcium and magnesium. If the atmospheric values of *p*CO₂ are considered, the pH of the Archean oceans must have been close to ≥6.5 (Holland 2003). The initial salinity of the oceans probably ranged between 1.5 and 2 times the present values, and it must have remained high during the Archean, due to the absence of continental cratons, which are deemed necessary to sequester large quantities of halite [NaCl] and/or brines (Knauth 2005).

The oceanic temperature was estimated to have ranged between 0°C and 100°C during the Archean, as evidenced by the occurrence of pillow lavas, and cross-bedding or other sedimentary structures (Knauth 2005). It is assumed that the first ocean must have been completely anoxic (just like the atmosphere) and that the oxygen content increased little by little, although in a variable way. The solubility of oxygen in water is governed by temperature and salinity, and these variables have changed drastically through time on Earth (Knauth 2005). Estimates based on the content of cerium and carbonate mineral anomalies indicate that the concentration of oxygen in seawater was very low until at least 1.9 Ga (Komiya et al. 2008). This, with low or null oxygen concentration, allowed easily oxidizable organic molecules to remain in the environment (Parker et al. 2011). In this context, in primitive Earth, it has been estimated that the concentration of many organic compounds dissolved in the ocean would have ranged between 0.003 M and 0.03 M (Miller and Orgel 1974). Despite such low concentrations, some key organic reactions might have formed nonetheless.

5.4.3 GEOLOGICAL SETTINGS FOR HYDROTHERMAL SYSTEMS

After the discovery of the first marine hydrothermal springs (Ballard and Van Andel 1977; Corliss et al. 1979) some researchers proposed those environments as possible niches

for the origin of life (Corliss et al. 1980; Corliss et al. 1981; Baross and Hoffman 1985). Corliss et al. (1981) suggested that hydrothermal systems could be “*ideal sites for abiotic synthesis*” [sic] due to the high availability of geochemical variables (*i.e.*, water, rocks, gases, thermal energy, gradients in chemical concentration, temperature, and pH). The combination of these variables would eventually lead to the formation of “protocells” and the proliferation of the “*first organism in the vicinity of hydrothermal vents*” [sic]. As soon as these ideas were published, several experiments questioned the viability of these environments as plausible niches for the origin of life, due to the high instability of organic molecules at the conditions present in hydrothermal springs, namely, high pressures and temperatures (Bernhardt et al. 1984; White 1984; Miller and Bada 1988). Subsequently, it was proposed that hydrothermal systems could have been involved in the process of chemical evolution, but they were hardly propitious places for the origin of life (Miller and Bada 1988; Bada and Lazcano 2002; Becerra et al. 2007).

Later, the discovery of a different type of hydrothermal system, the “Lost City Hydrothermal Field” (LCHF) (Kelley et al. 2001, 2002; Proskurowski et al. 2008), rekindled such discussion. The LCHF is located on an ultramafic basement with smoother physicochemical conditions than black smokers, in association with lower temperature and alkaline fluids. This discovery reinforced the idea that important geochemical processes would have been likely in ancient settings and that they probably contributed to the synthesis of organics on primitive oceans (Kelley et al. 2001, 2002; Martin et al. 2008; Proskurowski et al. 2008; Konn et al. 2015; McDermott et al. 2015).

To support the idea of hydrothermal systems as “niches for chemical evolution,” it is fundamental at first to identify the natural settings where hydrothermal systems may occur. Then, to understand the physicochemical processes that occur, it is necessary to identify the geochemical variables involved on them (Table 5.4.1) and to evaluate those that could be involved in prebiotic chemical reactions. Such steps are necessary to guide systematic experimental studies that, in turn, will determine if such environments served as places for synthesis and complication or, instead, these were the environments in which decomposition predominated. It is necessary to take into account the geochemical variables in laboratory experiments, even if that means to increase the complexity of experiments (Holm and Andersson 2005; Kawamura 2011). It is also relevant to consider that some variables must have contributed to the increase in complexity of molecules on primitive Earth whereas other variables would have limited it (Cleaves 2013). For instance, during the LHB, Earth was exposed to a constant impact of bodies that might have terminated organics. However, already synthesized organics might have lingered on for subsequent reactions “protected” by hydrothermal vents and deep sediments (Holm 1992).

Many geological settings may harbor hydrothermal activity whose likeliness to be associated with chemical evolution needs to be tested. For that matter, in this section the geological, chemical and physical characteristics of selected settings

TABLE 5.4.1
Some Geochemical Variables at Hydrothermal Springs;
All Are Relevant for Studies of Chemical Evolution and
Origin of Life

Energy Sources	Dissolved Elements	Gradients	Minerals
Geothermal energy	Cl	Temperature	Sulfides
Thermal energy and electrochemical energy	Na	Concentration	Sulfates
	Ca	Salinity	Oxides
	K	pH	Halides
Radiation	Ba	Eh	Carbonates
From radionuclides embedded on minerals or in radionuclides in water	Fe	Pressure	Phosphates
	Mn	Mineralogy	Silicates
	Cu		Native elements
	Zn		
	Pb		
	Co		
	Cd		
	Ni		
	Mg		
	Ag		
	Hg		
	As		
	Sb		

that are widely distributed in time and space are described and evaluated. First of all, though, it is necessary to comprehensively describe some key geological notions.

A hydrothermal system is an environment where hot fluids circulate below the Earth's surface and may (or not) reach the surface, as hot springs or vents. There are two main components of a hydrothermal system: a heat source and a fluid phase. In addition, fluid circulation requires faults, fractures, and permeable lithologies (*e.g.*, Pirajno 2009). The most common heat sources comprise anomalously high geothermal gradients due to a broad panoply of magmatic foci or tectonic setting that implies crustal thinning. Fluid phases in such systems are typically aqueous (hence the hydro- prefix) that comprise vapor, supercritical fluids or water with very variable salinity (brines) or volatile contents, but these can also be CO₂, H₂S, hydrocarbons, and several other species (Roedder 1990), and even molten sulfur. The sources for such fluids are very variable as well: magmatic, sedimentary-diagenetic, meteoric, oceanic, metamorphic, etc. Such sources determine the physical and chemical characteristics of such fluids, which, in turn, determine the ability of fluids to mobilize and carry ions in solution and, therefore, the mineralogy of precipitates that were formed from them in key geological environments.

Therefore, hydrothermal systems can be classified according to their tectonic setting, the characteristics of their emplacement, including rock permeability, the sources for fluids and their physical and chemical major variables (*i.e.*, anions and cations in solution, pH, Eh, temperature, pressure, density, oxygen and sulfur fugacity, etc.), and the resulting mineral associations, among other geological variables. Upon such characteristics and their natural variations,

geological environments are typified, classified, and categorized for the sake of reasonably guiding further research or exploration endeavors. Such is the essential usefulness of the emphasis in branding types of mineral deposits (for fossil instances) and their active manifestations. Our understanding of the processes that govern the formation of (fossil) mineral deposits is boosted by the understanding of their presently active analogues, and *vice versa*. It is not always possible to resort to uniformitarianism to explain any geological process, but when conceptual models are wisely used, they can provide clues to the past or the present, which would not be obtained otherwise. Such is the reason for grouping fossil and present examples of key hydrothermal environments in this chapter (see Table 5.4.2). As for the matter of prebiotic synthesis, a variety of such environments have been invoked as likely sites to harbor the plausible chemical reactions thus involved. These can be classified between submarine and subaerial hydrothermal systems, and similar systems associated with impact cratering. The latter will not be discussed here; see Chapter 5.3 in this book (Chatterjee 2018) and references therein.

Mineral parageneses are a key for the definition of physicochemical parameters that characterize the conditions for mineral precipitation, including timing. Mineralization in submarine magmatic-hydrothermal systems (volcanogenic massive sulfide [VMS]-type systems) is a product of the chemical and thermal exchange among the ocean, the lithosphere, and the magmas emplaced within it and the fluids exsolved from them. Mineralization in submarine sedimentary-exhalative (SEDEX)-type systems is a product of the chemical and thermal exchange among the ocean, the lithosphere, and sedimentary brines. Mineralization in epithermal systems is a product of the chemical and thermal exchange among magmas and magmatic fluids, the lithosphere, and meteoric water, besides other plausible minor contributors. Mineralization in submarine seafloor serpentinization systems is a product of the chemical and thermal exchange among the ocean, the lithosphere, the mantle, and the fluids derived from them all. Mineralization in shallow submarine to subaerial hydrothermal systems may be the result of chemical and thermal exchange among the ocean, the lithosphere, magmas, magmatic fluids, sedimentary brines, and meteoric water. In all these cases, hydrothermal minerals can be found in many different ways, with regard to (1) type of mineralized structure (vein, veinlet, stockwork, lens, stratum, layer, etc.), (2) geometric relationship between mineralized structures and host rocks (stratiform, stratabound, and cross-cutting), (3) time relationship between mineralized structures and host rocks (syngenetic and epigenetic), (4) types of crystal aggregates (massive, disseminated, laminated, banded, etc.), and (5) grain size (fine to coarse). Several aspects in each category may coexist in each model for mineral deposition, and most of them may be exposed on the surface during the lifetime of hydrothermal systems due to syndepositional faulting, diapirism, or slope sliding. The latter, no matter how obvious it may be, means that some mineral association on the surface does not necessarily have been deposited there. This broadens the spectrum of mineral species that could have had a role in

Table 5.4.2. Comparison between shallow hydrothermal environments (Both fossil ore deposits and present examples)

Type of deposit and metallic associations	Tectonic setting	Association with volcanism	Main types of mineralizing fluids and mechanisms of formation	Range of temperatures	Other key characteristics of fluids and geological processes	Depth	Sources for sulfur	Mineral variability in surface exposures during hydrothermal activity (*)	Age distribution	Fossil examples	Presently active examples	Further readings
Volcanogenic massive sulfide deposits (VMS); Cu(-Pb-Zn-Ag-Au)	Arc to back-arc settings (Kuroko and Besshi types), and mid-ocean ridges (Cyprus type).	Close time, space and genetic association between volcanism and hydrothermal activity.	Magmatic, fresh marine, and modified marine water (evolved within the crust). Seafloor venting.	~100° to >500 °C. Important temperature gradients occur from central to peripheral vents.	Euxinic environment; pH very acidic to alkaline; reduced to oxidized fluids; broad variations in salinity (lower than seawater up to >50 wt.% NaCl equiv.); no bubbling unless in atypical shallow locations; sources for fluids are magmatic, fresh and deeply evolved seawater. Possible associated submarine brine and molten sulfur pools.	Generally ~2 km below sea level; known shallow examples.	Magmatic, also from seawater sulfate.	Sphalerite, galena, pyrite, chalcopyrite, pyrrhotite, wurtzite, bornite, covellite, arsenopyrite, marcasite, tetrahedrite-tennantite, löllingite, acanthite, cubanite, boulangerite, proussite-pyrargyrite, stannite, cassiterite, realgar, orpiment, cinnabar, microcrystalline varieties of silica, hematite, barite, anhydrite, gypsum, Mn and Fe oxides and hydroxides, native sulfur, talc, crysothite, chlorite, illite, smectite, montmorillonite, kaolinite, nontronite, jarosite, calcite, dolomite, siderite, ankerite, kutnohorite, native sulfur, cerussite. Possible precipitation of silica gels.	Since the Archean (ca. 3.5 Ga); numerous Paleozoic examples.	Pilbara craton (Australia), Noranda, Abitibi, Windy Craggy (Canada), Troodos ophiolite (Cyprus), Hokuroku and the Green Tuff region (Japan), Semail ophiolite (Oman), Iberian Pyrite Belt (Spain, Portugal), Almadén (Spain).	Mid-ocean ridges: Lucky Strike, Lost City, East Pacific Rise at 21°N, Sonne Field.	(Franklin 1996), (Barrie and Hannington 1999), (Allen et al. 2002), (Franklin et al. 2005), (Hannington et al. 2005), (Piercey 2011)
Sedimentary-exhalative deposits (SEDEX) and subaqueous brine pools; Zn-Pb-Ba(-Cu), Fe-Mn	Advanced stages of continental rifting, failed rifts, and passive continental margins.	None, but volcanic rocks can be present in the hosting sedimentary series.	Sedimentary brines, fresh marine, and modified marine water. Seafloor venting and precipitation from seawater combined.	~50° to <300 °C. Important temperature gradients possibly occurred (stratiform deposits are frequently separated from their hydrothermal feeders).	Euxinic environment; pH very acidic to alkaline; reduced to oxidized fluids; broad variations in salinity (lower than seawater up to <50 wt.% NaCl equiv. in brine pools); no bubbling unless in atypical shallow locations; sources for fluids are sedimentary brines fresh and deeply evolved seawater. Possible associated submarine brine pools.	Between a few hundreds of m and >1000 m below sea level.	Seawater sulfate.	Pyrite, galena, sphalerite, microcrystalline varieties of silica, barite, anhydrite, gypsum, pyrrhotite, marcasite, chalcopyrite, arsenopyrite, löllingite, siderite, ankerite, kutnohorite, dolomite, magnesite, calcite, aragonite, hematite, Mn and Fe oxides and hydroxides, Cu-Fe-Ag-Pb sulfosalts, nontronite, talc, jarosite, stevensite, atacamite, caminite, anglesite, montmorillonite, chlorite, apatite, cassiterite, scheelite, celsian, native sulfur, native silver.	Since the late Paleoproterozoic (ca. 1.8 Ga); Mesoproterozoic and Paleozoic.	Broken Hill, Mount Isa, McArthur River (Australia), Sullivan (Canada), Matahambre (Cuba), Rammelsberg, Meggen (Germany), Rajpura-Dariba (India), Molango (México), Gamsberg-Aggeneys (South Africa), Red Dog, Anarraq (USA).	Atlantis II Deep (Red Sea), Salton Sea, lakes in the East Africa Rift System (?).	(Russell et al. 1981), (Goodfellow et al. 1993), (Lydon 1996), (Jorge et al. 1997), (Hannington et al. 2005), (Leach et al. 2005), (Lyons et al. 2006), (van der Zwan et al. 2015), (Schardt 2016), (Sangster 2018).
Shallow submarine or sublacustrine to subaerial exhalative deposits; Mn-Fe-Cu-Zn-Co-Ba-Hg-As-Sb-Ag-Pb	Incipient to advanced stages of continental rifting, failed rifts, and passive continental margins; also shallow manifestations in volcanic arcs (similar to VMS deposits except for their depth).	Close time, space and genetic association between volcanism and hydrothermal activity, or none at all due to high heat flux related to crustal thinning.	Fresh marine, and modified marine water to magmatic. Seafloor venting to subaerial precipitation.	≤100 °C, eventually higher in magma-derived systems.	Oxidized to euxinic environments; pH very acidic to very alkaline (normally moderately acidic to alkaline); reduced to oxidized fluids; in general, salinities lower than seawater; bubbling very common; sources for fluids highly variable upon their geological location.	<~200 m below sea (or lake) level to subaerial.	Seawater sulfate or magmatic.	Opal, calcite, aragonite, barite, celestine, Mn and Fe oxides and hydroxides, microcrystalline varieties of silica, braunite, rhodochrosite, pyrite, marcasite, cinnabar, carlinite, orpiment, realgar, zeolites, illite, smectite, montmorillonite, chlorite, talc, kaolinite, zeolites, celadonite, apatite, native sulfur, native mercury, Pb-Cu-Ag oxychlorides. Precipitation of silica gels.	Since the Mesoproterozoic.	El Boleo-Lucifer and Concepción peninsula (Mexico), Wafangzi (China), Tatra Mts. (Poland), Valle del Azogue (Spain), Kueishantao (Taiwan), sedimentary phosphorites (?).	East Africa Rift System (including alkaline lakes), Milos island (Greece), Concepción bay (Mexico), Kueishantao (Taiwan), Kraternaya Bight (Russia), Bay of Plenty (New Zealand), Lihir island (Papua-New Guinea).	(Tiercelin et al. 1993), (Fan et al. 1999), (Tarasov et al. 2005), (Canet and Prol-Ledesma 2006), (Conly et al. 2011), (Papavassiliou et al. 2017).

Table 5.4.2. (Continued) Comparison between shallow hydrothermal environments (Both fossil ore deposits and present examples)

Type of deposit and metallic associations	Tectonic setting	Association with volcanism	Main types of mineralizing fluids and mechanisms of formation	Range of temperatures	Other key characteristics of fluids and geological processes	Depth	Sources for sulfur	Mineral variability in surface exposures during hydrothermal activity (*)	Age distribution	Fossil examples	Presently active examples	Further readings
Metalliferous black shales (and closely associated phosphorites); Zn-Cu-Pb(-Mo-Au-Ni-PGE-U-V-P-Se), Cu-Co-Zn, Sb-W-Hg, etc.	Intracontinental rift-related sedimentary basins.	Unclear, may be correlated with mantle plumes; may occur without associated magmatism or associated with mafic volcanism.	Sedimentary brines, fresh marine, and modified marine water. Seafloor venting? Precipitation from seawater? (Impact-related?).	~100° to >300 °C.	Speculative or ill-defined; euxinic environment (but some authors claim otherwise); pH acidic to alkaline; reduced to oxidized fluids; sedimentary to magmatic (related to mantle plumes, according to some authors) sources for fluids.	Between a few hundreds of m and >1000 m below sea level.	Seawater sulfate.	Pyrite, vaesite, gersdorffite, jordisite, millerite, polydymite, sphalerite, chalcopyrite, galena, clausthalite, illite, smectite, montmorillonite, kaolinite, apatite and other phosphates (particularly in sedimentary phosphorites), collophane, Mn and Fe oxides and hydroxides, dolomite, calcite, fluorite, barite, anhydrite, gypsum. Precipitation of colloidal phases (e. g., Ni-Mo sulfides and carbides).	Since the middle Paleoproterozoic (ca. 2.1 Ga) or earlier, peaking during the Paleozoic, associated with worldwide anoxic events (?) after the global oceanic oxygenation.	Willyama Supergroup (Australia), Selwyn Basin (Canada), Nunitang Formation (China), Bohemian massif (Czech Rep., Germany, Poland), Outokumpu, Talvivaara (Finland), Franceville Series (Gabon).	Black Sea, Caspian Sea, Ontong Java Plateau.	(Pašava 1993), (Coffin and Edholm 1994), (Mossman et al. 2005), (Laznicka 2006), (Johnson et al. 2017).
Seafloor serpentinization; Ni-Co-Cu-Fe, PGE-Au-Ag, Cr(-Ti-V)	Mid-ocean ridges, supra-subduction zones (back-arc and fore-arc settings), and incipient stages of continental rifting.	Close time, space and genetic association between volcanism (usually the spreading centers) and hydrothermal activity.	Magmatic, fresh marine, and modified marine water (evolved within the crust and/or slab-derived fluids). Precipitation from seawater, seafloor venting and ultramafic-host-rock combined.	< 450-500°C. Important temperature gradients occur from the seafloor to the oceanic crust inward.	Euxinic environment; pH acidic to alkaline; reduced to oxidized fluids; board variations in salinity (lower than seawater up to <40 wt.% NaCl equiv.); no bubbling; sources for fluids are magmatic (related to the dehydration of subduction slab in forearc settings), fresh and deeply evolved seawater.	Generally >2000 below sea level; known shallow examples.	Seawater sulfate, also magmatic.	Olivine, pyroxene, amphibole, plagioclase, serpentinite group minerals (antigorite, chrysotile, lizardite), (Fe)-brucite, talc, chlorite, fuchsite, Mg-rich clays (smectite, sepiolite, palygorskite) zeolite, amphibole, aragonite, calcite, dolomite, magnesite, garnet, clinzoisite, prehnite, pumpellyite, lawsonite, barite, spinel, magnetite, hematite, pyrite, calcopyrite, pentlandite, Co-pentlandite, hazdewoodite, millerite, marcasite, vallecite, violarite, Fe-Ni-(Co)-alloys, bornite, covellite, Platinum Group Minerals (PGM), native gold and minor Mg-Fe-hydroxychlorides (jovaita, pyromite-sjögrenite group).	Since the Phanerozoic (ophiolites) or earlier (ca. 3.5 Ga; Archean greenstone belts).	Greenstone belts: Isua (Greenland), Barberton (South Africa), Jormaa Complex (Finland), Ophiolites: Semal (Oman), Troodos (Cyprus), Zambales (Philippines), Mineoka (Japan), Leka (Norway).	Mid-ocean ridges: Mid-Atlantic Ridge at Lost City, Kane Fracture Zone and 15°20'N Fracture Zone, Hess Deep, Iberian Abisal Plain; Forearc seamounts: Izu-Ogasawara-Mariana	(Frost 1985), (Bach et al. 2004, 2006), (Früh-Green et al. 2004), (Deschamps et al. 2013), (Frost et al. 2013).
Epithermal deposits; Au-Ag, Ag-Pb-Zn-Au	Continental and island arcs; transform boundaries (minor setting).	Close time, space and genetic association between volcanism and hydrothermal activity.	Magmatic, fresh meteoric, and modified meteoric water. Epigenetic structures and subaerial precipitation (sinters).	~50° to ~400 °C. Important temperature gradients occur from central to peripheral springs.	Oxidized environment; pH very acidic to mildly alkaline; reduced to oxidized fluids; generally low salinities; bubbling and formation of aerosols common in geothermal fields; sources for fluids are magmatic, fresh to deeply evolved meteoric water.	Between >1500 m and subaerial paleosurfaces.	Magmatic, also sedimentary or metasedimentary.	Silica and carbonate minerals in sinters (mostly opal and calcite), kaolinite, alunite, native sulfur, barite, anhydrite, gypsum, celestine, Mn and Fe oxides and hydroxides, montmorillonite, illite, smectite, chlorite, epidote, calcite, dolomite, zeolites, adularia, quartz, chalcedony, cristobalite, tridymite, pyrite, cinnabar, realgar, orpiment, stibnite, and other minor sulfides and halides. Precipitation of silica gels.	Vastly Cenozoic; Known Archean and Paleoproterozoic examples.	Campbell (Canada), Emperor (Fiji), Kelian (Indonesia), Hishikari (Japan), Fresnillo, Pachuca, Tayolitha (México), Yanacocha (Perú), Lepanto, Baguio (Philippines), Comstock Lode, Summitville, Creede (USA).	Campi Flegrei (Italy), Los Azufres, Cerro Prieto (México), Taupo Volcanic Zone, White Island (New Zealand), Yellowstone, Steamboat Springs, The Geysers (USA).	(Corbett and Leach 1998), (Sillitoe and Hedenquist 2003), (Simmons et al. 2005), (Camprubi and Albinson 2006, 2007), (Hedenquist and Taran 2013), (Sillitoe 2015).

Source : Based loosely on Misra, K. C., Understanding Mineral Deposits, Kluwer Academic Publishers, Dordrecht, the Netherlands, 845 p, 1999; Jébrak, M., and Marcoux, E., Géologie des ressources minérales,

Ministère des ressources naturelles et de la faune du Québec, Québec, Canada, 667 p, 2008; Pirajno, F., *Hydrothermal Processes and Mineral Systems*, Springer, East Perth, Australia, 1250 p, 2009.

a Besides those in host rocks. The listed minerals would belong to precipitates or alteration assemblages on the surface or near it, but also to deeper areas that could be exposed by faulting or syndepositional slope sliding.

(?) Indicates debatable locations

chemical evolution, as one must account equally for minerals that were deposited on the surface and those that were formed somewhere else and eventually made available on the surface while hydrothermal activity still is on. The last (but not least) relevant characteristics for the matter would be the mineral species itself and its particular variation in chemical composition. However, in spite of the geological complexity of each family of depositional environments, many mineral families, groups and classes are shared by most of them (Table 5.4.2), namely silica-group minerals (or silica gels), clay minerals, serpentine minerals and other phyllosilicates, sulfides (especially base-metal sulfides, including arsenides, antimonides, etc.), sulfates, oxides (especially Fe and Mn oxides and hydroxides), phosphates, halides, native elements (including alloys), and many miscellaneous silicates (zeolites, feldspars, amphiboles, scapolites, epidote-group minerals, etc.). It is important to note that these are minerals that form as hydrothermal precipitates or replacements (passive and reactive associations, respectively), but also rock-forming minerals in host rocks should be added to the list above. Among the latter, zircon can be considered as a “cosmopolitan” mineral due to its resilience.

5.4.3.1 SUBAQUEOUS HYDROTHERMAL SYSTEMS

Submarine vents in association with magmas at or near mid-ocean ridges are usually described as the likeliest hydrothermal systems to be associated with the emergence of life on Earth (*i.e.*, Corliss et al. 1981; Nisbet and Sleep 2001). A common case for the formation of submarine hydrothermal vents occurs when seawater migrates through fractures into the crust and reaches the vicinity of a magmatic intrusion. While approaching the magmas, water is heated up by the anomalously high thermal gradient induced by their emplacement. Additionally, magmas release aqueous fluids upon their cooling down. Therefore, hydrothermal fluids in magma-related systems may come from magmatic, marine or meteoric sources. Similarly, sulfur, iron, copper, zinc, and other metals may come from magmas, ocean water or host rock leachates. The dissolved minerals nourish chemosynthetic bacteria that constitute the base of the food chain for a variety of invertebrates, including large tubeworms (*e.g.*, Levin 2009).

The importance of submarine hydrothermal vents for studies related to the origin of life lies in: (1) providing hot water to surficial environments, (2) upwelling fluids interact with seawater, provide agents for chemical imbalance, thus potentially allowing the synthesis of organic compounds, (3) they produce a rapid crystallization of carbonates and silicates at low temperatures; this increases the local potential to preserve microbial organisms as fossils and their chemical signatures, despite later diagenetic or low-grade metamorphic processes (Pope et al. 2006), and (4) even debatable, some authors suggest that the oldest forms of terrestrial life might have been autotrophic-thermophiles (Pope et al. 2006).

Submarine or sublacustrine hydrothermal systems can be divided into those linked to magmatism as both source for heat, water, and other chemical components, and those associated

with venting of basinal brines or other fluids. Such environments correspond, respectively, to volcanogenic massive sulfide (or VMS; Figure 5.4.1) and sedimentary-exhalative (or SEDEX; Figure 5.4.2) deposits and their present-day analogues, which are well-established types of ore deposits and depositional environments, both submarine. Another case, similar to the latter, is constituted by hydrothermal systems that are associated with early stages of continental rifting or lingering activity in more tectonically evolved environments (*e.g.*, along the eastern side of the Baja California peninsula; Canet and Prol-Ledesma 2006; Camprubí et al. 2008). Such systems may occur between shallow submarine and subaerial manifestations, including intertidal venting (Figure 5.4.3). Seafloor serpentinization and paleo-hydrothermal submarine systems associated with metalliferous deposits in black shales are also likely to be accounted among keen environments for prebiotic synthesis. Most theoretical and experimental approaches to prebiotic reactions have been carried out considering VMS-like hydrothermal systems, while neglecting the others. The following account does not intend to be exhaustive, but demonstrative of the variability of hydrothermal scenarios that might have had a role in chemical evolution. Some authors even proposed that BIFs could be related to hydrothermal activity (*e.g.*, Ohmoto et al. 2006), which could be at least the case of Algoma-type deposits (Jébrak and Marcoux 2008).

5.4.3.1.1 Volcanogenic Massive Sulfide-Type Systems

The so-called “black smokers” are the most conspicuous submarine hydrothermal manifestations in VMS-type systems (Figure 5.4.1) and are also interpreted to occur in SEDEX-type systems (Figure 5.4.2; see Larter et al. 1981; Boyce et al. 1983; Russell et al. 1989). These are hydrothermal fumaroles with abundant sulfides and sulfates in suspension that upon precipitation form mounds along favorable faults or within submarine calderas. In VMS systems associated with divergent margins, these are usually located close to mid-ocean ridges. In these fumaroles, due to their proximity to magmas, water may attain temperatures above 400°C and low pH (see Table 5.4.2; also, Von Damm et al. 1985; Camprubí et al. 2017). The latter facilitates the leaching of iron and other metals as the water seeps through the country rocks, which is a feature shared with the other systems hereby described. Such fluids come in contact with cold seawater, thus generating a rapid nucleation of sulfides and other minerals and resulting in a turbid suspension resembling a cloud of black smoke. Salinities of sulfide-rich ore-forming fluids are generally up to 20 wt.% NaCl equiv. although extremely high-salinity polysaline brines may eventually reach the sea bottom as well (up to 65 wt.% NaCl and ~44 wt.% KCl, at >500°C; Camprubí et al. 2017). That being the case, it is likely that brine pools can be associated with VMS-type systems. Another type of hydrothermal vents is dubbed “white smokers,” which are generally more distant from their heat source than the black ones (Figure 5.4.1). Black and white smokers may coexist in the same submarine hydrothermal field, but they generally represent proximal and distal vents, respectively, to the main

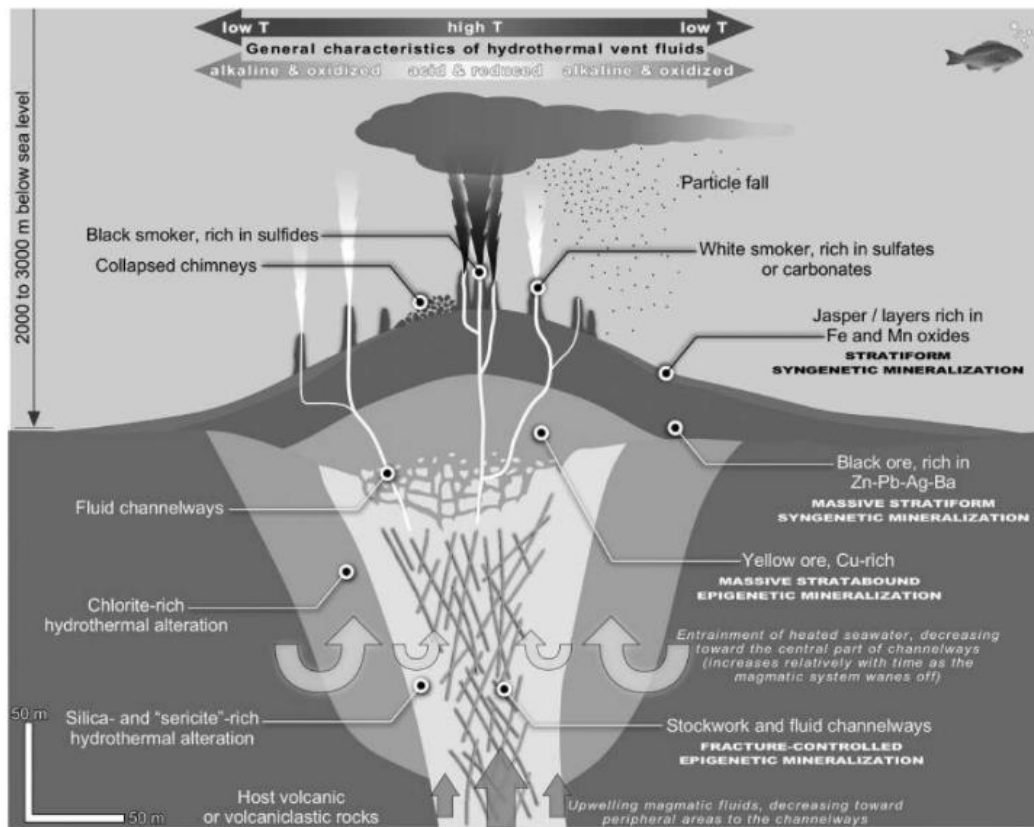


FIGURE 5.4.1 Structural section that combines evidence from active submarine magmatic-hydrothermal vents and from fossil volcanogenic massive sulfide (VMS) deposits, especially in Kuroko-type settings, including all typical styles of mineralization and hydrothermal assemblages. “Sericite,” not a valid mineral species name, stands for fillosilicates that range between illite and fine-grained muscovite. Key: T = temperature. (Adapted from Colín-García, M. et al., *Bol. Soc. Geol. Mex.*, 68, 599–620, 2016, and based on Lydon, J. W., *Volcanogenic massive sulphide deposits, Part 2: Genetic models*, in *Ore Deposit Models*, R. G. Roberts and P. A. Sheahan (Eds.), pp. 155–181, Geological Association of Canada, Geoscience Canada, Reprint Series, 3, St. John’s, Canada, 1988, and Hannington, M. D. et al., *Sea-floor tectonics and submarine hydrothermal systems*, in *Economic Geology One Hundredth Anniversary*, Vol. 1905–2005, J. W. Hedenquist, J. F. H. Thompson, and R. J. Goldfarb (Eds.), pp. 111–142, Society of Economic Geologist, 2005.)

upflow zone (Figure 5.4.1). However, white smokers correspond mostly to waning stages of such hydrothermal fields, as magmatic heat sources become progressively more distant from the source (due to magma crystallization) and hydrothermal fluids become dominated by seawater instead of magmatic water (see references in Table 5.4.2 for VMS systems). The temperature in white smokers can be as low as 40°C to 75°C and are alkaline (pH ranges between 9 and 9.8; Kelley et al. 2001). Mineralizing fluids from this type of vents are rich in calcium, and they form dominantly sulfate-rich (*i.e.*, barite and anhydrite) and carbonate deposits. These may form giant chimneys, the largest of which stand almost 60 m above the bottom of the ocean at the LCHF (Kelley et al. 2001). Hydrothermal fluids in this location contain methane, ethane, and propane and organic acids in the form of formate and acetate; these are produced in association with this hydrothermal system (Proskurowski et al. 2008). The global frequency distribution of depths for the occurrence of actualistic examples of VMS deposits (magmatic-hydrothermal seafloor

vents, either black or white smokers) shows a dominant range between 2000 and 3000 m (Figure 3 in Colín-García et al. 2016; Figures 2 and 3 in Hannington et al. 2005), which is consistent with calculated depths of fossil examples (see Table 5.4.2 and references therein). In spite of this, much shallower examples are known both in present-day manifestations as well as in fossil VMS deposits (*e.g.*, Camprubí et al. 2017).

Different mineral associations precipitate during the typical stages of mineralization that characterize the life span of VMS-type systems (Figure 5.4.1). Comprehensive reviews of this subject have been published (*e.g.*, Franklin et al. 1981, 2005; Lydon 1988; Ohmoto 1996; Barrie and Hannington 1999; Hannington et al. 2005). Minerals present in a hydrothermal system or a fossil VMS deposit are deposited passively or reactively. Mineral associations may vary (1) in different mineralized structures, either syngenetic (namely, passive precipitation in chimneys, mounds, and stratiform deposits) or epigenetic (structures that correspond to feeder channels, and replacements of host rocks or pre-existing

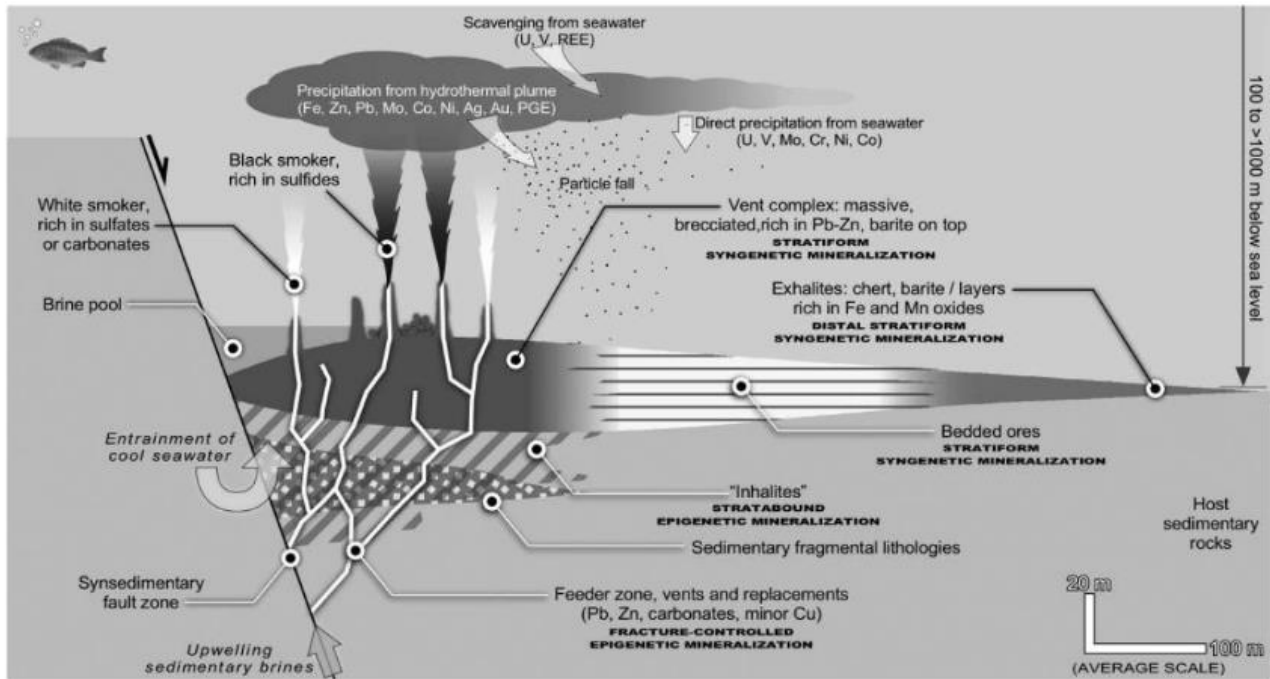


FIGURE 5.4.2 Structural section that combines evidence from active submarine non-magmatic hydrothermal vents, from fossil sedimentary-exhalative (SEDEX) deposits and from an analogy with VMS deposits (see Figure 5.4.1), including all typical styles of mineralization and hydrothermal assemblages. It is important to note that this model corresponds to proximal-to-vent deposits in the model of (Lydon 1996), because feeder zones in most SEDEX deposits, which are commonly more distal to vents than this model exemplifies, have not been found.

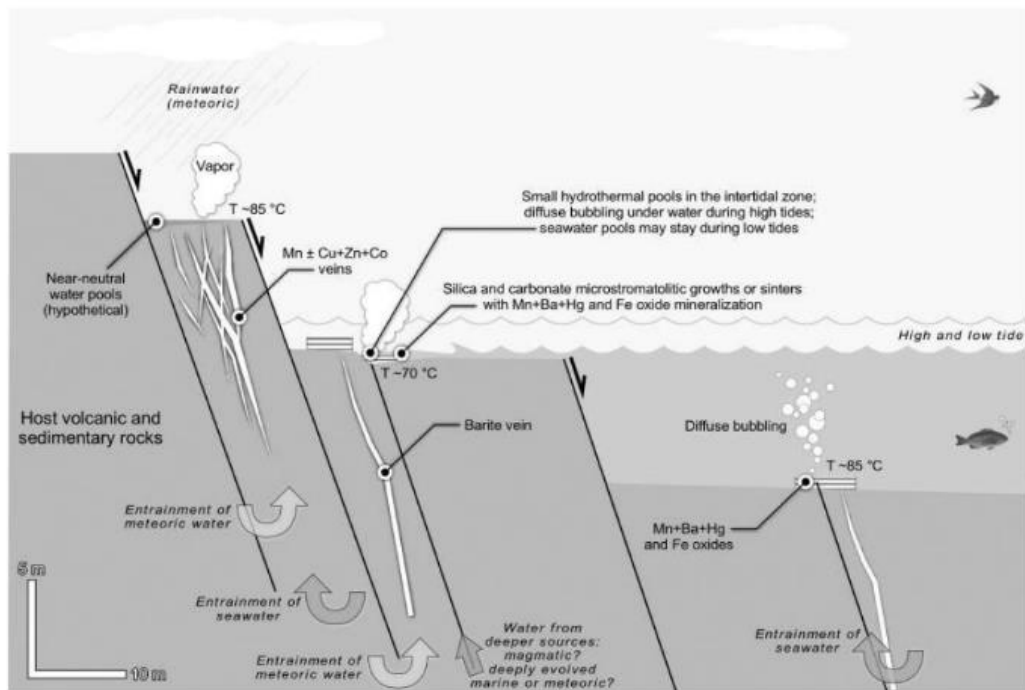


FIGURE 5.4.3 Structural section that combines evidence from active submarine non-magmatic (?) hydrothermal vents and from fossil Mn ± Cu + Zn + Co deposits that formed during early stages of continental rifting, as based in the models for evidence in the eastern Baja California Peninsula in Mexico. The intertidal and submarine hydrothermal manifestations illustrated here would be those around the Concepción Bay area and the ore deposits would be El Boleo, Lucifer, and those in the Concepción peninsula. (Model adapted from Canet, C., and Prol-Ledesma, R. M., *Bol. Soc. Geol. Mex.*, 58, 83–102, 2006; Camprubí, A. et al., *Island Arc*, 17, 6–25, 2008; and references therein.) The (?) here indicates a dubious origin or debatable origin for these vents.

massive sulfide bodies), or *structural zonation*, (2) from proximal to distal associations with respect to venting areas within the same stratigraphic horizon, or *horizontal zonation*, (3) from deep to shallow associations (*i.e.*, stockworks to mounds), or *vertical zonation*, (4) from early and climactic to late stages of mineralization (dominated by sulfides, and sulfates or oxides, respectively), or *temporal zonation*, and (5) in various volcano sedimentary contexts, depending essentially on the composition of volcanic rocks and, ultimately, on the tectonomagmatic context. The most common minerals in ore-bearing associations of VMS deposits (non-metamorphosed or oxidized) and their modern analogues are summarized in Table 5.4.2. The most common hydrothermal alteration assemblages are chloritic (including Mg-rich ones) and phyllic (dominated by “sericite,” mostly illite), and also silicification, deep and shallow talcose alteration, and ferruginous (including Fe oxides, carbonates, and sulfides) alteration. Although not necessarily associated with these systems, molten sulfur lakes may occur in association with submarine volcanism (de Ronde et al. 2015). The precipitation of silica and iron oxide gels in VMS-type systems is also possible (Grenne and Slack 2003).

5.4.3.1.2 Sedimentary-Exhalative-Type Systems

Sedimentary-exhalative systems and those associated with metalliferous black shales provide all geological and physicochemical characteristics that would have favored prebiotic reactions as effectively as VMS systems, such as temperature gradients, euxinic environments, and a wide range of depths of formation (see Table 5.4.2). Sedimentary-exhalative-type systems also provide strong mineralogical and geochemical gradients, and similar pH and Eh gradients to those in VMS-type systems. In addition, the occurrence of submarine brine pools in association with these environments (Figure 5.4.2), such as those interpreted for ore deposits (Boyce et al. 1983) and present-day examples found in the Red Sea (*e.g.*, Schardt 2016), provides strong salinity (and geochemical) contrasts among them, seawater, and more dilute vent fluids.

The problem in the involvement of SEDEX systems with prebiotic reactions resides in the age of the oldest examples of such systems, as no known deposits are older than late Paleoproterozoic (*ca.* 1.8 Ga; Lydon 1996). Metalliferous black shales can be significantly older (middle Paleoproterozoic, *ca.* 2.1 Ga or older; Mossman et al. 2005) than SEDEX or shallow submarine/sublacustrine deposits (see Section 5.4.3.1.3). However, neither type has yet been found to be old enough as to be coeval with prebiotic processes or, least of all, be involved with them. In contrast, Archean VMS deposits are numerous (*ca.* 3.5 Ga; Barrie and Hannington 1999). The striking lack of Archean SEDEX deposits can be associated with the *limiting effect of high reduced iron contents on the activity of reduced sulfur in anoxic oceans (sic, Goodfellow 1992)* in which *metals in hydrothermal fluids [...] were dispersed because a lack of reduced sulfur to precipitate them (sic, Misra 1999)*. Therefore, it is likely that SEDEX-type hydrothermal systems did effectively exist during the Archean, despite being unable to generate

sulfide deposits because reduced sulfur in the oceans would have been previously “sequestered” by iron to precipitate iron sulfides directly from seawater. After the oxygenation of Earth’s oceans SEDEX deposits formed, during worldwide anoxic events of the Paleozoic, as might also be the case for Proterozoic deposits (Misra 1999).

Sedimentary-exhalative-type systems (Figure 5.4.2) span different mineralogical styles that are similar to those in VMS-type systems, although their mineral associations are typically more diverse than in the latter. Comprehensive reviews of this subject are published (*e.g.*, Russell et al. 1981; Goodfellow et al. 1993; Hannington et al. 2005; Leach et al. 2005; Lyons et al. 2006; Sangster 2018). Massive and layered sulfide deposits, and exhalites are similar to syngenetic stratiform associations in VMS deposits, whereas “inhalites” are similar to epigenetic stratabound associations in VMS deposits. Exhalites can be constituted by silica-rich, nontronite, montmorillonite, chlorite, carbonate, phosphate, and Fe-Mn oxide-hydroxide layers, and all deposits normally show strong mineralogical banding. Although the SEDEX term is usually reserved to Pb-Zn deposits, their mineralogical diversity allows to classify them into barite, Sb-W-Hg in black shales, Fe-Mn, Sn, and base-metal deposits (Jorge et al. 1997). The latter are subdivided into (type I) deposits with metallic sulfides alone, (type II) deposits with metallic sulfides and exhalites (chert + barite), and (type III) deposits with metallic sulfides, Fe-Mn oxide-hydroxide layers, and exhalites (Sangster and Hillary 1998). Unlike VMS-type systems, feeder zones are rarely found (supra-vent systems; Figure 5.4.2). The most common minerals in ore-bearing associations of SEDEX deposits (non-metamorphosed or oxidized) and their modern analogues are summarized in Table 5.4.2. A particular feature found in association with active SEDEX-type systems is the occurrence of submarine brine pools (*e.g.*, Schardt 2016). Owing to the relatively shallow character that these systems may have, gasohydrothermal activity (bubbling) can be common.

5.4.3.1.3 Shallow Subaqueous Hydrothermal Systems

Hydrothermal systems that are associated with early stages of continental rifting (and later stages as well) share some similarities with SEDEX systems, starting with their specific tectonic setting (early to late stages of continental rifting, respectively). The former, however, stretches between shallow submarine (up to ~200 m deep; neritic zone) or sublacustrine to subaerial hydrothermal to gasohydrothermal systems, including intertidal environments, at temperatures <100°C. The associated aqueous fluids have generally weaker gradients in pH and Eh than in VMS- and SEDEX-type environments, although the genetic variability of these systems, between magmatic-derived and sedimentary-marine-meteoritic, implies a large chemical variation within this group of environments. Also, intertidal environments provide an interesting gradient, which is implied by low- and high-tide cycles, with thermochemical gradients between upwelling fluids and seawater that can be pooled during low tides (Figure 5.4.3). In addition, the occurrence of gasohydrothermal fluids in this environment

induces generalized diffuse bubbling (*e.g.*, Tarasov et al. 1990; Vázquez-Figueroa et al. 2009; Canet et al. 2010). Diffuse bubbling is normally absent in VMS- and SEDEX-type environments due to high pressures from the water column above them, unless these are atypically shallow. Such gases are rich in CO₂ in most cases, in N₂ and CH₄ in systems that interacted with sedimentary rocks, and in H₂S in association with fumarolic activity (Canet and Prol-Ledesma 2006, and references therein). Little is known about the oldest possible ages of the fossil deposits generated in this environment because of their scarcity in the geological record, but the oldest known example is the Mesoproterozoic Wafangzi Deposit in China (Fan et al. 1999). However, with regard to the most likely geodynamic setting for these systems, which encompasses incipient to advanced stages of continental rifting, the crustal dynamics in the Archean could have furnished plenty of such systems.

Shallow submarine/sublacustrine to subaerial hydrothermal systems are as mineralogically diverse as their possible geological settings. Some of them could be ascribed to VMS- or SEDEX-type environments and their characteristic tectonic settings (see Table 5.4.2 and Canet and Prol-Ledesma 2006). However, a tectonic setting that is seemingly the most characteristic for these systems, which is represented by incipient stages of continental rifting and into advanced stages but confined to the resulting passive margins (Figure 5.4.3). Sedimentary phosphorites may perhaps be the largest deposits in association with such environments (*e.g.*, those formed during the breakup of Pangea in NE Mexico and during the Miocene rifting-off of the Baja California peninsula; see Camprubí [2013]), and a possible hydrothermal origin has been postulated for them (*e.g.*, Slack et al. 2015; Caird et al. 2017), although it is not a necessary condition (Jébrak and Marcoux 2008). Such phosphorites are constituted by amorphous to cryptocrystalline apatite-group phases, generally carbonate-fluorapatite or francolite and rarely hydroxylapatite (Jébrak and Marcoux 2008). Note that phosphorites can be associated with SEDEX deposits and metalliferous black shales as well. However, the most common minerals in shallow settings are silica-group minerals and microcrystalline varieties, carbonates, barite, Fe-Mn oxides and hydroxides and pyrite. Silica minerals and carbonates are most characteristic forming sinters, microstromatolitic growths and veins. Intertidal environments are characteristic to this group of environments (Figure 5.4.3), which means high and low tides twice a day, but also fully subaerial pools are possible in association with Mn ± Cu+Zn+Co deposits. Both tide variations onto hydrothermal venting and permanent subaerial ponds imply the plausibility of concentration mechanisms. The latter is also valid for epithermal systems (see Section 5.4.3.2). Besides all the possible minerals in the various settings in which such hydrothermal systems occur, the precipitation of silica gels is also possible (Tiercelin et al. 1993). Owing to the shallow character of these systems, gasohydrothermal activity (diffuse bubbling; Figure 5.4.3) is very common.

5.4.3.1.4 Seafloor Serpentinization Systems

The seafloor serpentinization processes consist in the hydration of the oceanic lithosphere, which is mainly formed by mantle peridotites (*i.e.*, dunites, harzburgites, lherzolites, and piroxenites) and lower crustal plutonic rocks. These rocks comprise ~20% or more of the ocean crust and are usually located in the vicinity of spreading ridges, passive margins, arc-subduction environments and could constitute the host rocks for VMS-type systems. The serpentinization process constitute a sequence of exothermic reactions at variable temperatures (below 450°C–500°C), which provide strong mineralogical and geochemical gradients controlled by pH and Eh changes in hydrothermal fluids that were derived from seawater and/or the mantle (*e.g.*, Früh-Green et al. 2004; Alt and Shanks 2006; Klein et al. 2009; Deschamps et al. 2013; Frost et al. 2013; see Table 5.4.2). The process starts with the hydration of olivine to form serpentinite and ferroan brucite, in presence of high pH and reducing fluids, thus promoting the dissolution of sulfides from the peridotitic host rock. The evolution of the system results in the formation of magnetite, from the breakdown of ferroan brucite in presence of SiO₂-rich, acidic, and oxidizing fluids, subsequently releasing significant amounts of H₂ and forming sulfides, oxides, and metal alloys (*e.g.*, Alt and Shanks 1998, 2003; Bach et al. 2004, 2006). A byproduct of serpentinization under highly reducing conditions is the venting of methane- and hydrogen-rich fluids, which can lead to the formation of carbonate mounds and chimneys similar as those described in the LCHF (Kelley et al. 2001). Mixing zones of these reduced hydrothermal fluids with seawater above peridotite outcrops (subseafloor mixing zones, according to Klein et al. 2015) represent niches for chemolithoautotrophic microbial communities associated with the serpentinization of the oceanic mantle (*e.g.*, Alt and Shanks 1998; Kelley et al. 2001; Früh-Green et al. 2004). Fossil examples of seafloor serpentinization systems are found as ancient sections of the Earth's oceanic crust (*i.e.*, ophiolitic sequence defined at the Penrose Conference, 1972) (Juteau and Maury 1997). The temporal frequency of ophiolites ranges between the Archean (*i.e.*, greenstone belts; de Wit 2004) and the Phanerozoic (Table 5.4.2; Misra 1999), thus suggesting that the modern plate tectonics, the formation of oceanic crust, and the seafloor serpentinization systems operated since the early Archean (Furnes et al. 2014).

The mineralogical styles shown in seafloor serpentinization systems are similar to those described in VMS- and SEDEX-type systems, while their mineral assemblages depend largely on the primary mineral association of the altered peridotitic rocks. For comprehensive reviews on this subject see (Sakai et al. 1990; Alt and Shanks 1998, 2003; Kelley et al. 2001; Klein and Bach 2009; Frost et al. 2013; Schwarzenbach et al. 2014, 2016; Klein et al. 2015). Sulfide-rich serpentinites, talc-rich serpentinites, carbonate-rich serpentinites (associated with magnesite deposits), listvenites (*i.e.*, CO₂- and SiO₂-rich serpentinites), and rodingites (hydrated gabbros with calcium silicates) are products of the hydrothermal alteration (*i.e.*, carbonation and/or silicification) of serpentinites. These

serpentinites are enriched in sulfides, oxides, alloys, and metallic and non-metallic elements (Co, Ni, Fe, Cu, Zn, Mn, Na, Ca, K, and S) relative to peridotitic protoliths (Uçurum 1998, 2000; Hansen et al. 2005; Tsikouras et al. 2006; Nasir et al. 2007; Falk and Kelemen 2015; Hinsken et al. 2017), which are key minerals/elements to promote prebiotic reactions. The types of serpentines listed previously, especially fossil examples associated with magnesite deposits, are currently the subject of numerous studies due to their usefulness as a “natural laboratory” for CO₂ sequestration and storage (Hansen et al. 2005; Kelemen et al. 2011; Beinlich et al. 2012; Power et al. 2013; Falk and Kelemen 2015). The most common minerals in ore-bearing associations of seafloor serpentinization deposits (non-metamorphosed or oxidized) and their modern analogues are summarized in Table 5.4.2.

5.4.3.2 SUBAERIAL HYDROTHERMAL SYSTEMS

Aside from those mentioned above for shallow submarine/sublacustrine to subaerial exhalative deposits in continental rifts, hydrothermal manifestations are abundant in subaerial settings, particularly in association with convergent plate boundaries (continental and island volcanic arcs), but also occur in transform boundaries. For instance, hydrothermal activity is known to occur in the Salton Sea, in association with the San Andreas Fault System but, unlike volcanic arcs, this case is normally placed among modern equivalents to SEDEX deposits and their associated subaqueous brine pools (see Table 5.4.2 and Figure 5.4.2). The most relevant and numerous recent/active hydrothermal fields are found in geothermal and magmatic-hydrothermal contexts, which are normally considered as the modern analogues of low-sulfidation and high-sulfidation epithermal deposits, respectively (which, in both cases, may include intermediate-sulfidation deposits); (Simmons et al. 2005; Camprubí and Albinson 2006, 2007; Sillitoe 2015). The uppermost part of such systems has a tendency to display wide variations in temperature, salinity, volatile content, pH, and redox potential (Figure 5.4.4) and hence the broad range in reactivity between the associated hydrothermal fluids and host rocks. Additionally, such differences in physicochemical variables and reactivity determine broad mineralogical variations on the surface or near it. The above variables are largely controlled by the vertical or lateral nearness of hydrothermal discharge zones to their parental intrusions (see Figure 1 in Sillitoe 2015) and the geological and hydrological characteristics in each area (White and Hedenquist 1990). Besides the broad temperature and salinity gradients that may occur in the actual variety of such environments, the occurrence of deep hypogene low- to intermediate-sulfidation fluids (generally near-neutral and reduced; geothermal context) or high- to intermediate-sulfidation fluids (acidic and oxidized; magmatic-hydrothermal context) determines (1) the possible zonation of alteration assemblages around the fluid conduits, and (2) the mineralogy of the mineral precipitates (if any) that may occur on the surface. In addition to the

“original” physicochemical characteristics of hydrothermal fluids, their chemical characteristics may vary depending on the occurrence of (relatively) near-surface boiling, which may generate H₂SO₄-rich fluids locally in steam-heated grounds (shallow hypogene acidic fluids), independently from the composition of pre-boiling fluids (e.g., Sillitoe 2015). This means that hydrothermal fluids of any kind that undergo boiling may generate acidic fluids upon condensation of boiled-off steam, and the associated alteration assemblages and surficial hydrothermal features.

Acidic fluids from either deep or shallow hypogene sources generate alteration assemblages that result from extremely reactive to relatively mild reactions between fluids and host rocks, from proximal to distal areas to hydrothermal upflow. No surface sinter deposits, either carbonate- or silica-rich, can be expected from highly reactive high-sulfidation type fluids. In this environment, silica is the only residue after extreme acid leaching of every other mineral, or as a late overprint. Common hydrothermal manifestations of the high-sulfidation type are high-temperature solfataras and fumaroles centered on recent volcanic edifices, and hyper-acidic crater lakes. Near-neutral low-sulfidation type fluids, on the contrary, may develop sinter deposits in hot spring environments unless the hydrothermal discharge occurs in high-relief terrains. Common hydrothermal manifestations of the low-sulfidation type are hot springs and geysers. Common manifestations associated with steam-heated grounds are fumaroles, steaming grounds, and mud pots (or mud “volcanoes”). The position of the groundwater table is sensitive to seasonal variations in rainwater availability, climatic and tectonic changes, or several other phenomena (e.g., Sillitoe 2015).

Paleosurface features for the various types of subaerial/sublacustrine magmatic-hydrothermal systems (*i.e.*, epithermal-like systems; Figure 5.4.4) and their mineralogy were summarized in detail by Sillitoe (2015) as (1) steam-heated grounds, with opal/chalcedony, alunite, kaolinite and smectite, (2) groundwater table silicification, with opal/chalcedony, (3) lacustrine amorphous silica sediments, with opal and cristobalite, (4) hydrothermal eruption craters and breccias, with illite and smectite, (5) hot spring sinter, with opal/chalcedony, (6) hot spring travertine, with calcite and aragonite, (7) hydrothermal chert, with opal/chalcedony, and (8) silicified lacustrine sediments, with opal/chalcedony. See their occurrence and nature schematized in Figure 11 by Sillitoe (2015), as replacements, open-space, or on-surface (subaerial or subaqueous) precipitation. Cases 6 to 8 (particularly case 6) occur distally to their hydrothermal upflow zone, which implies that their temperatures are lower than in proximal features and their chemical characteristics are attenuated by interaction with meteoric water. Such features and their particular mineral assemblages may be found topping various hydrothermal alteration assemblages in association with either acidic or near-neutral to alkaline fluids (high-sulfidation and intermediate- to low-sulfidation fluids, respectively), but not necessarily. Alteration assemblages in the uppermost part of these systems are characteristically zoned as follows, from the central portion of hydrothermal upflow outwards into

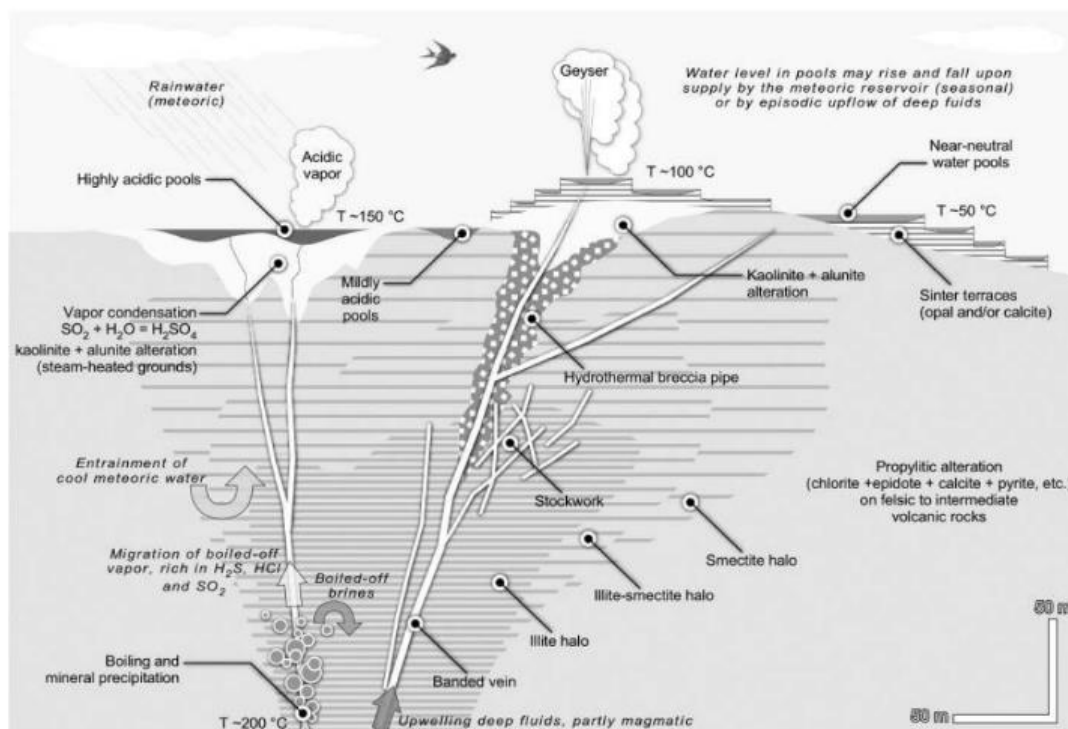


FIGURE 5.4.4 Structural section that combines evidence from active geothermal fields with neutral to alkaline fluids and from the uppermost portion of fossil low-sulfidation epithermal deposits, including all typical styles of mineralization and hydrothermal assemblages. (Loosely based on Buchanan, L. J., Precious metal deposits associated with volcanic environments in the Southwest, in: *Relations of Tectonics to Ore Deposits in the Southern Cordillera*, Vol. 14, W. R. Dickinson and W. D. Payne (Eds.), pp. 237–262, Arizona Geological Society Digests, 1981; Corbett, G. J., and Leach, T. M., *Southwest Pacific Rim Gold-Copper Systems: Structure, Alteration and Mineralisation*, Society of Economic Geologists, Boulder, CO, Special Publications No. 6. 238 p, 1998; Albinson, T. et al., Controls on formation of low-sulfidation epithermal deposits in Mexico: Constraints from fluid inclusion and stable isotope data, in: *New Mines and Discoveries in Mexico and Central America*, T. Albinson and C. E. Nelson (Eds.), pp. 1–32, Society of Economic Geologist Special Publications No. 8, 2001.)

non-altered host rocks (see Stoffregen 1987; Corbett and Leach 1998; Camprubí and Albinson 2006, 2007):

1. High-sulfidation systems: residual quartz (with opal, cristobalite and tridymite), advanced argillic (from silica + alunite to alunite + kaolinite outwards), argillic (from kaolinite + silica to kaolinite + silica + smectite outwards), and illite- or smectite-rich phyllic, from montmorillonite to chlorite-rich propylitic alteration, including zeolites and carbonates (calcite and dolomite), in association with the most alkaline fluids;
2. Intermediate- to low-sulfidation systems: phyllic to propylitic alteration, with the same mineral assemblages as those described for high-sulfidation systems.

Additionally, all the features in the uppermost portions of epithermal deposits and their modern analogues may have anomalously high concentrations of Mn, As, Sb, Hg, Tl, Se, Au, Ag, Ga, and W (Hedenquist et al. 2000; Sillitoe 2015). These anomalies occur in association with minerals such as pyrite, cinnabar, stibnite, orpiment, realgar, native sulfur, livingstonite, corderoite, several amorphous phases, and, exceptionally,

borates (Sillitoe 2015, and references therein). The precipitation of silica gels in epithermal systems is very common. The occurrence in present-day geothermal fields (broadly regarded as the active examples of epithermal deposits) of phenomena such as geysers and phreatomagmatic eruptions add another interesting feature for prebiotic reactions: the formation of aerosols and the occurrence of minute mineral particles alongside them (see subsequent sections).

Other possible hydrothermal environments associated with volcanism that might have harbored similar conditions as epithermal-type systems are Algoma-type BIFs, which were formed during the Archean. Such deposits are rich in magnetite, hematite, siderite, pyrite, pyrrhotite, quartz (as cherts), chlorites, amphiboles, feldspars, biotite, chalcopyrite, and apatite, and the precipitation of colloidal silica would have also occurred (Jébrak and Marcoux 2008).

5.4.4 PREBIOTIC EXPERIMENTS RELATED TO HYDROTHERMAL VENTS

Even if hydrothermal vent systems effectively harbored chemical synthesis, it is necessary to remind that the formation of relevant molecules is only the first step toward the origin of

life. The permanence of molecules in these environments is a crucial factor to guarantee the formation of more complex molecules (even polymers) that are necessary for the emergence of living beings. In the forthcoming sections some experiments that aimed to reproduce the environmental conditions in some hydrothermal systems are discussed.

Although hydrothermal systems are the combination of a broad number of geochemical variables, the vast majority of experiments that consider the “conditions of hydrothermal springs” have been initially oriented to test the effect of high temperatures on prebiotic reactions. Thermal energy has been considered as a synonym of energy in hydrothermal systems and other energy sources have been neglected. Therefore, the research in the matter started by testing the stability of organic molecules at high temperatures, which is one of the most straightforward possibilities. Lately, pressure has also been incorporated in simulations as many of the experiments deal with the simulation of deep submarine environments where the pressure is a critical variable. In submarine environments pressure affects the physical state of fluids: water and other molecules (CO_2 and CH_4) behave as supercritical fluids, hence their high efficiency as solvents for organics (Holm 1992).

5.4.4.1 STABILITY OF ORGANICS AT HIGH TEMPERATURES AND PRESSURES

The stability of organic molecules exposed to high temperatures is a fundamental issue. The endurance of molecules allows to increase their concentration and the chance for further chemical reactions. The formation of polymers, such as nucleic acids, proteins, and polysaccharides, requires a low decomposition rate of the monomers that constitute them. Some groups of molecules are seemingly good candidates to be the objects in these experiments; the tested molecules include amino acids, sugars, nitrogenous bases, and organic acids, among others (Table 5.4.3). Half-life values ($t_{1/2}$) provide an estimate of the time span molecules may last in the environments under the tested environmental conditions, for an excellent review of half-lives values see Weber (2004) and references therein.

Amino acids are essential molecules for life and their behavior has been largely studied. Amino acids at high temperatures (*i.e.*, 250°C) and pressures (*i.e.*, 250 atm) are very short-lived, as they are stable for only a few hours (Abelson 1954; Bernhardt et al. 1984; White 1984; Miller and Bada 1988; Bada et al. 1995). These results would suggest that hydrothermal springs in such conditions would not fit the requirements for being considered “niches for chemical evolution.” However, it is essential to emphasize that most of these experiments do not incorporate many of the physicochemical parameters (*e.g.*, oxidation state, pH, dissolved gas species, presence of inorganic surfaces, etc.). Also, such studies did not recreate the entire natural variability in temperature and pressure and their existing gradients even at the scale of a single vent. Consequently, the stability of the organic molecules could have been largely underestimated (Holm and Andersson 2005).

Other relevant molecules are sugars, which are essential constituents of nucleic acids and the basis for structural polymers in cells. The studies regarding the thermolysis of sugars (Larralde et al. 1995) showed that these compounds are very unstable ($t_{1/2}$ ribose ≈ 77 min) at temperatures as low as 100°C. The same behavior is observed for nitrogenous bases. The half-life of adenine is $t_{1/2} \approx 1$ year at 100°C (Levy and Miller 1998), which is a very short availability for further reactions. Similarly, considering the effect of pH and high pressures (*e.g.*, 7.2 MPa), uracil and adenine are even more labile ($t_{1/2} < 1$ h) than in the previous case (White 1984; Balodis et al. 2012). All in all, this only emphasizes the high lability of organic molecules at relatively high temperatures, as they have much lower fusion and decomposition points than inorganic compounds.

5.4.4.2 TEMPERATURE GRADIENTS

Even if energy is necessary for promoting chemical reactions, the temperatures of some actual hydrothermal fluids may attain up to 400°C (Von Damm 2013; James et al. 2014), which are excessively high for organic molecules. It is an immense problem, considering that these high temperatures could have existed in some environments during the Archean (Shibuya et al. 2010). However, as explained in sections above, such temperatures are not constant in time and space; high-temperature vents are commonly located in submarine areas at temperatures nearing 0°C, which implies the occurrence of strong thermal gradients. *In situ* studies at present-day hydrothermal vent systems demonstrate the existence of such gradients: just 15 cm around the hydrothermal vents temperature drops at least 30°C from the vent (Chevaldonné et al. 1991; Bates et al. 2010). The spatial variability of the temperature, associated with the turbulent mixing of the fluids in this type of environments, could considerably increase the stability of the organic molecules.

However, temperature is not the only variable that may present broad gradients, such is also the case of pressure, pH, Eh, ionic concentration, mineralogy, etc. Such gradients, besides representing an undeniable fact in natural hydrothermal systems, could also have contributed to increase the stability of organic molecules. Recently, attention has been paid to gradients in the experimental field and some attempts have been made indeed.

A first approximation is to estimate the half-life of molecules at different temperatures. Levy and Miller (1998) demonstrated that at 100°C, nucleobases have short half-lives ($t_{1/2} \approx 1$ year for A and G, $t_{1/2} \approx 12$ years for U, and $t_{1/2} \approx 19$ days for C). However, the half-lives of same molecules at 0°C leapt various orders of magnitude, to the point that all of them presented values in the order of 10^6 years. In other experiments, Larralde et al. (1995) tested the stability of sugars and found that the stability ribose increased from 73 min at 100°C to 44 years at 0°C. Such experiments can only encourage working with temperature gradients, ideally in congruence with those determined in natural examples.

The design and use of flow reactors brought a new perspective in the field, as they permit the generation of thermal

TABLE 5.4.3

Some Relevant Experiments in Prebiotic Chemistry Simulating Physicochemical Conditions of Hydrothermal Vents

Type of Study	Variables Used (Ω)	Description of the Experiments	Organic Molecule Used	Mineral	Main Findings	Reference
Decomposition	T	Solutions of amino acids (AAs) sealed in Pyrex glass	Ala, Arg, HCl, Asp, Cys, Glu, Gly, His, HCl, HyPro, Ile, Leu, Lys, HCl, Met, Phe, Pro, Ser, Thr, Tyr, Val	N.A.	Interconversion of amino acids (i.e., methylamine from glycine; ethylamine from alanine; glycine, alanine, and ethanolamine from serine, etc.). There is an order of relative thermal stability at temperatures between 216°C and 280°C: (1) Asp, Thr, Ser, Arg, HCl; (2) Lys-HCl, His-HCl, Met; (3) Tyr, Gly, Val, Leu, Ile; (4) Ala, Pro, Hyp, Glu.	Vallentyne (1964)
Decomposition	T	Amino acid in water solutions	Glu, PCA (pyroglutamic acid)	N.A.	Kinetic parameters	Povoledo and Vallentyne (1964)
Decomposition	T	Hydrolysis and decomposition of biomolecules in solutions at 250°C (pH = 7, potassium phosphate buffer).	Free amino acids, nucleic bases, peptide bonds, phosphodiester bonds	N.A.	The $t_{1/2}$ of peptide bonds on alanine oligomers is close to 7 min. A fast breakdown of other oligomers (Ala-Asp and Glu-Ala). Short half-life for proteins (1.08 s for (Ala) ₃).	White (1984)
Decomposition	T, P	Amino acid decomposition (6 h of incubation at 250°C and 260 bar).	Ala, Arg, Asp, Glu, Gly, His, Ile, Leu, Lys, Met, Phe, Ser, Thr, Tyr, Val	N.A.	Amino acids are drastically affected by high temperature and pressure. Some amino acids are almost quantitatively transformed or decomposed (Asp, Glu, Ser, Thr, Cys, Trp); apolar amino acids as well as His, Lys, Arg and Phe are partially degraded.	Bernhardt et al. (1984)
Decomposition	T, P, pH	Decomposition of solutions of amino acids at 250°C, 265 atm, and pH = 7.	Ala, Leu, Ser, Asp	N.A.	Leu $t_{1/2}$ is 15–20 min; Asp (<1 min), and Ser (few minutes) decomposed more rapid than Leu; Ala is more stable than Leu. Gly is produced during the heating experiment.	Miller and Bada (1988)
Decomposition	T, P, M	Amino acid and oligomers at high temperatures, at both high and low pressure.	Gly, Di-Gly, L-Ala, L-Glu	Magnetite	Dipeptide hydrolysis and amino acid decomposition have a first-order rate law. Magnetite accelerates the decomposition.	Qian et al. (1993)
Decomposition	T, P, M	Kinetics of thermal decarboxylation of aqueous solutions of acetic acid and sodium acetate (335°C and 355°C) in contact with surfaces as potential catalysts. Different pressures were used.	Acetic acid and sodium acetate	Quartz, fused quartz, calcite, natural pyrite, titanium oxide, Au, Ca-montmorillonite, Fe-montmorillonite, hematite, synthetic pyrite, and magnetite.	The decarboxylation of acetic acid and acetate catalyzed by the cleavage of the C-C bond, while the acetate molecule is adsorbed onto a surface. Oxidation of acetic acid occur with hematite and defected magnetite.	Bell et al. (1994)
Decomposition	T, P, M, pH	Amino acids, at high temperatures (240°C), buffered solutions (pH = 7).	Ala, Gly + Leu, ethylamine	Quartz-fayalite-magnetite mixture	Amino acids are irreversibly destroyed by heating at 240°C. Equilibrium thermodynamic calculations are not applicable to organics under submarine vent conditions.	Bada et al. (1995)
Decomposition	T	Determination of half-lives of sugars (aldopentoses and aldohexoses). Decomposition at pH 4–8 and, temperatures from 40°C to 120°C.	Ribose	N.A.	Ribose $t_{1/2}$ are very short (73 min at pH 7.0 and 100°C and 44 years at pH 7.0 and 0°C). The other sugars also have short half-lives (2-deoxyribose, ribose 5-phosphate, and ribose 2,4-bisphosphate).	Laralde et al. (1995)
Decomposition	T, redox	Amino acids at different temperatures, controlling the oxidation state of the environment.	Ala, bAla, aABA, Asp, Glu, Gly, Leu, Ser, Val	N.A.	The decomposition rate is lower in high hydrogen fugacity environments.	Kohara et al. (1997)

(Continued)

TABLE 5.4.3 (Continued)

Some Relevant Experiments in Prebiotic Chemistry Simulating Physicochemical Conditions of Hydrothermal Vents

Type of Study	Variables Used (Ω)	Description of the Experiments	Organic Molecule Used	Mineral	Main Findings	Reference
Decomposition	T, pH	Half-lives of nucleic bases at 100°C and pH = 7.	Adenine, Guanine, Cytosine, Uracil	N.A.	At 100°C the half-lives for nucleobases are very short. half-For A is 1 yr, G is 0.8 yr, U is 12 yr, and T is 56 yr. C has half-life of 19 days. At 0°C, the half-life of A is 6×10^5 yr, G is 1.3×10^6 yr, U is 3.8×10^8 yr, and T is 20×10^8 yr.	Levy and Miller (1998)
Decomposition	T, P, M, redox	Stability of amino acids, under redox buffered hydrothermal conditions; 200°C and 50 bar in Teflon-coated autoclaves.	Ala, Asp, Leu, Ser	Pyrite-pyrrhotite-magnetite (PPM) to constrain the oxygen fugacity. K-feldspar-muscovite-quartz (KMQ) to control the hydrogen ion activity.	Gly, and Ala were formed, from Ser. Decomposition rates of Leu, Ala and Asp lower in experiments containing the PPM assemblage.	Andersson and Holm (2000)
Decomposition	T, P	Influence of P (22.2 and 40.0 MPa) and T (250°C, 300°C, 350°C, 374°C, 400°C) in the processes.	Gly	N.A.	Formation of Di-Gly, Tri-Gly (traces), diketopiperazine and a 433 Da product. P and T influence both dimerization and decomposition. Maximum dimers formation at 350°C–375°C 22.2 and 40 Mpa.	Alargov et al. (2002)
Decomposition	T, P	High temperature (200°C–340°C) and high pressure (20 MPa), in a continuous-flow tubular reactor.	Ala, Asp, Leu, Phe, Ser	N.A.	Degradation rates Asp > Ser > Phe > Leu > Ala. Two main reaction paths: <i>deamination</i> (Asp) to produce ammonia and organic acids, and <i>decarboxylation</i> to produce carbonic acid and amine. Production of glycine and alanine from serine.	Sato et al. (2004)
Decomposition	T, P	Hydrothermal reaction kinetics. Followed by a custom-built spectrophotometric reaction cell. <i>In situ</i> observations.	Asp	Reactor type. Non-inert (Ti-6-4/Au reactor) Inert reactor (Au reactor).	The reaction kinetics of Asp is complicated, and highly dependent on experimental conditions (P, T, catalytic surfaces).	Cox and Seward (2007a)
Decomposition	T, P	Hydrothermal reaction kinetic. A custom spectrophotometric reaction cell was constructed. <i>In situ</i> observations. Experiments performed at 120°C–165°C and 20 bar.	α -Ala, β -Ala, Gly	N.A.	Under certain hydrothermal conditions, α -Ala, Gly, and β -Ala undergo dimerization and cyclization reaction pathways.	Cox and Seward (2007b)
Decomposition	T, P	Decomposition of the amino acids sub- and supercritical water. The effect of T (250°C–450°C), and residence time (2.5–35 s), P (34 and 24 MPa), and reactant concentration (1.0% and 2.0%, w:v).	Ala, Gly	N.A.	Decarboxylation and amino acid deamination reactions were proposed for both molecules. Ala is decomposed in lactic acid and ethylamine. Gly is decomposed in methylamine	Klingler et al. (2007)
Decomposition	T, M	The effect of iron oxide and sulfide minerals on decomposition reactions of amino acids.	Nva, Ala	Iron oxide and sulfide minerals. Mineral assemblage hematite-magnetite-pyrite (HMP) and pyrite-pyrrhotite-magnetite (PPM).	Nva decomposes by (1) decarboxylation followed by oxidative deamination, and by (2) deamination directly to valeric acid. Ala decomposes in acetic and propionic acids, CO ₂ and NH ₃ . Minerals accelerated decomposition rates. Decomposition is faster in presence HMP than PPM. Surface catalysis and production of dissolved sulfur compounds are probably responsible of the decomposition.	McCollom (2013)

(Continued)

TABLE 5.4.3 (Continued)

Some Relevant Experiments in Prebiotic Chemistry Simulating Physicochemical Conditions of Hydrothermal Vents

Type of Study	Variables Used (Ω)	Description of the Experiments	Organic Molecule Used	Mineral	Main Findings	Reference
Decomposition	T, M	Role of relevant minerals and mineral mixtures in the thermal behavior of an amino acid (200°C–250°C).	Gly	Mineral matrices: montmorillonite, nontronite, kaolinite, salts, artificial sea salt, gypsum, magnesite, picritic basalt, and three samples that simulate the Martian regolith.	Glycine intercalated in some phyllosilicates was well protected against thermomelanoid, survived unaltered or been transformed into the cyclic dipeptide (DKP) and linear peptides up to (Gly) ₆ .	Dalai et al. (2017)
Decomposition	T, P, M, redox	Decomposition of aspartate (200°C and 15.5 bars in gold capsules) with and without a mineral product of serpentinization, and at reducing conditions (NH ₄ Cl and H _{2(aq)})	Aspartate	Brucite	The reaction products vary significantly depending on the reaction conditions. Fluids including just aspartate formed: fumarate, maleate, malate, acetate, and succinate and glycine (both in traces). Under reducing conditions, the main product was succinate and amino acids glycine, α -alanine, and β -alanine.	Estrada et al. (2017)
Stability	T, M _d	The thermal stability of amino acids in seafloor hydrothermal systems is tested.	Ala, Asp, Gaba, Glu, Gly, Leu, Met, Ser.	Carbonaceous ooze. Calcite, with minor amounts of quartz and huntite and traces of illite, smectite and chlorite.	The upper limit temperature for the stable presence was 150°C and 200°C. AAs cannot be synthesized or survive at temperatures higher than 250°C.	Ito et al. (2006)
Stability	T, pH	Reactions of amino acids under subcritical water conditions (220°C–290°C).	Ala, Arg, Asp, Cys, Glu, Gly, His, Ile, Leu, Lys, Met, Phe, Pro, Ser, Thr, Tyr, Val.	N.A.	A decrease in the overall stability in amino acids mixtures. Most of the amino acids decompose at acidic and near-natural pH, stable at basic pH.	Abdelmoez et al. (2007)
Stability	T, pH, M	Evaluation of the thermal stability of amino acids under alkaline hydrothermal conditions (an aqueous solution of NaCl and Na ₂ CO ₃) at elevated temperature (100°C–300°C).	Ala, Arg, Asp, Bala, Gaba, Glu, Gly, His, Ile, Leu, Lys, Met, Or, Phe, Pro, Ser, Thr, Tyr, Val	Siliceous ooze	Compared with decomposition at neutral conditions, the decomposition rates are lower under alkaline conditions.	Yamaoka et al. (2007)
Stability	T, P, redox	Stability of adenine under hydrothermal conditions, at 300°C under fugacities of CO ₂ , N ₂ , and H ₂	Adenine	Iron	The gases improve the stability of adenine. The concentration of adenine decreased rapidly during the first 24 h of the experiment, then kept decreasing slowly. Adenine was still present in the hydrothermal solution after ~200 h.	Franiatte et al. (2008)
Stability	T, M	Effect of the mineralogical and chemical properties of host sediments on the thermal stability of amino acids.	Ala, Arg, Asp, B-Ala, Gaba, Glu, Gly, His, Ile, Leu, Lys, Met, Phe, Pro, Ser, Thr, Tyr, Val	Siliceous ooze: silica minerals (mostly quartz and minor opaline silica); moderate amounts of calcite and minor amounts of smectite and illite. Montmorillonite Saponite (synthesized).	Amino acids protected from decomposition by amorphous silica and silicate minerals via adsorption and/or binding. The optimal temperature for amino acids was below 150°C. Amino acids are more stable at higher temperatures when associated with silicates.	Ito et al. (2009)

(Continued)

TABLE 5.4.3 (Continued)

Some Relevant Experiments in Prebiotic Chemistry Simulating Physicochemical Conditions of Hydrothermal Vents

Type of Study	Variables Used (Ω)	Description of the Experiments	Organic Molecule Used	Mineral	Main Findings	Reference
Stability	T, P, pH	Ionization constants of nucleic bases at 250°C and 7.2 MPa	Adenine, Uracil	N.A.	Uracil and adenine decomposition occurred by one-step and two-step processes. Phosphate buffer solution enhances the stability of nucleic acid bases.	Balodis et al. (2012)
Stability	T, pH, redox	The effects of temperature (25°C, 150°C, 200°C, and 250°C) pH (6 and 10) and redox state (13 mM aqueous H ₂) of hydrothermal fluids. Reaction times from 3 to 36 min.	Glu	N.A.	Glutamic acid at high-temperatures cyclizes and forms pyroglutamate. The formed products (succinate, formate, carbon dioxide, and ammonia) depend on the temperature, pH, and the redox state.	Lee et al. (2014)
Oligomerization	T, M	Amino acids.	Gly, Phe, Tyr	(Ni,Fe)S surfaces.	The formation of oligopeptides was pH dependent. Dipeptide formation (L-Phe, L-Tyr, D,L-Tyr and Gly).	Huber and Wächtershäuser (1998)
Oligomerization	T, P, pH, M	Amino acids in a flow reactor with temperature gradients (T = 250°C, at 24 MPa, pH 2.5)	Gly+Ala	CuCl ₂	Exponential growth of the products, as a consequence of previous cycles formation, function as templates for the next cycle. At least six different oligopeptides were detected; Ala-Gly, Gly-Ala, Ala-Ala, Gly-Ala-Ala, Ala-Ala-Ala, Ala-Ala-Ala-Ala.	Ogata et al. (2000)
Oligomerization	T, pH, S _r	Oligomerization in a flow reactor (temperature gradient from 110°C to 0°C at pH 3). Dissolved ZnCl ₂	AMP	N.A.	Synthesis of oligonucleotides in the absence of condensing agents.	Ogasawara et al. (2000)
Oligomerization	T	Amino acid solution heating at different temperatures (200°C–350°C) in a supercritical flow reactor. The stability of some amino acids (ω - and α -amino acids) under hydrothermal conditions was explored.	Gly	N.A.	Oligomers, up to tetra-Gly, formed at 200°C–350°C. No glycine oligopeptides were produced at 400°C. ω -Amino acids and glutamic acid exhibited higher stability than other α -amino acids.	Islam et al. (2003)
Oligomerization	T	Hydrothermal stability of alanine oligopeptides.	(Ala) ₃ , (Ala) ₄ , (Ala) ₅	N.A.	Small excess of oligopeptides longer than the starting ones. Elongation of (Ala) ₄ and (Ala) ₅ was possible in Ala excess. Elongation is competitive with degradation.	Kawamura (2005)
Oligomerization	T	Amino acid solution heating at different T (160°C, 220°C, and 260°C).	Gly	Gold hydrothermal reaction cells.	Peptide synthesis (di-Gly, tri-Gly) is favored in hydrothermal fluids. Rapid recycling of products from cool into near-supercritical fluids will enhance peptide chain elongation.	Lemke et al. (2009)
Oligomerization	T	In a hydrothermal microflow reactor, the synthesis of oligopeptide-like molecules at 250°C–310°C.	Glu, Asp		Synthesis of oligopeptide-like molecules of length up to 20-mers from Glu and Asp.	Kawamura and Shimahashi (2008)
Oligomerization	T, pH	Dimerization rate of glycine, the effects of pH (ranging from 3.1 to 10.9) and temperature (120°C, 140°C, 160°C, and 180°C) were tested.	Gly	N.A.	Dimerization increases at basic pH (7–10). The dimerization rate increases with temperature (150°C). Gly dimerizes most under alkaline pH (~9.8) at about 150°C.	Sakata et al. (2010)

(Continued)

TABLE 5.4.3 (Continued)

Some Relevant Experiments in Prebiotic Chemistry Simulating Physicochemical Conditions of Hydrothermal Vents

Type of Study	Variables Used (Ω)	Description of the Experiments	Organic Molecule Used	Mineral	Main Findings	Reference
Oligomerization	T	The production of phosphodiester bond and formation of mononucleotides capable of base pairing after hydration-dehydration cycles (85°C).	AMP, UMP	N.A.	The cycles of hydration and dehydration drive the synthesis of ester bonds. Oligomers resembling RNA are synthesized. Some of the products have properties suggesting secondary structures, including duplex species stabilized by hydrogen bonds.	DeGuzman et al. (2014)
Oligomerization	T, M, pH	The effect of elemental composition, pH, presence of clay, doping with small organic compounds, ribonucleotide activation on RNA oligomerization.	AMP, Imidazole-activated AMP (ImpA)	Iron-sulfide synthesized chimneys. Montmorillonite.	Nucleotide oligomerization—for both the activated and unactivated nucleotide—can occur in synthetic alkaline hydrothermal chimneys. Generation of oligomers (up to 4 units) with imidazole-activated ribonucleotides.	Burcar et al. (2015)
Synthesis	T, M	Heating of NH_4HCO_3 solution with C_2H_2 , H_2 and O_2 (produced <i>in situ</i>).	Acetylene	Calcium carbide. Calcium.	Amino acids (Gly, Ala, Asp, Glu, Pro, Ser, Leu, Ile, Lys, Val, Thr) and amines formed at 200°C–275°C, no formation at <150°C.	Marshall (1994)
Synthesis	T	Formation of lipids through Fischer-Tropsch-type synthesis of aqueous solutions.	Formic acid or oxalic acid	N.A.	Heating at 175°C for 2–3 days, lipid compounds from C_2 to $>\text{C}_{35}$ (n-alkanols, n-alkanoic acids, n-alkenes, n-alkanes and alkanones).	McCollom et al. (1999)
Synthesis	T, P, M	Reactivity of organic acids and acid anions (325°C, 350 bars) in the presence of the mineral assemblages.	Acetic acid, sodium acetate, valeric acid	(1) Hematite + magnetite + pyrite (HMP). (2) Pyrite + pyrrhotite + magnetite (PPyM) (3) Hematite + magnetite (HM)	Acetic acid and acetate decompose by decarboxylation and oxidation. Reactions are catalyzed by minerals: magnetite promotes decarboxylation; hematite promotes oxidation. The oxidation reaction is much faster. Valeric acid decomposed faster than acetic acid under similar conditions.	McCollom and Seewald (2003b)
Synthesis		Decomposition of formic acid and formate and the production of formate from CO_2 reduction (175°C–260°C). Experiments conducted in gold-TiO ₂ reactors	Formic acid and formate	Hematite, Magnetite. Serpentinized olivine, Ni-Fe alloy	Minerals had no effect on the stability of formic acid or formate. The quantity of formate in hydrothermal fluids could be controlled by an equilibrium with dissolved CO_2 at the oxidation state and pH of the fluid.	McCollom and Seewald (2003a)
Synthesis	T, P, M	Conversion of CO_2 into organic compounds in hydrothermal conditions (300°C and 30 MPa).	CO_2 and H_2	Cobalt-bearing magnetite.	Formation of CH_4 , C_2H_6 , and C_3H_8 , but also n-C ₄ H ₁₀ and n-C ₅ H ₁₂ .	Ji et al. (2008)
Synthesis	T, M	N-bearing molecules, to synthesize ammonia, at different T (200°C, 70°C, and 22°C).	Dinitrogen, nitrate	Fe and Ni metal, awaruite (Ni ₈₀ Fe ₂₀) and tetraaenite (Ni ₅₀ Fe ₅₀), alloys bearing Fe and Ni.	Nitrite and nitrate are converted to ammonium rapidly. The reaction of dinitrogen is slower. Reduction is strongly temperature-dependent. Metals were more reactive than alloys.	Smirnov et al. (2008)
Synthesis	T	Amino acids synthesis in function of temperature, heating time, starting material composition and concentration.	NH_4HCO_2		Amino acids synthesized (Gly, Ala, Asp, Glu, Ser) from simple precursors under submarine hydrothermal systems conditions. Degradation is privileged in such conditions. Synthesis at lower temperatures.	Aubrey et al. (2009)

(Continued)

TABLE 5.4.3 (Continued)

Some Relevant Experiments in Prebiotic Chemistry Simulating Physicochemical Conditions of Hydrothermal Vents

Type of Study	Variables Used (Ω)	Description of the Experiments	Organic Molecule Used	Mineral	Main Findings	Reference
Synthesis/ Precipitation	T, M	Pyrophosphate synthesis in inorganic precipitates simulating hydrothermal chimney structures in thermal and/or ionic gradients.	FeCl ₂ ·4H ₂ O, Na ₂ S·9H ₂ O, K ₂ HPO ₄ , Sodium silicate solution (Na ₂ O/26.5% SiO ₂), Na-acetyl phosphate	Iron mineral films.	Poi was synthesized. Iron-rich membranes with incorporated phosphates were generated.	Barge et al. (2014)
Cycling	T, S	Laboratory simulation of hydrothermal pools under cycles of hydration and dehydration at 85°C in an atmosphere of CO ₂ and monovalent salts	Mixtures of AMP and UMP	N. A.	1:1 are cycled in the presence of monovalent salts, a polymerization reaction yields a product with	Da Silva et al. (2015)
Adsorption	T, M	Adsorption-desorption experiments at 80°C for 10 days.	Lys	Na-smectite (smectite (>90%), a small amount of cristobalite (<10%) and traces of calcite and quartz.	Thermal treatment originates stronger smectite-lysine binding, by H bonds between NH ₃ ⁺ lysine groups and smectite basal O atoms.	Cuadros et al. (2009)
Microsphere formation	T, P	Aqueous solution with amino acids (Gly, Ala, Val and Asp) in glass tubes, heated at 200°C, 250°C, 300°C, and 350°C, at 134 atm, buffered (pH 7.2).	Gly, Ala, Val, Asp	N.A.	Formation of microspheres at temperatures above 250°C. Polar amino acids are needed for the microsphere formation. Microspheres are made of peptide-like polymers.	Yanagawa and Kojima (1985)
Reaction	T	Decarboxylation of an amino acid solution as a function of pH.	α -Ala	N.A.	Arrhenius parameters were determined. The addition of KCl resulted in a reduction of the decarboxylation rate.	Li et al. (2002)
Reactivity	T, M	Pyruvate reactions in presence of transition-metal sulfide minerals, at moderate temperatures (25°C–110°C).	Pyr	Pyrrhotite, troilite, arsenopyrite, pyrite, marcasite, sphalerite, chalcocopyrite	Amino acids and fatty acids were formed. Formation of lactate, propionate, and alanine, among others.	Novikov and Copley (2013)
Concentration	T, M	To test if channels within the mineral could act as act as natural Clusius-Dickel thermal diffusion column and increase local amphiphile concentrations.	Oleic acid	Borosilicate microcapillaries.	Microcapillaries act as a thermal diffusion column and concentrated the molecule. Vesicle formation.	Budin et al. (2009)
Mineral precipitation	T, pH	Raman spectroscopy to study ancient hydrothermal iron sulfide formation (growth temperatures from 40°C to 80°C).	Aqueous alkaline solutions containing bisulfide and silicate injected into iron (II) solutions.	N.A.	Formation of mackinawite and greigite iron sulfide phases. Mackinawite was probably the dominant catalyst in ancient pre-biotic chemistry.	White et al. (2015)

Source: Colín-García, M. et al., *Bol. Soc. Geol. Mex.*, 68, 599–620, 2016.

Note: All amino acids are abbreviated according to the IUPAC indications.

Key: ABA = aminobutyric acid, Ala = alanine, AMP = adenosine monophosphate, Arg = arginine, Asp = asparagine, Cys = cysteine, Gaba = gamma-aminobutyric acid, Glu = glutamic acid, Gly = glycine, His = histidine, Hyp = hydroxyproline, Ile = isoleucine, Leu = leucine, Lys = lysine, Met = methionine, Nva = norvaline, Orn = ornithine, PCA = pyroglutamic acid, Phe = phenylalanine, Pro = proline, Pyr = pyruvate, Ser = serine, Thr = threonine, Tyr = tyrosine, Val = valine.

(Ω) Variables used refer to: T = temperature, P = pressure, M = minerals, S = salts, redox estate, and pH.

gradients. The use of those equipment showed that it is not only possible for organic molecules to remain in these environments, but it is also feasible to form more complex molecules, such as oligomers. This was tested for amino acids that formed oligopeptides (Imai et al. 1999; Ogata et al. 2000; Islam et al. 2003); similarly, oligonucleotides were formed from the repeatedly circulation of nucleotides between hot and cold regions, even in the absence of condensation agents (Ogasawara et al. 2000). These experiments have been completed with theoretical approaches that suggest that thermal gradients in mineral pores could favour the accumulation of molecules (Braun and Libchaber 2002; Baaske et al. 2007; Mast et al. 2013; Niether et al. 2016).

5.4.4.3 REDOX STATE AND DISSOLVED GASES

Hydrothermal vents harbor a high diversity of chemical species. Currently, some of these dissolved species in hydrothermal fluids are the fuel for microbial communities thriving in these environments (Martin et al. 2008). It has been proposed that the wide availability of gases and/or dissolved elements (CO_2 , H_2S , H_2 , CH_4 , NH_3 , Co, Fe, Mg, SO_4^{2-} , and Mn) (Tivey 2007; Martin et al. 2008) in hydrothermal systems could have been the basis of the first metabolic routes (Wächtershäuser 1990; Russell and Martin 2004; Martin et al. 2008). Certainly, dissolved chemical species in these environments may have promoted or inhibit the reactivity of organic molecules.

More recently, several research groups have delved into the effect of various geochemical variables on the stability of organic molecules. In general, the experiments suggest that the geochemical variables are intrinsically related to the fate of the organic molecules. That implies that in these environments small changes in environmental conditions could have promoted chemical changes. Investigations (Kohara et al. 1997) and (Lee et al. 2014) showed that the decomposition rate of some amino acids (*i.e.*, glycine, glutamic acid, and alanine) was much slower in environments with high hydrogen fugacity. In other experiments, the decomposition of amino acids decreases under buffered conditions, as the pyrite-pyrrhotite-magnetite system acts as a redox buffer (Andersson and Holm 2000). However, the redox condition also affects the decomposition pathways. There are two possible decomposition reactions of amino acids under hydrothermal conditions: *deamination* to produce ammonia and organic acids, and *decarboxylation* to produce carbonic acid and amines (Sato et al. 2004). It has been shown that some amino acids (*i.e.*, glycine and alanine) may preferably undergo dimerization and then cyclization reactions, instead of decomposition, depending on the experimental conditions (mineral surface, temperature, residence time, and redox state; (Cox and Seward 2007b, 2007c). In addition, depending on temperature and pressure, there may be a selection of the decomposition mechanism (Klingler et al. 2007).

Experiments with nitrogenous bases (Franiatte et al. 2008) showed that under an atmosphere containing CO_2 , N_2 , and H_2 , adenine was present after ≈ 200 hours of

heating at 300°C . On the other hand, the decomposition reactions (*e.g.*, dehydrogenation) may depend on the redox state of the system.

5.4.4.4 pH GRADIENTS

There is a great debate about the role of proton gradients in the origin of life, as the electrochemical gradients across the membranes could have boosted metabolism (Jackson 2016; Lane 2017). It is very feasible that the pH values in hydrothermal vent systems could also be involved in the chemical behavior of organic molecules. On-site measurements showed that hydrothermal fluids at high temperatures (*e.g.*, $>350^\circ\text{C}$) and with acidic pH (close to 5) change their pH toward neutrality when they come in contact with oceanic water (Ding et al. 2005). Similarly, theoretical studies explain that it is possible to have a gradient of up to 6 pH units (that is, six orders of magnitude) at a micrometric scale in hydrothermal vents (Möller et al. 2017). Experimentally, Sakata et al. (2010) showed that dimerization of glycine is most efficient at alkaline pH (≈ 9.8) due to differences in dissociation states of the molecule (*i.e.*, Gly^\pm and Gly^- fractions are approximately equal at this pH). Also, the decarboxylation of alanine is three times higher in pH values where the zwitterion predominates, although the presence of dissolved ions (*i.e.*, KCl) reduces it (Li et al. 2002).

5.4.4.5 EXPERIMENTS THAT INCLUDE MINERALS

One of the most important characteristics of hydrothermal vents is their high mineralogical diversity. The broad diversity of minerals in hydrothermal springs of any type could be a crucial parameter in the formation and production of complex organic molecules in prebiotic experiments (Colín-García et al. 2016). The role that minerals could have played in prebiotic reactions is complex but can be envisioned as follows: (1) catalysts of reactions, both decomposition and formation of more complex species, (2) templates where organics can organize and constitute more complex molecules, (3) protective agents, sheltering molecules from decomposition in the media, and (4) concentrating agents—the concentration of organics in contact with solids increases and some organic reactions can be promoted. The specific role that minerals play depends on variables including: chemical composition of minerals and their impurities, solubility of minerals, redox potential in the environment, pH, temperature, ionic force, and, of course, the characteristics of the organic molecule. Minerals affect at different degrees the thermal decomposition of organics; actually, many experiments have been performed in order to specifically understand the effect of minerals on the chemical reactions related to prebiotic chemistry experiments (Table 5.4.3).

In order to evaluate the effect of the mineralogical and chemical properties of host sediments on the thermal stability of amino acids (Ito et al. 2006) reported almost full decomposition of amino acids (90.1% at 200°C and 99.7% at 300°C) in experiments including calcareous sediments and

NaCl solutions. Also, they suggested that the temperature roof for having stable amino acids probably varies between 150°C and 200°C (Ito et al. 2006). Later, the same group demonstrated that at the very same conditions siliceous ooze served as a better protection for amino acid than calcareous sediments (Ito et al. 2009). Yamaoka et al. (2007) also studied the effect of siliceous ooze in the decomposition of amino acids, but under alkaline hydrothermal conditions (by enrichment of Na₂CO₃ and volatile gases). They found that decomposition is inhibited in alkaline conditions and, even more, amino acids remained even after heating for 240 hours at 300°C. Dalai et al. (2017) investigated how minerals and mineral mixtures change the formation of a black water-soluble thermal polymer (“thermomelanoid”) of glycine. When the experiment was carried out in the presence of phyllosilicates, these minerals precluded the formation of the polymer; instead, glycine remained unaltered or was even transformed to the cyclic dipeptide diketopiperazine (DKP) or polymerized up to Gly₆.

It has also been tested the role of sulfides in prebiotic reactions. Novikov and Copley (2013) demonstrated that pyrite favors the synthesis of amino acids and fatty acids from pyruvate (an important precursor for organic molecules and already synthesized under simulated hydrothermal vent conditions). Qian et al. (1993) showed that magnetite increases the decomposition of amino acids at high pressures and temperatures. In addition, the presence of mineral substrates (*e.g.*, iron oxides and sulfides) accelerates the decomposition rates of some amino acids (norvaline; McCollom 2013).

A series of experiments (McCollom and Seewald 2003a) showed that minerals such as hematite, magnetite, serpentinized olivine, and NiFe alloy had little effect on the stability of some species (formate and formic acid, the simplest organic acid, and acid anion present in natural waters). However, minerals influenced both the pH and concentration in CO₂ of fluids, and, in turn, dissolved CO₂ determined the amount of formate that was present. Acetic acid and acetate (intermediates in metabolism) decompose rapidly in the presence of minerals containing metal ions (*e.g.*, calcium- and iron-bearing montmorillonite, pyrite, hematite, and magnetite) as they act as catalysts in the decarboxylation reaction (Bell et al. 1994).

Stereoselectivity is also promoted by minerals. Fuchida et al. (2017) heated (at 120°C) DL-alanine in presence of olivine and water to investigate the formation of the diastereoisomers of diketopiperazine (DKP). Olivine was an efficient catalyst to form DKP and determined the preferential formation of one of these dipeptides.

Studies that included other types of variables demonstrated that minerals can also have a representative role in the behavior of organic molecules. For example, the presence of dissolved ions may favor the protection of amino acids against thermal decomposition, probably due to the formation of complexes with dissolved ions (*e.g.*, Ca²⁺ and Mg²⁺) that, in turn, increase their sorption onto mineral surfaces (Dalai et al. 2017). Likewise, thermal treatment from a hydrated phase can favor the concentration of amino acids in clays due to the increase in hydrogen bonds between the tetrahedron

bed and the amino group of the amino acid (Cuadros et al. 2009). Also, the stability of formate and formic acid could be affected more by dissolved CO₂ contents and the pH of the fluid than by the presence of some minerals (*e.g.*, hematite, magnetite, and serpentine; McCollom and Seewald 2003b).

5.4.5 SUMMARY OF RELEVANT GEOLOGICAL AND MINERALOGICAL ASPECTS FOR EXPERIMENTAL STUDIES WITH REGARD TO PREBIOTIC SYNTHESIS

Physicochemical variables such as temperature, pressure, composition of solutes in aqueous brines or supercritical fluids, pH, and Eh are obvious key factors that control prebiotic synthesis. In addition, the role of minerals in prebiotic chemistry is acknowledged nowadays as no lesser factor (see the previous sections; Schoonen et al. 2004; Cleaves et al. 2012). The broad variety of factors that have an influence on prebiotic chemistry come from an even broader variety of natural environments (Figures 5.4.5 through 5.4.8, which stretch far more generously than those visible in deep submarine VMS-type hydrothermal vents, either acidic or alkaline (see Table 5.4.2). In other words, many natural settings interesting as models for prebiotic studies can be found outside VMS-type hydrothermal vents.

Natural systems keep resisting experimental simplifications but also have a great potential for furnishing new possibilities for experimental patterns. It is in such spirit that we may now summarize from the above the following variables and “situations,” as it were, in order to direct future experimental endeavors as much close to nature as possible.

1. Physicochemical gradients: temperature gradients, pH gradients, Eh gradients, salinity gradients, ionic force gradients, *p*CO₂ gradients, and O₂ and S₂ fugacity gradients (virtually all hydrothermal systems in early sections of this paper). All natural hydrothermal systems show strong natural variations (Hazen and Sverjensky 2010) in all these cases with respect to (A) upwelling hydrothermal fluids themselves, and (B) the contrast between them and the environment they may encounter (whether it is a rock, air, seawater, a lake, or a puddle). As consequence, the value distribution of all variables may behave fractally across space and time—for instance, temperature decreases and pH increases from the central to the peripheral vents in VMS and SEDEX mounds, but they also do so in the lifetime of a particular vent and as the whole hydrothermal system wanes. The most obvious differences that arise for a given variable when comparing two or more types of hydrothermal systems have to do with how extreme is the range of variation of a given physicochemical variable, as such general ranges overlap in all the types of systems considered hereby. For example, all ranges of temperatures in Table 5.4.2 are those of

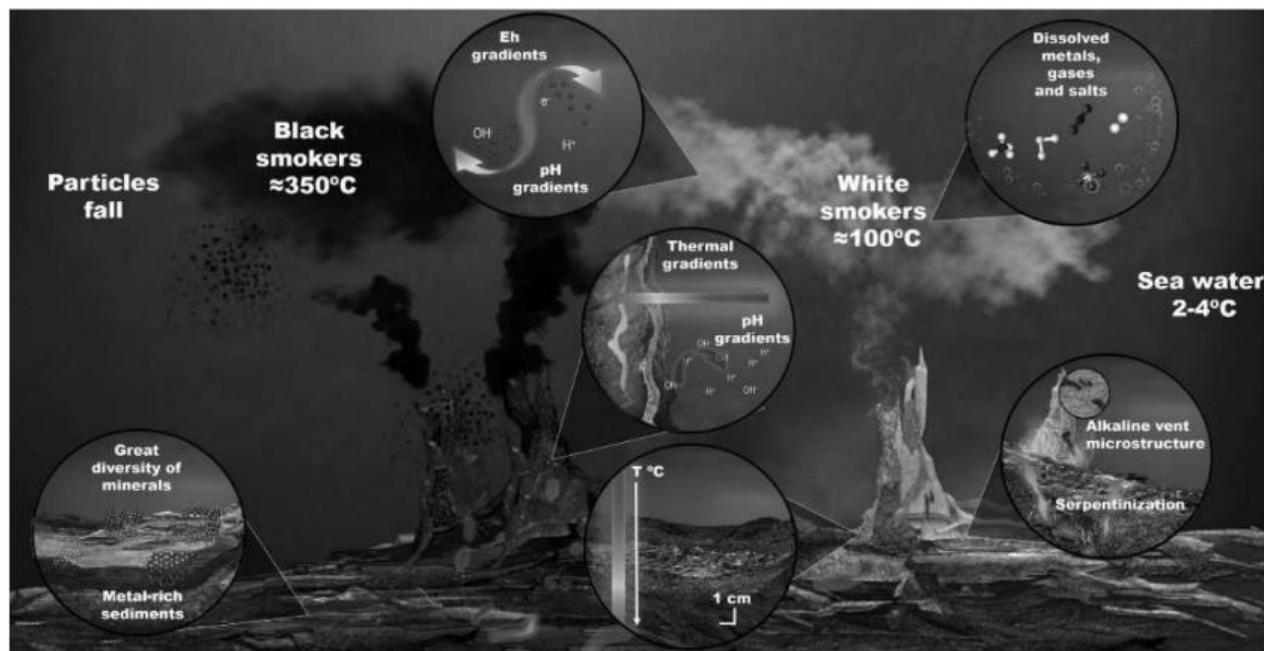


FIGURE 5.4.5 Representation of structures, processes, and gradients of key variables on the seafloor in association with hydrothermal systems of the volcanogenic massive sulfide (VMS) type, as of Figure 5.4.1.

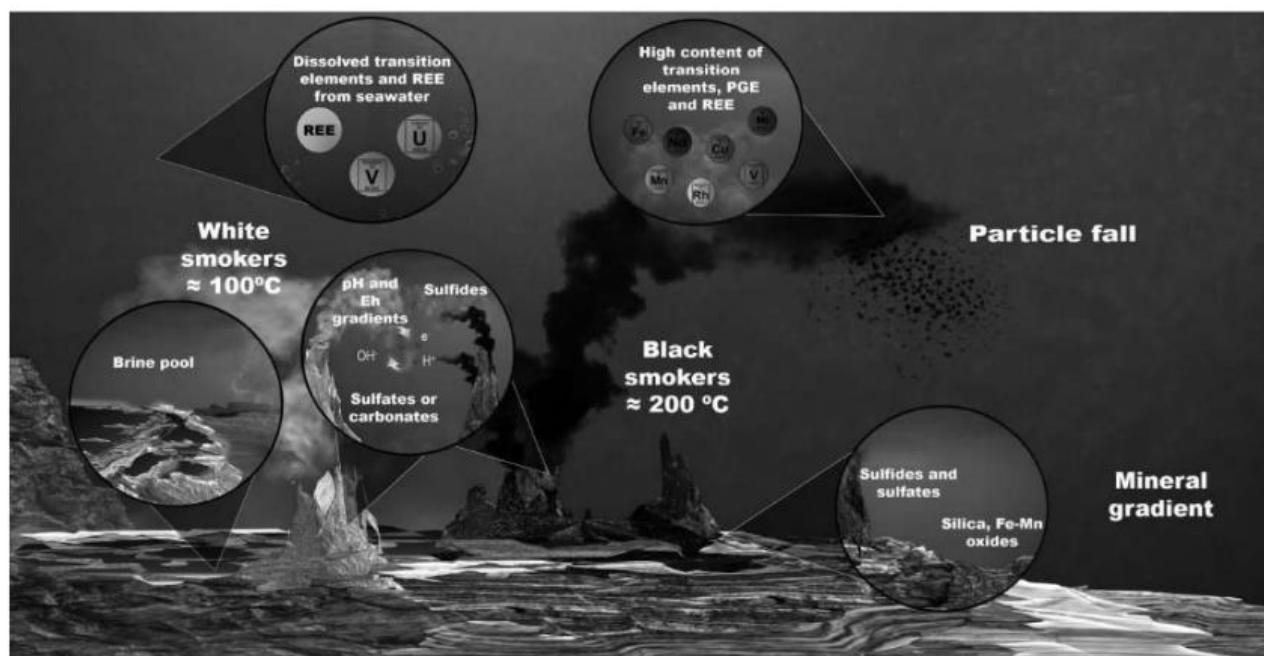


FIGURE 5.4.6 Representation of structures, processes, and gradients of key variables on the seafloor in association with hydrothermal systems of the sedimentary-exhalative (SEDEX) type, as of Figure 5.4.2.

typical stages of mineral deposition (ore associations in particular), but the general variation of temperature stretches down to the environmental temperature for each case ($\sim 0^{\circ}\text{C}$ in deep seawater and $\sim 25^{\circ}\text{C}$ in continental systems). In addition, all the (paleo-) hydrothermal systems considered in this paper have

a multi-episodic behavior, which means that each hydrothermal pulse has physicochemical characteristics that may differ greatly from those of preceding or later pulses.

2. Mineralogical gradients across a mineral deposit or compositional gradients within the same mineral

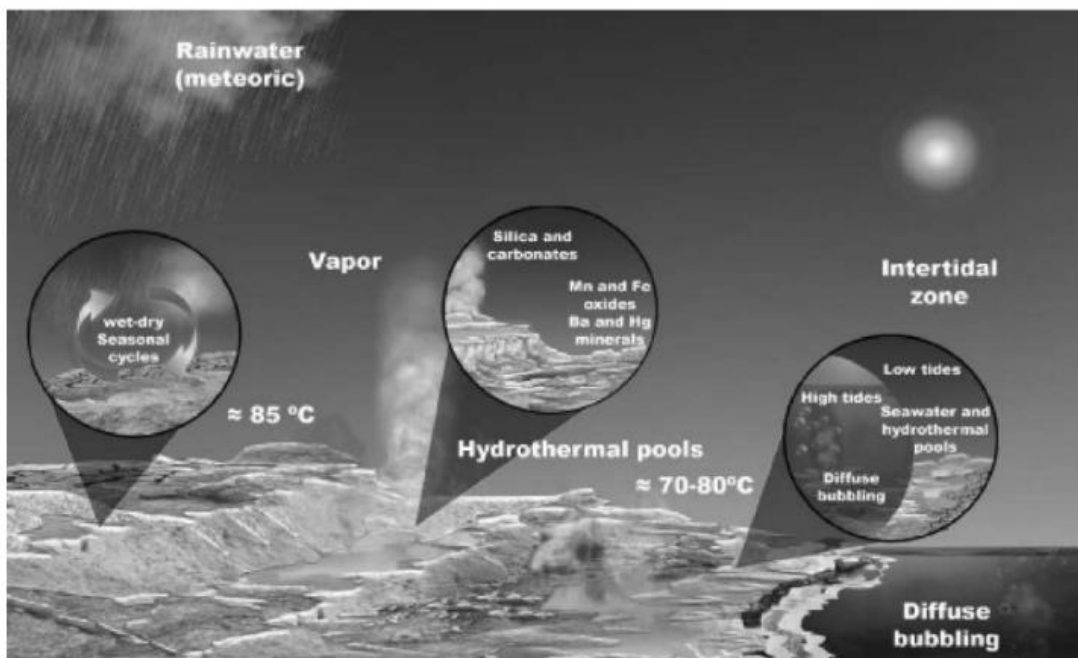


FIGURE 5.4.7 Representation of structures, processes, and gradients of key variables in shallow submarine to subaerial hydrothermal systems that occur during early stages of continental rifting, as of Figure 5.4.3.

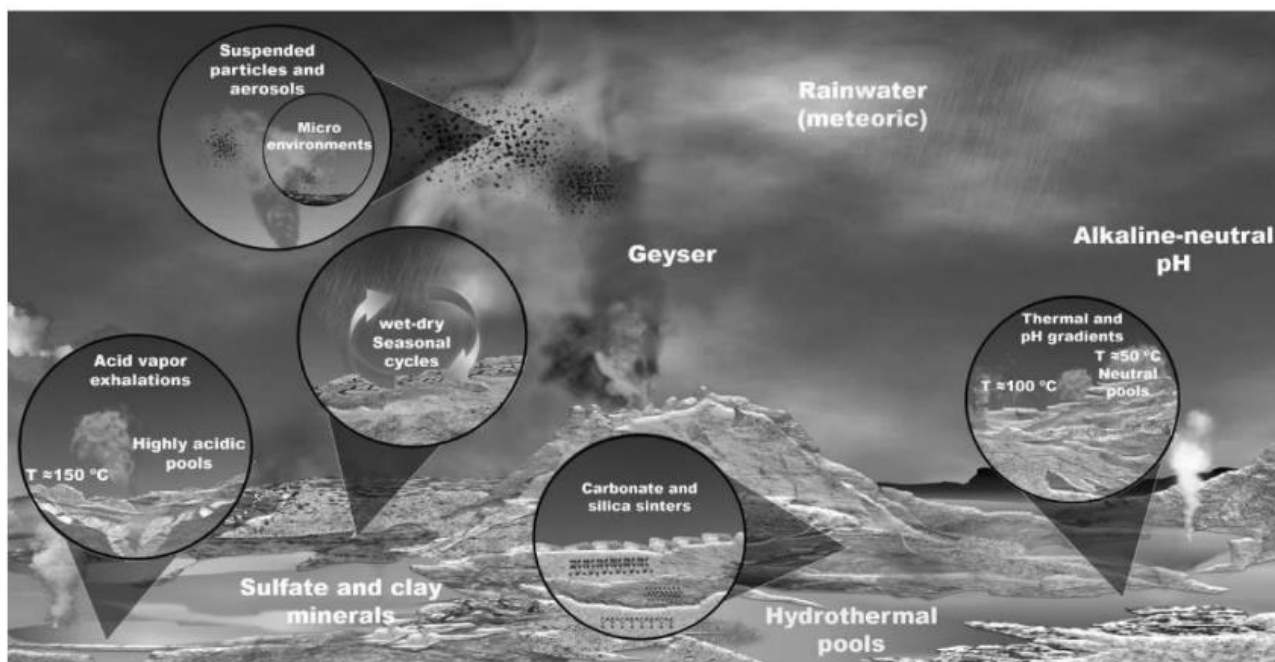


FIGURE 5.4.8 Representation of structures, processes, and gradients of key variables on the surface in association with active geothermal fields and epithermal deposits, as of Figure 5.4.4.

(virtually all systems). Most hydrothermal systems share minerals from about the same mineralogical hierarchical categories (silica, carbonates, sulfates, sulfides, clay minerals, etc.), but the distribution of such minerals may vary among different types of hydrothermal systems and even among different

vents of the same system. Strong mineralogical contrast may occur at very variable stretches, from millimeters to meters, even fractally in the same deposit (e.g., within the internal banding of a single mineralized chimney and on the surface from core to rim of venting in a VMS mineralized vent). There

is no straightforward explanation for such variation, which is multifactorial in nature. It may even happen that high-temperature fluids cross low-temperature mineral associations and vice versa. Additionally, minerals show natural variations in composition that may vary among different types of hydrothermal systems (*i.e.*, sphalerite may attain very different Fe contents) and even down to crystal scale.

3. Grain-size gradients (virtually all systems). Ever since their formation, crystals may naturally vary between coarse-grained to cryptocrystalline, even into amorphous phases. This is an important aspect for experimental matters because as grain size decreases, the overall specific surface of a mineral aggregate increases. Also, the grain size of a mineral aggregate can be relatively homogeneous or inhomogeneous. Grain size may be highly variable since the very moment in which a mineral aggregate is deposited, but grain sizes can be greatly modified during the life span of a hydrothermal system. Indeed, minerals can be “ground” by fracturing and deformed by diapiric ascent or slope sliding; the grain size of a mineral may increase due to thermal recrystallization (or replacement by another mineral), and gels and amorphous phases may eventually crystallize. However, these processes do not necessarily occur during the life span of a hydrothermal system, and these are issues that need to be addressed case by case.
4. Occurrence of silica and/or Fe-Mn oxide gels, or colloidal phases (VMS, shallow subaqueous systems, epithermal, black shales, SEDEX, Algoma-type BIF). Can the presence of silica and other inorganic species from gels have any role in the oligomerization of organic species? It has been demonstrated that amino acids interact with the surface of silica by different mechanism (Rimola et al. 2013 and reference therein). Moreover, once adsorbed, amino acids react to give DKP cyclic intermediates, which constitute a full research area, the study of the thermal transformations of amino acids catalyzed by silica (Rimola et al. 2013 and reference therein).
5. Occurrence of liquid interfaces with highly contrasting physicochemical characteristics. Such is the case of the interfaces among submarine brine pools, less saline hydrothermal fluids, and even less saline and cooler seawater (VMS and SEDEX); among some of these and hot molten sulfur (VMS and submarine volcanoes); or between two aqueous fluids with contrasting salinities, which will not mix easily on the continental surface (geothermal/epithermal). The experimental work concerning prebiotic synthesis is generally carried out between a liquid phase with dissolved organic molecules and a solid phase, which is the most common situation in natural hydrothermal systems. However, it is yet to be tested whether

some of the situations described previously may have a role in prebiotic chemistry.

6. Seasonal gradients for water supply (epithermal and other continental systems) or invasion/retreat of seawater upon low and high tides twice a day (shallow subaqueous systems). These gradients imply the variation in time of water availability either by (A) seasonality of meteoric recharge that may not compensate the evaporation of puddled water, or (B) the occurrence of puddles in intertidal areas filled with upwelling hydrothermal fluids and variable amounts of seawater. The relevance and potential of fluctuations in wet/dry or hydration/dehydration cycles for prebiotic synthesis have been already pointed out by Damer and Deamer (2015).
7. Occurrence of diffuse bubbling (epithermal, shallow subaqueous systems, including exceptionally shallow VMS and SEDEX systems) or aerosols with or without the occurrence of minute mineral particles alongside them in association with geysers, mud pots, or phreatomagmatic eruptions (geothermal/epithermal and other subaerial to shallow submarine/sublacustrine hydrothermal manifestations). It has been demonstrated that in bubbles and aerosols, many chemical reactions occur, and both types of interfaces represent heterogeneous microenvironments. Bubbles become more stable as they adsorb dissolved materials, thus concentrating these; afterward, the stabilized bubbles that contain organics act as nucleation sites for larger bubbles. This mechanism increases the concentration of organics (Lerman 2010) that could react to form more complex molecules.
8. Transition metals, which are available in aqueous solution elsewhere in all the hydrothermal systems described in the previous sections, may be effective catalysts for abiotic reactions that are involved in prebiotic synthesis by means of natural gases at temperatures $\leq 200^{\circ}\text{C}$ (Horita 2001).

5.4.6 FINAL CONSIDERATIONS

Hydrothermal systems in oceanic (submarine) or continental settings (subaerial, sublacustrine) may have played an important role in the synthesis of organic compounds in the early Earth. In order to understand the role of the various geological environments in prebiotic chemistry, a multidisciplinary approach is necessary, which includes chemistry and geology. There are many environments, both ancient and recent, that can be called hydrothermal. Although many experiments have been conducted to simulate the conditions of the most conspicuous environments (mostly VMS-type systems, both white and black smokers), little effort has been devoted to understanding the possible contributions to organic synthesis stemming from other likely hydrothermal environments. In this work, the possible role of other hydrothermal environments is highlighted, provided that their characteristics

also provide physicochemical variables, a broad variety of minerals, and a natural variability that could have been relevant in the synthesis of organic molecules from inorganic compounds. In order to contribute to a consensus on whether the participation of hydrothermal environments to chemical evolution was constructive or destructive, it is necessary to design more accurate experiments that combine not only the known physicochemical variables, but also their gradients in space and time. In this sense, recent literature in this matter increasingly aims at reproducing physicochemical conditions that are closer to natural gradients than earlier work. Although multivariable approaches to prebiotic chemistry are hard to manage, they will surely prove to be worthwhile endeavors, especially those that get as close as possible to the natural diversity of hydrothermal systems. In addition, the approach on which this paper relies provides many possibilities for conducting experiments that use heterogeneous interfaces of many kinds that would be firmly based on actual natural hydrothermal systems.

ACKNOWLEDGMENTS

The support of DGAPA-PAPIIT (No. IG100116 and IA203217) is acknowledged.

REFERENCES

- Abdelmoez, W., Nakahasi, T., and H. Yoshida. 2007. Amino acid transformation and decomposition in saturated subcritical water conditions. *Ind. Eng. Chem. Res.* 46: 5286–5294.
- Abelson, P. H. 1954. Amino acids in fossils. *Science* 119: 576.
- Alargov, D., Deguchi, S., Tsujii, K., and K. Horikoshi. 2002. Reaction behaviors of glycine under super- and subcritical water conditions. *Orig. Life Evol. Biosph.* 32: 1–12.
- Albinson, T., Norman, D. I., Cole, D., and B. A. Chomiak. 2001. Controls on formation of low-sulfidation epithermal deposits in Mexico: Constraints from fluid inclusion and stable isotope data. In: *New Mines and Discoveries in Mexico and Central America*, T. Albinson and C. E. Nelson (Eds.), *Soc. Econ. Geol. Spec. Publ.* pp. 1–32. No. 8. Boulder, CO.
- Allen, R. L., Weihed, P., Blandell, D. et al. 2002. Global comparisons of volcanic-associated massive sulphide districts. *Geol. Soc. Lond. Spec. Publ.* 204: 13–37.
- Alt, J. C., and W. C. Shanks. 1998. Sulfur in serpentinized oceanic peridotites: Serpentinization processes and microbial sulfate reduction. *J. Geophys. Res. B: Solid Earth* 103: 9917–9929.
- Alt, J. C., and W. C. Shanks. 2003. Serpentinization of abyssal peridotites from the MARK area, Mid-Atlantic Ridge: Sulfur geochemistry and reaction modeling. *Geochim. Cosmochim. Acta* 67: 641–653.
- Alt, J. C., and W. C. Shanks. 2006. Stable isotope compositions of serpentinite seamounts in the Mariana forearc: Serpentinization processes, fluid sources and sulfur metasomatism. *Earth Planet. Sci. Lett.* 242: 272–285.
- Andersson, E., and N. G. Holm. 2000. The stability of some selected amino acids under attempted redox constrained hydrothermal conditions. *Orig. Life Evol. Biosph.* 30: 9–23.
- Aubrey, A. D., Cleaves, H. J., and J. L. Bada. 2009. The role of submarine hydrothermal systems in the synthesis of amino acids. *Orig. Life Evol. Biosph.* 39: 91–108.
- Baaske, P., Weinert, F. M., Duhr, S., Lemke, K. H., Russell, M. J., and D. Braun. 2007. Extreme accumulation of nucleotides in simulated hydrothermal pore systems. *PNAS* 104: 9346–9351.
- Bach, W., Garrido, C. J., Paulick, H., Harvey, J., and M. Rosner. 2004. Seawater-peridotite interactions: First insights from ODP Leg 209, MAR 15 N. *Geochim. Geophys. Geosyst.* 5: Q09F26.
- Bach, W., Paulick, H., Garrido, C. J., Ildefonse, B., Meurer, W. P., and S. E. Humphris. 2006. Unraveling the sequence of serpentinization reactions: Petrography, mineral chemistry, and petrophysics of serpentinites from MAR 15 N (ODP Leg 209, Site 1274). *Geophys. Res. Lett.* 33: L13306.
- Bada, J. L., and A. Lazcano. 2002. Some like it hot, but not the first biomolecules. *Science* 296: 1982–1983.
- Bada, J. L., and A. Lazcano. 2009. The origin of life. In *Evolution: The First Four Billion Years*, M. Ruse and J. Travis (Eds.), pp. 49–79. Cambridge, MA: Harvard University Press.
- Bada, J. L., Miller, S. L., and M. Zhao. 1995. The stability of amino acids at submarine hydrothermal vent temperatures. *Orig. Life Evol. Biosph.* 25: 111–118.
- Ballard, R. D., and T. H. Van Andel. 1977. Morphology and tectonics of the inner rift valley at lat 36°50'N on the Mid-Atlantic Ridge. *GSA Bull.* 88: 507–530.
- Balodis, E., Madekufamba, M., Trevani, L. N., and P. R. Tremaine. 2012. Ionization constants and thermal stabilities of uracil and adenine under hydrothermal conditions as measured by in situ UV–visible spectroscopy. *Geochim. Cosmochim. Acta.* 93: 182–204.
- Barge, L. M., Doloboff, I. J., Russell, M. J., Vander Velde, D., White, L. M., Stucky, G. D., Baum, M. M., Zeytounian, J., Kidd, R., and I. Kanik. 2014. Pyrophosphate synthesis in iron mineral films and membranes simulating prebiotic submarine hydrothermal precipitates. *Geochim. Cosmochim. Acta* 128: 1–12.
- Baross, J. A., and S. E. Hoffman. 1985. Submarine hydrothermal vents and associated gradient environments as sites for the origin and evolution of life. *Orig. Life Evol. Biosph.* 15: 327–345.
- Barrie, C. T., and M. D. Hannington. 1999. Classification of volcanic-associated massive sulfide deposits based on host-rock deposition. *Rev. Econ. Geol.* 8: 1–11.
- Bates, A. E., Lee, R. W., Tunnicliffe, V., and M. D. Lamare. 2010. Deep-sea hydrothermal vent animals seek cool fluids in a highly variable thermal environment. *Nat. Commun.* 1: 14.
- Becerra, A., Delage, L., Islas, S., and A. Lazcano. 2007. The very early stages of biological evolution and the nature of the last common ancestor of the three major cell domains. *Annu. Rev. Ecol. Evol. Syst.* 38: 361–379.
- Beinlich, A., Plümper, O., Hövelmann, J., Austrheim, H., and B. Jamtveit. 2012. Massive serpentinite carbonation at Linnajavri, N-Norway. *Terra Nova* 24: 446–455.
- Bell, J. L. S., Palmer, D. A., Barnes, H. L., and S. E. Drummond. 1994. Thermal decomposition of acetate: III. Catalysis by mineral surfaces. *Geochim. Cosmochim. Acta* 58: 4155–4177.
- Bernhardt, G., Lüdemann, H. D., Jaenicke, R., König, H., and K. O. Stetter. 1984. Biomolecules are unstable under “black smoker” conditions. *Naturwissenschaften* 71: 583–586.
- Bowring, S. A., and I. S. Williams. 1999. Priscoan (4.00–4.03 Ga) orthogneisses from northwestern Canada. *Contrib. Mineral. Petrol.* 134: 3–16.
- Bowring, S., Housh, T., and C. Isachsen. 1990. *The Acasta Gneisses: Remnant of Earth's Early Crust*, Vol. 1, pp. 319–343. LPI Conference on the Origin of the Earth.
- Boyce, A. J., Coleman, M. L., and M. J. Russell. 1983. Formation of fossil hydrothermal chimneys and mounds from Silvermines, Ireland. *Nature* 306: 545–550.

- Braun, D., and A. Libchaber. 2002. Trapping of DNA by thermophoretic depletion and convection. *Phys. Rev. Lett.* 89: 188103.
- Buchanan, L. J. 1981. Precious metal deposits associated with volcanic environments in the Southwest. In: *Relations of Tectonics to Ore Deposits in the Southern Cordillera*, Vol. 14, W. R. Dickinson and W. D. Payne (Eds.), pp. 237–262. Tucson, AZ: Arizona Geological Society Digests.
- Budin, I., Bruckner, R. J., and J. W. Szostak. 2009. Formation of protocell-like vesicles in a thermal diffusion column. *J. Am. Chem. Soc.* 131: 9628–9629.
- Burcar, B. T., Barge, L. M., Trail, D., Watson, E. B., Russell, M. J., and L. B. McGown. 2015. RNA oligomerization in laboratory analogues of alkaline hydrothermal vent systems. *Astrobiology* 15: 509–522.
- Caird, R. A., Pufahl, P. K., Hiatt, E. E., Abram, M. B., Rocha, A. J. D., and T. K. Kyser. 2017. Ediacaran stromatolites and intertidal phosphorite of the Salitre Formation, Brazil: Phosphogenesis during the Neoproterozoic Oxygenation Event. *Sediment. Geol.* 350: 55–71.
- Camprubí, A. 2013. Tectonic and metallogenic history of Mexico. In *Tectonics, Metallogeny, and Discovery: The North American Cordillera and Similar Accretionary Settings*, Vol. 17, M. Colpron, T. Bissig, B. G. Rusk, and J. F. H. Thompson (Eds.), pp. 201–243. Boulder, CO: Society of Economic Geologist Special Publications.
- Camprubí, A., and T. Albinson. 2006. Depósitos epitermales en México: Actualización de su conocimiento y reclasificación empírica. *Bol. Soc. Geol. Mex.* 58: 27–81.
- Camprubí, A., and T. Albinson. 2007. Epithermal deposits in México – an update of current knowledge, and an empirical reclassification. In *Geology of México: Celebrating the Centenary of the Geological Society of Mexico*, Vol. 422, S. A. Alaniz-Álvarez and A. F. Nieto-Samaniego (Eds.), pp. 377–415. Boulder, CO: Special Paper of the Geological Society of America.
- Camprubí, A., Canet, C., Rodríguez-Díaz, A. A., Prol-Ledesma, R. M., Villanueva-Estrada, R. E., Blanco-Florido, D., and A. López-Sánchez. 2008. Geology, mineral deposits and hydrothermal activity in Bahía Concepción, Baja California Sur, Mexico. *Island Arc* 17: 6–25.
- Camprubí, A., González-Partida, E., Torró, L., Alfonso, P., Miranda-Gasca, M. A., Martini, M., Canet, C., and F. González-Sánchez. 2017. Mesozoic volcanogenic massive sulfide (VMS) deposits in Mexico. *Ore Geol. Rev.* 81: 1066–1083.
- Canet, C., and R. M. Prol-Ledesma. 2006. Procesos de mineralización en manantiales hidrotermales submarinos someros, ejemplos en México. *Bol. Soc. Geol. Mex.* 58: 83–102.
- Canet, C., Prol-Ledesma, R. M., Dando, P. R., Vázquez-Figueroa, V., Shumilin, E., Birosta, E., Sánchez, A., Robinson, C. J., Camprubí, A., and E. Tauler. 2010. Discovery of massive gas seepage along the Wagner Fault, northern Gulf of California. *Sediment. Geol.* 228: 292–303.
- Cavosie, A., Valley, J., and S. Wilde. 2005. Magmatic $\delta^{18}\text{O}$ in 4400–3900 Ma detrital zircons: A record of the alteration and recycling of crust in the Early Archean. *Earth Planet. Sci. Lett.* 235: 663–681.
- Chatterjee, S. 2018. Hydrothermal impact crater lakes and the origin of life. In *Handbook of Astrobiology*, V. Kolb (Ed.). Boca Raton, FL: Taylor & Francis Group.
- Chevaldonné, P., Desbruyères, D., and M. L. Haître. 1991. Time-series of temperature from three deep-sea hydrothermal vent sites. *Deep-Sea Res. A. Oceanogr. Res. Pap.* 38: 1417–1430.
- Chyba, C., and C. Sagan. 1992. Endogenous production, exogenous delivery and impact-shock synthesis of organic molecules: An inventory for the origins of life. *Nature* 355: 125–132.
- Cleaves, H. 2013. Prebiotic chemistry: Geochemical context and reaction screening. *Life* 3: 331–345.
- Cleaves II, H. J., Scott, A. M., Hill, F. C., Leszczynski, J., Sahai, N., and R. Hazen. 2012. Mineral–organic interfacial processes: Potential roles in the origins of life. *Chem. Soc. Rev.* 41: 5502–5525.
- Cnossen, I., Sanz-Forcada, J., Favata, F., Witasse, O., Zegers, T., and N. F. Arnold. 2007. Habitat of early life: Solar X-ray and UV radiation at Earth’s surface 4–3.5 billion years ago. *J. Geophys. Res. Planets* 112: E02008.
- Cockell, C. S. 2006. The origin and emergence of life under impact bombardment. *Philos. Trans. R. Soc. Lond. Ser. B.* 361: 1845–1856.
- Coffin, M. F., and O. Eldholm. 1994. Large igneous provinces: Crustal structure, dimensions, and external consequences. *Rev. Geophys.* 32: 1–36.
- Colín-García, M., Heredia, A., Cordero, G., Camprubí, A., Ortega-Gutiérrez, F., Negrón-Mendoza, A., Beraldi, H., and S. Ramos-Bernal. 2016. Hydrothermal vents and prebiotic chemistry: A review. *Bol. Soc. Geol. Mex.* 68: 599–620.
- Conly, A. G., Scott, S. D., and H. Bellon. 2011. Metalliferous manganese oxide mineralization associated with the Boléo Cu–Co–Zn district, Mexico. *Econ. Geol.* 106: 1173–1196.
- Corbett, G. J., and T. M. Leach. 1998. *Southwest Pacific Rim Gold-Copper Systems: Structure, Alteration and Mineralisation*. Boulder, CO: Society of Economic Geologists. Special Publications No. 6. 238 p.
- Corliss, J. B., Dymond, J., Gordon, L. I. et al. 1979. Submarine thermal aprings on the galápagos rift. *Science* 203: 1073–1083.
- Corliss, J. B., Baross, J. A., and Hoffman, S. E. 1980. Submarine hydrothermal systems: A probable site for the origin of life. Corvallis, OR: School of Oceanography, Oregon State University.
- Corliss, J. B., Baross, J. A., and S. E. Hoffman. 1981. An hypothesis concerning the relationship between submarine hot springs and the origin of life on Earth. *Oceanol. Acta* 4: 59–69.
- Cox, J. S., and T. M. Seward. 2007a. The reaction kinetics of alanine and glycine under hydrothermal conditions. *Geochim. Cosmochim. Acta* 71: 2264–2284.
- Cox, J. S., and T. M. Seward. 2007b. The hydrothermal reaction kinetics of aspartic acid. *Geochim. Cosmochim. Acta* 71: 797–820.
- Cox, J. S., and T. M. Seward. 2007c. The reaction kinetics of alanine and glycine under hydrothermal conditions. *Geochim. Cosmochim. Acta* 71: 2264–2284.
- Cuadros, J., Aldega, L., Vetterlein, J., Drickamer, K., and W. Dubbin. 2009. Reactions of lysine with montmorillonite at 80°C: Implications for optical activity, H⁺ transfer and lysine–montmorillonite binding. *J. Colloid Interface Sci.* 333: 78–84.
- Da Silva, L., Maurel, M. C., and D. Deamer. 2015. Salt-promoted synthesis of RNA-like molecules in simulated hydrothermal conditions. *J. Mol. Evol.* 80: 86–97.
- Dalai, P., Pleyer, H. L., Strasdeit, H., and S. Fox. 2017. The influence of mineral matrices on the thermal behavior of glycine. *Orig. Life Evol. Biosph.* 47: 427–452.
- Damer, B. and D. Deamer. 2015. Coupled phases and combinatorial selection in fluctuating hydrothermal pools: A scenario to guide experimental approaches to the origin of cellular life. *Life* 5: 872–887.
- de Ronde, C. E. J., Chadwick, W. W. Jr., Ditchburn, R. G., Embley, R. W., Tunnicliffe, V., Baker, E. T., Walker, S. L., Ferrini, V. L., and S. M. Merle. 2015. Molten sulfur lakes of intraoceanic arc volcanoes. In *Volcanic Lakes*, D. Rouwet, B. Christenson, F. Tassi, and J. Vandemeulebroeck (Eds.), pp. 261–288. Berlin, Germany: Springer-Verlag.

- de Wit, M. J. 2004. *Archean Greenstone Belts Do Contain Fragments of Ophiolites*, *Developments in Precambrian Geology*, Vol. 13, pp. 599–614. Elsevier.
- DeGuzman, V., Vercoutere, W., Shenasa, H., and D. Deamer. 2014. Generation of oligonucleotides under hydrothermal conditions by non-enzymatic polymerization. *J. Mol. Evol.* 78: 251–262.
- Delays, L., and A. Lazcano. 2005. Prebiological evolution and the physics of the origin of life. *Phys. Life Rev.* 2: 47–64.
- Deschamps, F., Godard, M., Guillot, S., and K. Hattori. 2013. Geochemistry of subduction zone serpentinites: A review. *Lithos* 178: 96–127.
- Ding, K., Seyfried, W. E., Zhang, Z., Tivey, M. K., Von Damm, K. L., and A. M. Bradley. 2005. The in situ pH of hydrothermal fluids at mid-ocean ridges. *Earth Planet. Sci. Lett.* 237: 167–174.
- Draganić, I. G., Bjergbakke, E., Draganić, Z. D., and K. Sehested. 1991. Decomposition of ocean waters by potassium-40 radiation 3800 Ma ago as a source of oxygen and oxidizing species. *Precambrian Res.* 52: 337–345.
- Estrada, C. F., Mamajanov, I., Hao, J., Sverjensky, D. A., Cody, G. D., and R. M. Hazen. 2017. Aspartate transformation at 200°C with brucite [Mg(OH)₂], NH₃, and H₂: Implications for prebiotic molecules in hydrothermal systems. *Chem. Geol.* 457: 162–172.
- Falk, E. S., and P. B. Kelemen. 2015. Geochemistry and petrology of listvenite in the Samail ophiolite, Sultanate of Oman: Complete carbonation of peridotite during ophiolite emplacement. *Geochim. Cosmochim. Acta.* 160: 70–90.
- Fan, D., Ye, J., and J. Li. 1999. Geology, mineralogy, and geochemistry of the Middle Proterozoic Wafangzi ferromanganese deposit, Liaoning Province, China. *Ore Geol. Rev.* 15: 31–53.
- Ferrari, F., and E. Szuszkiewicz. 2009. Cosmic rays: A review for astrobiologists. *Astrobiology* 9: 413–436.
- Franiatte, M., Richard, L., Elie, M., Nguyen-Trung, C., Perfetti, E., and D. E. LaRowe. 2008. Hydrothermal stability of adenine under controlled fugacities of N₂, CO₂ and H₂. *Orig. Life Evol. Biosph.* 38: 139–148.
- Franklin, J. M. 1996. Volcanic-associated massive sulphide base metals. In: *Geology of Canadian Mineral Deposit Types*, Vol. 8, O. R. Eckstrand, W. D. Sinclair, and R. I. Thorpe (Eds.), pp. 158–183. Ottawa, Canada: Geological Survey of Canada, Geology of Canada.
- Franklin, J. M., Gibson, H. L., Jonasson, I. R., and A. G. Galley. 2005. Volcanogenic massive sulfide deposits. In *Economic Geology One Hundredth Anniversary*, Vol. 1905–2005, J. W. Hedenquist, J. F. H. Thompson, and R. J. Goldfarb (Eds.), pp. 523–560. Littleton, CO: Society of Economic Geologists.
- Franklin, J. M., Lydon, J. W., and D. M. Sangster. 1981. Volcanic-associated massive sulfide deposits. In *Economic Geology Seventy-Fifth Anniversary*, B. J. Skinner (Ed.), pp. 485–627. Lancaster, PA: Economic Geology Publishing Company.
- Frost, B. R. 1985. On the stability of sulfides, oxides, and native metals in serpentinite. *J. Petrol.* 26: 31–63.
- Frost, B. R., Evans, K. A., Swapp, S. M., Beard, J. S., and F. E. Mothersole. 2013. The process of serpentinitization in dunite from New Caledonia. *Lithos* 178: 24–39.
- Früh-Green, G. L., Connolly, J. A., Plas, A., Kelley, D. S., and B. Grobety. 2004. Serpentinization of oceanic peridotites: Implications for geochemical cycles and biological activity. In *The Subseafloor Biosphere at Mid-ocean Ridges*, W. S. D. Wilcock, E. F. Delong, D. S. Kelley, J. A. Baross, and S. C. Cary (Eds.), pp. 119–136. Washington, DC: American Geophysical Union.
- Fuchida, S., Naraoka, H., and H. Masuda. 2017. Formation of diastereoisomeric piperazine-2,5-dione from DL-Alanine in the Presence of Olivine and Water. *Orig. Life Evol. Biosph.* 47: 83–92.
- Furnes, H., de Wit, M., and Y. Dilek. 2014. Precambrian greenstone belts host different ophiolite types. In *Evolution of Archean Crust and Early Life, Modern Approaches in Solid Earth Sciences*, Vol. 7, Y. Dilek and H. Furnes (Eds.), pp. 1–22. Dordrecht, the Netherlands: Springer.
- Gladman, B., Dones, L., Levison, H. F., and J. A. Burns. 2005. Impact seeding and reseeded in the inner solar system. *Astrobiology* 5: 483–496.
- Goodfellow, W. D. 1992. Chemical evolution of the oceans as discerned from the temporal distribution of sedimentary exhalative (SEDEX) Zn-Pb-Ag deposits. In *International Geological Congress, Kyoto, Japan, Programs and Abstracts*, p. 185.
- Goodfellow, W. D., Lydon, J. W., and R. J. W. Turner. 1993. Geology and genesis of stratiform sediment-hosted (SEDEX) zinc-lead-silver sulphide deposits. *Geol. Assoc. Can. Spec. Pap.* 40: 201–252.
- Grenne, T., and J. F. Slack. 2003. Paleozoic and Mesozoic silica-rich seawater: Evidence from hematitic chert (jasper) deposits. *Geology* 31: 319–322.
- Hannington, M. D., de Ronde, C. E. J., and S. Petersen. 2005. Sea-floor tectonics and submarine hydrothermal systems. In *Economic Geology One Hundredth Anniversary*, Vol. 1905–2005, J. W. Hedenquist, J. F. H. Thompson, and R. J. Goldfarb (Eds.), pp. 111–142. Littleton, CO: Society of Economic Geologists.
- Hansen, L. D., Dipple, G. M., Gordon, T. M., and D. A. Kellett. 2005. Carbonated serpentinite (listwanite) at Atlin, British Columbia: A geological analogue to carbon dioxide sequestration. *Can. Mineral.* 43: 225–239.
- Hazen, R. M., and D. A. Sverjensky. 2010. Mineral surfaces, geochemical complexities, and the origins of life. *Cold Spring Harb. Perspect Biol.* 2: a002162.
- Hedenquist, J. W., Arribas, A. Jr., and E. Urien-Gonzalez. 2000. Exploration for epithermal gold deposits. *Rev. Econ. Geol.* 13: 245–277.
- Hedenquist, J. W., and Y. A. Taran. 2013. Modeling the formation of advanced argillic lithocaps: Volcanic vapor condensation above porphyry intrusions. *Econ. Geol.* 108: 1523–1540.
- Hinsken, T., Bröcker, M., Strauss, H., and F. Bulle. 2017. Geochemical, isotopic and geochronological characterization of listvenite from the Upper Unit on Tinos, Cyclades, Greece. *Lithos* 282: 281–297.
- Holland, H. D. 2003. The geologic history of seawater. In *Treatise on Geochemistry*, Vol. 6, K. K. Turekian and H. D. Holland (Eds.), pp. 583–625. Oxford, UK: Elsevier Science.
- Holm, N. G. 1992. Why are hydrothermal systems proposed as plausible environments for the origin of life? In *Marine Hydrothermal Systems and the Origin of Life: Report of SCOR Working Group 91*, N. G. Holm (Ed.), pp. 5–14. Dordrecht, the Netherlands: Springer.
- Holm, N. G., and E. Andersson. 2005. Hydrothermal simulation experiments as a tool for studies of the origin of life on Earth and other terrestrial planets: A review. *Astrobiology* 5: 444–160.
- Horita, J. 2001. Carbon isotope exchange in the system CO₂–CH₄ at elevated temperatures. *Geochim. Cosmochim. Acta* 65: 1907–1919.
- Huber, C., and G. Wächtershäuser. 1998. Peptides by activation of amino acids with CO on (Ni, Fe)S surfaces. *Orig. Life Evol. Biosph.* 281: 670–672.
- Iizuka, T., Horie, K., Komiya, T., Maruyama, S., Hirata, T., Hidaka, H., and B. F. Windley. 2006. 4.2 Ga zircon xenocryst in an Acasta gneiss from northwestern Canada: Evidence for early continental crust. *Geology* 34: 245–248.

- Iizuka, T., Komiya, T., and S. Maruyama. 2007. Chapter 3.1: The early Archean Acasta Gneiss Complex: Geological, geochronological and isotopic studies and implications for early crustal evolution. In *Developments in Precambrian Geology*, M. J. van Kranendonk, R. H. Smithies, and V. C. Bennett (Eds.), pp. 127–147. Amsterdam, the Netherlands: Elsevier.
- Imai, E.-I., Honda, H., Hatori, K., Brack, A., and K. Matsuno. 1999. Elongation of oligopeptides in a simulated submarine hydrothermal system. *Science* 283: 831–833.
- Islam, M. N., Kaneko, T., and K. Kobayashi. 2003. Reaction of amino acids in a supercritical water-flow reactor simulating submarine hydrothermal systems. *Bull. Chem. Soc. Jpn.* 76: 1171–1178.
- Ito, M., Gupta, L. P., Masuda, H., and H. Kawahata. 2006. Thermal stability of amino acids in seafloor sediment in aqueous solution at high temperature. *Org. Geochem.* 37: 177–188.
- Ito, M., Yamaoka, K., Masuda, H., Kawahata, H., and L. P. Gupta. 2009. Thermal stability of amino acids in biogenic sediments and aqueous solutions at seafloor hydrothermal temperatures. *Geochem. J.* 43: 331–341.
- Jackson, J. B. 2016. Natural pH gradients in hydrothermal alkali vents were unlikely to have played a role in the origin of life. *J. Mol. Evol.* 83: 1–11.
- Jacobsen, S. B. 2003. How old is planet Earth? *Science* 300: 1513–1514.
- James, R. H., Green, D. R. H., Stock, M. J., Alker, B. J., Banerjee, N. R., Cole, C., German, C. R., Huvenne, V. A. I., Powell, A. M., and D. P. Connelly. 2014. Composition of hydrothermal fluids and mineralogy of associated chimney material on the East Scotia Ridge back-arc spreading centre. *Geochim. Cosmochim. Acta* 139: 47–71.
- Jébrak, M., and E. Marcoux. 2008. *Géologie des ressources minérales*. Québec, Canada: Ministère des ressources naturelles et de la faune du Québec, 667 p.
- Ji, F., Zhou, H., and Q. Yang. 2008. The abiotic formation of hydrocarbons from dissolved CO₂ under hydrothermal conditions with cobalt-bearing magnetite. *Orig. Life Evol. Biosph.* 38: 117–125.
- Johnson, S. C., Large, R. R., Coveney, R. M., Kelley, K. D., Slack, J. F., Steadman, J. A., Gregory, D. D., Sack, P. J., and S. Meffre. 2017. Secular distribution of highly metalliferous black shales corresponds with peaks in past atmosphere oxygenation. *Miner. Deposita* 52: 791–798.
- Jorge, S., Melgarejo, J. C., and M. P. Alfonso. 1997. Sedimentos exhalatixos y sus derivados metamórficos. In *Atlas de Asociaciones Minerales en Lámina Delgada*, J. C. Melgarejo (Ed.), pp. 287–308. Barcelona, Spain: Edicions Universitat de Barcelona – Fundació Folch.
- Juteau, T., and R. Maury. 1997. *Géologie de la Croûte Océanique*. Petrologie et Dynamique: Endogènes, 569 p. Dunod, Montrouge (Haus-de-Seine), France.
- Kasting, J. F. 1993a. Earth's early atmosphere. *Science* 259: 920–926.
- Kasting, J. F. 1993b. Evolution of the Earth's atmosphere and hydrosphere. In *Organic Geochemistry Topics in Geobiology*, Vol. 11. M. H. Engel, and S. A. Macko (Eds.), pp. 611–623. Boston, MA: Springer.
- Kawamura, K. 2005. Behaviour of RNA under hydrothermal conditions and the origins of life. *Int. J. Astrobiol.* 3: 301–309.
- Kawamura, K. 2011. Development of micro-flow hydrothermal monitoring systems and their applications to the origin of life study on Earth. *Anal. Sci.* 27: 675–675.
- Kawamura, K., and M. Shimahashi. 2008. One-step formation of oligopeptide-like molecules from Glu and Asp in hydrothermal environments. *Naturwissenschaften* 95: 449–454.
- Kelemen, P. B., Matter, J., Streit, E. E., Rudge, J. F., Curry, W. B., and J. Blusztajn. 2011. Rates and mechanisms of mineral carbonation in peridotite: Natural processes and recipes for enhanced, in situ CO₂ capture and storage. *Annu. Rev. Earth Planet. Sci.* 39: 545–576.
- Kelley, D. S., Karson, J. A., Blackman, D. K. et al. 2001. An off-axis hydrothermal vent field near the Mid-Atlantic Ridge at 30°N. *Nature* 412: 145–149.
- Kelley, D. S., Baross, J. A., and Delaney, J. R. 2002. Volcanoes, fluids, and life at mid-ocean ridge spreading centers. *Annu. Rev. Earth Planet. Sci.* 30: 385–491.
- Klein, F., and W. Bach. 2009. Fe–Ni–Co–O–S phase relations in peridotite–seawater interactions. *J. Petr.* 50: 37–59.
- Klein, F., Bach, W., Jöns, N., McCollom, T., Moskowicz, B., and T. Berquó. 2009. Iron partitioning and hydrogen generation during serpentinization of abyssal peridotites from 15 N on the Mid-Atlantic Ridge. *Geochim. Cosmochim. Acta* 73: 6868–6893.
- Klein, F., Humphris, S. E., Guo, W., Schubotz, F., Schwarzenbach, E. M., and W. D. Orsi. 2015. Fluid mixing and the deep biosphere of a fossil Lost City-type hydrothermal system at the Iberia Margin. *PNAS* 112: 12036–12041.
- Klingler, D., Berg, J., and H. Vogel. 2007. Hydrothermal reactions of alanine and glycine in sub- and supercritical water. *J. Supercrit. Fluids* 43: 112–119.
- Knauth, L. P. 2005. Temperature and salinity history of the Precambrian ocean: Implications for the course of microbial evolution. *Palaeogeogr. Palaeoclimatol. Palaeoecol.* 219: 53–69.
- Kohara, M., Gamo, T., Yanagawa, H., and K. Kobayashi. 1997. Stability of amino acids in simulated hydrothermal vent environments. *Chem. Lett.* 26: 1053–1054.
- Komiya, T., Hirata, T., Kitajima, K., Yamamoto, S., Shibuya, T., Sawaki, Y., Ishikawa, T., Shu, D., Li, Y., and J. Han. 2008. Evolution of the composition of seawater through geologic time, and its influence on the evolution of life. *Gondwana Res.* 14: 159–174.
- Komiya, T., Maruyama, S., Masuda, T., Nohda, S., Hayashi, M., and K. Okamoto. 1999. Plate tectonics at 3.8–3.7 Ga: Field evidence from the Isua accretionary complex, southern West Greenland. *J. Geol.* 107: 515–554.
- Konn, C., Charlou, J. L., Holm, N. G., and O. Mousis. 2015. The production of methane, hydrogen, and organic compounds in ultramafic-hosted hydrothermal vents of the mid-atlantic ridge. *Astrobiology* 15: 381–399.
- Lane, N. 2017. Proton gradients at the origin of life. *BioEssays* 39: 1600217.
- Larralde, R., Robertson, M. P., and S. L. Miller. 1995. Rates of decomposition of ribose and other sugars: Implications for chemical evolution. *PNAS* 92: 8158–8160.
- Larter, R. C. L., Boyce, A. J., and M. J. Russell. 1981. Hydrothermal pyrite chimneys for the Ballynoe baryte deposits, Silvermines, County Tipperary, Ireland. *Miner. Deposita* 16: 309–318.
- Lazcano, A., and S. L. Miller. 1994. How long did it take for life to begin and evolve to cyanobacteria? *J. Mol. Evol.* 39: 546–554.
- Laznicka, P. 2006. *Giant Metallic Deposits, Future Sources of Industrial Minerals*. Heidelberg, Germany: Springer, 732 p.
- Leach, D. L., Sangster, D. F., Kelley, K. D., Large, R. R., Garven, G., Allen, C. R., Gutzmer, J., and S. Walters. 2005. Sediment-hosted lead-zinc deposits: A global perspective. In *Economic*

- Geology One Hundredth Anniversary*, Vol. 1905–2005, J. W. Hedenquist, J. F. H. Thompson, and R. J. Goldfarb (Eds.), pp. 561–607. Littleton, CO: Society of Economic Geologists.
- Lee, N., Foustoukos, D. I., Sverjensky, D. A., Cody, G. D., and R. M. Hazen. 2014. The effects of temperature, pH and redox state on the stability of glutamic acid in hydrothermal fluids. *Geochim. Cosmochim. Acta* 135: 66–86.
- Lemke, K. H., Rosenbauer, R. J., and D. K. Bird. 2009. Peptide synthesis in early Earth hydrothermal systems. *Astrobiology* 9: 141–146.
- Lerman, L. 2010. The primordial bubble: Water, symmetry-breaking, and the origin of life. In *Water and Life: The Unique Properties of Water*, R. M. Lynden-Bell, S. C. Morris, J. D. Barrow, J. L. Finney, and C. Harper (Eds.), pp. 259–290. Boca Raton, FL: CRC Press.
- Levin, H. 2009. *The Earth through Time*. Hoboken, NJ: John Wiley & Sons, 624 p.
- Levy, M., and S. L. Miller. 1998. The stability of the RNA bases: Implications for the origin of life. *PNAS* 95: 7933–7938.
- Li, J., Wang, X., Klein, M. T., and T. B. Brill. 2002. Spectroscopy of hydrothermal reactions, 19: pH and salt dependence of decarboxylation of α -alanine at 280–330°C in an FT-IR spectroscopy flow reactor. *Int. J. Chem. Kinet.* 34: 271–277.
- Lydon, J. W. 1988. Volcanogenic massive sulphide deposits, Part 2: Genetic models. In *Ore Deposit Models*, R. G. Roberts and P. A. Sheahan (Eds.), pp. 155–181. St. John's, Canada: Geological Association of Canada, Geoscience Canada, Reprint Series, 3.
- Lydon, J. W. 1996. Sedimentary exhalative sulphides (sedex). In *Geology of Canadian Mineral Deposit Types*, Vol. 8, O. R. Eckstrand, W. D. Sinclair, and R. I. Thorpe (Eds.), pp. 130–152. Ottawa-Ontario, Canada: Geological Survey of Canada, Geology of Canada.
- Lyons, T. W., Gellatly, A. M., McGoldrick, P. J., and L. C. Kah. 2006. Proterozoic sedimentary exhalative (SEDEX) deposits and links to evolving global ocean chemistry. *Geol. Soc. Am. Mem.* 198: 169–184.
- Marshall, W. L. 1994. Hydrothermal synthesis of amino acids. *Geochim. Cosmochim. Acta* 58: 2099–2106.
- Martin, W., Baross, J., Kelley, D., and M. J. Russell. 2008. Hydrothermal vents and the origin of life. *Nat. Rev. Microbiol.* 6: 805–814.
- Mast, C. B., Schink, S., Gerland, U., and D. Braun. 2013. Escalation of polymerization in a thermal gradient. *PNAS* 110: 8030–8035.
- McCormell, T. M. 2013. The influence of minerals on decomposition of the *n*-alkyl- α -amino acid norvaline under hydrothermal conditions. *Geochim. Cosmochim. Acta* 104: 330–357.
- McCormell, T. M., Ritter, G., and Simoneit, B. R. T. 1999. Lipid synthesis under hydrothermal conditions by Fischer-Tropsch-type reactions. *Orig. Life Evol. Biosph.* 29: 153–166.
- McCormell, T. M., and J. S., Seewald. 2003a. Experimental constraints on the hydrothermal reactivity of organic acids and acid anions: I. Formic acid and formate. *Geochim. Cosmochim. Acta* 67: 3625–3644.
- McCormell, T. M., and J. S. Seewald. 2003b. Experimental study of the hydrothermal reactivity of organic acids and acid anions: II. Acetic acid, acetate, and valeric acid. *Geochim. Cosmochim. Acta* 67: 3645–3664.
- McDermott, J. M., Seewald, J. S., German, C. R., and S. P. Sylva. 2015. Pathways for abiotic organic synthesis at submarine hydrothermal fields. *PNAS* 112: 7668–7672.
- Miller, S. L. 1953. A production of amino acids under possible primitive Earth conditions. *Science* 117: 528–529.
- Miller, S. L. 1993. The prebiotic synthesis of organic compounds on the early Earth. In *Organic Geochemistry: Principles and Applications*, M. H. Engel, and S. A. Macko (Eds.), pp. 625–636. Boston, MA: Springer US.
- Miller, S. L., and L. E. Orgel. 1974. *The Origins of Life on the Earth*. Englewood Cliffs, NJ: Prentice-Hall.
- Miller, S. L., and J. L. Bada. 1988. Submarine hot springs and the origin of life. *Nature* 334: 609–611.
- Misra, K. C. 1999. *Understanding Mineral Deposits*. Dordrecht, the Netherlands: Kluwer Academic Publishers, 845 p.
- Mojzsis, S. J., Arrhenius, G., McKeegan, K. D., Harrison, T. M., Nutman, A. P., and C. R. L. Friend. 1996. Evidence for life on Earth before 3,800 million years ago. *Nature* 384: 55–59.
- Möller, F. M., Kriegel, F., Kieß, M., Sojo, V., and D. Braun. 2017. Steep pH gradients and directed colloid transport in a microfluidic alkaline hydrothermal pore. *Angew. Chem.* 56: 2340–2344.
- Mossman, D. J., Gauthier-Lafaye, F., and S. E. Jackson. 2005. Black shales, organic matter, ore genesis and hydrocarbon generation in the Paleoproterozoic Franceville Series, Gabon. *Precambrian Res.* 137: 253–272.
- Nasir, S., Al Sayigh, A. R., Al Harthy, A., Al-Khribash, S., Al-Jaaidi, O., Musllam, A., Al-Mishwat, A., and S. Al-Bu'saidi. 2007. Mineralogical and geochemical characterization of listwaenite from the Semail Ophiolite, Oman. *Chem Erde.* 67: 213–228.
- Niether, D., Afanasenkau, D., Dhont, J. K. G., and S. Wiegand. 2016. Accumulation of formamide in hydrothermal pores to form prebiotic nucleobases. *PNAS* 113: 4272–4277.
- Nisbet, E. G., and N. H. Sleep. 2001. The habitat and nature of early life. *Nature* 409: 1083–1091.
- Novikov, Y., and S. D. Copley. 2013. Reactivity landscape of pyruvate under simulated hydrothermal vent conditions. *PNAS* 110: 13283–13288.
- Nutman, A. P., Allaart, J. H., Bridgwater, D., Dimroth, E., and M. Rosing. 1984. Stratigraphic and geochemical evidence for the depositional environment of the early Archaean Isua supra-crustal belt, southern West Greenland. *Precambrian Res.* 25: 365–396.
- Ogasawara, H., Yoshida, A., Imai, E., Honda, H., Hatori, K., and K. Matsuno. 2000. Synthesizing oligomers from monomeric nucleotides in simulated hydrothermal environments. *Orig. Life Evol. Biosph.* 30: 519–526.
- Ogata, Y., Imai, E., Honda, H., Hatori, K., and K. Matsuno. 2000. Hydrothermal circulation of seawater through hot vents and contribution of interface chemistry to prebiotic synthesis. *Orig. Life Evol. Biosph.* 30: 527–537.
- Ohmoto, H. 1996. Formation of volcanogenic massive sulfide deposits: The Kuroko perspective. *Ore Geol. Rev.* 10: 135–177.
- Ohmoto, H., Watanabe, Y., Yamaguchi, K. E., Naraoka, H., Haruna, M., Kakegawa, T., Hayashi, K.-I., and Y. Kato. 2006. Chemical and biological evolution of early Earth: Constraints from banded iron formations. In *Evolution of Early Earth's Atmosphere, Hydrosphere, and Biosphere – Constraints from Ore Deposits*, Vol. 198, S. E., Kesler and H. Ohmoto (Eds.), pp. 291–333. Geological Society of America Memoir.
- Papavassiliou, K., Voudouris, P., Kanellopoulos, C., Glasby, G., Alfieris, D., and I. Mitsis. 2017. New geochemical and mineralogical constraints on the genesis of the Vani hydrothermal manganese deposit at NW Milos Island, Greece: Comparison with the Aspro Gialoudi deposit and implications for the formation of the Milos manganese mineralization. *Ore Geol. Rev.* 80: 594–611.

- Parker, E. T., Cleaves, H. J., Callahan, M. P., Dworkin, J. P., Glavin, D. P., Lazcano, A., and J. L. Bada. 2011. Prebiotic synthesis of methionine and other sulfur-containing organic compounds on the primitive Earth: A contemporary reassessment based on an unpublished 1958 Stanley Miller experiment. *Orig. Life Evol. Biosph.* 41: 201–212.
- Pašava, J. 1993. Anoxic sediments—an important environment for PGE: An overview. *Ore Geol. Rev.* 8: 425–445.
- Piercey, S. J. 2011. The setting, style, and role of magmatism in the formation of volcanogenic massive sulfide deposits. *Miner. Deposita* 46: 449–471.
- Pirajno, F. 2009. *Hydrothermal Processes and Mineral Systems*. East Perth, Australia, Springer, 1250 p.
- Pope, K. O., Kieffer, S. W., and D. E. Ames. 2006. Impact melt sheet formation on Mars and its implication for hydrothermal systems and exobiology. *Icarus* 183: 1–9.
- Povolo, D., and J. R. Vallentyne. 1964. Thermal reaction kinetics of the glutamic acid-pyroglytamic acid system in water. *Geochim. Cosmochim. Acta.* 28: 731–734.
- Power, I. M., Wilson, S. A., and G. M. Dipple. 2013. Serpentinization for CO₂ sequestration. *Elements* 9: 115–121.
- Proskurowski, G., Lilley, M. D., Seewald, J. S., Früh-Green, G. L., Olson, E. J., Lupton, J. E., Sylva, S. P., and D. S., Kelley. 2008. Abiogenic hydrocarbon production at lost city hydrothermal field. *Science* 319: 604–607.
- Qian, Y., Engel, M. H., Macko, S. A., Carpenter, S., and J. W. Deming. 1993. Kinetics of peptide hydrolysis and amino acid decomposition at high temperature. *Geochim. Cosmochim. Acta* 57: 3281–3293.
- Rimola, A., Costa, D., Sodupe, M., Lambert, J.-F., and P. Ugliengo. 2013. Silica surface features and their role in the adsorption of biomolecules: computational modeling and experiments. *Chem. Rev.* 113: 4216–4313.
- Roedder, E. 1990. Fluid inclusion analysis—prologue and epilogue. *Geochim. Cosmochim. Acta* 54: 495–508.
- Ruiz-Mirazo, K., Briones, C., and A. de la Escosura. 2014. Prebiotic Systems Chemistry: New Perspectives for the Origins of Life. *Chem. Rev.* 114: 285–366.
- Russell, M. J., and W. Martin. 2004. The rocky roots of the acetyl-CoA pathway. *Trends Biochem. Sci.* 29: 358–363.
- Russell, M. J., Hall, A. J., and D. Turner. 1989. In vitro growth of iron sulphide chimneys: Possible culture chambers for origin-of-life experiments. *Terra Nova* 1: 238–241.
- Russell, M. J., Solomon, M., and J. L. Walshe. 1981. The genesis of sediment-hosted, exhalative zinc + lead deposits. *Miner. Deposita* 16: 113–127.
- Ryder, G. 2003. Bombardment of the Hadean Earth: Wholesome or Deleterious? *Astrobiology* 3: 3–6.
- Sakai, R., Kusakabe, M., Noto, M. and T. Ishii. 1990. Origin of waters responsible for serpentinization of the Izu-Ogasawara-Mariana forearc seamounts in view of hydrogen and oxygen isotope ratios. *Earth Planet. Sci. Lett.* 100: 291–303.
- Sakata, K., Kitadai, N., and T. Yokoyama. 2010. Effects of pH and temperature on dimerization rate of glycine: Evaluation of favorable environmental conditions for chemical evolution of life. *Geochim. Cosmochim. Acta* 74: 6841–6851.
- Sangster, D. F. 2018. Toward an integrated genetic model for vent-distal SEDEX deposits. *Miner. Deposita* 53: 509–527.
- Sangster, D. F., and E. M. Hillary. 1998. SEDEX lead-zinc deposits: Proposed sub-types and their characteristics. *Explor. Min. Geol.* 7: 341–357.
- Sato, N., Quitain, A. T., Kang, K., Daimon, H., and K. Fujie. 2004. Reaction kinetics of amino acid decomposition in high-temperature and high-pressure water. *Ind. Eng. Chem. Res.* 43: 3217–3222.
- Schardt, C. 2016. Hydrothermal fluid migration and brine pool formation in the Red Sea: Atlantis II Deep. *Miner. Deposita* 51: 89–111.
- Schoonen, M., Smirnov, A., and C. Cohn. 2004. A perspective on the role of minerals in prebiotic synthesis. *AMBIO* 33: 539–551.
- Schwarzenbach, E. M., Gazel, E., and M. J. Caddick. 2014. Hydrothermal processes in partially serpentinized peridotites from Costa Rica: Evidence from native copper and complex sulfide assemblages. *Contrib. Mineral. Petrol.* 168: 1079.
- Schwarzenbach, E. M., Caddick, M. J., Beard, J. S., and R. J. Bodnar. 2016. Serpentinization, element transfer, and the progressive development of zoning in veins: Evidence from a partially serpentinized harzburgite. *Contrib. Mineral. Petrol.* 171: 5.
- Schwille, P. 2017. How simple could life be? *Angew. Chem. Int. Ed.* 56: 10998–11002.
- Shibuya, T., Komiya, T., Nakamura, K., Takai, K., and S. Maruyama. 2010. Highly alkaline, high-temperature hydrothermal fluids in the early Archean ocean. *Precambrian Res.* 182: 230–238.
- Sillitoe, R. H. 2015. Epithermal paleosurfaces. *Miner. Deposita* 50: 767–793.
- Sillitoe, R. H., and J. W. Hedenquist. 2003. Linkages between volcanotectonic settings, ore-fluid compositions, and epithermal precious metal deposits. *Soc. Econ. Geol. Spec. Publ.* 10: 314–343.
- Simmons, S. F., White, N. C., and D. A. John. 2005. Geological characteristics of epithermal precious and base metal deposits. In *Economic Geology One Hundredth Anniversary*, Vol. 1905–2005, J. W. Hedenquist, J. F. H. Thompson, and R. J. Goldfarb (Eds.), pp. 485–522. Littleton, CO: Society of Economic Geologist.
- Slack, J. F., Selby, D., and J. A. Dumoulin. 2015. Hydrothermal, biogenic, and seawater components in metalliferous black shales of the brooks range, Alaska: Synsedimentary metal enrichment in a carbonate ramp setting. *Econ. Geol.* 110: 653–675.
- Smirnov, A., Hausner, D., Laffers, R., Strongin, D. R., and M. A. Schoonen. 2008. Abiotic ammonium formation in the presence of Ni-Fe metals and alloys and its implications for the Hadean nitrogen cycle. *Geochem. Trans.* 9: 5.
- Stoffregen, R. E. 1987. Genesis of acid-sulfate alteration and Au–Cu–Ag mineralization at Summitville, Colorado. *Econ. Geol.* 82: 1575–1591.
- Stüeken, E. E., Anderson, R. E., Bowman, J. S., Brazelton, W. J., Colangelo-Lillis, J., Goldman, A. D., Som, S. M., and J. A. Baross. 2013. Did life originate from a global chemical reactor? *Geobiology* 11: 101–126.
- Tarasov, V. G., Gebruk, A. V., Mironov, A. N., and L. I. Moskalev. 2005. Deep-sea and shallow-water hydrothermal vent communities: Two different phenomena? *Chem. Geol.* 224: 5–39.
- Tarasov, V. G., Propp, M. V., Propp, L. N., Zhirmunsky, A. V., Namsaraev, B. B., Gorlenko, V. M., and D. A. Starynin. 1990. Shallow-water gasohydrothermal vents of Ushishir volcano and the ecosystem of Kraternaya Bight (the Kurile Islands). *Mar. Ecol.* 11: 1–23.
- Tiercelin, J. J., Pflumio, C., Cartec, M., Boulègue, J., Gente, P., Rolet, J., Coussement, C., Stetter, K. O., Huber, R., Buku, S., and W. Mifundu. 1993. Hydrothermal vents in the Lake Tanganyika, East Africa Rift System. *Geology* 21: 499–502.
- Tivey, M. K. 2007. Generation of seafloor hydrothermal vent fluids and associated mineral deposits. *Oceanography* 20: 50–65.

- Tsikouras, B., Karipi, S., Grammatikopoulos, T. A., and K. Hatzipanagiotou. 2006. Listwaenite evolution in the ophiolite melange of Iti Mountain (continental Central Greece). *Eur. J. Mineral.* 18: 243–255.
- Uçurum, A. 1998. Application of the correspondence-type geostatistical analysis on the Co, Ni, As, Ag and Au concentrations of the listwaenites from serpentinites in the Divrigi and Kuluncak Ophiolitic Mélanges. *Turk. J. Earth Sci.* 7: 87–96.
- Uçurum, A. 2000. Listwaenites in Turkey: Perspectives on formation and precious metal concentration with reference to occurrences in east-central Anatolia. *Ofioliti* 25: 15–29.
- Vallentyne, J. R. 1964. Biogeochemistry of organic matter—II Thermal reaction kinetics and transformation products of amino compounds. *Geochim. Cosmochim. Acta* 28: 157–188.
- Valley, J. W., Peck, W. H., King, E. M., and S. A. Wilde. 2002. A cool early Earth. *Geology* 30: 351–354.
- van der Zwan, F. M., Devey, C. W., Augustin, N., Almeev, R. R., Bantan, R. A., and A. Basaham. 2015. Hydrothermal activity at the ultraslow- to slow-spreading Red Sea Rift traced by chlorine in basalt. *Chem. Geol.* 405: 63–81.
- Vázquez-Figueroa, V., Canet, C., Prol-Ledesma, R. M., Sánchez, A., Dando, P., Camprubí, A., Robinson, C. J., and G. Hiriart Le Bert. 2009. Batimetría y características hidrográficas (Mayo, 2007) en las Cuencas de Consag y Wagner, Norte del Golfo de California, México. *Bol. Soc. Geol. Mex.* 61: 119–127.
- Von Damm, K. L. 2013. Controls on the chemistry and temporal variability of seafloor hydrothermal fluids. In *Seafloor Hydrothermal Systems: Physical, Chemical, Biological, and Geological Interactions*, pp. 222–247. Washington, DC: American Geophysical Union.
- Von Damm, K. L., Edmond, J. M., Grant, B., Measures, C. I., Walden, B., and R. F. Weiss. 1985. Chemistry of submarine hydrothermal solutions at 21 °N, East Pacific Rise. *Geochim. Cosmochim. Acta* 49: 2197–2220.
- Wacey, D., Kilburn, M. R., Saunders, M., Cliff, J., and M. D. Brasier. 2011a. Microfossils of sulphur-metabolizing cells in 3.4-billion-year-old rocks of Western Australia. *Nat. Geosci.* 4: 698–703.
- Wacey, D., Mcloughlin N., and M. D. Brasier. 2008. Looking through windows onto the earliest history of life on earth and mars. In *From Fossils to Astrobiology: Records of Life on Earth and Search for Extraterrestrial Biosignatures*, J. Seckbach and M. Walsh (Eds.), pp. 39–68. Dordrecht, the Netherlands: Springer.
- Wacey, D., Saunders, M., Cliff, J., and M. D. Brasier. 2011b. Microfossils of sulphur-metabolizing cells in 3.4-billion-year-old rocks of Western Australia. *Nature* 4: 698–702.
- Wächtershäuser, G. 1990. The case for the chemoautotrophic origin of life in an iron-sulfur world. *Orig. Life Evol. Biosph.* 20: 173–176.
- Walker, S. I. 2017. Origins of life: A problem for physics, a key issues review. *Rep. Prog. Phys.* 80: 092601.
- Weber, A. L. 2004. Kinetics of organic transformations under mild aqueous conditions: Implications for the origin of life and its metabolism. *Orig. Life Evol. Biosph.* 34: 473–495.
- White, N. C., and Hedenquist, J. W. 1990. Epithermal environments and styles of mineralization: Variations and their causes, and guidelines for exploration. *J. Geochem. Explor.* 36: 445–474.
- White, L. M., Bhartia, R., Stucky, G. D., Kanik, I., and M. J. Russell. 2015. Mackinawite and greigite in ancient alkaline hydrothermal chimneys: Identifying potential key catalysts for emergent life. *Earth Planet. Sci. Lett.* 430: 105–114.
- White, R. H. 1984. Hydrolytic stability of biomolecules at high temperatures and its implication for life at 250°C. *Nature* 310: 430–432.
- Wilde, S. A., Valley, J. W., Peck, W. H., and C. M. Graham. 2001. Evidence from detrital zircons for the existence of continental crust and oceans on the Earth 4.4 Gyr ago. *Nature* 409: 175–178.
- Yamaoka, K., Kawahata, H., Gupta, L. P., Ito, M., and H. Masuda. 2007. Thermal stability of amino acids in siliceous ooze under alkaline hydrothermal conditions. *Org. Geochem.* 38: 1897–1909.
- Yanagawa, H., and K. Kojima. 1985. Thermophilic microspheres of peptide-like polymers and silicates formed at 250°C. *J. Biochem.* 97: 1521–1524.

Capítulo III

Metodología

Este trabajo consiste en una serie de estudios enfocados en explorar el papel de los sistemas hidrotermales desde la perspectiva de la evolución química. Estos experimentos abarcan la síntesis de materia prima para llevar a cabo reacciones químicas, así como el análisis de la estabilidad y reactividad de diversas moléculas orgánicas. De igual manera, se estudian las interacciones entre moléculas orgánicas y minerales con el fin de establecer cuál es el destino de diversos compuestos en un entorno específico.

De acuerdo a la Figura 3.1., la Tesis abarca cuatro experimentos básicos: 1) la termólisis del HCN; 2) la caracterización y propiedades térmicas del HCN-DTP; 3) la polimerización de aminoácidos en entornos hidrotermales; y 4) la sorción de aminoácidos considerando el efecto de iones disueltos.

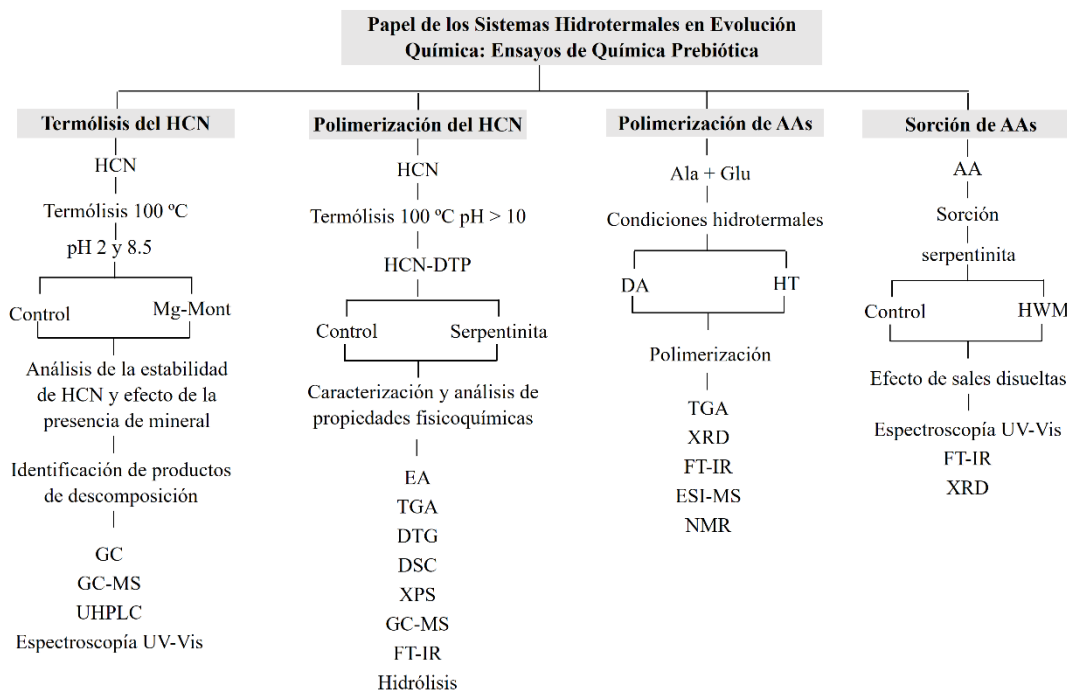


Figura 3.1. Resumen de la metodología.

Nota: **HCN:** Ácido cianhídrico; **AAs:** Aminoácidos; **EA:** Análisis elemental; **TGA:** Análisis termogravimétrico; **TG-MS:** Análisis termogravimétrico acoplado a espectrometría de masas; **DTG:** Análisis térmico diferencial; **DSC:** Calorimetría diferencial de barrido; **GC:** Cromatografía de gases; **GC-MS:** Cromatografía de gases acoplada a espectrometría de masas; **UHPLC:** Cromatografía líquida de ultra alta eficiencia; **XRD:** Difracción de Rayos X; **FT-ICR MS:** Espectrometría de masas por resonancia ion-ciclotrón con transformada de Fourier; **XPS:** Espectroscopía fotoelectrónica de Rayos X; **FT-IR:** Espectroscopía Infrarrojo con transformada de Fourier; **UV-Vis Spectroscopy:** Espectroscopía UV-Visible; **HWM:** Modelo de agua hidrotermal; **Mg-Mont:** Montmorillonita de Magnesio; **HCN-DTP:** Polímero térmico derivado de HCN; **pHpzc:** Punto de carga cero; **NMR:** Resonancia Magnética Nuclear; **DA:** Tratamiento de activación en seco; **HT:** Tratamiento hidrotermal submarino (alta temperatura-presión).

1. Materiales

1.1. Aminoácidos (AAs)

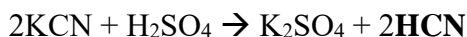
Se emplearon los aminoácidos glicina (Gly, G), L-alanina (Ala, A), ácido L-glutámico (Glu, E) y ácido L-aspartico (Asp, D) de Sigma-Aldrich® (99% de pureza) (Ver Capítulos VI y VII).

1.2. Minerales

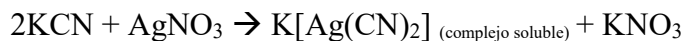
La Mg-Mont fue preparada a partir de la muestra SWy-2cNa-Mont Crook County, Wyoming, USA. La sílice pirogénica (SiO₂) fue proporcionada por Evonik Industries® (Aerosil 380). La serpentinita fue proporcionada por el profesor Fernando-Ortega (Instituto de Geología, UNAM). La muestra se obtuvo del Complejo Acatlán, SO de México (González-Mancera *et al.* 2009) (Ver Capítulos V, VI y VII).

1.3. Síntesis de ácido cianhídrico (HCN)

La producción de HCN en disolución acuosa y libre de oxígeno se realizó de acuerdo al procedimiento de Azamar y Draganic (1982) (Fig. 3.2.). Su formación se basa en la reacción entre un cianuro alcalino y un ácido fuerte (Ver Capítulos IV y V).



- Titulación (Método de Liebig)



1.4. Preparación de Montmorillonita de Magnesio (Mg-Mont)

La Mg-Mont fue preparada a partir de la muestra SWy-2cNa-Mont Crook County, Wyoming, USA. La muestra fue lavada con una disolución 2 N de $MgCl_2 \cdot 6H_2O$. La muestra seca se caracterizó por medio de difracción de rayos X para cuantificar las diferencias del espacio interlamilar de la arcilla (Fig. 3.3.). El procedimiento se repitió dos veces para confirmar la distancia interlamilar reportada en otros trabajos (Barshad 1950) (Ver Capítulo IV).

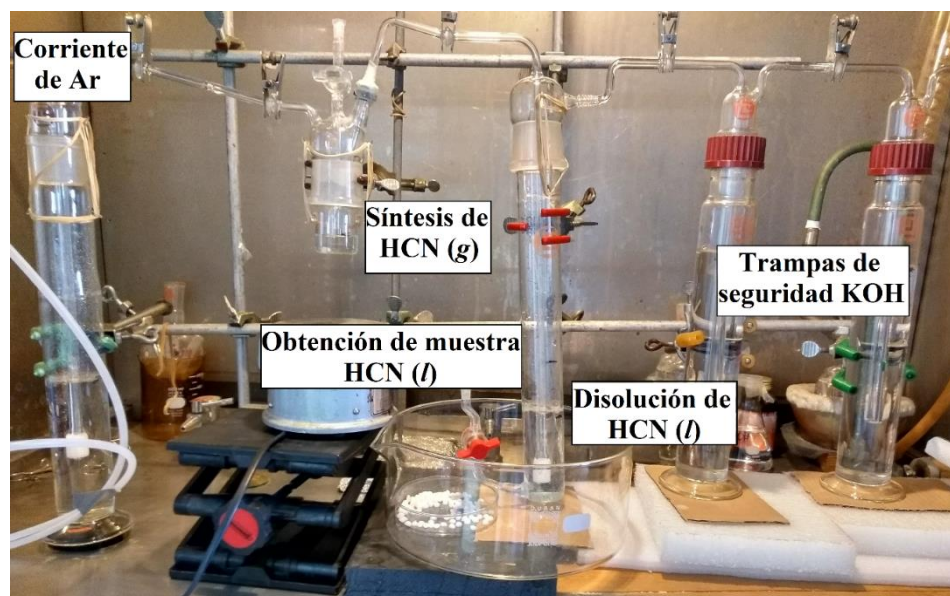


Figura 3.2. Síntesis de HCN

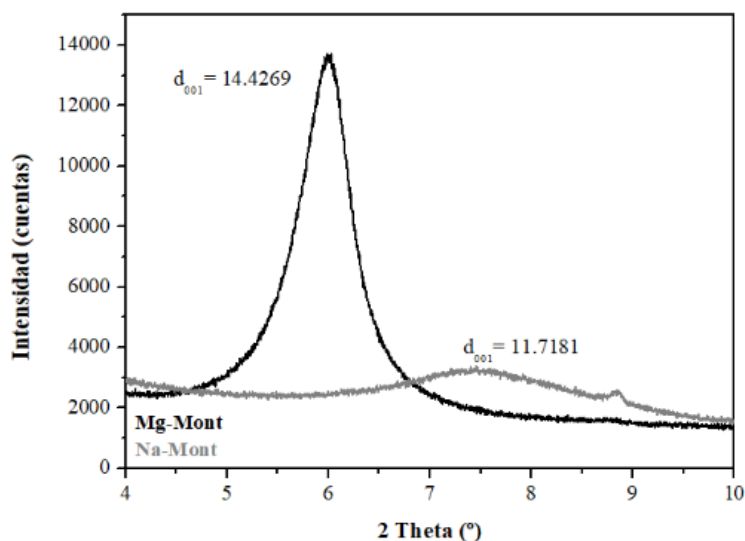


Figura 3.3. Difractograma de las muestras de Mg-Mont y Na-Mont.

2. Métodos

2.1. Lavado de minerales

Para eliminar la materia orgánica de la muestra, se llevó a cabo el siguiente procedimiento: los fragmentos de mineral (<2 cm) se lavaron con solución de KOH (3% v/v) por 30 min (1 g de mineral: 10 mL de solución). Después, el mineral se lavó con agua destilada (30 min) para eliminar el exceso de KOH. Posteriormente, la muestra se lavó con solución de HNO₃ (3% v / v) (1 g de mineral:10 mL de disolución) por 30 min. Finalmente, el mineral se limpió con agua destilada para eliminar el exceso de ácido. El mineral se secó a temperatura ambiente. El pH del punto de carga cero (*pHpzc*, por sus siglas en inglés) se obtuvo mediante el método propuesto por Ibanez *et al.* (2008) (Ver Capítulos IV, V, y VII).

2.2. Termólisis

Los experimentos de termólisis (Fig. 3.4.A) se llevaron a cabo en un sistema estático a una temperatura de ~ 100 °C. Se colocaron alícuotas de la disolución de HCN (0.1 mol L⁻¹, 5 mL) en ampollas de vidrio y se calentaron durante distintos periodos de tiempo (Fig. 3.4.B). Se realizaron experimentos con HCN y HCN en presencia de Mg-Mont en una proporción 100 mg Mg-Mont: 5 mL HCN. Ambos experimentos se realizaron a pH ácido (pH ~ 2) y pH básico (pH ~ 8.5) (ver Capítulo IV). La síntesis del polímero térmico de HCN (HCN-DTP, *hydrogen cyanide-derived thermal polymer*) (Fig. 3.4.C) (ver Capítulo V) se realizó a partir de la termólisis (50 h) de una disolución de HCN (0.15 mol L⁻¹) a pH > 10. Los experimentos en presencia de serpentinita se realizaron en una proporción 500 mg Mg-Mont: 5 mL HCN (Fig. 3.4.D) (Ver Capítulos IV y V).

2.3. Tratamiento de activación en seco (DA, dry activation)

Se realizó la deposición de diferentes cargas de (A+E) sobre SiO₂ mediante el procedimiento de impregnación por humedad incipiente (*IWI*, *Incipient wetness impregnation*) de acuerdo a Bouchoucha *et al.* (2011). Se adicionaron 10 mL de disolución de AAs en agua destilada con la concentración requerida a 1 g de SiO₂ produciendo una pasta homogénea. Las muestras se secaron a temperatura ambiente bajo una corriente de aire /N₂. Todas las muestras se prepararon con una relación A:E que correspondieron a una relación molar 1: 1 (Tabla 3.1; Fig. 3.5.A) (ver Capítulo VI)

Tabla 3.1. Preparación de muestras para la deposición de diferentes cargas de (A+E)/SiO₂.

%	Ala (mg)	Glu (mg)	SiO ₂ (g)
3	11.31	18.69	1
3.5	13.2	21.8	1
4	15.08	24.91	1
5	18.85	31.14	1
6	22.62	37.37	1

Para los experimentos en *condiciones hidrotermales subaéreas* se utilizó la muestra con 3.5% (A + E)/SiO₂. La muestra se activó térmicamente en un tubo en “U” bajo flujo de aire seco. El tubo se colocó en un horno tubular y se calentó hasta 205 °C con una rampa de 5 °C min⁻¹. La muestra se mantuvo a la temperatura final durante 20 min.

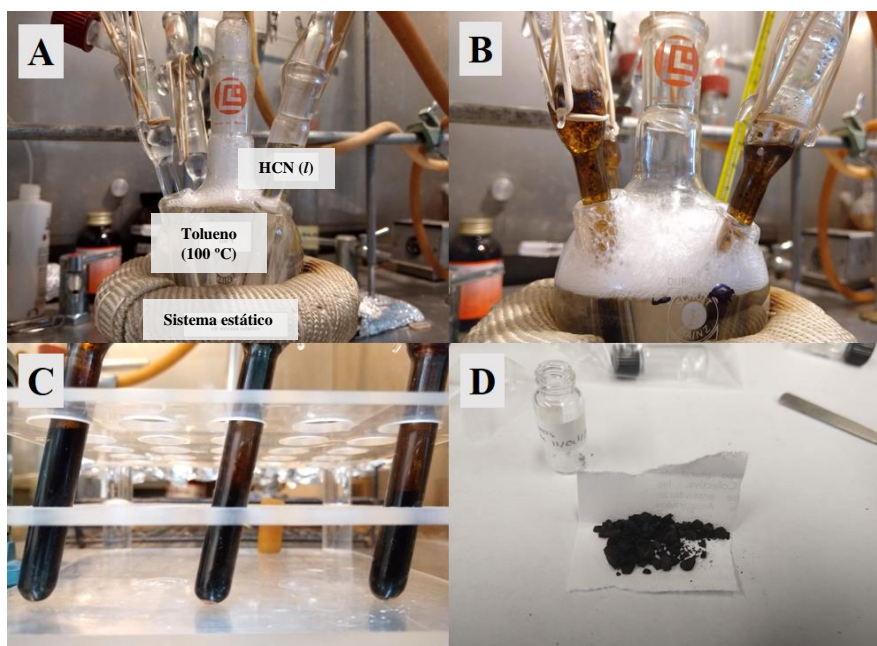


Figura 3.4. A) Sistema estático para experimentos de termólisis, B) Termólisis de HCN a pH básico después de 50 h, C) Polimerización de HCN a pH básico y D) Muestra de serpentinita + HCN-DTP.

2.4. Tratamiento hidrotermal submarino (alta temperatura-presión) (HT, hydrothermal treatment)

Las simulaciones de las condiciones hidrotermales submarinas se llevaron a cabo en un recipiente a presión Reactor Parr® 4600-4700 (Fig. 5B). Las condiciones para todos los experimentos fueron 230 °C y 2.8 MPa durante 1 hora. La muestra consiste en 10 mL de disolución de AAs:300 mg de SiO₂. La concentración inicial de la disolución de un solo aminoácido fue de 0.05 M. En el sistema mixto, A+E, la concentración fue de cada aminoácido fue 0.025 mol L⁻¹ (Fig. 3.5.B) (ver Capítulo VI).

2.5.Desorción

Para analizar las moléculas orgánicas retenidas en las superficies minerales después del proceso de DA, se realizaron tratamientos de desorción. En general, se agregó 1 mL de H₂O por 10 mg de muestra. Las muestras resultantes se agitaron manualmente y se centrifugaron durante 10 minutos a 5000 rpm. En todos los casos, la fase líquida se filtró con acrodiscos (0.4-0.25 µm) para remover el material particulado (ver Capítulo VI).

2.6. Modelo de agua hidrotermal (HWM, hydrothermal water model)

El HWM se preparó de acuerdo con la propuesta de Zaia (2012). Con base en la composición original (De Ronde *et al.* 1997) se eliminó el aporte de amonio (NH₄⁺) debido a que está relacionado con la descomposición de materia orgánica o un subproducto de microorganismos y por ende, no es consistente con un escenario prebiótico (ver Capítulo VII).

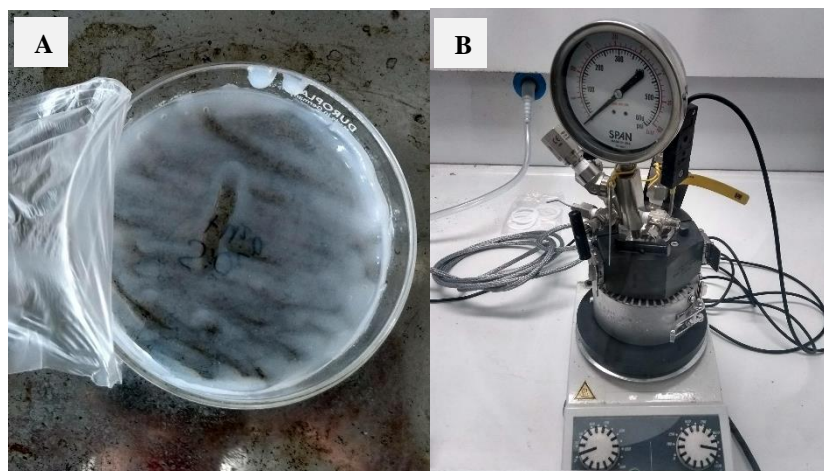


Figura 3.5. A) Muestra de A+E/SiO₂ por el método de IWI y B) Reactor Parr utilizado para experimentos de tratamiento hidrotermal submarino.

2.7. Sorción de aminoácidos en serpentinita

La sorción de aminoácidos se realizó utilizando una disolución de 3 mL (AA [0.2 mmol L⁻¹] en agua hidrotermal) y 100 mg de serpentinita (tamaño de partícula <250 µm) a temperatura ambiente. El valor de pH *per se* de las disoluciones fue pH ≈ 11-12. Las muestras se agitaron durante 1 hora y se centrifugaron durante 15 minutos a 23, 000 rpm. El sobrenadante se analizó colorimétricamente con espectrómetro UV-visible, utilizando el método de ninhidrina propuesto por Mundo *et al.* (2017). De igual manera, se realizaron experimentos de control (sorción en agua destilada). Las sorciones se realizaron con agua desionizada a diferentes valores de pH a la misma concentración de aminoácidos [0.2 mmol L⁻¹]: pH básico ≈ 10-12, ajustado con disolución de KOH (0.1 mol L⁻¹) (consistente con el valor *per se* del HWM), natural (pH natural de la disolución de aminoácidos en agua desionizada) y pH ácido ≈ 2-3, ajustado con disolución de HCl (0.1 mol L⁻¹). Todos los experimentos se realizaron por quintuplicado (ver Capítulo VII).

3. Técnicas analíticas y de caracterización

Análisis elemental. El polímero térmico derivado de HCN se examinó para la determinación de las fracciones másicas de carbono, hidrógeno y nitrógeno (en porcentaje con respecto al peso) en un analizador elemental Perkin Elmer®, modelo CNHS-2400 (ver Capítulo V).

Análisis térmico. Las mediciones de termogravimetría, análisis térmico diferencial y calorimetría diferencial de barrido se realizaron en un analizador térmico simultáneo modelo SDTQ-600 / Thermo Star de TA Instruments®. El análisis térmico se realizó en modo isotérmico durante 20 minutos. Se programó una rampa de calentamiento de 10 °C min⁻¹ hasta 1000 °C en atmósfera de argón (100 mL min⁻¹). Para el análisis de las principales especies durante la descomposición térmica dinámica de los procesos de fragmentación de la muestra se utilizó un sistema de termogravimetría acoplado que utiliza un detector selectivo de masas de tipo cuadrupolo en modo de impacto electrónico (Thermostar QMS200 M3®) (Capítulo V). Por otro lado, el análisis de TG de los experimentos del Capítulo VI se llevó a cabo en un analizador TA Instrument SDT Q600® con una velocidad de calentamiento de 5 °C min⁻¹ hasta 800 °C bajo flujo de aire seco (100 mL min⁻¹) (Ver Capítulos IV, V, y VI).

Cromatografía de gases. El HCN remanente fue seguido por cromatografía de gases (Varian® Serie 2400 con detector de ionización de flama) en una columna de acero inoxidable (1/8 de pulgada y 4 m de longitud) empacada con Chromosorb-102 (100/120). Gas acarreador, N₂; flujo 30 mL min⁻¹. El régimen de temperatura fue de 60-250 °C, con una velocidad de calentamiento de 6 °C min⁻¹. Se inyectó un volumen de 2 µL (ver Capítulo IV).

Cromatografía de gases acoplada a espectrometría de masas. Diversas moléculas orgánicas polares se caracterizaron por CG-EM usando un sistema Agilent® 6859 GC acoplado a un MSD 5975 VL con detector de triple eje que funciona en modo de impacto electrónico a 70 eV. Se utilizaron columnas HP-5 MS (30 m x 0.25 mm de d.i. x 0.25 µm de espesor). Se utilizó el método desarrollado por Ruiz-Bermejo *et al.* (2012) y Marín-Yaseli *et al.* (2016). Después de la termólisis, las muestras se liofilizaron para eliminar el H₂O. Enseguida, se agregaron 100 µL de BSTFA + TMCS [N, O bis (trimetilsilil) trifluoroacetamida con Me₃SiCl, Thermo Scientific Co®, EE. UU.] al material seco y se calentó durante 3 h a 80 °C. A continuación, se inyectaron 2 µL de muestra derivatizada (temperatura del inyector 220 °C, temperatura del detector 300 °C; He como gas acarreador) (ver Capítulo IV y V).

Cromatografía líquida de ultra alta eficiencia. Se utilizó un equipo UltiMate 3000, Thermo Scientific Co®, con detector UV-vis (Dionex Ultimate 3000 VWD). Se caracterizaron algunos ácidos carboxílicos presentes en la fase acuosa de las muestras de termólisis de HCN utilizando una columna de exclusión aniónica (Altech, 7.8*300 mm) y una fase móvil de 1.5 mmol L⁻¹ de H₂SO₄ con un flujo de 0.6 ml min⁻¹. La detección se realizó a una longitud de onda (λ) de $\lambda = 210$ nm. Para el caso del DAMN, se utilizó una columna Waters® Cortez 2.7 μ m (4.6*150 mm). La fase móvil fue: X) acetato de amonio 0.1 mol L⁻¹ y Y) Metanol: H₂O en una proporción 50:50. La proporción de X:Y fue 90:10, respectivamente. La detección se realizó a una $\lambda = 293$ nm. Respecto a la detección de aldehídos y cetonas se utilizó como fase móvil acetonitrilo y H₂O en una proporción 70:30. La detección se realizó a una longitud de onda $\lambda = 360$ nm (ver Capítulo IV).

Prueba de ninhidrina para la derivatización de aminoácidos. Se preparó una disolución amortiguadora de acetatos (100 mL) a partir de una disolución de ácido acético 0.2 mol L⁻¹ y acetato de sodio 0.2 mol L⁻¹ en una proporción 17.6:82.4 con un pH de 5.4. El reactivo de ninhidrina se preparó en las siguientes proporciones: 7.5 mL buffer de acetatos: 22.5 mL de etilenglicol (C₂H₆O₂): 600 mg de ninhidrina: 750 μ L de cloruro estañoso (SnCl₂). El procedimiento consiste en colocar en un tubo de ensayo 1 mL de la muestra problema + 1 mL de reactivo de ninhidrina y agitar vigorosamente. Enseguida, calentar en un baño de agua hirviendo durante 10 minutos. Dejar enfriar y añadir 2 mL de etanol al 50 % y agitar vigorosamente. El cambio de color de la muestra a púrpura indica la presencia de aminoácidos. Finalmente, se mide la absorbancia a una $\lambda = 570$ nm en un espectrofotómetro UV-vis (Varian ® Cary 100 Scan). La metodología se basó en Mundo *et al.* (2017) (ver Capítulo VII).

Prueba de detección de urea. La urea se identificó mediante el método DAM (diacetilmonoxima) propuesto por Negrón-Mendoza *et al.* (1986). Las muestras problema se analizan a partir del siguiente procedimiento: mezclar 1 mL de la muestra problema + 1 mL de disolución de catalizador (FeCl₂ 1.6 mmol L⁻¹ + tiosemicarbazida 5 mmol L⁻¹ + H₂SO₄ 1.3 mol L⁻¹ + H₃PO₄ 4 mol L⁻¹) + 1 mL de la disolución DAM (140 mmol L⁻¹). La muestra es agitada y calentada a baño maría a 80 °C durante 13 minutos (es necesario tapar los tubos de ensayo). Dejar enfriar la muestra. Finalmente, se mide la absorbancia a una $\lambda = 526$ nm en un espectrofotómetro UV-vis (Varian ® Cary 100 Scan) (ver Capítulo IV).

Espectroscopía Infrarrojo (Fourier Transform Infrared (FT-IR) Spectroscopy, por sus siglas en inglés). Los espectros de infrarrojo de las muestras se obtuvieron con un espectrómetro FT-IR (Nicolet®, modelo NEXUS 67) configurado con un accesorio de reflectancia DRIFT (Harrick, modelo Praying Mantis DRP®). Los espectros se obtuvieron en pastillas de CsI en la región espectral de 4000–450 cm⁻¹, con una resolución espectral de 2 cm⁻¹ (ver Capítulo V).

Espectrometría de masas por resonancia de ion-ciclotrón con transformada de Fourier. Tanto la disolución de desorción después de DA como el sobrenadante después de HT se analizaron por FT-ICR. Los análisis se realizaron en un equipo FT-ICR Bruker, SolarixXR®. Se prepararon alícuotas de sobrenadantes y se mezclaron con MeOH: H₂O al 50:50% v: HCOOH al 0.1% para promover la formación de especies protonadas. El análisis se realizó considerando el modo de ionización positiva (Bedoin, 2018) (ver Capítulo VI).

Hidrólisis. Las muestras se hidrolizaron utilizando el método desarrollado por Ferris *et al.* (1974). Las condiciones para la hidrólisis ácida fueron HCl 6N / 100–110 ° C / 16–24 h; para la hidrólisis básica, fueron NaOH 0.1 N / 100 ° C / 6 h. Después del tratamiento, el producto se analizó mediante CG-EM (ver Capítulo V).

Prueba de hidrazonas para la derivatización de aldehídos y cetonas. Las muestras tratadas se derivatizaron con una disolución de 2,4-dinitrofenilhidrazina (C₆H₆N₄O₄) 0.2 mol L⁻¹ siguiendo el método de Fuentes Carreón (2018) (ver Capítulo IV).

Difracción de Rayos X. La caracterización de la muestra de serpentinita se realizó mediante un difractómetro EMPYREAN® equipado con filtro de hierro, tubo de cobalto, filtro de níquel de enfoque fino y detector PIXcel3D. La medición se realizó en el intervalo angular 2θ de 4 ° a 80 ° con un tamaño de paso de 0.003 ° (2 Theta) y un tiempo de integración de 40 s por paso. La identificación se realizó utilizando el software HighScore (PANalytical®) y las bases de datos ICSD (base de datos de estructura de cristal inorgánico) e ICDD (Centro internacional de datos de difracción). La cuantificación se realizó mediante el método RIR (índice de intensidad de referencia) (ver Capítulo V y VII). Las muestras sólidas de Aerosil 380 se analizaron por XRD usando un difractómetro Bruker® D8 Avance utilizando radiación Cu Kα (λ = 1.5404 Å). Los patrones de XRD se registraron entre 10 y 40 ° 2θ con un tamaño de paso de 0.05 ° (Capítulo VI).

Espectroscopía fotoelectrónica de Rayos X. El análisis XPS de la fase III se realizó en una cámara de ultra alto vacío equipada con un analizador de electrones hemisférico y con el uso de una fuente de rayos X Al Kα (1486.6 eV) con una apertura de 7 mm x 20 mm . La presión base en la cámara fue de 1 x 10⁻⁹ mbar y los experimentos se realizaron a temperatura ambiente. La muestra se analizó preparando una pastilla que consiste en una muestra de aproximadamente 100 mg, obtenida después de triturar y prensar la fase III (mineral + HCN-DTP). Asimismo, se analizó la fase III como muestra global (roca cubierta por el polímero). La descomposición máxima en diferentes componentes se formó, después de la resta de fondo, como una deconvolución de las curvas Lorentzianas y Gaussianas. El cálculo de las relaciones atómicas entre los elementos identificados se derivó de las intensidades de los picos integrales y los factores de sensibilidad proporcionados por el fabricante (ver Capítulo V).

Referencias

- Azamar J. y Draganic I. (1982) Equipo para la preparación de compuestos tóxicos en solución acuosa y en atmósfera controlada: Cianuros para experimentos en Química de Radiaciones
- Barshad I (1950) The effect of the interlayer cations on the expansion of the mica type of crystal lattice. American Mineralogist: Journal of Earth and Planetary Materials 35:225–238
- Bedoin, Lise. (2018) Informe de Maestría, Sorbonne Université.

- Bouchoucha M, Jaber M, Onfroy T, et al (2011) Glutamic Acid Adsorption and Transformations on Silica. *The Journal of Physical Chemistry C* 115:21813–21825. <https://doi.org/10.1021/jp206967b>
- Colín-García M, Negrón-Mendoza A, Ramos-Bernal S (2009) Organics Produced by Irradiation of Frozen and Liquid HCN Solutions: Implications for Chemical Evolution Studies. *Astrobiology* 9:279–288. <https://doi.org/10.1089/ast.2006.0117>
- De Ronde CEJ, Channer DM deR., Faure K, et al (1997) Fluid chemistry of Archean seafloor hydrothermal vents: Implications for the composition of circa 3.2 Ga seawater. *Geochimica et Cosmochimica Acta* 61:4025–4042. [https://doi.org/10.1016/S0016-7037\(97\)00205-6](https://doi.org/10.1016/S0016-7037(97)00205-6)
- Ferris JP, Wos JD, Noonan DW, Oró J (1974) Chemical evolution: XXI. The Amino Acids Released on Hydrolysis of HCN Oligomers. *J Mol Evol* 3:225–231. <https://doi.org/10.1007/BF01797455>
- González-Mancera G, Ortega-Gutiérrez F, Proenza JA, Atudorei V (2009) Petrology and geochemistry of Tehuiztzingo serpentinites (Acatlán Complex, SW Mexico). *Boletín de la Sociedad Geológica Mexicana* 61:419–435
- Ibanez JG, Hernandez-Esparza M, Doria-Serrano C, et al (2008) The Point of Zero Charge of Oxides. In: *Environmental Chemistry*. Springer New York, New York, NY, pp 70–78
- Marín-Yaseli MR, González-Toril E, Mompeán C, Ruiz-Bermejo M (2016) The role of aqueous aerosols in the “glyoxylate scenario”: an experimental approach. *Chemistry—A European Journal* 22:12785–12799
- Mundo, B., Cruz, A. y Colin M (2017) Cuantificación de aminoácidos libres por reacción con ninhidrina
- Negrón-Mendoza, A., Chacón, B.E., Perezgasga, L. & Torres, J.L. (1986) Determinación de urea por el método de DAM
- Ruiz-Bermejo M, de la Fuente JL, Rogero C, et al (2012) New Insights into the Characterization of ‘Insoluble Black HCN Polymers.’ *Chemistry & Biodiversity* 9:25–40. <https://doi.org/10.1002/cbdv.201100036>
- Zaia DAM (2012) Adsorption of amino acids and nucleic acid bases onto minerals: a few suggestions for prebiotic chemistry experiments. *International Journal of Astrobiology* 11:229–234. <https://doi.org/10.1017/S1473550412000195>

Disponibilidad de materia prima para llevar a cabo reacciones

HCN y sistemas hidrotermales


Ensayos de Química Prebiótica I

Artículo de investigación

Villafañe-Barajas, S. A., Colín-García, M., Negrón-Mendoza, A., & Ruiz-Bermejo, M. (2020). An experimental study of the thermolysis of hydrogen cyanide: the role of hydrothermal systems in chemical evolution. *International Journal of Astrobiology*, 1-10.

Resumen El ácido cianhídrico (HCN) es considerado una molécula fundamental en los experimentos de química prebiótica ya que pudo haber tenido un papel crucial como materia prima para formar moléculas más complejas, así como intermediario en diversas reacciones químicas. Sin embargo, existen varias incógnitas acerca de los escenarios primitivos en donde esta molécula podría haber estado disponible. Los sistemas hidrotermales han sido considerados como reactores abióticos y nichos de evolución química aunque números experimentos han mostrado que las altas temperaturas y presiones podrían ser adversas respecto a la estabilidad de las moléculas orgánicas. En consecuencia, es necesario realizar experimentos sistemáticos enfocados en estudiar la síntesis, la estabilidad, la reactividad y el destino de diversos compuestos orgánicos (*e.g.*, HCN) en escenarios hidrotermales. En este trabajo, realizamos una serie de experimentos enfocados en estudiar la estabilidad y destino del HCN simulando un escenario hidrotermal simple (*i.e.*, termólisis de HCN a 100 °C, a pH básico y ácido, y en presencia de Mg-Mont). Nuestros resultados muestran que el comportamiento de esta molécula depende directamente de las condiciones ambientales. Sin embargo, las condiciones que permiten la formación de una amplia diversidad de moléculas orgánicas son predominantemente alcalinos y ausencia de mineral. Finalmente, resaltamos la importancia de los sistemas hidrotermales y los productos de descomposición del HCN en la evolución química.

An experimental study of the thermolysis of hydrogen cyanide: the role of hydrothermal systems in chemical evolution

Saúl A. Villafaña-Barajas¹, María Colín-García² , Alicia Negrón-Mendoza³
and Marta Ruiz-Bermejo⁴

Research Article

Cite this article: Villafaña-Barajas SA, Colín-García M, Negrón-Mendoza A, Ruiz-Bermejo M (2020). An experimental study of the thermolysis of hydrogen cyanide: the role of hydrothermal systems in chemical evolution. *International Journal of Astrobiology* 1–10. <https://doi.org/10.1017/S1473550420000142>

Received: 19 March 2020
Revised: 1 June 2020
Accepted: 8 June 2020

Key words:
Chemical evolution; hydrogen cyanide;
hydrothermal vents; prebiotic chemistry;
stability; thermolysis

Author for correspondence:
María Colín-García,
E-mail: mcolin@geologia.unam.mx

¹Posgrado en Ciencias de la Tierra, Universidad Nacional Autónoma de México, Ciudad Universitaria, 04510 Cd. Mx, México; ²Instituto de Geología, Universidad Nacional Autónoma de México, Ciudad Universitaria, 04510 Cd. Mx, México; ³Instituto de Ciencias Nucleares, Universidad Nacional Autónoma de México, Ciudad Universitaria, 04510 Cd. Mx, México and ⁴Centro de Astrobiología (INTA-CSIC). Dpto. Evolución Molecular, Ctra. Torrejón-Ajalvir, km 4, Torrejón de Ardoz, 28850 Madrid, Spain

Abstract

Hydrogen cyanide (HCN) is considered a fundamental molecule in prebiotic chemistry experiments due to the fact that it could have an important role as raw material to form more complex molecules, as well as it could be an intermediate molecule in chemical reactions. However, the primitive scenarios in which this molecule might be available have been widely discussed. Hydrothermal systems have been considered as abiotic reactors and ideal niches for chemical evolution. Nevertheless, several experiments have shown that high temperatures and pressures could be adverse to the stability of organic molecules. Thus, it is necessary to carry out systematic experiments to study the synthesis, stability and fate of organic molecules in hydrothermal scenarios. In this work, we performed experiments focused on the stability and fate of HCN under a simple hydrothermal system scenario: the thermolysis of HCN at 100°C, at acidic and basic pH and in the presence of Mg-montmorillonite. Furthermore, we analysed the products from HCN thermolysis and highlighted the role of these chemical species as prebiotic molecules under a hydrothermal scenario.

Introduction

Hydrogen cyanide (HCN) is suggested as a central molecule in chemical evolution because it is proposed as a ‘chemical block’ of the three pillars of the prebiotic chemistry (Islam and Powner, 2017). Several experiments have shown that HCN is an important precursor of organic molecules such as carboxylic acids, amino acids, purines, pyrimidines and other carbonyl compounds (Sanchez *et al.*, 1967; Draganić and Draganić, 1980; Niketić *et al.*, 1983; Ferris and Hagan, 1984; Schwartz *et al.*, 1984; Draganić *et al.*, 1985a; Borquez *et al.*, 2005; Matthews, 2005; Ruiz-Bermejo *et al.*, 2013; Sutherland, 2016).

However, one of the biggest problems in considering any primitive conditions is the availability of raw material in the environment and its concentration (Miller, 1987). These are fundamental criteria to consider any primitive scenario and the kind of reactions that could have happened on the primitive Earth. Regarding this, several mechanisms could have contributed to the inventory of HCN on early Earth by the action of different energy sources (*e.g.* photolysis, shock waves, electrical discharges of lightning and volcanism; Ferris and Hagan, 1984; Holm and Neubeck, 2009; Tian *et al.*, 2011; Parkos *et al.*, 2016; Ferus *et al.*, 2017; Rimmer and Rugheimer, 2019). Likewise, the extraterrestrial input from meteorites and comets was possibly an important source of HCN (Matthews and Minard, 2006; Colín-García *et al.*, 2009; Mumma and Charnley, 2011; Pizzarello, 2012). In general, the mechanisms for the synthesis of HCN are based in reactions between an oxidizing agent (*e.g.* CO, CO₂), a source of nitrogen (*e.g.* NH₃, N₂) and a reducing agent (*e.g.* H₂, H₂O) (for more details, see Ferris and Hagan, 1984). In addition, cyanide species in the form of complexes with sulphur/ferrous ions could have been present in the primitive oceans or in the vicinity of hydrothermal systems (Mukhin, 1974; Arrhenius *et al.*, 1994; Keefe and Miller, 1996; Dzombak *et al.*, 2006; Holm and Neubeck, 2009).

The concentration of HCN is a critical parameter. High concentrations (>0.1 mol l⁻¹) could have favoured the polymerization of the molecule, while lower concentrations (<0.01 mol l⁻¹) might have favoured its hydrolysis (Sanchez *et al.*, 1968; Miyakawa *et al.*, 2002). Besides, these mechanisms are highly dependent on pH.

There is no agreement about the concentration of HCN on early Earth. For instance, it has been proposed that it was possible to reach high concentrations of HCN at the surface of the water (floating HCN patches >1 mol l⁻¹; Fábán *et al.*, 2014). Other models propose

that concentration *per se* in the primitive oceans was very low (10^{-10} – 10^{-13} mol l⁻¹) (Stribling and Miller, 1987; Miyakawa *et al.*, 2002). Hence, it is necessary to consider primitive environments where the production of HCN was continuous and then chemical reactions could have taken place to increase the chemical complexity. One plausible scenario may be the hydrothermal systems.

Holm and Neubeck (2009) suggested a possible mechanism for HCN production under hydrothermal conditions from CH₄, NH₃ and other dissolved species (*i.e.* N₂, CO). The main reactions are as follows:

- (1) CH₄ + NH₃ → HCN + 3H₂
- (2) 2CH₄ + N₂ → 2HCN + 3H₂
- (3) CO + NH₃ → HCN + H₂O

In the same way, based on theoretical models, it has been proposed that HCN can coexist with their precursor molecules (*e.g.* CO, CO₂, H₂ and N₂) under hydrothermal conditions (Shock, 1992; Schulte and Shock, 1995; LaRowe and Regnier, 2008). Such species may be available in these environments (Table 1) when the hydrothermal fluids are mixed with seawater. Particularly, alkaline fluids, resulted from the serpentinization processes, could have an essential role in the release of several dissolved species and consequently in the formation of organic compounds (Konn *et al.*, 2015; McDermott *et al.*, 2015). Brandes *et al.* (1998) showed that N₂ could be transformed into NO₂, NO₃ and ammonia in the presence of minerals under hydrothermal conditions. Additionally, abiotic nitrogen reduction could have taken place within primordial hydrothermal vents, supplying some ammonia for the synthesis of C-H-O-N compounds *via* abiotic processes (Schoonen and Xu, 2001).

Consequently, if HCN can be produced under hydrothermal conditions, it is crucial to study its stability and reactivity considering some of the available geochemical variables in hydrothermal systems, such as different pH values, high temperatures and in the presence of inorganic surfaces.

On the one hand, it is well known that both hydrolysis and polymerization of HCN are pH-dependent (Sanchez *et al.*, 1967; Ferris and Hagan, 1984). Besides, it has been proven that some minerals adsorb HCN and/or increase its hydrolysis. This has been demonstrated theoretically and experimentally using ferrierite (Namba *et al.*, 2000), double-layered hydroxides (Zhao *et al.*, 2015), zeolites (Kotdawala *et al.*, 2008; Demir *et al.*, 2012), titanium oxides (Ma *et al.*, 2017) and serpentinite and clays (Colín-García *et al.*, 2010; Colín-García *et al.*, 2014). Nonetheless, it is necessary to consider all these variables together.

Here, we present an experimental approach of the HCN thermolysis under a simple hydrothermal scenario. In this study, it was considered that it is possible to find relatively warm fluids, generated by the hydrothermal fluids upwelling in chimneys and their diffusion within the medium. The selected temperature (100°C) could be very likely present surrounding the hot chimneys; since it has been reported a temperature difference (50°C) on fluids in a centimetre scale, result of turbulent mixing and venting activity (Fornari *et al.*, 1998; Bates *et al.*, 2010; Mittelstaedt *et al.*, 2012). In the study of the reactivity and fate of HCN and its decomposition products, it is important to consider some prebiotic scenarios, such as the surroundings of submarine and subaerial hydrothermal systems (Colín-García *et al.*, 2018), and to explore their potential implications for chemical evolution.

Materials and methods

Synthesis of HCN

HCN solution (0.1 M) was produced *in situ* by the reaction between KCN and H₂SO₄. HCN gas was dissolved in Milli Q water into an Ar atmosphere (Azamar and Draganić, 1982). The concentration was determined by titration with an aqueous solution of AgNO₃ (Draganić *et al.*, 1973).

Preparation of Mg²⁺-montmorillonite

Mg-montmorillonite (Mg-Mont) was prepared from SWy-2cNa-Mont Crook County, Wyoming, USA (Na-Mont), according to the following procedure: 40 g of Na-Mont was washed with a saturated solution of MgCl₂·6H₂O (2 N) for 24 h. The suspension was then centrifuged for 30 min at 20 000 rpm and washed with deionized water by shaking for 24 h. The suspension was centrifuged and lyophilized. This procedure was repeated three times. The dry powder sample was analysed by X-ray diffraction to quantify the differences of the interlamellar space of the clay. It was corroborated that Mg²⁺ had completely replaced Na⁺. Mg-Mont was used as magnesium was a common element on early Earth and because it is present in a wide variety of minerals in hydrothermal systems (Holm, 2012; Colín-García *et al.*, 2016, 2018).

Thermolysis

Thermolysis experiments were carried out in a static system at ≈100°C (Fig. 1). Aliquots of the HCN solution (0.1 M, 5 ml) were placed in glass tubes of 8 ml with stopcocks; the headspace was air. A ball flask with wells was filled up with toluene. Toluene was heated until boiling; samples were heated for different periods of time by conduction. All tests were carried out in triplicate. Controls and experiments including Mg-Mont were performed with 100 mg Mg-Mont by 5 ml HCN (0.1 M) at acidic and basic pH. The pH was modified and adjusted to 2 or 8.5, adding drops of HCl or KOH solution (0.1 M), respectively. The greater time exposition to heat for each sample was HCN_{acid}: 141.5 h, HCN/Mont_{acid}: 160 h, HCN_{basic}: 143 h and HCN/Mont_{basic}: 159.5 h. The aqueous phase of the samples was analysed to quantify changes of the organic molecule.

Analysis of samples

The treated samples were analysed by different analytical techniques:

Gas chromatography (GC)

The remnant HCN was followed by GC (Varian Series 2400 with flame ionization detector) on a stainless-steel column (1/8 inch and 4 m length) packed with Chromosorb-102 (100/120 mesh). The carrier gas was N₂ with a flow rate of 30 ml min⁻¹. The temperature regime was 60–250°C, with a heating rate of 6°C min⁻¹. The detector temperature was 200°C. A volume of 2 µl was injected.

GC-MS

The GC-MS analysis was done in a 6859 network GC system coupled to a 5975 VL MSD with triple-axis detector operating in electron-impact mode at 70 eV (Agilent). HP-5 MS columns (30 m × 0.25 mm i.d. × 0.25 µm film thickness) were used; the analysis was carried out using the method developed by Ruiz-Bermejo *et al.* (2012) to detect polar organic compounds. After thermolysis,

Table 1. Temperature, pH and dissolved species in fluids of some hydrothermal systems and seawater

Physicochemical conditions	Environment				
	Hydrothermal system				Seawater*
	Lucky Stricke ⁵	Menez Gwen ⁵	Lost City*	Rainbow*	
Temperature (°C)	172–324	275–284	40–93	365	7
pH	3.5–3.7	4.2–4.3	9–11	2.8	8
Chemical species (mmol)					
H ₂	3.3–725	44.2	0.25–0.43	16	–
CO ₂	15.0–26.6	22.6–28.8	–	16	2.3
CH ₄	0.30–0.88	1.2–1.49	0.13–0.28	2.5	–
N ₂	0.5–2.1	1.2–1.49	–	–	–

Based on: ⁵Charlou *et al.* (2000); *Schrenk *et al.* (2004) and references therein.

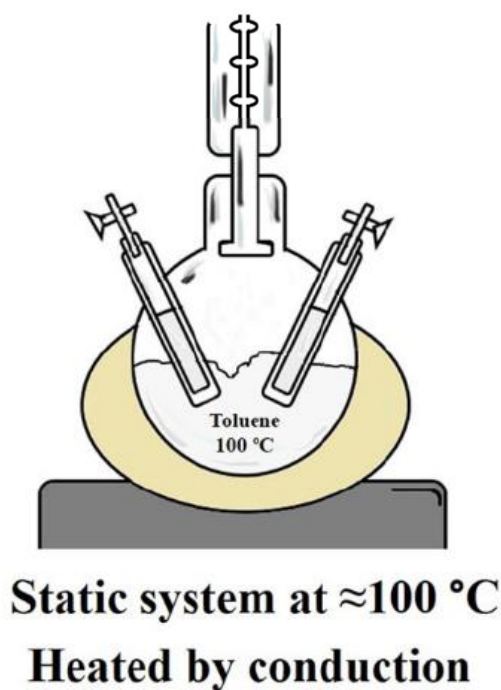


Fig. 1. Static heating system. A ball flask with wells is filled up with toluene; the system is heated until boiling, and samples are heated by conduction.

samples were freeze-dried to remove H₂O. Then, 100 μl of BSTFA + TMCS [N,O bis(trimethylsilyl)trifluoroacetamide with Me₃SiCl, Thermo Scientific Co, Waltham, MA, USA] was added to dry material and heated for 3 h at 80°C. Next, 2 μl of derivatized sample was injected (injector temperature 220°C, detector temperature 300°C and flow rate 1.1 ml min⁻¹; He as a carrier gas).

Ultra-high performance liquid chromatography (UHPLC)

The aqueous component was analysed by UHPLC (UltiMate 3000 UHPLC chromatograph, Thermo Scientific Co) with a UV-Vis

detector (Dionex UltiMate 3000 VWD). For carboxylic acids, we used an Alltech anion exclusion column (7.8 \times 300 mm) and 1.5 mmol⁻¹ of H₂SO₄ as a mobile phase, with a flow rate of 0.6 ml min⁻¹. The detection wavelength (λ) was $\lambda = 210\text{ nm}$. For diaminomaleonitrile (DAMN) detection, a Waters Cortex 2.7 μm , 4.6 \times 150 mm column was used; the mobile phase was (A) ammonium acetate 0.1 mol l⁻¹ and (B) methanol:water 50:50, with a 90 A:10 B ratio and a flow rate of 0.5 ml min⁻¹. The detection wavelength was $\lambda = 293\text{ nm}$.

UV-Vis spectroscopy

Urea was identified using the DAM method. The detection wavelength was $\lambda = 526\text{ nm}$ (Negrón-Mendoza *et al.*, 1986).

Results and discussion

Thermolysis

Figure 2 shows the thermolysis of HCN at acidic (2) and basic (8.5) pH, as well as in the presence of Mg-Mont. According to the species distribution diagram of HCN (Fig. 3), at pH = 2, HCN is the dominant species. However, at pH = 8.5, there is a considerable amount of cyanide (~20%). The availability of cyanide ions is crucial because, as we will discuss below, it is directly related to the polymerization process.

It is possible to identify some trends about the behaviour of HCN in both acidic and basic conditions (Fig. 2). It is noticeable that in acidic pH, the decomposition of HCN is low, but the presence of Mg-Mont increases its decomposition. Some experiments have shown that the half-life time for the hydrolysis of HCN is only a few minutes (Sanchez *et al.*, 1968; Stribling and Miller, 1987; Miller and Bada, 1988). However, Schäfer and Bonn (2000) demonstrated that hydrolysis of HCN_(g), as a function of temperature and in the presence of H₂O and N₂, is relatively slow until 700°C. It is well understood that hydrolysis of HCN yields formamide and, eventually, formic acid (Sanchez *et al.*, 1967; Ferris *et al.*, 1973; Schwartz *et al.*, 1984; Miyakawa *et al.*, 2002; Borquez *et al.*, 2005).

Some experiments have used inorganic surfaces to investigate the hydrolysis of HCN and suggested that this could be the result of the participation of acid sites at catalysts (Nanba *et al.*, 2000; Ma *et al.*, 2017). The catalytic activity of clay minerals may result from Brønsted acidity, Lewis acidity, presence of redox-active

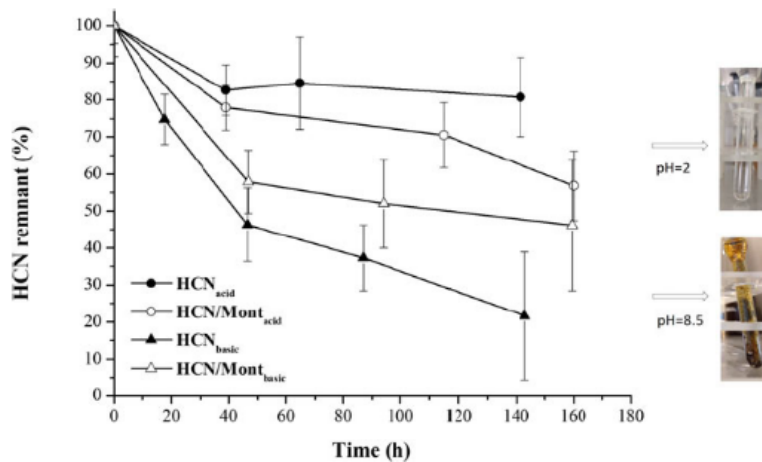


Fig. 2. Thermolysis of HCN at 100°C. Under acid conditions (pH = 2) the HCN remains relatively stable, but in the presence of Mg-Mont, the decomposition increases. At basic pH values (pH = 8.5) and in the absence of clay, the transformation of HCN is more efficient.

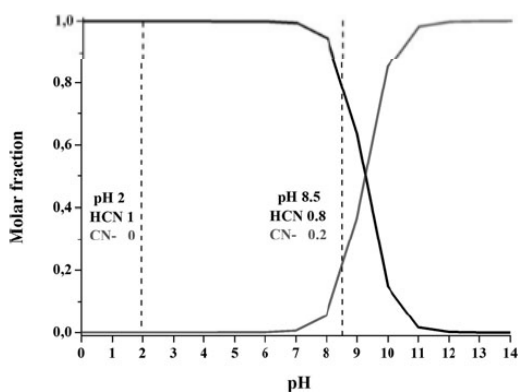


Fig. 3. Species distribution diagram for HCN.

species and/or introduction of catalytic species along the crystal structure (Adams and McCabe, 2006). In addition, the acidity at the surface of Mg-Mont may be the result of terminal hydroxyl groups, the bridging of oxygens and exchangeable cations. Likewise, Mg^{2+} has greater polarizing ability and, in consequence, it can dissociate the water in the interlamellar channel, releasing a proton to the medium (Frenkel, 1974; Nikalje *et al.*, 2000). In addition, the interaction of HCN with the Brønsted acid sites by hydrogen bonding in the lattice of clay would increase the hydrolysis of HCN (Cruz, 1974; Jamis *et al.*, 1995). Although one experimental report suggested that HCN at acidic conditions may be sorbed onto montmorillonite (Colín-García *et al.*, 2014), the HCN:Mont relationship in our experiments suggests that hydrolysis is the predominant mechanism, rather than sorption.

At basic pH, the decomposition of HCN is lower in the presence of clay. Although HCN hydrolysis at basic pH is possible, it has been demonstrated that polymerization until tetramer, DAMN, is the dominant mechanism (Miyakawa *et al.*, 2002; Borquez *et al.*, 2005).

Ferris *et al.* (1979) showed that in the presence of montmorillonite, the oligomerization of HCN is inhibited, suggesting an interaction with HCN oligomers, and not with HCN itself. In

other words, they found that clay catalysed the decomposition of tetramer, DAMN, to form diiminosuccinonitrile (DISN); consequently, the degradation of DAMN involves the release of HCN to the medium. According to this hypothesis, our results are congruent with the greater concentration of free HCN in the presence of clay (Fig. 2). The decomposition of tetramer could be the result of oxidation reactions, mediated by the hydrolysis process and/or the presence of Fe^{3+} in the clay lattice (Ferris *et al.*, 1982).

In summary, the results suggest that the hydrolysis process, at acidic pH and at 100°C, is the dominant mechanism of transformation of HCN. However, at basic pH and at 100°C, the polymerization of HCN is the dominant reaction (Fig. 2). In addition, the change in colour (yellow to brown) of basic samples, after treatment, is evidence of the polymerization process. The presence of Mg-Mont has two effects: on the one hand, it increases the hydrolysis of HCN (at acidic pH) and, on the other, it inhibits the oligomerization of HCN at basic pH. In order to evaluate the effect of pH on HCN-thermal products, several analytic studies were performed to identify organic molecules in the aqueous component.

Products of HCN thermolysis

Some intermediate species with great prebiotic importance can be formed from HCN under several experimental conditions (Ruiz-Bermejo *et al.*, 2013). In this work, only the aqueous phase from HCN thermolysis, the supernatant, was analysed. The organic richness of this aqueous phase will determine the best geochemical conditions in which the products of HCN thermolysis can undergo subsequent reactions in a dynamic environment. The nature, availability and reactivity of the organic molecules dissolved in the medium will determine the importance of HCN on hydrothermal environments. The supernatants of each experiment, with the greater time exposition to heat, were analysed by different qualitative methods.

Aldehydes

Only in the acidic sample heated without clay, a small peak associated with formaldehyde (HCHO) was detected by GC, both by retention time and co-injection of the standard (Fig. 4). Although

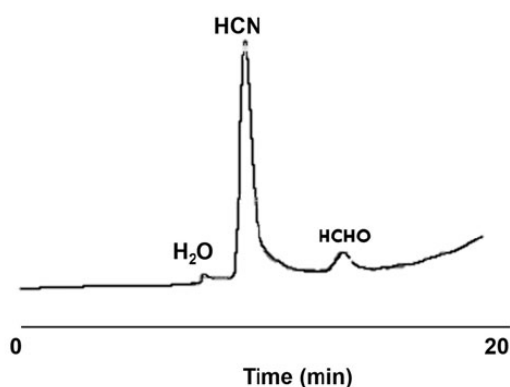


Fig. 4. Gas chromatogram of volatile products from the sample of HCN thermolysis at acidic pH without Mg-Mont. The formation of formaldehyde (HCHO) is shown.

the decomposition of formic acid – formed by hydrolysis of HCN – under hydrothermal conditions has as major products CO₂ and H₂ (Yu and Savage, 1998), it has been suggested that formaldehyde can also be a reaction product (Nelson and Engelder, 1925). In addition, the production of formaldehyde from the radiolysis of HCN has been reported (Negrón-Mendoza *et al.*, 1983). Even if derivatization by Brady's method (in which carbonyl groups are identified by the formation of 2,4-dinitrophenylhydrazones) (Shriner *et al.*, 1982) was performed for all samples, none of them showed positive results; this may be associated with a very low concentration of produced aldehydes in the samples.

Urea

Several researches have shown that urea is a product of HCN oligomerization. Specifically, it may be a product of oxidation/hydrolysis of DAMN (Ferris *et al.*, 1973, 1974b; Ferris and Ryan, 1973; Ferris and Edelson, 1978; Ferris and Hagan, 1984). Our experiments showed that urea is formed only by thermolysis of slightly basic HCN solutions (pH = 8.5) and even in the presence of Mg-Mont (Fig. 5). In addition, urea concentration was greater in the sample without clay. This is consistent with the HCN polymerization mechanism previously mentioned. In other words, and in agreement with Fig. 2, HCN polymerizes better in the absence of clay mineral; and, in consequence, the formation of the tetramer should be higher. Hence, the oxidation/hydrolysis reaction of DAMN at high temperatures led to the formation of an important amount of free urea (≈40% higher concentration than the sample with mineral).

Urea has been considered an important prebiotic molecule due to its participation in synthesis reactions of pyrimidines (Robertson and Miller, 1995; Menor-Salván *et al.*, 2009), and its role in hydrothermal scenarios was highlighted (Holm, 1992). Likewise, it has also been found in HCN-radiolysis experiments (Draganić *et al.*, 1985a, b; Vujošević *et al.*, 1990; Colín-García *et al.*, 2009).

Carboxylic acids

The formation of some carboxylic acids by thermolysis of HCN was confirmed (Fig. 6). Among the main carboxylic acids identified are: oxalic, maleic, glycolic and formic acid, which were also identified by GC-MS. The formation of formic acid corroborates that, at pH = 2, hydrolysis is the main reaction. In addition, the

peaks of oxalic and maleic acid may be a result of the decomposition of formic acid along thermolysis; in other words, they are secondary products.

The samples under basic pH show more production of carboxylic acids than in acidic conditions. The main reaction involves the formation of oxalic acid, which could be the result of oxidation of DAMN and the reaction between DISN with water and other nucleophiles (Ferris *et al.*, 1982; Schwartz *et al.*, 1984). Additionally, the presence of Mg-Mont seems to affect the reaction products (a predominant unidentified peak, with $R_t \sim 8.5$ min, was detected on the sample without mineral). Moreover, the sample with clay showed a higher remnant of HCN, which is consistent with Fig. 2. Clay mineral inhibits the polymerization process, and hence, a higher amount of free HCN is available. Negrón-Mendoza *et al.* (2001) reported that the presence of Na-Mont in HCN radiolysis significantly affects the amount and diversity of carboxylic acids formed.

Other options to explain the formation of carboxylic acids may be by reactions between aldehydes (e.g. formaldehyde) and the cyanide ion through the formation of cyanohydrins as intermediates; as well as the formation of other nitriles (e.g. cyanate, cyanogen, cyanoacetylene, glyconitrile), which are produced from decomposition (*i.e.* hydrolysis, oxidation) of HCN (Kemp and Kohnstam, 1956; Brotherton and Lynn, 1959; Ferris *et al.*, 1968; Wang *et al.*, 1987).

Diaminomaleonitrile

Among oligomers of HCN, DAMN has drawn great attention because it has been pointed out as a gateway for the synthesis of purine and pyrimidines (Zubay, 2000). The analysis of the aqueous phase of heated samples shows that DAMN is present only in the basic solutions (Fig. 7), as previously mentioned (Miyakawa *et al.*, 2002; Borquez *et al.*, 2005). Even though Yuasa and Ishigami (1977) showed that DAMN is also formed in the presence of Mg oxides, which suggests that divalent metals would favour the HCN oligomerization, the presence of a clay mineral seems to inhibit the synthesis of DAMN (the sample with clay showed a considerably lower amount of this oligomer). As mentioned above, the decomposition of DAMN may occur by its hydrolysis and/or oxidation by Fe³⁺ in the clay lattice (Begland *et al.*, 1974; Ferris *et al.*, 1982). Another possibility is that the lower amount of free DAMN in the sample with Mg-Mont may be the result of surface retention of this oligomer, as this has been reported to happen with other surfaces (Thissen *et al.*, 2015; Toh *et al.*, 2019). This is an important result because, although the HCN thermolysis under alkaline conditions yields DAMN, eventually, its interaction with the available clays in the medium would constrain the oligomerization process.

CG-MS analysis

To corroborate some of the species that we characterized and some free amino acids, a derivatization of samples, without the common hydrolysis procedure, was performed. Hydrolysis can affect the original amount and nature of the soluble fraction, and this procedure is focused on HCN-derived polymers (Ruiz-Bermejo *et al.*, 2013). As we mentioned above, this study is only focused on the soluble fraction of samples.

Glycine and alanine traces were detected only in the acidic sample without clay by GC-MS (data not shown). In both basic samples, it was also possible to corroborate the presence of urea, oxalic and glycolic acid by GC-MS. In addition, intermediate species such as carbamic acid, ethanolamine, glycerol, succinic

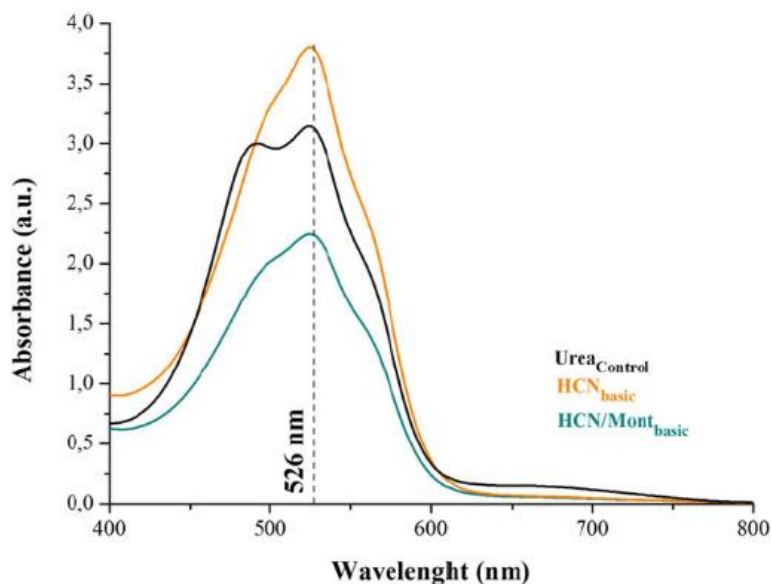


Fig. 5. Urea is a product of the thermolysis of HCN under slightly basic solutions. The spectrum UV-Vis shows the specific absorption band of the complex formed by the reaction of DAM.

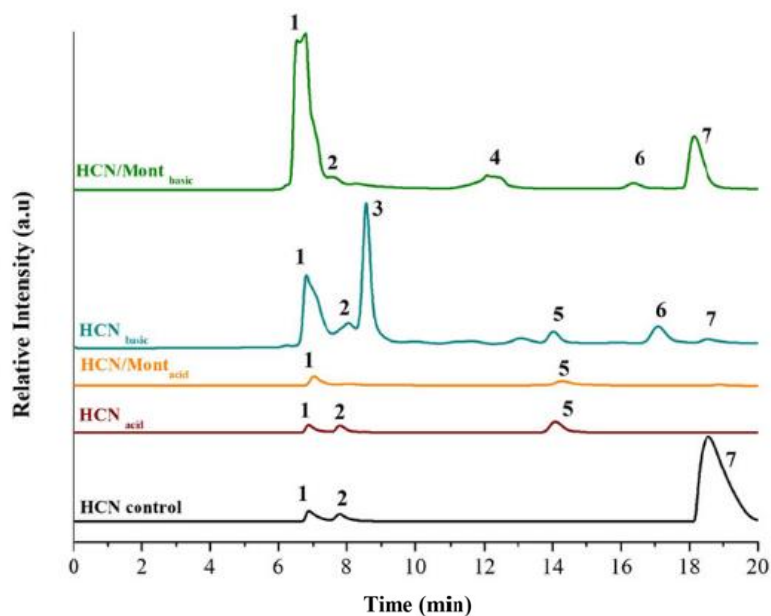


Fig. 6. UHPLC chromatograms of carboxylic acids formed by HCN-thermolysis. Under basic conditions, the formation of carboxylic acids is higher than at acidic pH. Legend: (1) oxalic acid, (2) maleic acid, (3) not characterized, (4) glycolic acid, (5) formic acid, (6) not characterized and (7) HCN.

and propanoic acid were detected in basic solution fractions. It should be mentioned that, in general, free amino acids are not detected in our HCN experiments. Only after acid hydrolysis of HCN oligomers, synthesized either by thermal energy or ionizing radiation, are a significant amount of amino acids released (Ferris *et al.*, 1974a; Draganić *et al.*, 1985a, b; Vujošević *et al.*, 1990; Ruiz-Bermejo *et al.*, 2013; Marin-Yaseli *et al.*, 2016). The

formation of free amino acids can be explained by common Strecker synthesis among HCN, aldehydes and ammonia. Some authors have reported the viability of this mechanism under submarine conditions (Schulte and Shock, 1995; Andersson and Holm, 2000). Other pathways for amino acid production [like the synthesis from ethanolamine (detected in this study by GC-MS) using metal powder and Friedel-Crafts reactions

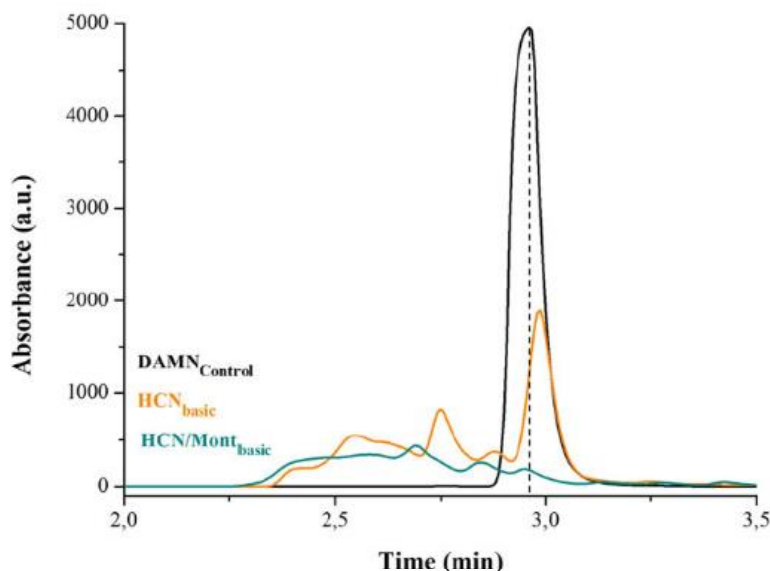


Fig. 7. UHPLC chromatogram of HCN thermolysis samples. Only in basic medium did the HCN thermolysis yield DAMN. However, Mg-Mont may inhibit the polymerization of HCN.

catalysed by minerals] have been proposed under alkaline hydrothermal scenarios (Zhang *et al.*, 2017; Ménez *et al.*, 2018).

In summary, the thermolysis of acidic samples shows that the formation of formic acid by hydrolysis of HCN is the predominant mechanism. In addition, the presence of Mg-Mont increases the transformation of HCN. The formation of formaldehyde and small carboxylic acids, in acidic conditions, may well be the result of decomposition of formic acid. Differently, the thermolysis at basic conditions showed a higher formation of organic molecules. In the case of the sample without clay, the amount of recovered HCN was lower with the consequent high formation of DAMN. Likewise, semi-quantitative analysis showed that a high amount of urea and oxalic acid was present. Finally, the higher amount of free HCN and the lower amount of urea and DAMN in the sample with Mg-Mont corroborate that clay inhibits the oligomerization of HCN at basic conditions.

Relevance for chemical evolution

Our experiments showed that, even considering a simple hydrothermal simulation, HCN thermolysis may be an important starting point for the production of several organic molecules. If the synthesis of HCN under hydrothermal conditions is continuous, these systems could have had a considerable role as 'abiotic reactors and chemical evolution niches', as they were originally proposed (Corliss *et al.*, 1980; Baross and Hoffman, 1985). It is important to highlight that geochemical conditions of the environment are crucial because they are directly related to the formation/destruction mechanisms of more complex organic compounds. Although some experiments suggest that both HCN and some thermolysis products are unstable under hydrothermal conditions (Sanchez *et al.*, 1968; Stribling and Miller, 1987; Miller and Bada, 1988; Holm, 1992; Yu and Savage, 1998; Cleaves II, 2008), it is necessary to take into account several points that, according to our criteria, could be underestimated.

The first is that hydrothermal systems are very complex environments with many geochemical variables, and hence, they are more than high-pressure and high-temperature environments. In this way, new approaches are considering the role of several combined parameters (*i.e.* pH, redox state, dissolved gases and/or mineral surfaces) on the stability of compounds. In general, these new approaches have shown that the fate and stability of organic molecules are intrinsically related to these variables (Holm and Andersson, 2005; Colín-García *et al.*, 2016, 2018).

Additionally, the chemical species are not isolated. In other words, the availability of different species in the same environment could favour the subsequent reactions. For instance, the presence of aldehydes and ammonia would favour the polymerization of HCN (Voet and Schwartz, 1983).

Additionally, the molecules are not exposed to the highest temperature all the time. At the moment that the hydrothermal fluids are mixed with seawater, new temperature and/or pH gradients can harbour more suitable conditions (Chevaldonné *et al.*, 1991; Bates *et al.*, 2010) and favour the stability and polymerization of organic molecules (Ogasawara *et al.*, 2000; Ogata *et al.*, 2000; Islam *et al.*, 2003).

This approximation about the role of the HCN thermolysis process in the formation of organic molecules suggests that surroundings of hydrothermal environments (<100°C), such as sub-aerial alkaline environments, could have been an important source of free organic compounds on early Earth. It is necessary to design and carry out more complex experiments that would consider coupled variables present in hydrothermal systems to gain a detailed understanding of the behaviour of organic molecules under several geochemical conditions.

Acknowledgements. SAVB acknowledges Posgrado en Ciencias de la Tierra UNAM, CONACyT (Ph.D. grant 697442 and the financial support for a research stay grant) and the Laboratorio de Evolucion Química (ICN-UNAM) for the use of its facilities. ANM acknowledges PAPIIT (IN110919). M.R.B. used the research facilities of the Centro de Astrobiología (CAB), and was supported by the Instituto Nacional de

Técnica Aeroespacial 'Eteban Terradas' (INTA) and by the Spanish Ministerio de Ciencia, Innovación y Universidades ESP2017-89053-C2-2-P. M.C-G acknowledges the financial support from the CONACyT A1-S-24341 and DGAPA-PAPIIT IA203217 research grants, and from the Instituto de Geología (UNAM). The authors are indebted to Claudia Camargo, Jorge A. Cruz Castañeda and Adriana Meléndez-López for their technical assistance.

References

- Adams JM and McCabe RW (2006) Chapter 10.2 clay minerals as catalysts. *Developments in Clay Science* 1, 541–581.
- Andersson E and Holm NG (2000) The stability of some selected amino acids under attempted redox constrained hydrothermal conditions. *Origins of Life and Evolution of Biospheres* 30, 9–23.
- Arrhenius T, Arrhenius G and Paplawsky W (1994) Archean geochemistry of formaldehyde and cyanide and the oligomerization of cyanohydrin. *Origins of Life and Evolution of Biospheres* 24, 1–17.
- Azamar JA and Draganić IG (1982) *Equipo Para la Preparación de Compuestos Tóxicos en Solución Acuosa Y en Atmósfera Controlada: Cianuros Para Experimentos en Química de Radiaciones*. Mexico D.F.: Informe Técnico Departamento de Química, CEN, UNAM.
- Baross JA and Hoffman SE (1985) Submarine hydrothermal vents and associated gradient environments as sites for the origin and evolution of life. *Origins of Life and Evolution of Biospheres* 15, 327–345.
- Bates AE, Lee RW, Tunnicliffe V and Lamare MD (2010) Deep-sea hydrothermal vent animals seek cool fluids in a highly variable thermal environment. *Nature Communications* 1, 1–6.
- Begland RW, Hartter DR, Jones FN, Sam DJ, Sheppard WA, Webster OW and Weigert FJ (1974) Hydrogen cyanide chemistry. VIII. New chemistry of diaminomaleonitrile. Heterocyclic synthesis. *Journal of Organic Chemistry* 39, 2341–2350.
- Borquez E, Cleaves HJ, Lazcano A and Miller SL (2005) An investigation of prebiotic purine synthesis from the hydrolysis of HCN polymers. *Origins of Life and Evolution of Biospheres* 35, 79–90.
- Brandes JA, Bactor NZ, Cody GD, Cooper BA, Hazen RM and Yoder HS (1998) Abiotic nitrogen reduction on the early Earth. *Nature* 395, 365–367.
- Brotherton TK and Lynn JW (1959) The synthesis and chemistry of cyanogen. *Chemical Reviews* 59, 841–883.
- Charoul JL, Donval JP, Douville E, Jean-Baptiste P, Radford-Knoery J, Fouquet Y, Dapigny A and Stievenard M (2000) Compared geochemical signatures and the evolution of Menez Gwen (37°50'N) and lucky strike (37°17'N) hydrothermal fluids, south of the Azores Triple Junction on the Mid-Atlantic Ridge. *Chemical Geology* 171, 49–75.
- Chevaldonné P, Desbruyères D and Håitre ML (1991) Time-series of temperature from three deep-sea hydrothermal vent sites. Deep sea research part A. *Oceanographic Research Papers* 38, 1417–1430.
- Cleaves HJ II (2008) The prebiotic geochemistry of formaldehyde. *Precambrian Research* 164, 111–118.
- Colín-García M, Negrón-Mendoza A and Ramos-Bernal S (2009) Organics produced by irradiation of frozen and liquid HCN solutions: implications for chemical evolution studies. *Astrobiology* 9, 279–288.
- Colín-García M, Ortega-Gutiérrez F, Ramos-Bernal S and Negrón-Mendoza A (2010) Heterogeneous radiolysis of HCN adsorbed on a solid surface. *Nuclear Instruments and Methods in Physics Research* 619, 83–85.
- Colín-García M, Heredia A, Negrón-Mendoza A, Ortega F, Pi T and Ramos-Bernal S (2014) Adsorption of HCN onto sodium montmorillonite dependent on the pH as a component to chemical evolution. *International Journal of Astrobiology* 13, 310–318.
- Colín-García M, Heredia A, Cordero G, Camprubí A, Negrón-Mendoza A, Ortega-Gutiérrez F, Bernaldi H and Ramos-Bernal S (2016) Hydrothermal vents and prebiotic chemistry: a review. *Boletín de la Sociedad Geológica Mexicana* 68, 599–620.
- Colín-García M, Villafaña-Barajas S, Camprubí A, Ortega-Gutiérrez F, Colás V and Negrón-Mendoza A (2018) 5.4 Prebiotic chemistry in hydrothermal vent systems. In *Handbook of Astrobiology*, Kolb, V. edn, Boca Raton, FL.: Publisher: CRC Press, pp. 297–329.
- Corliss JB, Baross JA and Hoffman SE (1980) Submarine hydrothermal systems: a probable site for the origin of life, *Corvallis, or School of Oceanography, Oregon State University*. 44 pp.
- Cruz M (1974) Adsorption and transformation of HCN on the surface of copper and calcium montmorillonite. *Clays and Clay Minerals* 22, 417–425.
- Demir B, Salmas RE, Ahunbay MG and Yurtsever M (2012) Monte Carlo simulations of HCN adsorption in LTA zeolites. in: *Proceedings of the International Conference on Innovations in Chemical Engineering and Medical Sciences*. Dubai, United Arab Emirates: IEEE pp. 11–15.
- Draganić IG and Draganić ZD (1980) Radiation-chemical aspects of chemical evolution and radiation chemistry of simple cyano compounds. *Radiation Physics and Chemistry* 15, 195–201.
- Draganić I, Draganić Z, Petković L and Nikolić A (1973) Radiation chemistry of aqueous solutions of simple RCN [hydrogen or alkyl cyanide] compounds. *Journal of the American Chemical Society* 95, 7193–7199.
- Draganić ZD, Draganić IG, Azamar JA, Vujošević SI, Berber MD and Negrón-Mendoza A (1985a) Radiation chemistry of overirradiated aqueous solutions of hydrogen cyanide and ammonium cyanide. *Journal of Molecular Evolution* 21, 356–363.
- Draganić ZD, Vujošević SI, Negrón-Mendoza A, Azamar JA and Draganić IG (1985b) Radiation chemistry of a multicomponent aqueous system relevant to chemistry of cometary nuclei. *Journal of Molecular Evolution* 22, 175–187.
- Dzombak DA, Ghosh RS and Wong-Chong GM (2006) *Cyanide in Water and Soil: Chemistry, Risk, and Management*. Boca Raton: CRC/Taylor & Francis, 601 pp.
- Fábián B, Szöri M and Jedlovsky P (2014) Floating patches of HCN at the surface of their aqueous solutions – Can they make 'HCN world' plausible? *Journal of Physical Chemistry C* 118, 21469–21482.
- Ferris JP and Edelson EH (1978) Chemical evolution. 31. Mechanism of the condensation of cyanide to hydrogen cyanide oligomers. *Journal of Organic Chemistry* 43, 3989–3995.
- Ferris JP and Hagan WJ (1984) HCN and chemical evolution: the possible role of cyano compounds in prebiotic synthesis. *Tetrahedron* 40, 1093–1120.
- Ferris JP and Ryan TJ (1973) Chemical evolution. XIV. Oxidation of diaminomaleonitrile and its possible role in hydrogen cyanide oligomerization. *Journal of Organic Chemistry* 38, 3302–3307.
- Ferris JP, Sanchez RA and Orgel LE (1968) Studies in prebiotic synthesis. *Journal of Molecular Biology* 33, 693–704.
- Ferris JP, Donner DB and Lobo AP (1973) Possible role of hydrogen cyanide in chemical evolution: investigation of the proposed direct synthesis of peptides from hydrogen cyanide. *Journal of Molecular Biology* 74, 499–510.
- Ferris JP, Wos JD, Nooner DW and Oró J (1974a) Chemical evolution: XXI. The amino acids released on hydrolysis of HCN oligomers. *Journal of Molecular Evolution* 3, 225–231.
- Ferris JP, Wos JD, Ryan TJ, Lobo AP and Donner DB (1974b) Biomolecules from HCN. *Origins of Life* 5, 153–157.
- Ferris JP, Edelson EH, Mount NM and Sullivan AE (1979) The effect of days on the oligomerization of HCN. *Journal of Molecular Evolution* 13, 317–330.
- Ferris JP, Hagan WJ, Alvis KW and McCrea J (1982) Chemical evolution 40. Clay-mediated oxidation of diaminomaleonitrile. *Journal of Molecular Evolution* 18, 304–309.
- Ferus M, Kubelík P, Knížek A, Pastorek A, Sutherland J and Civiš S (2017) High energy radical chemistry formation of HCN-rich atmospheres on early Earth. *Scientific Reports* 7, 1–9.
- Fornari DJ, Shank T, Von Damm KL, Gregg TKP, Lilley M, Levai G, Bray A, Haymon RM, Perfit MR and Lutz R (1998) Time-series temperature measurements at high-temperature hydrothermal vents, east pacific rise 9° 49'–51'N: evidence for monitoring a crustal cracking event. *Earth and Planetary Science Letters* 160, 419–431.
- Frenkel M (1974) Surface acidity of montmorillonites. *Clays and Clay Minerals* 22, 435–441.
- Holm NG (ed.) (1992) *Marine Hydrothermal Systems and the Origin of Life*. Dordrecht, The Netherlands: Springer, 250 pp.
- Holm NG (2012) The significance of Mg in prebiotic geochemistry. *Geobiology* 10, 269–279.
- Holm NG and Andersson E (2005) Hydrothermal simulation experiments as a tool for studies of the origin of life on Earth and other terrestrial planets: a review. *Astrobiology* 5, 444–460.

- Holm NG and Neubeck A (2009) Reduction of nitrogen compounds in oceanic basement and its implications for HCN formation and abiotic organic synthesis. *Geochemical Transactions* 10, 1–11.
- Islam S and Powner MW (2017) Prebiotic systems chemistry: complexity overcoming clutter. *Chem* 2, 470–501.
- Islam MN, Kaneko T and Kobayashi K (2003) Reaction of amino acids in a supercritical water-flow reactor simulating submarine hydrothermal systems. *Bulletin of the Chemical Society of Japan* 76, 1171–1178.
- Jamis J, Drljaca A, Spiccia L and Smith TD (1995) FTIR spectroscopic study of the adsorption of hydrogen cyanide by metal-oxide pillared clays. *Chemistry of Materials* 7, 2078–2085.
- Keefe AD and Miller SL (1996) Was ferrocyanide a prebiotic reagent? *Origins of Life and Evolution of Biospheres* 26, 111–129.
- Kemp IA and Kohnstam G (1956) The decomposition of inorganic cyanates in water. *Journal of Chemical Society (Resumed)* 191, 900–911.
- Konn C, Charlou JL, Holm NG and Mouis O (2015) The production of methane, hydrogen, and organic compounds in ultramafic-hosted hydrothermal vents of the Mid-Atlantic ridge. *Astrobiology* 15, 381–399.
- Kotdawala RR, Kazantzis N and Thompson RW (2008) Molecular simulation studies of adsorption of hydrogen cyanide and methyl ethyl ketone on zeolite NaX and activated carbon. *Journal of Hazardous Materials* 159, 169–176.
- LaRowe DE and Regnier P (2008) Thermodynamic potential for the abiotic synthesis of adenine, cytosine, guanine, thymine, uracil, ribose, and deoxyribose in hydrothermal systems. *Origins of Life and Evolution of Biospheres* 38, 383–397.
- Ma Y, Wang F, Wang X, Ning P, Jing X and Cheng J (2011) The hydrolysis of hydrogen cyanide over Nb/La–TiO_x catalyst. *Journal of the Taiwan Institute of Chemical Engineers* 70, 141–149.
- Marin-Yaseli MR, González-Toril E, Mompeán C and Ruiz-Bermejo M (2016) The role of aqueous aerosols in the ‘glyoxylate scenario’: an experimental approach. *Chemistry – A European Journal* 22, 12785–12799.
- Matthews CN (2005) The HCN world. In Seckbach J (ed.), *Origins*. Dordrecht: Kluwer Academic Publishers, pp. 121–135.
- Matthews CN and Minard RD (2006) Hydrogen cyanide polymers, comets and the origin of life. *Faraday Discussions* 133, 393–401.
- McDermott JM, Seewald JS, German CR and Sylva SP (2015) Pathways for abiotic organic synthesis at submarine hydrothermal fields. *PNAS* 112, 7668–7672.
- Ménez B, Pisapia C, Andreani M, Jamme F, Vanbellingen QP, Brunelle A, Richard L, Dumas P and Réfrégiers M (2018) Abiotic synthesis of amino acids in the recesses of the oceanic lithosphere. *Nature* 564, 59–63.
- Menor-Salván C, Ruiz-Bermejo DM, Guzmán MI, Osuna-Esteban S and Veintemillas-Verdaguer S (2009) Synthesis of pyrimidines and triazines in ice: implications for the prebiotic chemistry of nucleobases. *Chemistry – A European Journal* 15, 4411–4418.
- Miller SL (1987) Which organic compounds could have occurred on the prebiotic Earth? *Cold Spring Harbor Symposium on Quantitative Biology* 52, 17–27.
- Miller SL and Bada JL (1988) Submarine hot springs and the origin of life. *Nature* 334, 609–611.
- Mittelstaedt E, Escartin J, Gracias N, Olive J-A, Barreyre T, Davaille A, Cannat M and Garcia R (2012) Quantifying diffuse and discrete venting at the tour Eiffel vent site, lucky strike hydrothermal field. *Geochemistry, Geophysics, Geosystems* 13, 1–18.
- Miyakawa S, Cleaves HJ and Miller SL (2002) The cold origin of life: a. Implications based on the hydrolytic stabilities of hydrogen cyanide and formamide. *Origins of Life and Evolution of Biospheres* 32, 195–208.
- Mukhin LEV (1974) Evolution of organic compounds in volcanic regions. *Nature* 251, 50–51.
- Mumma MJ and Charnley SB (2011) The chemical composition of comets – emerging taxonomies and natal heritage. *Annual Review of Astronomy and Astrophysics* 49, 471–524.
- Nanba T, Obuchi A, Akaratiwa S, Liu S, Uchisawa J and Kushiya S (2000) Catalytic hydrolysis of HCN over H-ferrierite. *Chemistry Letters* 29, 986–987.
- Negrón-Mendoza A, Draganić ZD, Navarro-González R and Draganić IG (1983) Aldehydes, ketones, and carboxylic acids formed radiolytically in aqueous solutions of cyanides and simple nitriles. *Radiation Research* 95, 248.
- Negrón-Mendoza A, Chacón BE, Perezgasga L and Torres JL (1986) *Determinación de Urea por el Método de DAM*. Mexico: Informe Técnico Q-02–86, CEN-UAM, 7 pp.
- Negrón-Mendoza A, Ramos-Bernal S, Cruz E and Juárez JM (2001) Radiolysis of HCN in heterogeneous phase. *Radiation Physics and Chemistry* 61, 771–772.
- Nelson WL and Engelder CJ (1925) The thermal decomposition of formic acid. *Journal of Physical Chemistry* 30, 470–475.
- Nikalje MD, Phukan P and Sudalai A (2000) Recent advances in clay-catalyzed organic transformations. *Organic Preparations and Procedures International* 32, 1–40.
- Niketić V, Draganić ZD, Nešković S, Jovanović S and Draganić IG (1983) Radiolysis of aqueous solutions of hydrogen cyanide (pH~6): compounds of interest in chemical evolution studies. *Journal of Molecular Evolution* 19, 184–191.
- Ogasawara H, Yoshida A, Imai E, Honda H, Hatori K and Matsuno K (2000) Synthesizing oligomers from monomeric nucleotides in simulated hydrothermal environments. *Origins of Life and Evolution of Biospheres* 30, 519–526.
- Ogata Y, Imai E, Honda H, Hatori K and Matsuno K (2000) Hydrothermal circulation of seawater through hot vents and contribution of interface chemistry to prebiotic synthesis. *Origins of Life and Evolution of Biospheres* 30, 527–537.
- Parkos D, Pikus A, Alexeenko A and Melosh HJ (2016) HCN production from impact ejecta on the early Earth, in: *AIP Conference Proceedings*. AIP Publishing, 1/86. 1/0001-1-1/000-8.
- Pizzarello S (2012) Hydrogen cyanide in the Murchison meteorite. *Astrophysical Journal Letters*. 754, L27. 1–3
- Rimmer PB and Rugheimer S (2019) Hydrogen cyanide in nitrogen-rich atmospheres of rocky exoplanets. *Icarus* 329, 124–131.
- Robertson MP and Miller SL (1995) An efficient prebiotic synthesis of cytosine and uracil. *Nature* 375, 772–774.
- Ruiz-Bermejo M, de la Fuente JL, Rogero C, Menor-Salván C, Osuna-Esteban S and Martín-Gago JA (2012) New insights into the characterization of ‘insoluble black HCN polymers’. *Chemistry and Biodiversity* 9, 25–40.
- Ruiz-Bermejo M, Zorzano M-P and Osuna-Esteban S (2013) Simple organics and biomonomers identified in HCN polymers: an overview. *Life (Chicago, IL)* 3, 421–448.
- Sanchez RA, Ferris JP and Orgel LE (1967) Studies in prebiotic synthesis. II. Synthesis of purine precursors and amino acids from aqueous hydrogen cyanide. *Journal of Molecular Biology* 30, 223–253.
- Sanchez RA, Ferris JP and Orgel LE (1968) Studies in prebiotic synthesis. *Journal of Molecular Biology* 38, 121–128.
- Schäfer S and Bonn B (2000) Hydrolysis of HCN as an important step in nitrogen oxide formation in fluidised combustion. Part 1. Homogeneous reactions. *Fuel* 79, 1239–1246.
- Schoonen MAA and Xu Y (2001) Nitrogen reduction under hydrothermal vent conditions: implications for the prebiotic synthesis of C-H-O-N compounds. *Astrobiology* 1, 133–142.
- Schrenk MO, Kelley DS, Bolton SA and Baross JA (2004) Low archaeal diversity linked to seafloor geochemical processes at the lost city hydrothermal field, Mid Atlantic Ridge. *Environmental Microbiology* 6, 1086–1095.
- Schulte M and Shock E (1995) Thermodynamics of Strecker synthesis in hydrothermal systems. *Origins of Life and Evolution of Biospheres* 25, 161–173.
- Schwartz AW, Voet AB and Veen M (1984) Recent progress in the prebiotic chemistry of HCN. *Origins of Life and Evolution of the Biosphere* 14, 91–98.
- Shock EL (1992) Hydrothermal organic synthesis experiments. In Holm NG (ed.), *Marine Hydrothermal Systems and the Origin of Life*. Dordrecht, The Netherlands: Springer, pp. 135–146.
- Shriner RM, Fuson C, Reynold C, Curtin Y, David C and Dominguez XA Tr (1982) *Identificación Sistemática de Compuestos Orgánicos*. Mexico: Limusa, 479 pp.
- Stribling R and Miller SL (1987) Energy yields for hydrogen cyanide and formaldehyde syntheses: the HCN and amino acid concentrations in the primitive ocean. *Origins of Life and Evolution of Biospheres* 17, 261–273.

- Sutherland JD (2016) The origin of life – out of the blue. *Angewandte Chemie International Edition* 55, 104–121.
- Thissen H, Koegler A, Salwiczek M, Easton CD, Qu Y, Lithgow T and Evans RA (2015) Prebiotic-chemistry inspired polymer coatings for biomedical and material science applications. *NPG Asia Materials* 7, e225. 1–9 pp.
- Tian F, Kasting JF and Zahnle K (2011) Revisiting HCN formation in Earth's early atmosphere. *Earth and Planetary Science Letters* 308, 417–423.
- Toh RJ, Evans R, Thissen H, Voelcker NH, d'Ischia M and Ball V (2019) Deposition of aminomalononitrile-based films: kinetics, chemistry, and morphology. *Langmuir* 35, 9896–9903.
- Voet AB and Schwartz AW (1983) Prebiotic adenine synthesis from HCN – evidence for a newly discovered major pathway. *Bioorganic Chemistry* 12, 8–17.
- Vujošević SI, Negrón-Mendoza A and Draganić ZD (1990) Radiation-induced polymerization in dilute aqueous solutions of cyanides. *Origins of Life and Evolution of Biospheres* 20, 49–54.
- Wang YL, Lee HD, Beach MW and Margerum DW (1987) Kinetics of base hydrolysis of cyanogen and 1-cyanoformamide. *Inorganic Chemistry* 26, 2444–2449.
- Yu J and Savage PE (1998) Decomposition of formic acid under hydrothermal conditions. *Industrial & Engineering Chemistry Research* 37, 2–10.
- Yuasa S and Ishigami M (1977) Geochemically possible condensation of hydrogen cyanide in the presence of divalent metal compounds. *Geochemical Journal* 11, 247–252.
- Zhang X, Tian G, Gao J, Han M, Su R, Wang Y and Feng S (2017) Prebiotic synthesis of glycine from ethanolamine in simulated Archean alkaline hydrothermal vents. *Origins of Life and Evolution of Biospheres* 47, 413–425.
- Zhao Q, Tian S, Yan L, Zhang Q and Ning P (2015) Novel HCN sorbents based on layered double hydroxides: sorption mechanism and performance. *Journal of Hazardous Materials* 285, 250–258.
- Zubay G (2000) *Origins of Life: On Earth and in the Cosmos*. Academic Press, 564 pp

Síntesis de moléculas orgánicas

Polimeros de HCN y sistemas hidrotermales

Ensayos de Química Prebiótica II


Artículo de Investigación

Villafañe-Barajas, S. A., Ruiz-Bermejo, M., Rayo-Pizarroso, P., & Colín-García, M. (2020). Characterization of HCN-Derived Thermal Polymer: Implications for Chemical Evolution. *Processes*, 8(8), 968.

Resumen Los polímeros derivados del ácido cianhídrico (HCN) han sido reconocidos como precursores de moléculas orgánicas relevantes en el campo de la química prebiótica y las ciencias de los materiales. Sin embargo, aún se desconoce la naturaleza de estos polímeros así como sus propiedades fisicoquímicas y las vías químicas que llevan a su síntesis. Aunque se ha propuesto que el HCN pudo haber estado disponible en entornos hidrotermales y pudo ser una molécula esencial en la serie de pasos que llevo a la síntesis de diversas moléculas orgánicas más complejas, muy pocos experimentos han utilizado especies de cianuro considerando escenarios hidrotermales. En este trabajo, sintetizamos un polímero térmico derivado del HCN (*HCN-DTP*, por sus siglas en inglés) simulando un ambiente hidrotermal alcalino (*i.e.*, HCN (l) 0.15 M, 50 h, 100 °C, pH > 10). De igual manera, caracterizamos su posible estructura química, su comportamiento térmico y el efecto de hidrólisis en la liberación de moléculas orgánicas. El análisis elemental y la espectroscopia infrarroja sugieren un importante grado de oxidación. El análisis térmico permite concluir que el polímero es considerablemente más estable que otros polímeros derivados de HCN, sintetizados en condiciones similares. De igual manera, es posible identificar la liberación gradual de varios compuestos volátiles a lo largo de diferentes eventos térmicos. En general, los resultados sugieren una macro estructura que podría estar formada por grupos amida e hidroxilo unidos a la cadena reticular principal con enlaces químicos conjugados (C = O, N = O, -O - C = N). Finalmente, el tratamiento de hidrólisis mostró las mejores condiciones de pH para la liberación de moléculas orgánicas. La posibilidad de sintetizar polímeros térmicos derivados del HCN en probables condiciones hidrotermales primitivas y su comportamiento posterior podría ser relevante para considerar a estos sistemas como nichos de evolución química importantes durante la Tierra primitiva.

Article

Characterization of HCN-Derived Thermal Polymer: Implications for Chemical Evolution

Saul A. Villafañe-Barajas ¹, Marta Ruiz-Bermejo ², Pedro Rayo-Pizarroso ² and María Colín-García ^{3,*} 

¹ Posgrado en Ciencias de la Tierra, Universidad Nacional Autónoma de México, Ciudad Universitaria, Cd. Mx 04510, Mexico; saulvillafanephd@gmail.com

² Centro de Astrobiología (CSIC-INTA), Dpto. Evolución Molecular, Ctra. Torrejón-Ajalvir, km 4, Torrejón de Ardoz, 28850 Madrid, Spain; ruizbm@cab.inta-csic.es (M.R.-B.); prayo@cab.inta-csic.es (P.R.-P.)

³ Instituto de Geología, Universidad Nacional Autónoma de México, Ciudad Universitaria, Cd. Mx 04510, Mexico

* Correspondence: mcolin@geologia.unam.mx; Tel.: +52-(55)-56224300-164

Received: 28 June 2020; Accepted: 4 August 2020; Published: 11 August 2020



Abstract: Hydrogen cyanide (HCN)-derived polymers have been recognized as sources of relevant organic molecules in prebiotic chemistry and material sciences. However, there are considerable gaps in the knowledge regarding the polymeric nature, the physicochemical properties, and the chemical pathways along polymer synthesis. HCN might have played an important role in prebiotic hydrothermal environments; however, only few experiments use cyanide species considering hydrothermal conditions. In this work, we synthesized an HCN-derived thermal polymer simulating an alkaline hydrothermal environment (i.e., HCN (l) 0.15 M, 50 h, 100 °C, pH approximately 10) and characterized its chemical structure, thermal behavior, and the hydrolysis effect. Elemental analysis and infrared spectroscopy suggest an important oxidation degree. The thermal behavior indicates that the polymer is more stable compared to other HCN-derived polymers. The mass spectrometric thermal analysis showed the gradual release of several volatile compounds along different thermal steps. The results suggest a complicate macrostructure formed by amide and hydroxyl groups, which are joined to the main reticular chain with conjugated bonds (C=O, N=O, –O–C=N). The hydrolysis treatment showed the pH conditions for the releasing of organics. The study of the synthesis of HCN-derived thermal polymers under feasible primitive hydrothermal conditions is relevant for considering hydrothermal vents as niches of chemical evolution on early Earth.

Keywords: HCN-derived thermal polymer; thermolysis; alkaline hydrothermal systems; chemical evolution

1. Introduction

Hydrogen cyanide, HCN, has been considered as a paramount raw material to reach high chemical complexity in the field of prebiotic chemistry and chemical evolution [1–4]. HCN could have been formed from different endogenic sources, on early Earth [3,5–9], or it could be formed exogenically and then carried to Earth [4,10–12].

The concentration of HCN on primitive environments is still discussed. Some authors argue that it must be low (10^{-10} – 10^{-13} mol L⁻¹; [13,14]); recently, Fábian et al. [15] proposed the formation of floating HCN patches with a >1 mol L⁻¹ concentration. In addition, Holm and Neubeck [5] suggested that HCN could have been produced under hydrothermal conditions from CH₄, NH₃, and other dissolved species (i.e., N₂, CO). The main reactions are as follows:





It is well known that HCN solutions spontaneously polymerize [16]. During the polymerization of HCN, an insoluble black polymer is formed under different synthesis conditions [17,18]. After hydrolysis treatments, these complex polymers release an important number of organic molecules [2,17,19–21]; recently, their applications on material sciences have been studied [22–25]. It has been demonstrated that the possible chemical structure and the thermal properties of these polymers directly depend on the conditions of the synthesis (e.g., raw material, temperature, concentration, reaction time, and atmosphere). Therefore, the HCN-derived polymers should be considered as a family of complex substances [18,26].

The synthesis of these complex materials has been dominated by the use of cyanide salts (e.g., sodium, potassium, and ammonia salts) dissolved in aqueous medium in a broad range of temperatures (from -20 up to 100 °C) at alkaline conditions ($\text{pH} > 8$) (e.g., [18,26–28]). Other experiments have synthesized HCN-derived polymers by heating formamide [29,30], aminomalononitrile, AMN, [24] and diaminomaleonitrile, DAMN [18].

There is robust information about the mechanisms and chemical conditions that lead to the formation of DAMN from HCN, cyanide (CN^-), and intermediate species, such as AMN [31–34]. There are also some proposals about their polymeric structure [18,20,28,35–39]. However, the pathways for the formation of HCN-derived polymers remain unsolved; new approaches suggest that hydrolysis/oxidation reactions along polymerization directly affect the physicochemical properties of these materials [26,28].

HCN polymers might have had an important role in chemical evolution; nonetheless, there are several inconsistencies regarding the initial concentration of HCN and the primitive scenario where polymers could have been formed [4,13,14]. It has been proposed that HCN could have experienced important reactions in prebiotic hydrothermal environments, and it could be an essential part of the stepwise series to produce successively more complex organic molecules [5,40–46]. Nonetheless, only a few research studies have used cyanide species in hydrothermal experiments [47–49] (for more details, see Aubrey et al., 2009 [46]).

There is a growing interest in the chemistry of HCN solutions in prebiotic chemistry studies. In addition, alkaline environments are shown to be very relevant for studies related to the origin of life [50,51]. However, the synthesis of HCN polymers under simulated hydrothermal conditions has been scarcely explored. In a recent paper [52], we studied the thermolysis of HCN under simulating HV conditions; along with the identification of formed products in solution in this experiment, we also detected the formation a black polymer. Hence, as we are interested in a systematic study of HCN under HV conditions, an HCN-derived thermal polymer (HCN-DTP) from a hydrogen cyanide solution was synthesized and characterized in detail in order to better constrain the properties of these fascinating substances. For characterization, we used a method previously developed for the analysis and systematic characterization of HCN-derived polymers that consisted of elemental analysis, infrared spectroscopy (IR), thermogravimetric (TG) and mass spectrometric thermal analysis (TG-MS), hydrolysis treatment, and GC-MS analysis, in order to gain information about its structure, nature, thermal behavior, and to evaluate its role as a precursor of organic molecules [17,18,26–28,53–55]. This comprehensive analytical study shows the identification of single biomolecules of interest in the chemical evolution research but also gives clues about the complex nature of the macrostructure of the HCN-DTP. It is necessary to know the relationships among the synthesis conditions, the structure, and the properties of the HCN polymers, in order to increase our knowledge about the possible role of HCN polymerization in prebiotic chemistry. These would lead to the generation of polymeric structures with potential properties fit for new or secondary reactions in unexplored prebiotic scenarios. In addition, these polymers would have potential applications in material sciences [18]. Interestingly, the HCN-DTP here described presents characteristics not previously reported.

2. Materials and Methods

Production of HCN. HCN solution (0.15 M) was produced in situ by the reaction between KCN and H₂SO₄. HCN gas was dissolved into Milli Q water under an argon atmosphere. The concentration of HCN was determined by titration with an aqueous solution of AgNO₃ [56]. The reaction for producing HCN is not scalable and must be carried out with many precautions due to the high toxicity of HCN. Although the concentration of HCN solution (0.15 M) could be higher than the feasible concentration on primitive environments, it was chosen according to previous reports that consider it as a practical and a consistent concentration for the polymerization of HCN [57].

After synthesis, the pH of the HCN solution was adjusted to approximately 10 by adding drops (approximately 10 µL) of a concentrated KOH solution (0.1 M) until the desired pH was reached; this was done to have an important amount of free cyanide in solution, thus avoiding a high potassium concentration. It has been observed that the formation of HCN polymers is favored in alkaline media [18], and we wanted to induce the formation of the polymer and prevent its hydrolysis.

Synthesis of HCN-derived thermal polymer. Experiments were carried out in a static system at 100 °C. Aliquots of the HCN solution (0.15 M, 5 mL) were placed in glass tubes and heated for 50 h. After the thermolysis treatment, the sample was cooled at room temperature. Then, it was possible to identify two different fractions: a soluble fraction (brown yellow) and a black viscous fraction, the HCN-DTP. HCN-DTP (black fraction) was separated from the rest of the soluble fraction (yellow) by centrifugation (10 min, 15 °C, 23,000 rpm). The procedure was carried out four times in order to have a considerable amount of the material (approximately 50 mg), since the yield of the polymer is low [18,26]. The reaction temperature and the pH were both chosen considering conditions surrounding alkaline hydrothermal environments [58]. In addition, this temperature was selected to synthesize organic molecules, and to favor the polymerization reactions of HCN, cyanide salts, and DAMN (for more details, see reference [2]). In contrast with previous reports [2,29,47,59], HCN-DTP does not form appreciable solid particles, although it was prepared above the concentration that favors polymerization reaction (>0.01 M) [14,31]. Recently, Ruiz-Bermejo and co-workers [18,26] have proved that high temperatures and low concentrations of raw material (i.e., up to 90 °C and <1 M) resulted in a low yield of the polymer. According to this, the nature of HCN-DTP is the result of the domain of hydrolysis/oxidation reactions over polymerization during thermolysis (see below). Therefore, the common insoluble black HCN polymers [17] do not have the same nature that the HCN-DTP produced in this experiment. Finally, the fractions were freeze-dried under reduced pressure, resulting in two fractions: a yellow oily precipitate and a black solid powder (HCN-DTP). In this report, different analyses were carried out with the black solid powder.

Elemental analysis. The content of C, N, H, and oxygen was measured. The HCN-derived thermal polymer was examined for the determination of the mass fractions of carbon, hydrogen, and nitrogen (in percentage with respect to weight) in a PerkinElmer® Elemental Analyzer, model CNHS-2400. The percentage of oxygen of the sample was calculated by difference.

FT-IR spectroscopy. Spectra were obtained with a FT-IR spectrometer (Nicolet®), model NEXUS 67) configured with a DRIFT reflectance accessory (Harrick, model Praying Mantis DRP). The spectra were obtained in CsI pellets in the 4000–450 cm⁻¹ spectral region, with a spectral resolution of 2 cm⁻¹.

Thermal analysis. Thermogravimetry (TG), differential thermal analysis (DTG), and differential scanning calorimetry (DSC) measurements were performed in a simultaneous thermal analyzer model SDTQ-600/Thermo Star from TA Instruments®. Thermal analysis was performed in an isothermal mode for 20 min; then, a heating ramp of 10 °C/min was programmed until 1000 °C under an argon atmosphere (100 mL/min). A coupled TG-MS system using an electron-impact quadrupole mass-selective detector (model Thermostar QMS200 M3) was used to analyze the main species during the dynamic thermal decomposition of the fragmentation processes of the sample.

Hydrolysis. HCN-DTP was hydrolyzed using the method developed by Ferris [19] that consisted of an acid hydrolysis followed by a basic hydrolysis. The conditions for acid hydrolysis were HCl 6N/100–110 °C/16–24 h; for basic hydrolysis, they were NaOH 0.1 N/100 °C/6 h. After treatment,

the product was analyzed by GC-MS in a 6859 network GC system coupled to a 5975 VL MSD with triple-axis detector operating in the electron-impact (EI) mode at 70 eV (Agilent®); an HP-5 MS column (30 m × 0.25 mm i.d. × 0.25 µm film thickness) was used; the analysis was carried out using the derivatization method and the GC oven program developed by Marín-Yaseli [60] to detect polar organic compounds. When available, the identified compounds were confirmed against authentic standard mass spectra and retention times. Other organic compounds were identified by searching their mass spectra in the NIST (The National Institute of Standards and Technology) database. For identification purposes, we considered only peaks with a signal-to-noise ratio over 10. Those peaks whose match probability in the database were below 90%, and/or those that were tentatively or ambiguously identified were considered unidentified and are not discussed in this paper.

3. Results

3.1. Elemental Analysis

Elemental analysis shows that the synthesized polymer (HCN-DTP) is compositionally different from other HCN-derived polymers; it is highly oxidized. The elemental composition of HCN-DTP, in percentage, was C 23.2%, H 3.1%, N 19.9%, and O 53.8%. The oxygen concentration (%) was calculated by subtraction of the experimental elemental analysis data. When these results are compared to other syntheses under analogous conditions (i.e., cyanide source, alkaline aqueous solution, [>0.1], >25 °C, free oxygen) (Table S1), it is evident that the content of hydrogen is very similar. However, values of carbon and nitrogen are almost half that reported. This depletion is counteracted by the considerably higher content of oxygen in our sample compared with the values founded in analogous experiments [18,26–28,54]. Even, at similar initial concentrations and high temperatures in other experiments (i.e., 0.1 M NH_4CN , 80 °C during 96 h), only the hydrogen content is similar to our results (e.g., C 38–40%; N 37–39%; H 3–4%; O 16–20%) (Table S1). The depletion of nitrogen can be related to the effect of high temperatures, which increase denitrogenation, hydrolysis, and oxidation processes, throughout polymerization; this process results in oxidized macrostructures [26]. In addition, previous experiments that used net HCN [e.g., DuPont (E.I. Du Pont de Nemours & Co., Inc., Wilmington, DE, USA) $\text{HCN}_{(g)} + \text{H}_2\text{O}_{(l)}$ and $\text{HCN}_{(l)} + \text{NH}_{3(aq)}$ 0 °C, 4 days] did not show similar trends. The higher oxygen value reported in other experiments is around 25%; it has been associated with a long-time reaction (i.e., one month) and different synthesis and storage conditions [27].

The oxygen content could depend on the polymerization conditions, such as the presence of ammonium in the reaction medium, the temperature, the reaction time, and the raw material [26,28]. In addition, HCN-derived polymers are hygroscopic, and they can absorb a considerable amount of water from air moisture [18]. In fact, thermograms suggest that our sample retains around approximately 10% of H_2O (peak at 55 °C in the DTG curve, see below), and furthermore, the real amount of structural oxygen is around 43.8%. Even considering these contributions, the oxygen content is unexpectedly high. Hence, other mechanisms should be related to the oxidation of the polymer, such as hydrolysis and oxidation reactions [3,26,36].

The molar ratios calculated for HCN-DTP were C/N 1.36; H/N 2.18; O/N 1.93. This suggests that our polymer contains about approximately 2 atoms of oxygen and 2 atoms of hydrogen per nitrogen. The molecular formula proposed is $\text{C}_{15}\text{H}_{24}\text{N}_{11}\text{O}_{21}$. This indicates that our HCN-DTP polymer has a great amount of oxygenated functional groups in the polymeric structure, and it differs from other already studied HCN polymers. In order to identify these functional groups, a Fourier transform infrared (FT-IR) study was performed.

3.2. Fourier Transform Infrared (FT-IR) Spectroscopy

The IR-light exposition generates a complex band-pattern for HCN-DTP; those bands can be associated with functional groups. Although IR spectra provide important information about the functional groups that constitute these polymers, there is not enough information to associate a

spectrum with a specific synthesis method. The IR reflectance spectra of HCN-derived polymers prepared under diverse experimental conditions (Table S1 Supplementary Information) show similar bands [17,18,26,27,61] to the bands identified in our polymer.

Figure 1 shows the IR spectrum of HCN-DTP. As in previous reports, the FT-IR spectra are divided into four main regions: region I (3700–3000 cm^{-1}), region II (2275–2000 cm^{-1}), region III (1825–1000 cm^{-1}), and region VI (centered at 660 cm^{-1}) [26] (Figure 1). Region I can be assigned mainly to N-containing groups of primary and secondary amines (3338 cm^{-1} , -NH asymmetric stretch; 3211 cm^{-1} , -NH₂ symmetric stretch). In addition, OH groups of carboxylic acids and/or methyl groups in aliphatic compounds (2964 cm^{-1} ; OH stretch, -CH₃ asymmetric and symmetric stretch) may overlap. Markedly, the bands at 2798 and 2713 cm^{-1} have not been reported before. These bands are associated with CH₃ symmetric stretch and attached with aromatic groups and/or nitrogen and oxygen atoms [62].

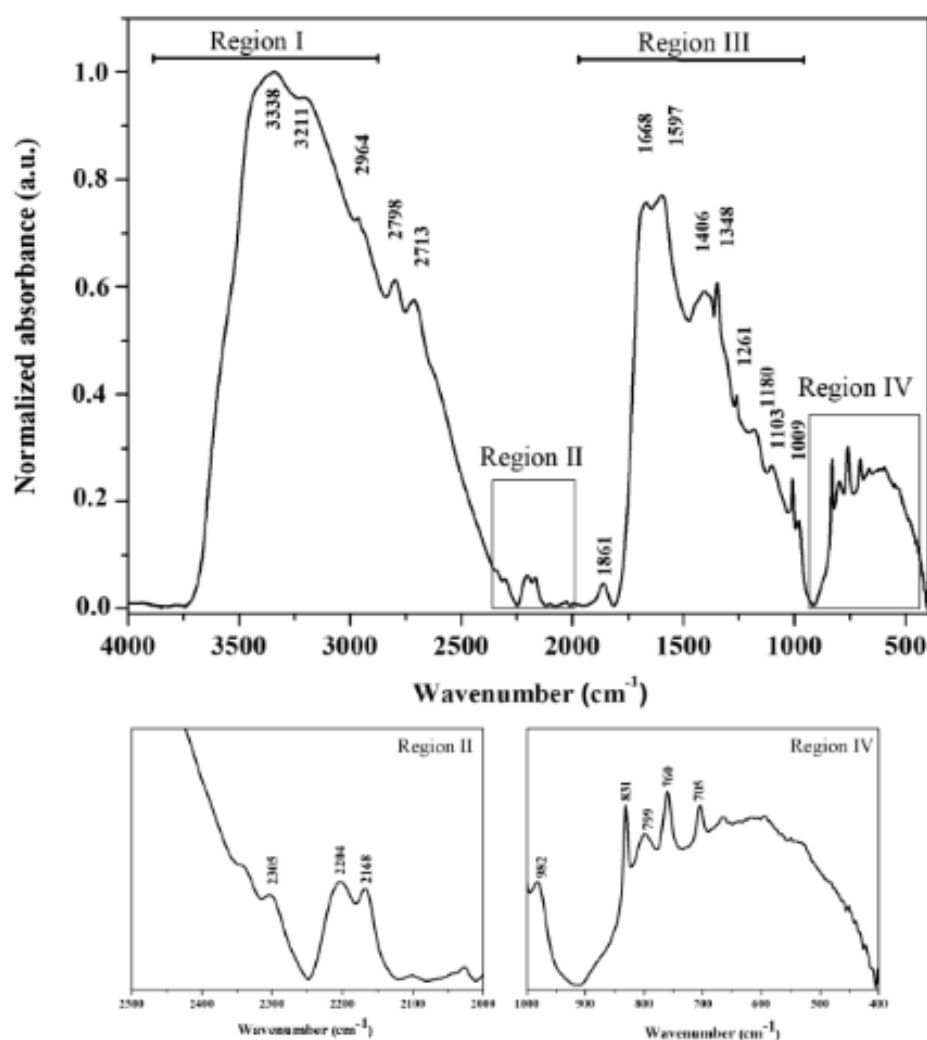


Figure 1. Fourier transform infrared (FT-IR) spectrum of hydrogen cyanide (HCN)-derived thermal polymer. Four regions can be recognized; the band assignments are given in the text and summarized in Table S2.

Region II is characteristic of nitrile groups. In general, three well-defined absorption bands are displayed in this region (at 2305, 2204, and 2168 cm^{-1}); their intensity and position vary depending on synthesis conditions [27]. The first band is associated with isocyanates groups (NCO asymmetric

stretch), while the band at 2204 cm^{-1} may be related with azides and or cyanamides ($\text{N}=\text{N}=\text{N}$ asymmetric stretch, $-\text{C}=\text{N}$ stretch). Some authors have reported a clear band at 2200 cm^{-1} due to $\text{C}\equiv\text{N}$ stretching on HCN polymers formed from formamide [29,30]. However, the possible interaction among bonds such as $\text{X}\equiv\text{Y}$ and $\text{X}=\text{Y}=\text{Z}$ (where X, Y, and Z can be carbon, oxygen, or nitrogen atoms) must be considered. The band at 2168 cm^{-1} is related to the same functional groups, such as carbodiimide groups [17]. In addition, there are appreciable bands around 2340 , 2100 , and 2026 cm^{-1} .

The third spectral region displays several bands with well-resolved peaks. The band at 1861 cm^{-1} can be associated to carbonyl compounds ($\text{C}=\text{O}$ stretch). Additionally, bands at 1668 and 1597 cm^{-1} may correspond to overtones, and a combination of esters, ketones, amides, and carboxylic acids functional groups. The presence of these bands can be related with hydrolysis at high temperatures, and/or oxidation reactions that yield oxygenated groups [18]. Moreover, the IR spectrum exhibits bands that may correspond to $-\text{CH}_3$ and $-\text{CH}_2$ in unsaturated or cyclic compounds (1406 and 1348 cm^{-1}) associated with adjacent electronegative atoms, such as nitrogen and oxygen (e.g., CH_3 , CH_2 asymmetric/symmetric stretching, wagging and bending vibrations, NO_2 symmetric stretch, NCO symmetric stretch, $\text{H}-\text{C}-\text{H}$ bending). Previous reports [18] have proposed that the absorption bands in this region can be associated with amide bonds and/or heteroaromatic or heterocyclic groups. Likewise, the peak at 1261 cm^{-1} could be linked with amide bonds, esters, or amines. The last relevant signals (Region IV) could be associated with $-\text{CH}_3$ and $-\text{CH}_2$ groups and/or $\text{C}-\text{C}$ stretch with no H on central carbon in straight and branched chains (1180 , 1103 , and 1009 cm^{-1}), and aliphatic insaturation and/or substituted aromatics (982 , 831 , 799 , 760 , and 705 cm^{-1}) [62].

New kinetic studies, considering the polymerization of aqueous solutions of NH_4CN at different temperatures, showed that the shape and width of the bands at approximately 3340 and 1645 cm^{-1} can be interpreted as a highly conjugated macrostructure, and that it could be related with the presence of oxygenated functional groups (i.e., $-\text{COOH}$ and $-\text{CONH}_2$) at $90\text{ }^\circ\text{C}$ [26]. In our case, the band in Region I is centered at 3338 cm^{-1} , while the band at 1645 cm^{-1} is divided in two well-defined peaks (1668 and 1597 cm^{-1}) (see above).

Therefore, the elemental analysis and the infrared spectra analysis suggest that HCN-DTP shows a higher degree of hydrolysis and/or oxidation than other polymers (Table S1). The structure of this polymer can be composed by a greater number of conjugated bonds [e.g., $\text{C}=\text{C}$, $\text{C}=\text{N}$ and $\text{C}=\text{O}$ groups (heterocyclic system)] resulted from the hydrolysis and oxidation of the main chains [18,26].

3.3. TG, DTG and DSC Analysis

Thermal analyses were conducted to characterize in detail the polymer and its thermal behavior. Thermal analysis was chosen since many properties of a complex sample can be obtained, as described as follows. The TG relates the behavior of a sample's weight and physicochemical phenomena. Through DTG, it is possible to gain information of the temperature and enthalpy at which thermal phenomena occur; and DSC was used to study the thermal transitions of the polymer while it is heated.

The TG thermogram of HCN-DTP is shown in Figure 2. In accordance with earlier reports about the thermogravimetric behavior of HCN-derived polymers, three stages can be identified: (I) a drying state ($<150\text{ }^\circ\text{C}$), (II) a pyrolysis stage ($150\text{--}450\text{ }^\circ\text{C}$), and (III) a carbonization stage ($>450\text{ }^\circ\text{C}$) [17,18,27,28,53].

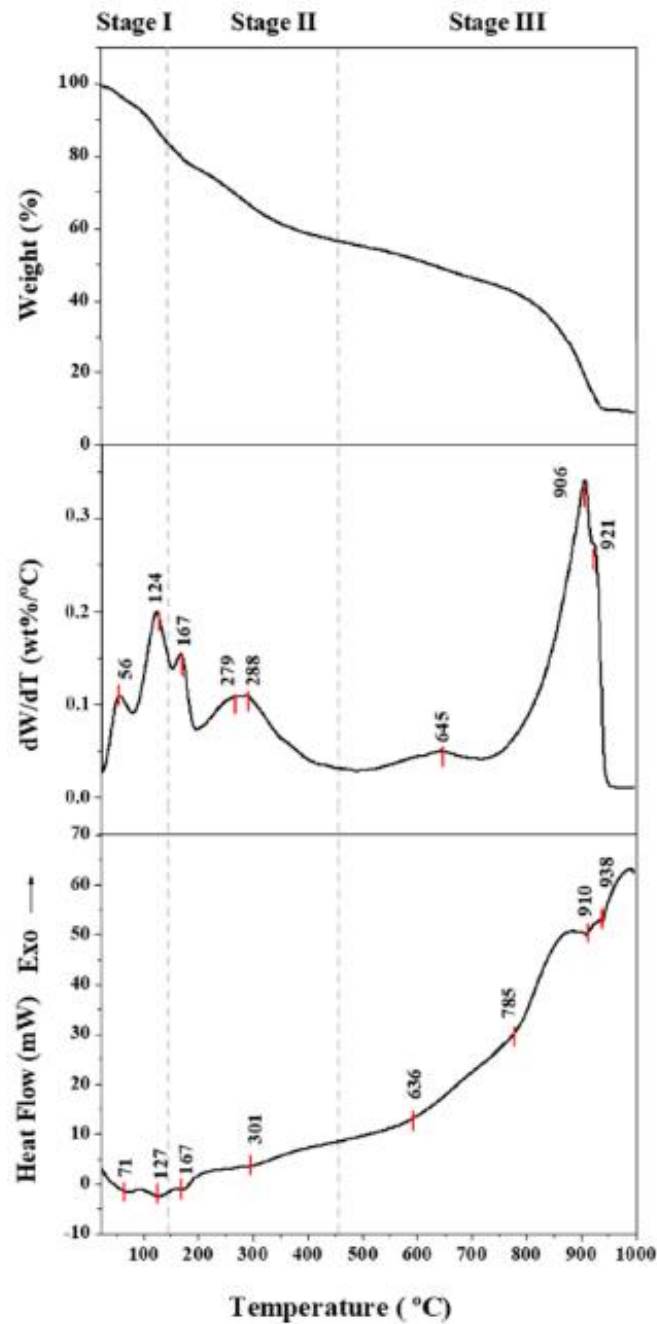


Figure 2. Thermogravimetric (TG), differential thermal analysis (DTG), and differential scanning calorimetry (DSC) curves. The predominant thermal peak around 900 °C is markedly different from previous reports. The DTG curve shows common decomposition steps related with HCN-derived polymers. However, the peak at 167 °C and the peaks around 900 °C are unique of our sample. The DSC curve shows multiple thermal decomposition steps. In general, each peak has its corresponding peak in the DTG curve.

At the first stage, there is a mass loss in our sample of about 17.2 wt %. In this stage, only one peak has been reported [18,27,28]. However, two other evident peaks (at 55 and 124 °C) can be observed in our sample, which suggests two main decomposition steps during the evaporation process. The dehydration occurs at low temperatures (<90 °C), which suggests the general degradation profiles of HCN-derived polymers [18,27,28]. The first peak (i.e., 55 °C) is related to the release of volatile compounds such as NH₃ or H₂O, which are retained in the polymer (approximately 10 wt %). The predominant peak around 124 °C could be associated with the mass loss from the structure of the polymer. Accordingly, the value of mass loss during the first stage is 7.83 wt %. This value is consistent with previous reports (HCN-derived polymer samples present an average value close to 7.8%) [18,27,28]. It should be mentioned that the systematic procedure development by Ruiz-Bermejo and co-workers [17] consists of washing the solid insoluble black polymer in order to remove the soluble part that may be retained by the polymer. As we did not have appreciable solid particles during synthesis, this step was not carried out (see above). Therefore, it should be considered that the peaks at the first stage may correspond to the soluble part retained by the polymer.

The first stage corresponds to the vaporization of moisture and the desorption of water. Likewise, it has been reported that the differences among HCN-derived polymers in this stage may be linked with the tendency to absorb atmospheric moisture (hydrophilicity) [18]. The synthesis of HCN-DTP was performed under argon atmosphere, and furthermore, the polymerization reaction was performed under depleted oxygen conditions. The higher hydrophilicity of our sample may be related with moisture directly acquired from aqueous medium resulted from hydrolysis reactions (e.g., hydrolysis of nitriles, urea, and/or diiminosuccinonitrile, DISN [32,33]). Hence, the peak at 124 °C in our sample could be linked with another thermal event, the degradation of other organic molecules, such as urea, which are ionically adsorbed on the polymer backbone.

The mass loss at the second stage (26.1%) and the last stage (46.8%) are similar to other HCN-derived polymers' behavior, corresponding to a mass loss of approximately 25 wt % and 48 wt %, respectively [18,27,28]. The second thermal degradation is associated with the thermal decomposition of the weakest bonds (e.g., side groups on the main chain); while the third stage is related with the breaking of the main chain. Previous reports [18,27,28] have suggested a correlation between the mass loss at these stages, with longer polymerization time, and furthermore, a higher thermal stability. In addition, two clear DTG peaks appear at 167 °C, and around approximately 280 °C, a well-defined peak is also found at 288 °C, and a slight shoulder is around 279 °C. Due to the proximity of these peaks, we will refer only to the peaks at 167 °C and 288 °C as part of the second stage (Figure 2). These peaks may be related with secondary scissions, which are associated with relative high stability structures [28]. Although, in general, two well-defined peaks at >200 °C are identified in this second zone, other peaks can be present depending on the HCN-derived polymer (e.g., aqueous polymerization of DAMN at 80 °C and DuPont's sample show clear peaks above 390 °C) [18,27,28]. No peaks have been reported at the second degradation stage at temperatures <200 °C. Hence, the sharp peak around 167 °C might be associated with a specific thermal decomposition step in HCN-DTP.

Significant differences, due to thermal degradation of the main chain of HCN-derived polymers, are associated with the third stage [18,27,28]. Our sample yields approximately 10 wt % of char residue at 1000 °C, which is lower than the reported values (i.e., >15 wt %) (Table S1). A slow rate of weight loss around 642 °C is consistent with the general behavior of HCN-derived polymers [18,27,28]. Moreover, two predominant peaks are found at 906 °C and 921 °C, with a rate of weight loss that is quite fast, which are the main degradation events of our sample. Char forming reaction can be associated with the last peak (approximately 921 °C) under coupled thermal events. This result suggest that the HCN-DTP is more stable than the predominant HCN-derived polymer (i.e., synthesized from cyanide salts, AMN or DAMN) [18,27,28]; this difference may be associated with the synthesis procedure. It has been suggested that the high thermal properties of HCN-derived polymers are related with the high interaction between polymer chains and rigid chain-stiffening (cross-linked structures and rigid chains with hetero/aromatic structures along the backbone); their decomposition involves the chemical conversion of side chains [28]. Likewise, the presence of an oxygen atmosphere seems to have an effect

during the last part of thermal degradation, since there is no char residue due to thermo-oxidation processes [27,28].

As our polymer was synthesized under free oxygen atmosphere, the greatest peaks around 900 °C may be related with a char-forming reaction that is a result of important cross-linking reaction associated with oxygen atoms inside the polymer structure. Only one study reported a relevant degradation step around 900 °C [28]. This high thermal stability can be associated with a higher oxygen content in the HCN polymers, which depends on polymerization reactions or on the oxygenated functional groups in the macromolecular structure due to hydrolytic processes. Some plausible structures have been reported for oxidized HCN-derived polymers which are enriched in keto groups, amino acids, hydroxy acids, primary amides, and carboxylic acids; these structures are the result of hydrolysis reaction from imine, amino nitriles, cyanohydrins, cyano, and amide groups, respectively [28].

Although the thermal behavior of HCN-derived thermal polymer is complex, characteristic peaks are summarized in Table 1. In general, we can associate each peak with endothermic (DSC) degradation processes. The analysis of the DTG curves shows at least seven predominant peaks associated with different thermal events. These peaks are numbered according to gradual appearance, as a function of temperature.

Table 1. Characteristic temperatures for the thermal decomposition of HCN-thermal derived polymer under argon atmosphere. DTG maxima with the corresponding rates of weight loss, dW/dt , and DSC peaks observed in the samples.

Peak	Stage I (25–150 °C) Evaporation			Stage II (150–450 °C) Low Thermal Decomposition				Stage III (450–1000 °C) High Thermal Decomposition			
	DTG	dW/dt (wt %/°C)	DSC T_{peak} (°C)	Peak	DTG	dW/dt (wt %/°C)	DSC T_{peak} (°C)	Peak	DTG	dW/dt (wt %/°C)	DSC T_{peak} (°C)
1	56	0.11	71	3	167	0.15	167	5	636	0.05	636
2	124	0.20	127	4	279	0.11					785
					288	0.11	301	6	906	0.34	910
								7	921	0.27	938

The DSC thermogram is shown in Figure 2 along with its corresponding peak temperatures (T_{peak}) (Table 1). The different peaks can be attributed to several decomposition/oxidation reactions associated with deamination, dehydration, and decyanation as the main reactions. At higher temperatures, random breaking by heteroatom bridges can occur [28]. Finally, carbonaceous char could result from cyclization (exothermic events associated with the heating of nitrile polymers), scission, and cross-linking reactions. The cyclization may occur during HCN polymerization, through nitrile groups forming a stable ladder backbone [17,27,28]. Two endothermic peaks are clearly observed around 900 °C.

In summary, the high oxidation degree of the structure of the HCN-DTP could result from a continuous hydrolysis, deamination, and decyanation process, along polymerization. These reactions generate a complex macromolecular structure that is essentially a polyamide with intra and inter amide bonds, as suggested recently [28].

3.4. Mass Spectrometric Thermal Analysis

The functional groups of the decomposition residues were determined by in situ mass spectrometry (MS). It was possible to detect several volatile species from the thermal decomposition and fragmentation processes of the HCN-DTP polymer (Figure 3). As in the thermogravimetric analysis, we considered the same three thermal decomposition stages to compare its analysis with DTG and DSC curves. Several signals have been observed for MS peaks in a wide range of temperatures. Major signals have been quite well characterized, and they are associated with H_2O , NH_4^+ ($m/z = 18$), and OH and NH_3 ($m/z = 17$, Figure 3a) [27,28,53]. Clear MS peaks at 61, 122, and 293 °C are observed for the H_2O/NH_4^+ profile. A broad peak, from 700 up to 850 °C, is present. Two evident signals at 61 °C and

markedly at 172 °C related with other amine species (i.e., $m/z = 15$, NH , $m/z = 16$, NH_2 and $m/z = 17$, NH_3/OH) and NO ($m/z = 30$) are observed. Two broad peaks can be recognized among 200–600 °C for NH and NO (Figure 3a), and it may contribute to the predominant signal on the second stage (279–288 °C) (Table 1). These profiles (Figure 3a) coincide with the first four mass loss observed on DTG curves (Figure 2) and are associated with deamination process, and the releasing of physisorbed water. Besides the mentioned products, other obvious MS peaks are present with a considerable intensity. Probably, carbon and/or nitrogen species (e.g., C^+ ($m/z = 12$); N/CH_2^+ ($m/z = 14$); CO/N_2 ($m/z = 28$); HCO ($m/z = 29$) and $\text{CO}_2/\text{HC}(=\text{NH})\text{NH}_2$ ($m/z = 44$); Figure 3b) contribute to the mass loss at the first stage (approximately 122 °C) and along a broad temperature interval on the second stage (172 and 250–303 °C). For example, the profiles of $m/z = 12$ (e.g., C) and $m/z = 44$ (e.g., $\text{CO}_2/\text{HC}(=\text{NH})\text{NH}_2$) show similar behavior. A first peak appears around 122 °C, two signals appear at the second stages (i.e., 172 and 253–273 °C), and three clear signals appear at the third stage (i.e., for CO_2 ; 643, 793, and 903 °C). In general, these temperature profiles display similar MS peaks to those ion currents corresponding to scission and/or depolymerization mechanisms (i.e., deamination, denitrogenation, decarboxylation, and decyanogenation) [27,28,53]. The signal at $m/z = 44$ also can be attributed to the hydrolytic cleavage of the amide linkage, which can lead to the formation of two fragments with NH_2 and COOH end groups.

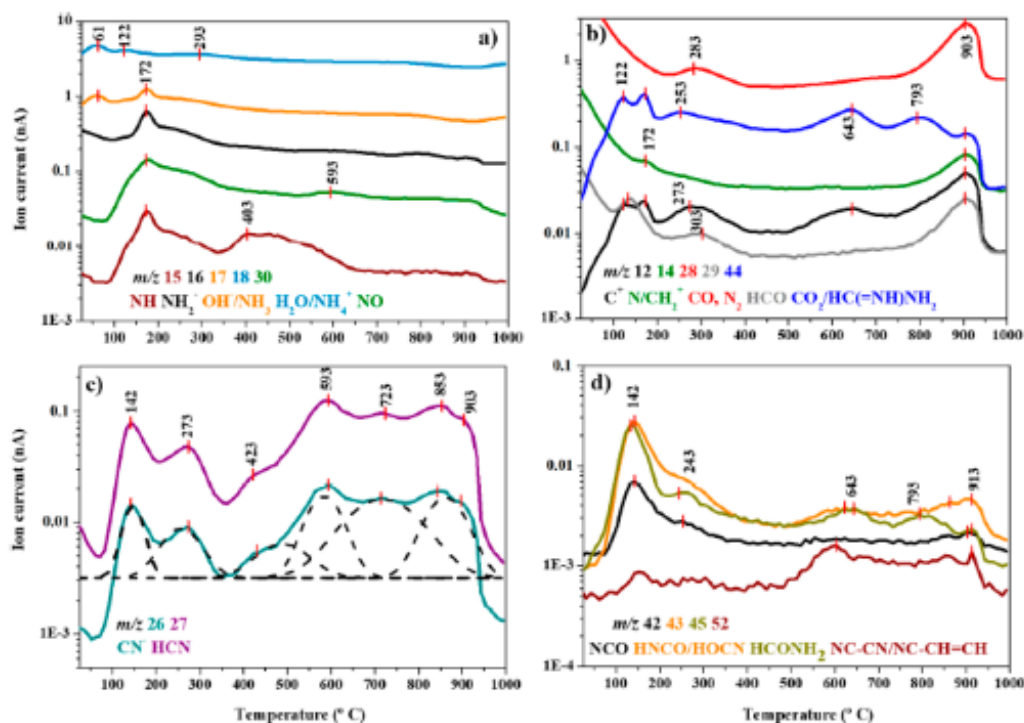


Figure 3. Ion intensity curves for HCN-derived thermal polymer. Deamination and decarboxylation mechanisms during pyrolysis stages dominate over dehydration. (a) Major signals associated with the releasing of amines and water; (b) signals associated with carbon and nitrogen species released through scission and/or depolymerization mechanisms; (c) cyanide and HCN curves; and (d) signals associated with the cleavage of the polymer chain through the release of larger species.

As was mentioned before, the most intense peak on the DTG curve is around 900 °C. The profiles of carbon/nitrogen species show a well-defined and intense peak around 903 °C (Figure 3b); this peak is the

result of diverse species that could include C^+ , CH_2^+ , CO , HCO , $CO_2/HC(=NH)NH_2$ through cracking of the HCN polymer main chain, such as $-N=N-$ or $-HC=O$ or $-N=C=O$ and/or by decarboxylation.

Cyanide and hydrogen cyanide curves for $m/z = 26$ and $m/z = 27$, respectively, are shown in Figure 3c. In order to examine carefully these profiles, an analysis based on a Gaussian function for the deconvolution method was performed. The deconvolution analysis shows at least six peaks that resemble very well the last six predominant peaks on the DTG profile (Figure 2). It must be considered that although the profile resembles the general decomposition process, the intensity of the signals associated to cyanide species are less intense (approximately 10 times) than the signals associated with the decarboxylation process (Figure 3b). However, it is possible to deduce that decyanogenation of the polymer takes place over a wide range of temperatures (from 142 up to 903 °C).

Finally, the TG-MS profiles for $m/z > 30$ (Figure 3d) produce clear signals along the first two thermal stages (i.e., 142 and 243 °C) that may be the result of the cleavage of the polymer chain through the release of NCO ($m/z = 42$), isocyanic acid, and/or cyanic acid ($m/z = 43$), the corresponding deprotonated derivate of formamidine ($^+C(=NH)NH_2$ $m/z = 43$), formamide ($m/z = 45$), and $NC-CH=CH^-$ ($m/z = 52$). Other appreciable peaks are characteristic for the third stage (i.e., 643, 793, and 913 °C). The fragment at $m/z = 52$ can be attributed to dinitrile $NC-CN$ or mononitrile derivative (the fragment $NC-CH=CH^-$) from polyaminonitrile, as it has been suggested in previous reports [27,28,53]. No more important signals were detected for $m/z > 52$.

In general, the TG-MS profiles and DTG curves are consistent with the thermal behavior of HCN-DTP. Table 2 shows a simpler view of the contribution of each volatile species related with different thermal stages.

Table 2. Summary of detected feasible volatile species associated with each stage of thermal decomposition and fragmentation processes of HCN-derived thermal polymer (HCN-DTP).

Probable Species	MS Peaks (m/z)	DTG Peaks (°C)						
		55	124	167	279–288	642	906	921
C^+	12							
N, CH_2^+	14							
NH	15							
NH_2	16							
OH^+, NH_3	17							
H_2O/NH_4^+	18							
^+CN	26							
HCN	27							
CO, N_2	28							
N_2H, HCO	29							
NO	30							
NCO	42							
$HNCO, HOCN$	43							
CO_2	44							
$^+C(=NH)NH$	45							
$HCONH_2$	45							
$NC-CN,$ $NC-CH=CH$	52							
STAGES		STAGE I		STAGE II		STAGE III		

Note: Except for water, ammonia, and nitrile oxides, all species contribute with the greatest thermal step showed on the DTG curve.

In summary, it is possible to distinguish among species with punctual thermal events from those that decomposed gradually. The first stage (<150 °C) seems to be associated with the release of physisorbed water, deamination, and the cleavage of the polymer chain through the release of high mass species. The second and the last stages are the result of continuous decyanogenation, deamination, and decarboxylation mechanisms. The almost identical behavior between the carbon profile and carbon dioxide suggests that decarboxylation is the main thermal decomposition process, which is consistent with a high oxygenated structure of the polymer.

The HCN-DTP polymer is extremely complex, and many of its functional groups were determined by in situ mass spectrometry. The potential of this polymer as a source for organic molecules motivated

macrostructure) results in the releasing of organic molecules that were retained within the structure; this retention is lower at high temperatures. Since the high temperatures yields high stable macrostructures, the retention of organic molecules is not efficient (non-available retention spaces) and in consequence, the amount and diversity of molecules is limited. In addition, as the basic treatment was performed at a lower heating time, the pool of organic compounds is limited.

In summary, the systematic method followed in this report suggests that HCN-DTP can be understood as a highly oxidized macrostructure with conjugated carbon and nitrogen bonds. As it has been reported recently, the physicochemical properties of these materials are directly related with temperature and raw material, which favors hydrolytic and/or oxidative reactions during the polymerization of HCN [18,26]. The identification of the physicochemical properties of this polymer is crucial to propose a scenario where the HCN-DTP could have played an important role from the point of view of chemical evolution.

4. Discussion

Since the 1970s, it has been proposed that hydrogen cyanide can play an important role in the formation of complex organic molecules under hydrothermal conditions [5,40–46]. In addition, new ideas propose the surroundings of alkaline environments as ideal niches for a rich HCN chemistry [9,68,69]. If HCN was present in alkaline hydrothermal environments, as suggested by Holm and Neubeck [5], the reactions it will undergo would be crucial to understand its role in prebiotic reactions occurring on these environments. Figure 5 shows a possible scenario of the probable fate of HCN, as well as its thermal polymer, under a submarine alkaline hydrothermal system.

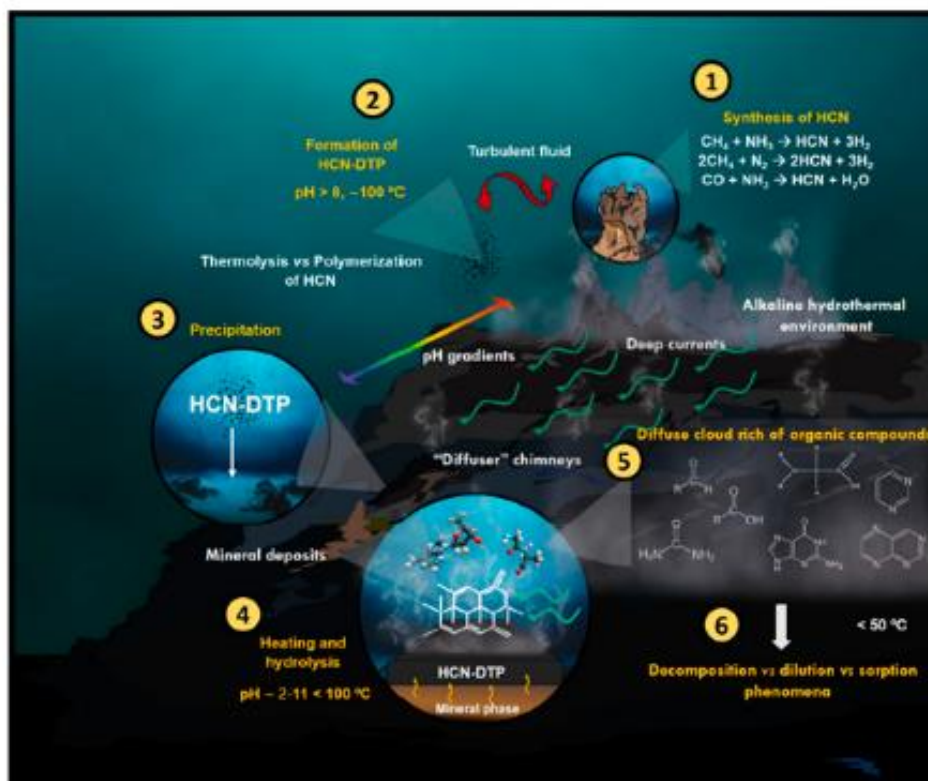


Figure 5. Probable fate of HCN and its thermal polymer (HCN-DTP) in a primitive submarine hydrothermal system. Each point is described in detail in the text.

The availability of HCN in submarine hydrothermal systems similar to the Lost City in the Hadean Earth [5,70,71] allow HCN through two main reaction pathways. As soon as the HCN is synthesized (from the released gases, e.g., CH₄, NH₃, CO, N₂) in hydrothermal fluids (Figure 5, Step 1), a continuous competition among hydrolysis [68] and polymerization reactions takes place [26,54]. In a recent paper [52], we showed that the thermolysis of HCN at relatively alkaline pH values (i.e., pH > 8) allows the formation of a kind of HCN-DTP.

Higher pH values (i.e., pH > 10) may favor the formation of the HCN-DTP polymer (Figure 5, Step 2) over HCN hydrolysis at relatively high temperatures (this work). Once HCN-DTP is formed, it will experience several phenomena; the turbulent fluids and the deep currents could spread it along the hydrothermal system. As it is essentially insoluble, eventually, it will precipitate (Figure 5, Step 3) at lower temperatures (<100 °C) and may interact with mineral surfaces.

In hydrothermal systems, there are both temperature and pH gradients naturally occurring (Figure 5, Step 4). The HCN polymer could be exposed to a wide temperature gradient (from 2 up to 350 °C), and along with pH variations, hydrolysis could accomplish. Hydrothermal deposits and venting sites along hydrothermal systems with temperatures below 100 °C represent big areas (spanning a few kilometers) [72–75]. In addition, the dynamic flux could generate important pH gradients through the circulation of fluids [76]. In this way, the polymer could be heated at temperatures as high as 300 °C at different pH values. Although the off-axis (e.g., the Lost City Hydrothermal System) ultramafic hosted hydrothermal systems are essentially alkaline environments, the contribution of acid fluids from relative near ultramafic on-axis systems (e.g., the Rainbow Hydrothermal System) [77] could favor acidic hydrolysis (pH < 3). As the thermal behavior suggests (see above), the heating (<300 °C) of HCN polymers would release several organic species to the environment. In particular, the acid hydrolysis coupled with heating would favor the release of organic compounds of prebiotic interest (e.g., aldehydes, carboxylic acids, amino acids, and N-heterocyclic compounds). These results are consistent with previous works that highlight the relevance of submarine alkaline hydrothermal systems. For example, La Rowe and Regnier [71], based on theoretical analysis, showed that under hydrothermal conditions (i.e., off-axis vent sites, 150 °C, 500 bars), HCN reacts with dissolved gases (e.g., CO₂, H₂, N₂), forming nucleobases through the formation of HCN polymer. A cloud rich of organic compounds could be formed surrounding hydrothermal systems (Figure 5, Step 5). The organic molecules could have persisted at high temperatures and pressures since, as it has been discussed, the fate of organic molecules depends on the particular environmental conditions [50,58]. For instance, it has been proven that some amino acids (e.g., lysine and glutamic acid) are thermally more stable under alkaline solutions at high temperatures (>200 °C) [78].

The species (organics, gases, ions, metals, and minerals) in hydrothermal systems could be transported [79] to other primitive environments, where they could follow decomposition, dilution, precipitation, and/or sorption processes [80] (Figure 5, Step 6). In this experiment, the release of adenine from HCN polymer was confirmed. The availability of N-heterocyclic compounds is crucial to the formation of RNA oligomers. It has been suggested that RNA polymerization could probably occur at conditions similar to those found on submarine hydrothermal systems [81]. The formation of other complex molecules, tholins, has been studied under alkaline conditions [82]. In this study, the formation of alkaline aqueous aerosols under reducing atmospheres (e.g., NH₃, CH₄, H₂) resulted in a great diversity of organic molecules, notably glyoxylic acid, which has a great relevance in the hypothesis of glyoxylate. This finding highlights that the synthesis of organics could be favored by alkaline conditions.

This research is part of a series of prebiotic chemistry experiments devoted to understanding the behavior of a very simple molecule (HCN) exposed to conditions found on Hydrothermal Vents Systems. In this research, the main objective was to characterize the produced polymer and to identify the released formed products. In the field of prebiotic chemistry, we try to find conditions that allowed the increase in the complexity of molecules through the simulation of feasible environments and including some likely variables in them. The formation of more complex molecules than those we

used as raw material could have led to the development of interactions among these molecules and thus accomplish a complex chemistry. Eventually, such scenarios could have preceded the origin of life on Earth.

5. Conclusions

HCN is abundant throughout the universe, and it can be easily formed in hydrothermal chimneys. In this work, we explored the synthesis and characterization of an HCN polymer produced under conditions resembling those of HV. Our results support the hypothesis developed by Nils Holm and co-workers about the relevance of alkaline systems to host a rich chemistry during the first steps of chemical evolution [5,83]. The synthesis of HCN-DTP polymer under assayed conditions, simulating alkaline hydrothermal conditions, reinforce the idea about considering those environments as relevant during early Earth for organic synthesis. HCN polymers are a huge group of macromolecules, and their study requires the use of different analytical techniques. The polymer synthesized in this experiment is very complex and presents chemical properties different from those of the already characterized polymers. After hydrolysis, it releases prebiotic relevant molecules such as purines, pyrimidines, carboxylic acids, and amino acids.

The next step in this study could be to focus on understanding the effect of ions and mineral surfaces in the synthesis of those polymers and to evaluate their effects on the production of complex organic molecules. In addition, as pressure is a key variable in submarine hydrothermal systems (since it affects the boiling point of water, and a change in pressure could affect the polymer yield and the selectivity of the reaction), in a future work, we aim to develop this idea.

Although this research focuses on studying the role of HCN-DTP in alkaline hydrothermal systems and its impact on chemical evolution, the conditions for its synthesis are easily applied to materials science. Likewise, characterizing its physicochemical properties may be useful for other approaches and expand to other research areas.

Supplementary Materials: The following are available online at <http://www.mdpi.com/2227-9717/8/8/968/s1>. Table S1: Summary of HCN-derived polymers from diverse synthesis, Table S2: Description and assignment of IR bands for HCN-DTP.

Author Contributions: Conceptualization, M.R.-B. and M.C.-G.; methodology M.R.-B.; validation, S.A.V.-B., P.R.-P., and M.R.-B.; formal analysis, S.A.V.-B. and P.R.-P.; investigation, S.A.V.-B.; resources, M.R.-B.; writing—original draft preparation, S.A.V.-B., M.C.-G. writing—review and editing, M.C.-G.; supervision, M.R.-B. and M.C.-G.; funding acquisition, M.R.-B. and M.C.-G. All authors have read and agreed to the published version of the manuscript.

Funding: This research was funded by the project ESP2017-89053-C2-2-P from the Spanish Ministerio de Ciencia, Innovación y Universidades; the project MDM-2017-0737 Centro de Astrobiología (CSIC-INTA), Unidad de Excelencia Maria de Maeztu from the Spanish State Research Agency (AEI), the DGAPA-PAPIIT (grant number IA203217), and CONACyT (grant A1-S-25341).

Acknowledgments: S.A.V.-B. acknowledges Posgrado en Ciencias de la Tierra UNAM, CONACyT (Ph. D. grant 697442 and the financial support for a research stay grant) and the technical assistance of Claudia Camargo. The Instituto de Ciencias Nucleares (UNAM), and Centro de Astrobiología (CAB) are acknowledged for the use of their facilities. M.R.-B. and P.R.-P. used the research facilities of the Centro de Astrobiología (CAB) and were supported by the Instituto Nacional de Técnica Aeroespacial “Esteban Terradas” (INTA) and by the Spanish State Research Agency (AEI) Centro de Astrobiología (CSIC-INTA), Unidad de Excelencia Maria de Maeztu. Additionally, the authors are grateful to M^a Teresa Fernández for performing the FT-IR spectra, and to the “Servicio de Análisis Térmico” of ICMN (CSIC, Spain).

Conflicts of Interest: The authors declare no conflict of interest. The funders had no role in the design of the study; in the collection, analyses, or interpretation of data; in the writing of the manuscript, or in the decision to publish the results.

References

1. Sutherland, J.D. The Origin of Life—Out of the Blue. *Angew. Chem. Int. Ed.* **2016**, *55*, 104–121. [[CrossRef](#)] [[PubMed](#)]

2. Ruiz-Bermejo, M.; Zorzano, M.P.; Osuna-Esteban, S. Simple Organics and Biomonomers Identified in HCN Polymers: An Overview. *Life* **2013**, *3*, 421–448. [CrossRef] [PubMed]
3. Ferris, J.P.; Hagan, W.J. HCN and chemical evolution: The possible role of cyano compounds in prebiotic synthesis. *Tetrahedron* **1984**, *40*, 1093–1120. [CrossRef]
4. Matthews, C.N.; Minard, R.D. Hydrogen cyanide polymers, comets and the origin of life. *Faraday Discuss.* **2006**, *133*, 393–401. [CrossRef]
5. Holm, N.G.; Neubeck, A. Reduction of nitrogen compounds in oceanic basement and its implications for HCN formation and abiotic organic synthesis. *Geochem. Trans.* **2009**, *10*, 9. [CrossRef]
6. Tian, F.; Kasting, J.F.; Zahnle, K. Revisiting HCN formation in Earth's early atmosphere. *Earth Planet. Sci. Lett.* **2011**, *308*, 417–423. [CrossRef]
7. Parkos, D.; Pikus, A.; Alexeenko, A.; Melosh, H.J. HCN production from impact ejecta on the early Earth. In Proceedings of the 30th International Symposium on Rarefied Gas Dynamics: RGD 30, Victoria, BC, Canada, 10–15 July 2016; AIP Publishing: Melville, NY, USA; Volume 1786, p. 170001.
8. Ferus, M.; Kubelik, P.; Knižek, A.; Pastorek, A.; Sutherland, J.; Civiš, S. High energy radical chemistry formation of HCN-rich atmospheres on early Earth. *Sci. Rep.* **2017**, *7*, 6275. [CrossRef]
9. Rimmer, P.B.; Shorttle, O. Origin of life's building blocks in carbon-and nitrogen-rich surface hydrothermal vents. *Life* **2019**, *9*, 12. [CrossRef]
10. Colin-García, M.; Negrón-Mendoza, A.; Ramos-Bernal, S. Organics produced by irradiation of frozen and liquid HCN solutions: Implications for Chemical Evolution Studies. *Astrobiology* **2009**, *9*, 279–288. [CrossRef]
11. Mumma, M.J.; Charnley, S.B. The chemical composition of comets—Emerging taxonomies and natal heritage. *Annu. Rev. Astron. Astrophys.* **2011**, *49*, 471–524. [CrossRef]
12. Pizzarello, S. Hydrogen cyanide in the Murchison meteorite. *Astrophys. J. Lett.* **2012**, *754*, L27. [CrossRef]
13. Stribling, R.; Miller, S.L. Energy yields for hydrogen cyanide and formaldehyde syntheses: The hcn and amino acid concentrations in the primitive ocean. *Orig. Life Evol. Biosph.* **1987**, *17*, 261–273. [CrossRef] [PubMed]
14. Miyakawa, S.; Cleaves, H.J.; Miller, S.L. The cold origin of life: A. Implications based on the hydrolytic stabilities of hydrogen cyanide and formamide. *Orig. Life Evol. Biosph.* **2002**, *32*, 195–208. [CrossRef] [PubMed]
15. Fábián, B.; Szóri, M.; Jedlovský, P. Floating Patches of HCN at the Surface of their aqueous solutions—Can they make “HCN World” Plausible? *J. Phys. Chem. C* **2014**, *118*, 21469–21482. [CrossRef]
16. Liebman, S.A.; Pesce-Rodriguez, R.A.; Matthews, C.N. Organic analysis of hydrogen cyanide polymers: Prebiotic and extraterrestrial chemistry. *Adv. Space Res.* **1995**, *15*, 71–80. [CrossRef]
17. Ruiz-Bermejo, M.; de la Fuente, J.L.; Rogero, C.; Menor-Salván, C.; Osuna-Esteban, S.; Martín-Gago, J.A. New insights into the characterization of ‘insoluble black HCN polymers. *Chem. Biodivers.* **2012**, *9*, 25–40. [CrossRef] [PubMed]
18. Ruiz-Bermejo, M.; José, L.; Carretero-González, J.; García-Fernández, L.; Aguilar, M.R. A Comparative Study on HCN Polymers Synthesized by Polymerization of NH₄CN or Diaminomaleonitrile in Aqueous Media: New Perspectives for Prebiotic Chemistry and Materials Science. *Chem. Eur. J.* **2019**, *25*, 11437–11455. [CrossRef]
19. Ferris, J.P.; Wos, J.D.; Nooner, D.W.; Oró, J. Chemical evolution: XXI. The Amino Acids Released on Hydrolysis of HCN Oligomers. *J. Mol. Evol.* **1974**, *3*, 225–231. [CrossRef]
20. Matthews, C.N.; Moser, R.E. Peptide synthesis from hydrogen cyanide and water. *Nature* **1967**, *215*, 1230–1234. [CrossRef]
21. Oró, J.; Kimball, A.P. Synthesis of purines under possible primitive earth conditions. I. Adenine from hydrogen cyanide. *Arch. Biochem. Biophys.* **1961**, *94*, 217–227. [CrossRef]
22. Thissen, H.; Koegler, A.; Salwiczek, M.; Easton, C.D.; Qu, Y.; Lithgow, T.; Evans, R.A. Prebiotic-chemistry inspired polymer coatings for biomedical and material science applications. *NPG Asia Mater.* **2015**, *7*, e225. [CrossRef]
23. Thissen, H.; Evans, R.; Koegler, A. Hydrogen Cyanide-Based Polymer Surface Coatings and Hydrogels. U.S. Patent 9,587,141, 17 May 2017.
24. Toh, R.J.; Evans, R.; Thissen, H.; Voelcker, N.H.; d'Ischia, M.; Ball, V. Deposition of Aminomalononitrile-Based Films: Kinetics, Chemistry, and Morphology. *Langmuir* **2019**, *35*, 9896–9903. [CrossRef] [PubMed]

25. D'Ischia, M.; Manini, P.; Moracci, M.; Saladino, R.; Ball, V.; Thissen, H.; Evans, R.A.; Puzzarini, C.; Barone, V. Astrochemistry and Astrobiology: Materials Science in Wonderland? *Int. J. Mol. Sci.* **2019**, *20*, 4079.
26. Mas, I.; de la Fuente, J.L.; Ruiz-Bermejo, M. Temperature effect on aqueous NH₄CN polymerization: Relationship between kinetic behaviour and structural properties. *Eur. Polym. J.* **2020**, *132*, 109719. [[CrossRef](#)]
27. José, L.; Ruiz-Bermejo, M.; Nna-Mvondo, D.; Minard, R.D. Further progress into the thermal characterization of HCN polymers. *Polym. Degrad. Stab.* **2014**, *110*, 241–251.
28. Ruiz-Bermejo, M.; de la Fuente, J.L.; Marin-Yaseli, M.R. The influence of reaction conditions in aqueous HCN polymerization on the polymer thermal degradation properties. *J. Anal. Appl. Pyrolysis* **2017**, *124*, 103–112.
29. Cataldo, F.; Patané, G.; Compagnini, G. Synthesis of HCN polymer from thermal decomposition of formamide. *J. Macromol. Sci. A Pure Appl. Chem.* **2009**, *46*, 1039–1048. [[CrossRef](#)]
30. Cataldo, F.; Lilla, E.; Ursini, O.; Angelini, G. TGA–FT-IR study of pyrolysis of poly (hydrogen cyanide) synthesized from thermal decomposition of formamide. Implications in cometary emissions. *J. Anal. Appl. Pyroly.* **2010**, *87*, 34–44. [[CrossRef](#)]
31. Sanchez, R.A.; Ferris, J.P.; Orgel, L.E. Studies in prebiotic synthesis. II. Synthesis of purine precursors and amino acids from aqueous hydrogen cyanide. *J. Mol. Biol.* **1967**, *30*, 223–253.
32. Ferris, J.P.; Ryan, T.J. Chemical evolution. XIV. Oxidation of diaminomaleonitrile and its possible role in hydrogen cyanide oligomerization. *J. Org. Chem.* **1973**, *38*, 3302–3307. [[CrossRef](#)]
33. Ferris, J.P.; Edelson, E.H. Chemical evolution. 31. Mechanism of the condensation of cyanide to hydrogen cyanide oligomers. *J. Org. Chem.* **1978**, *43*, 3989–3995. [[CrossRef](#)]
34. Ferris, J.P.; Donner, D.B.; Lotz, W. Chemical evolution. IX. Mechanism of the oligomerization of hydrogen cyanide and its possible role in the origins of life. *J. Am. Chem. Soc.* **1972**, *94*, 6968–6974. [[CrossRef](#)]
35. Völker, T. Polymere blausäure. *Angew. Chem.* **1960**, *72*, 379–384.
36. Ferris, J.P.; Edelson, E.H.; Auyeung, J.M.; Joshi, P.C. Structural studies on HCN oligomers. *J. Mol. Evol.* **1981**, *17*, 69–77.
37. Umemoto, K.; Takahasi, M.; Yokota, K. Studies on the structure of HCN oligomers. *Orig. Life Evol. Biosph.* **1987**, *17*, 283–293.
38. Mamajanov, I.; Herzfeld, J. HCN polymers characterized by solid state NMR: Chains and sheets formed in the neat liquid. *J. Chem. Phys.* **2009**, *130*, 134503.
39. Mamajanov, I.; Herzfeld, J. HCN polymers characterized by SSNMR: Solid state reaction of crystalline tetramer (diaminomaleonitrile). *J. Chem. Phys.* **2009**, *130*, 134504.
40. Mukhin, L.E.V. Evolution of organic compounds in volcanic regions. *Nature* **1974**, *251*, 50–51. [[CrossRef](#)]
41. Mukhin, L. Volcanic processes and synthesis of simple organic compounds on primitive earth. *Orig. Life* **1976**, *7*, 355–368. [[CrossRef](#)]
42. Dowler, M.J.; Ingmanson, D.E. Thiocyanate in Red Sea brine and its implications. *Nature* **1979**, *279*, 51–52. [[CrossRef](#)]
43. Corliss, J.B.; Baross, J.A.; Hoffman, S.E. An hypothesis concerning the relationships between submarine hot springs and the origin of life on earth. *Oceanol. Acta Spec. Issue* **1981**, *1*, 59–69.
44. Baross, J.A.; Hoffman, S.E. Submarine hydrothermal vents and associated gradient environments as sites for the origin and evolution of life. *Orig. Life Evol. Biosph.* **1985**, *15*, 327–345. [[CrossRef](#)]
45. Ferris, J.P. Chemical Markers of Prebiotic Chemistry in Hydrothermal Systems. In *Marine Hydrothermal Systems and the Origin of Life*; Holm, N.G., Ed.; Springer: Dordrecht, The Netherlands, 1992; pp. 109–134.
46. Aubrey, A.D.; Cleaves, H.J.; Bada, J.L. The Role of Submarine Hydrothermal Systems in the Synthesis of Amino Acids. *Orig. Life Evol. Biosph.* **2009**, *39*, 91–108. [[CrossRef](#)]
47. Lowe, C.U.; Rees, M.W.; Markham, R. Synthesis of Complex Organic Compounds from Simple Precursors: Formation of Amino-Acids, Amino-Acid Polymers, Fatty Acids and Purines from Ammonium Cyanide. *Nature* **1963**, *199*, 219–222. [[CrossRef](#)]
48. Hennes, R.-C.; Holm, N.; Engel, M. Abiotic synthesis of amino acids under hydrothermal conditions and the origin of life: A perpetual phenomenon? *Naturwissenschaften* **1992**, *79*, 361–365. [[CrossRef](#)]
49. Islam, M.N.; Kaneko, T.; Kobayashi, K. Determination of amino acids formed in a supercritical water flow reactor simulating submarine hydrothermal systems. *Jpn. Soc. Anal. Chem.* **2002**, *17*, i1631–i1634.
50. Colín-García, M.; Heredia, A.; Cordero, G.; Camprubi, A.; Negrón-Mendoza, A.; Ortega-Gutiérrez, F.; Beraldi, H.; Ramos-Bernal, S. Hydrothermal vents and prebiotic chemistry: A review. *Bol. Soc. Geol. Mex.* **2016**, *68*, 599–620. [[CrossRef](#)]

51. Sojo, V.; Herschy, B.; Whicher, A.; Camprubi, E.; Lane, N. The Origin of Life in Alkaline Hydrothermal Vents. *Astrobiology* **2016**, *16*, 181–197. [CrossRef] [PubMed]
52. Villafaña-Barajas, S.A.; Colín-García, M.; Negrón-Mendoza, A.; Ruiz-Bermejo, M. An experimental study of the thermolysis of hydrogen cyanide: The role of hydrothermal systems in chemical evolution. *Int. J. Astrobiol.* **2020**, 1–10. [CrossRef]
53. de la Fuente, J.L.; Ruiz-Bermejo, M.; Menor-Salván, C.; Osuna-Esteban, S. Thermal characterization of HCN polymers by TG–MS, TG, DTA and DSC methods. *Polym. Degrad. Stab.* **2011**, *96*, 943–948.
54. Fernández, A.; Ruiz-Bermejo, M.; de la Fuente, J.L. Modelling the kinetics and structural property evolution of a versatile reaction: Aqueous HCN polymerization. *Phys. Chem. Chem. Phys.* **2018**, *20*, 17353–17366.
55. Marin-Yaseli, M.R.; Moreno, M.; de la Fuente, J.L.; Briones, C.; Ruiz-Bermejo, M. Experimental conditions affecting the kinetics of aqueous HCN polymerization as revealed by UV–vis spectroscopy. *Spectrochim. Acta Part A* **2018**, *191*, 389–397.
56. Azamar, J.; Draganić, I. *Equipo para la preparación de compuestos tóxicos en solución acuosa y en atmósfera controlada: Cianuros para experimentos en Química de Radiaciones; Informe Técnico Q5; Departamento de Química, CEN, UNAM: Mexico City, Mexico, 1982; p. 16.*
57. Ferris, J.P.; Joshi, P.C.; Edelson, E.H.; Lawless, J.G. HCN: A plausible source of purines, pyrimidines and amino acids on the primitive earth. *J. Mol. Evol.* **1978**, *11*, 293–311. [CrossRef]
58. Colín-García, M.; Villafaña-Barajas, S.; Camprubi, A.; Ortega-Gutiérrez, F.; Colás, V.; Negrón-Mendoza, A. 5.4 Prebiotic Chemistry in Hydrothermal Vent Systems. In *Handbook of Astrobiology*; Kolb, V., Ed.; CRC Press: Boca Raton, FL, USA, 2018; pp. 297–329.
59. Matthews, C.N. Hydrogen cyanide polymers: From laboratory to space. *Planet. Space Sci.* **1995**, *43*, 1365–1370. [CrossRef]
60. Marin-Yaseli, M.R.; González-Toril, E.; Mompeán, C.; Ruiz-Bermejo, M. The Role of Aqueous Aerosols in the “Glyoxylate Scenario”: An Experimental Approach. *Chem. Eur. J.* **2016**, *22*, 12785–12799. [CrossRef]
61. Marin-Yaseli, M.R.; Cid, C.; Yagüe, A.I.; Ruiz-Bermejo, M. Detection of Macromolecular Fractions in HCN Polymers Using Electrophoretic and Ultrafiltration Techniques. *Chem. Biodivers.* **2017**, *14*, e1600241. [CrossRef] [PubMed]
62. Socrates, G. *Infrared and Raman Characteristic Group Frequencies: Tables and Charts*, 3rd ed.; Repr. as Paperback; Wiley: Chichester, UK, 2010; p. 366.
63. Schwartz, A.W.; Voet, A.B.; Veen, M. Recent progress in the prebiotic chemistry of HCN. *Orig. Life* **1984**, *14*, 91–98.
64. Minard, R.D.; Hatcher, P.G.; Gourley, R.C.; Matthews, C.N. Structural investigations of hydrogen cyanide polymers: New insights using TMAH thermochemolysis/GC-MS. *Orig. Life Evol. Biosph.* **1998**, *28*, 461–473.
65. Marin-Yaseli, M.R.; Mompeán, C.; Ruiz-Bermejo, M. A prebiotic synthesis of pterins. *Chem. Eur. J.* **2015**, *21*, 13531–13534. [CrossRef]
66. Borquez, E.; Cleaves, H.J.; Lazcano, A.; Miller, S.L. An investigation of prebiotic purine synthesis from the hydrolysis of HCN polymers. *Orig. Life Evol. Biosph.* **2005**, *35*, 79–90. [CrossRef]
67. Moser, R.E.; Claggett, A.R.; Matthews, C.N. Peptide formation from aminomalononitrile (HCN trimer). *Tetrahedron Lett.* **1968**, *9*, 1605–1608. [CrossRef]
68. Das, T.; Ghule, S.; Vanka, K. Insights into the origin of life: Did it begin from HCN and H₂O? *ACS Cent. Sci.* **2019**, *5*, 1532–1540. [CrossRef]
69. Toner, J.D.; Catling, D.C. Alkaline lake settings for concentrated prebiotic cyanide and the origin of life. *Geochim. Cosmochim. Acta* **2019**, *260*, 124–132. [CrossRef]
70. Smimov, A.; Hausner, D.; Laffers, R.; Strongin, D.R.; Schoonen, M.A. Abiotic ammonium formation in the presence of Ni-Fe metals and alloys and its implications for the Hadean nitrogen cycle. *Geochim. Trans.* **2008**, *9*, 5. [CrossRef]
71. LaRowe, D.E.; Regnier, P. Thermodynamic potential for the abiotic synthesis of adenine, cytosine, guanine, thymine, uracil, ribose, and deoxyribose in hydrothermal systems. *Orig. Life Evol. Biosph.* **2008**, *38*, 383–397. [CrossRef]
72. Lupton, J.E.; Delaney, J.R.; Johnson, H.P.; Tivey, M.K. Entrainment and vertical transport of deep-ocean water by buoyant hydrothermal plumes. *Nature* **1985**, *316*, 621–623. [CrossRef]
73. Little, S.A.; Stolzenbach, K.D.; Von Herzen, R.P. Measurements of plume flow from a hydrothermal vent field. *J. Geophys. Res.* **1987**, *92*, 2587–2596. [CrossRef]

74. Bemis, K.; Lowell, R.; Farough, A. Diffuse Flow on and Around Hydrothermal Vents at Mid-Ocean Ridges. *Oceanography* **2012**, *25*, 182–191. [CrossRef]
75. Mittelstaedt, E.; Escartin, J.; Gracias, N.; Olive, J.-A.; Barreyre, T.; Davaille, A.; Cannat, M.; Garcia, R. Quantifying diffuse and discrete venting at the Tour Eiffel vent site, Lucky Strike hydrothermal field. *Geochem. Geophys. Geosyst.* **2012**, *13*, 1–18. [CrossRef]
76. Holm, N.G.; Hennet, R.J.-C. Hydrothermal systems: Their varieties, dynamics, and suitability for prebiotic chemistry. In *Marine Hydrothermal Systems and the Origin of Life*; Springer: Dordrecht, The Netherlands, 1992; pp. 15–31.
77. Allen, D.E.; Seyfried, W.E. Serpentinization and heat generation: Constraints from Lost City and Rainbow hydrothermal systems. *Geochim. Cosmochim. Acta* **2004**, *68*, 1347–1354. [CrossRef]
78. Yamaoka, K.; Kawahata, H.; Gupta, L.P.; Ito, M.; Masuda, H. Thermal stability of amino acids in siliceous ooze under alkaline hydrothermal conditions. *Org. Geochem.* **2007**, *38*, 1897–1909. [CrossRef]
79. Stüeken, E.E.; Anderson, R.E.; Bowman, J.S.; Brazelton, W.J.; Colangelo-Lillis, J.; Goldman, A.D.; Som, S.M.; Baross, J.A. Did life originate from a global chemical reactor? *Geobiology* **2013**, *11*, 101–126. [CrossRef]
80. Omran, A.; Pasek, M. A Constructive Way to Think about Different Hydrothermal Environments for the Origins of Life. *Life* **2020**, *10*, 36. [CrossRef]
81. Burcar, B.T.; Barge, L.M.; Trail, D.; Watson, E.B.; Russell, M.J.; McGown, L.B. RNA Oligomerization in Laboratory Analogues of Alkaline Hydrothermal Vent Systems. *Astrobiology* **2015**, *15*, 509–522. [CrossRef]
82. Mompeán, C.; Marin-Yaseli, M.R.; Espigares, P.; González-Toril, E.; Zorzano, M.-P.; Ruiz-Bermejo, M. Prebiotic chemistry in neutral/reduced-alkaline gas-liquid interfaces. *Sci. Rep.* **2019**, *9*, 1–12. [CrossRef]
83. Holm, N.G.; Dumont, M.; Ivarsson, M.; Korn, C. Alkaline fluid circulation in ultramafic rocks and formation of nucleotide constituents: A hypothesis. *Geochem. Trans.* **2006**, *7*, 7. [CrossRef] [PubMed]



© 2020 by the authors. Licensee MDPI, Basel, Switzerland. This article is an open access article distributed under the terms and conditions of the Creative Commons Attribution (CC BY) license (<http://creativecommons.org/licenses/by/4.0/>).

Síntesis de moléculas orgánicas

Polimeros de HCN y sistemas hidrotermales

Ensayos de Química Prebiótica III





Artículo de investigación

Villafañe-Barajas, S. A., Ruiz-Bermejo, M., Rayo-Pizarroso, P., Gálvez-Martínez, S., Mateo-Martí, E., & Colín-García, M. (2021). A Lizardite–HCN Interaction Leading the Increasing of Molecular Complexity in an Alkaline Hydrothermal Scenario: Implications for Origin of Life Studies. *Life*, 11(7), 661.

Resumen El ácido cianhídrico, HCN, es una molécula fundamental en la evolución química y los experimentos de química prebiótica. Varias investigaciones han demostrado que los “polímeros derivados de HCN” liberan una cantidad importante de diferentes moléculas orgánicas después de los tratamientos de hidrólisis. Además, algunas investigaciones novedosas se han centrado en el estudio del papel de las superficies minerales durante la hidrólisis y/o polimerización de especies de cianuro, pero hasta ahora, el efecto de las superficies minerales no está claro. El papel de los minerales a lo largo de los procesos de evolución química pudo ser crucial porque indudablemente interactuaron con las moléculas orgánicas durante la Tierra primitiva mediante diferentes procesos. De esta forma, en este trabajo simulamos las probables interacciones entre HCN y serpentinita en condiciones hidrotermales alcalinas simples. Se estudió el efecto de la serpentinita durante la termólisis del HCN en condiciones básicas (*i.e.*, HCN (*l*) 0,15 M, 50 h, 100 °C, pH > 10). El polímero térmico derivado de HCN y el sobrenadante formado después del tratamiento fueron analizados mediante diversas técnicas analíticas complementarias. Los resultados obtenidos sugieren que: I) las superficies minerales podrían actuar como mediadoras en los mecanismos de producción de moléculas orgánicas como, por ejemplo, la polimerización de HCN; II) las propiedades térmicas y fisicoquímicas del polímero de HCN producido se ven afectadas por la presencia de la superficie mineral; y III) la serpentinita parece inhibir la formación de moléculas orgánicas en comparación con el experimento de control (sin mineral).

Article

A Lizardite–HCN Interaction Leading the Increasing of Molecular Complexity in an Alkaline Hydrothermal Scenario: Implications for Origin of Life Studies

Saúl A. Villafaña-Barajas ¹, Marta Ruiz-Bermejo ^{2,*}, Pedro Rayo-Pizarroso ², Santos Gálvez-Martínez ², Eva Mateo-Martí ² and María Colín-García ³

- ¹ Posgrado en Ciencias de la Tierra, Universidad Nacional Autónoma de México, Ciudad Universitaria, Mexico City 04510, Mexico; aquarium@comunidad.unam.mx
 - ² Departamento de Evolución Molecular, Centro de Astrobiología (CSIC-INTA), Ctra, Torrejón-Ajalvir, km 4, Torrejón de Ardoz, 28850 Madrid, Spain; prayo@cab.inta-csic.es (P.R.-P.); sgalvez@cab.inta-csic.es (S.G.-M.); mateome@cab.inta-csic.es (E.M.-M.)
 - ³ Instituto de Geología, Universidad Nacional Autónoma de México, Ciudad Universitaria, Mexico City 04510, Mexico; mcolin@geologia.unam.mx
- * Correspondence: ruizbm@cab.inta-csic.es; Tel.: +34-915206458; Fax: +34-915206410



Citation: Villafaña-Barajas, S.A.; Ruiz-Bermejo, M.; Rayo-Pizarroso, P.; Gálvez-Martínez, S.; Mateo-Martí, E.; Colín-García, M. A Lizardite–HCN Interaction Leading the Increasing of Molecular Complexity in an Alkaline Hydrothermal Scenario: Implications for Origin of Life Studies. *Life* **2021**, *11*, 661. <https://doi.org/10.3390/life11070661>

Academic Editor: Marie-Christine Maurel

Received: 17 May 2021

Accepted: 29 June 2021

Published: 6 July 2021

Publisher's Note: MDPI stays neutral with regard to jurisdictional claims in published maps and institutional affiliations.



Copyright: © 2021 by the authors. Licensee MDPI, Basel, Switzerland. This article is an open access article distributed under the terms and conditions of the Creative Commons Attribution (CC BY) license (<https://creativecommons.org/licenses/by/4.0/>).

Abstract: Hydrogen cyanide, HCN, is considered a fundamental molecule in chemical evolution. The named HCN polymers have been suggested as precursors of important bioorganics. Some novel researches have focused on the role of mineral surfaces in the hydrolysis and/or polymerization of cyanide species, but until now, their role has been unclear. Understanding the role of minerals in chemical evolution processes is crucial because minerals undoubtedly interacted with the organic molecules formed on the early Earth by different process. Therefore, we simulated the probable interactions between HCN and a serpentinite-hosted alkaline hydrothermal system. We studied the effect of serpentinite during the thermolysis of HCN at basic conditions (i.e., HCN 0.15 M, 50 h, 100 °C, pH > 10). The HCN-derived thermal polymer and supernatant formed after treatment were analyzed by several complementary analytical techniques. The results obtained suggest that: (I) the mineral surfaces can act as mediators in the mechanisms of organic molecule production such as the polymerization of HCN; (II) the thermal and physicochemical properties of the HCN polymer produced are affected by the presence of the mineral surface; and (III) serpentinite seems to inhibit the formation of bioorganic molecules compared with the control (without mineral).

Keywords: hydrogen cyanide; alkaline hydrothermal environments; organic molecules; serpentine minerals; prebiotic chemistry

1. Introduction

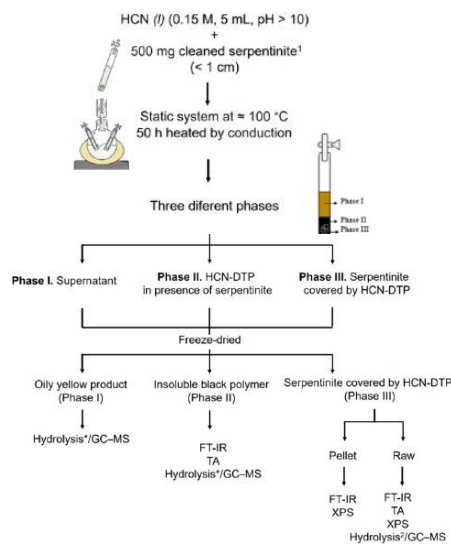
Currently, it is undoubted that several cyanide species may have had a crucial role in the previous steps for the origin of life [1–3], either as an important source of precursors to building blocks of RNA, proteins, and lipids [4–13] or as important chemical intermediates in phosphorylation reactions [14]. These cyanide species may have been scattered throughout some primitive environments such as the hydrothermal systems, either submarine or subaerial [15–20]. Hydrothermal environments, both subaerial and submarine, are considered ideal systems that allowed chemical evolution on Earth [21–23]. It has been proposed that serpentine-hosted hydrothermal systems may support favorable conditions for prebiotic pathways due to the coexistence of different geochemical variables on them [21,24–26]. Serpentinites are rocks formed mostly of serpentine-group minerals derived from metamorphism of mafic–ultramafic rocks that were abundant during the Hadean–Archean eons [27–30]. In general, these hydrous magnesium silicates are formed after low-temperature (<400 °C) hydration of ferromagnesian or magnesian minerals (e.g., olivine, orthopyroxene) formed in basic and ultrabasic rocks [31].

Because hydrothermal activity and the serpentinization process should have been common and widely distributed in the first 1000 Ma of the Earth's history [24,26,29,32–35], some authors have highlighted the interactions among cyanide species and geochemical variables present in hydrothermal environments and their aftermath in origin of life scenarios [2,36–41].

Recent papers have shown that hydrothermal fluids, during the serpentinization process, can lead to the occurrence of carbonaceous matter on mineral surfaces [42–44]. In addition, it has been shown that alkaline conditions and the dynamic surroundings that are present in hydrothermal systems are crucial for the transformation of cyanide species (e.g., cyanide salts and hydrogen cyanide, HCN) into other organic precursors with interesting roles in pre-RNA world scenarios [11,12,45–48]. Therefore, it seems necessary to study the role of serpentinite during the polymerization of HCN in order to simulate a feasible primitive geochemical scenario such as the surroundings of an alkaline hydrothermal system.

The polymerization of HCN has been widely studied [49–55]; however, few reports have focused on the polymerization of HCN onto mineral surfaces. Ferris et al. [56] found that the presence of montmorillonite inhibits the formation of oligomers because the clay decomposes the tetramer of HCN (i.e., diaminomaleonitrile, DAMN); this effect increases at higher temperatures [47]. However, Bocclair and coworkers [57] reported that layered double hydroxides (LDH) can favor the self-addition of cyanide at alkaline pH. On the other hand, the γ -irradiation of a heterogeneous sample of HCN/Na-montmorillonite inhibited the amount of carboxylic acids formed [58]. In addition, it has been shown that the properties (e.g., structure, kind of deposition, morphology) of aminomalononitrile-based films are modified by the presence of surfaces (e.g., quartz, glass, and silica; [59]). There is no comprehensive information about the role of mineral surfaces during HCN polymerization.

The dynamism of hydrothermal systems offers an interesting place for chemical reactions. For instance, the continuous transport of material along the surroundings of hydrothermal systems (i.e., the vent field that includes all active hydrothermal fluids (both at low (<100 °C) and high temperatures (<400 °C)) may involve the occurrence of thermolysis and polymerization reactions of raw material. Recently, we characterized a polymer formed from the thermolysis of HCN (i.e., HCN-DTP) [46] simulating a simple alkaline hydrothermal system. In this work, using the same synthesis conditions (i.e., HCN_(l) 0.15 M, 50 h, 100 °C, pH > 10), we studied the role of serpentinite related to the physicochemical properties of the formed polymer (HCN-DTP/serpentinite) as well as the nature of the supernatant and the mineral coated by an organic layer (Figure 1). Finally, we discuss the implications for chemical evolution studies.



1) Serpentinite was cleaned using KOH 3% v/v; H₂O; HNO₃ 3% v/v and characterized using XRD, FT-IR, and TA.

2) The hydrolysis procedure comprised two kinds of hydrolysis: acid (HCl 6N, 100–110 °C, 16–24 h) and basic (NaOH 0.1N, 100 °C, 6 h). Both procedures were carried out in each sample.

Figure 1. Processes followed for the synthesis and characterization of the HCN-DTP in presence of serpentinite.

2. Materials and Methods

2.1. Mineral/HCN Samples

Serpentinite was provided by Professor Fernando Ortega-Gutiérrez (Geology Institute, Universidad Nacional Autónoma de México, Ciudad Universitaria, 04510 Cd. Mx, Mexico). The sample was obtained from the Acatlán Complex, SW México [60]. In order to remove all the organic material on the sample, the following procedure was carried out: fragments of mineral (< 1 cm) were washed with a KOH solution (3% v/v) for 30 min (1 g mineral/10 mL solution). After that, the mineral was stirred in distilled water (30 min) to remove the KOH excess. Later, the sample was washed with HNO₃ solution (3% v/v) (1 g mineral/10 mL solution) for 30 min. Finally, the mineral was cleaned with distilled water to remove the acid excess. Mineral was dried at room temperature. XRD analysis was performed for mineralogical characterization of the serpentinite sample. The lizardite polymorph predominated in the sample. XRD spectra (Figure 2) showed distinctive diffraction peaks corresponding to lizardite (91%), antigorite (5%), and minor traces of magnetite and brucite (≈4%). Lizardite has the structural formula M₃T₂O₅(OH)₄, where M is mainly Mg and T is Si, although several common elements can be present in Table 2. Al³⁺, Ni, Mn²⁺, or Zn²⁺ [61–63]. In this mineral, 1:1 flat layers of sheets of SiO₄ tetrahedra and sheets of MgO₂(OH)₄ octahedra are linked by hydrogen bonds. The most common polytypic is the stacking of three layers without any lateral shift [64].

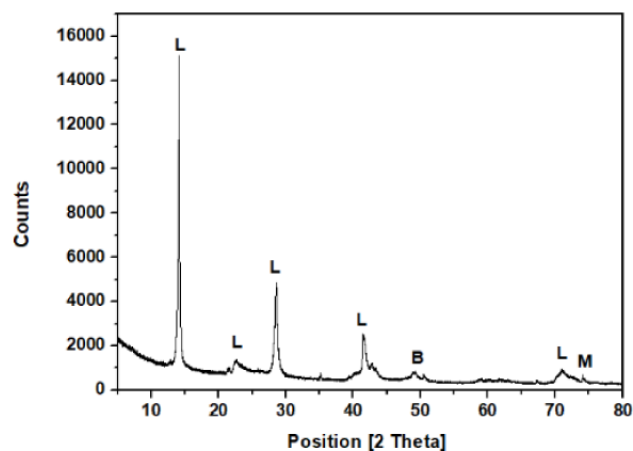


Figure 2. X-ray pattern for the serpentinite rock sample. Diffraction peaks were assigned based on previous works [61,63]. Legend: (L) lizardite $Mg_3Si_2O_5(OH)_4$, (M) magnetite (Fe_3O_4), and (B) brucite ($Mg(OH)_2$).

To confirm that the mineral sample was not contaminated, a mass spectroscopy thermal analysis was carried out for the cleaned serpentinite sample. Peaks related to OH^- and H_2O (at 619 and 696 °C) were detected; this corroborated that all organic material was removed from the serpentinite (figure not shown).

The HCN-DTP was synthesized in the presence of serpentinite as follows. HCN solution was produced in situ by the reaction between KCN and H_2SO_4 under argon atmosphere (for further details, please see Villafañe-Barajas et al., 2020 [46]). Once the desired concentration was reached (0.15 mol L^{-1}), the pH of the HCN solution was adjusted ($pH > 10$) with KOH solution (0.1 mol L^{-1}) to favor the availability of ^-CN and the formation of HCN-polymers. Finally, aliquots of HCN solution (0.15 mol L^{-1} , 5 mL) were prepared with 500 mg of the previously cleaned serpentinite in glass tubes and heated in a static system at 100 °C for 50 h. The selected temperature was consistent with the one found in the surroundings of alkaline hydrothermal environments. After treatment, three phases could be distinguished in the sample: I) supernatant (yellow soluble part), II) HCN-DTP (black polymer that was not adhered to mineral surface), and III) mineral + HCN-DTP (serpentinite covered by polymer). The three phases were analyzed by different analytical techniques (for more details, see Figure 1).

2.2. Analysis of Samples

2.2.1. FT-IR Spectroscopy (FT-IR)

The spectra were collected with a FT-IR spectrometer (Nicolet Thermo Fisher[®], model Nexus 67, MA, USA, software OMNIC) using CsI pellets. Using a DRIFT reflectance accessory (Harrik, model Praying Mantis DRP, New York, NY, USA), the spectra of Phases II and III in the $4000\text{--}450 \text{ cm}^{-1}$ spectral region (spectral resolution of 2 cm^{-1}) were obtained.

2.2.2. Thermal Analysis (TA)

A thermal analysis (thermogravimetry (TG), differential thermal analysis (DTG), and differential scanning calorimetry (DSC)) was performed with a TA instrument[®] (SDTQ-600/Thermo Star). The method involved operating in isothermal mode (20 min) and a heating ramp of 10 °C min^{-1} until 1000 °C under inert atmosphere (argon, flux 100 mL min^{-1}). The analysis of the main released species along dynamic thermal decomposition from

fragmentation process, were carried out with a coupled TG–MS system using an electron-impact quadrupole mass-selective detector (model Thermostar QMS200 M3).

2.2.3. XPS Spectroscopy Analysis

X-ray photoelectron spectroscopy analysis of Phase III was carried out in an ultrahigh-vacuum chamber equipped with a hemispherical electron analyzer and with the use of an Al K α X-ray source (1486.6 eV) with an aperture of 7 mm \times 20 mm. The base pressure in the chamber was 3×10^{-8} mbar, and the experiments were performed at room temperature. The sample was analyzed by preparing a pellet containing a sample of approximately 100 mg obtained after grinding and pressing the Phase III (mineral + HCN-DTP). Phase III was also analyzed as raw sample (rock covered by the polymer). The peak analysis in different components was shaped, after background subtraction, as a convolution of Lorentzian and Gaussian curves. Binding energies were calibrated against the binding energy of the C 1s peak at 285.0 eV. Calculation of the atomic relationships between the identified elements was derived from integral peak intensities and sensitivity factors supplied by Handbook of XPS [65].

2.2.4. Hydrolysis and GC–MS Analysis

To conduct a comparative analysis, a basic (NaOH 0.1N, 100 °C, 6 h) and acid (HCl 6N, 110 °C, 24 h) hydrolysis procedure was performed following previous reports [46,66]. After treatment, the samples (Phases I, II, and III) were analyzed by a GC system coupled to a 5975 VL MSD (Agilent®). The detection and characterization of different signals were performed as previously reported [9,46].

3. Results and Discussion

3.1. Fourier Transform Infrared (FT-IR) Spectroscopy

The FT-IR spectra of Phases II and III were registered and compared with their respective control samples. That means that the Phase II was compared to the polymer control HCN-DTP synthesized in the absence of mineral and the Phase III to a control serpentinite sample (Figure 3). This was done as a first step to evaluate the effect of the serpentinite in the cyanide polymerization process.

There were no appreciable differences between the spectra of the mineral alone and the Phase III (Figure 3A). The lack of differences between the naked mineral spectrum and the coated serpentinite is probably because the spectrum of the Phase III was registered using a pellet of the raw sample. As will be discussed below, the organic film represents a very low amount (in % weight) of the raw Phase III. Therefore, in relative proportion, the intensities of the mineral FT-IR features are much higher than those of the organic film; therefore, it was not possible to characterize the polymeric coating by this methodology. The FT-IR spectrum of the serpentinite described here (Figure 3A) is very similar to others spectra previously reported, with characteristic peaks centered at 3682 cm^{-1} , related to MgO-H stretching vibration modes, and at 974 cm^{-1} with a shoulder at 1068 cm^{-1} , corresponding to the Si–O–Si asymmetric stretching mode (for a detailed description of these FT-IR spectra, see, e.g., Rivero Crespo et al., 2019; [67]).

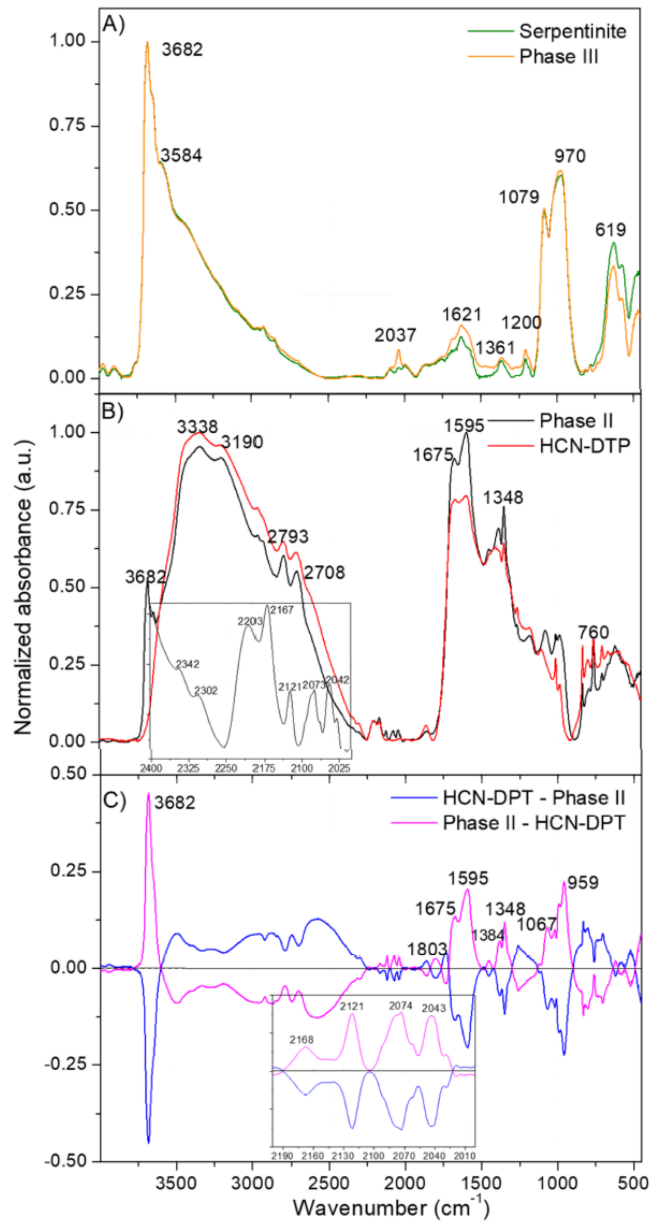


Figure 3. FT-IR spectra of (A) net serpentinite (clean control mineral) and serpentinite coated in a HCN-derived polymeric film (Phase III); (B) HCN-DTP polymer synthesized in the presence of serpentinite (Phase II) and control HCN-DTP polymer (synthesized in the absence of serpentinite); and (C) subtraction of the FT-IR spectra of the Phase II and the control HCN-DTP polymer.

On the other hand, the FT-IR spectra of the Phase II and the polymer control HCN-DTP present the same main features (Figure 3B). Detailed interpretations of these spectra were presented in Villafaña-Barajas et al. [46] indicating the generation of a highly conjugated macrostructure dominated by oxygenated functional groups. However, some slight but significant differences can be observed between the Phase II and the polymer control HCN-DTP (inset plot in Figure 3B and the subtraction of the spectra in Figure 3C). The subtraction of the FT-IR spectra of the Phase II and the polymer control HCN-DTP (pink line in Figure 3C) presents a clear feature at 3682 cm^{-1} and additional features at 959 and 1067 cm^{-1} , which can be related with the presence of residual serpentinite in the Phase II. The bands at 1803 , 1675 , and 1595 cm^{-1} may indicate a greater oxidation state for the Phase II, since these bands can be assigned to carbonyl compounds such as esters, ketones, amides, and carboxylic acids. Furthermore, the band at 1348 cm^{-1} can be related to $-\text{COO}$ groups in carboxylic acids salts (in this case, the counterions can come from the residual serpentinite). The features centered at 2168 , 2121 , 2074 , and 2043 cm^{-1} identified in the Phase II (inset plot Figure 3C) can be assigned to azide ($-\text{N}=\text{N}=\text{N}$), carbodiimide ($-\text{N}=\text{C}=\text{N}$), and isonitrile ($\text{N}\equiv\text{C}$) functional groups. Therefore, it seems that the serpentinite increases the hydrolysis in the HCN polymerization, resulting in highly oxidized products.

3.2. Thermal Analysis

Thermal analysis allowed characterization of the thermal behavior of the samples and finding notable differences between HCN polymers that were not evident using FT-IR spectroscopy. DTG and DSC curves are considered fingerprints to characterize and distinguish among HCN polymers with very similar FT-IR spectra [68,69]. As was done in the previous sections with the FT-IR spectra, the thermal curves of the Phase II were compared with those of the polymer control HCN-DTP and the curves for the Phase III with the control clean serpentinite (Figure 4). In addition, the thermal analysis of the Phase III was carried out under an air atmosphere. In accordance with previous reports, the thermogravimetric behavior of the samples was divided into three stages: I) drying stage ($<150\text{ }^{\circ}\text{C}$), II) pyrolysis stage ($150\text{--}450\text{ }^{\circ}\text{C}$), and III) carbonization stage ($>450\text{ }^{\circ}\text{C}$) [46,68–72]. The total weight loss of serpentinite was 12.6%, which agrees with previous reports, together with the DTG doublet in the carbonization stage (Figure 4A,C; Table 1) and with the DTA sharp exothermic peak at $823\text{ }^{\circ}\text{C}$ [73]. The thermal decomposition of this mineral leads to the dehydroxylation of the structure; the bound hydroxyl groups are removed from the serpentinite and liberated as water vapor [74]. The release of these groups reaches its maximum peaks at ~ 619 and $\sim 696\text{ }^{\circ}\text{C}$ as shown in the DTG curve (Figure 4C; Table 1). Likewise, the DSC and DTA curves (Figures 4E and 5) show a sharp exotherm peak at $\sim 823\text{ }^{\circ}\text{C}$, which indicates the complete formation of olivine (i.e., forsterite; Mg_2SiO_4) ([74,75].

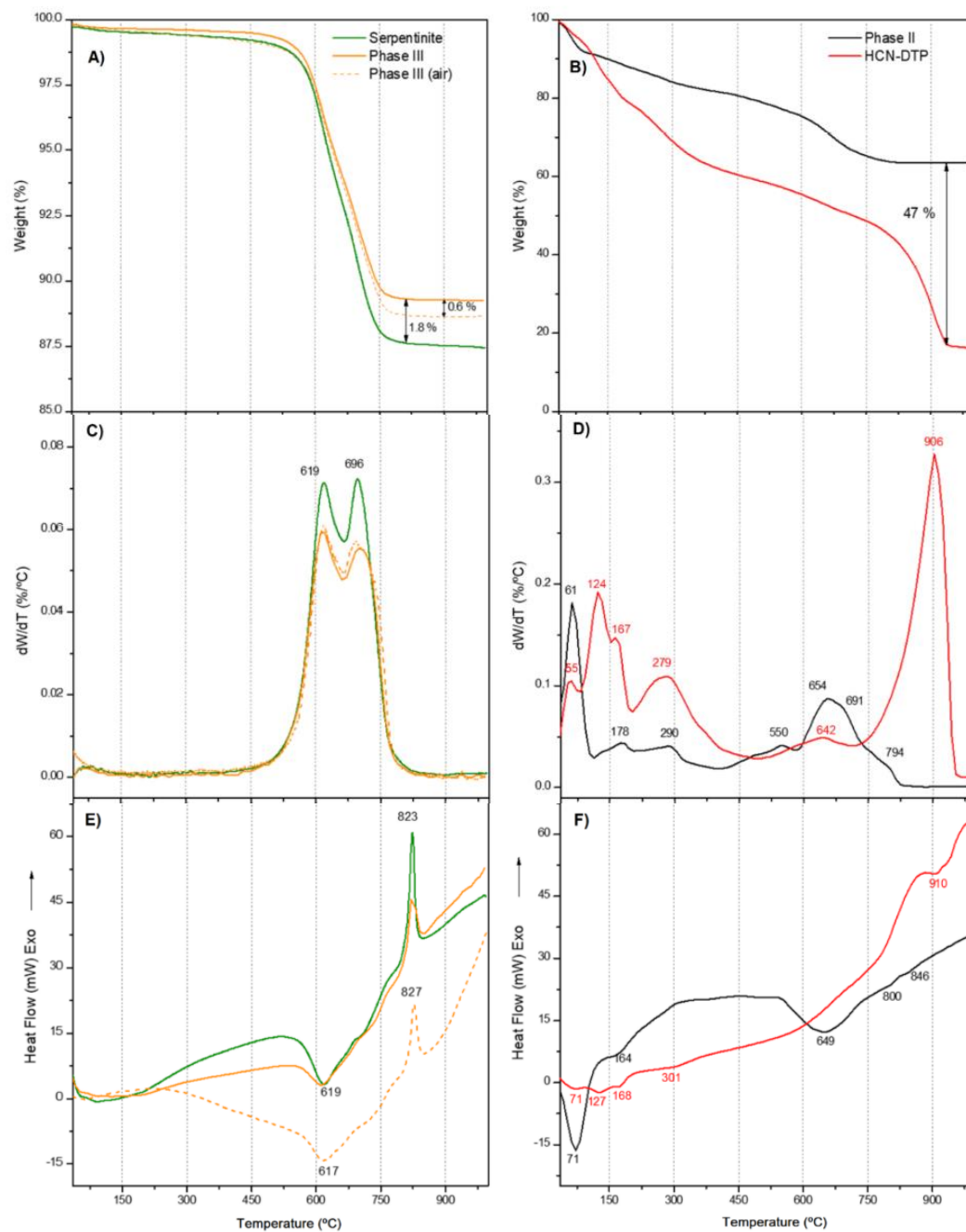


Figure 4. (A) and (B) TG curves; (C) and (D) DTG curves; (E) and (F) DSC curves. Note that an important amount of residue remained even at high temperatures. The most important decomposition step occurred along the third thermal stage. The identified stages were (I) drying stage (<150 °C), (II) pyrolysis stage (150–450 °C), and (III) carbonization stage (>450 °C).

Table 1. Characteristic temperatures for the thermal decomposition of samples. DTG maxima with the corresponding rates of weight loss, dW/dt , and DSC peaks observed in the samples.

Sample	Stage I (25–150 °C) Evaporation			Stage II (150–450 °C) Low Thermal Decomposition			Stage III (450–1000 °C) High Thermal Decomposition		
	DTG		DSC	DTG		DSC	DTG		DSC
	T_{max} (°C)	dW/dt (wt%/°C)	T_{peak} (°C)	T_{max} (°C)	dW/dt (wt%/°C)	T_{peak} (°C)	T_{max} (°C)	dW/dt (wt%/°C)	T_{max} (°C)
Serpentinite							619	0.07	619
							696	0.07	823
Phase II	61	0.18	71	178	0.04	164	550	0.04	649
				290	0.04		654	0.08	
							691	0.07	800
Phase III							794	0.03	846
							619	0.06	619
Phase III (Air)							696	0.05	823
							619	0.06	617
HCN-DTP	55	0.11	71	167	0.15	168	642	0.05	636
	124	0.20	127	279	0.11		906	0.34	910
				288	0.11	301	921	0.27	938

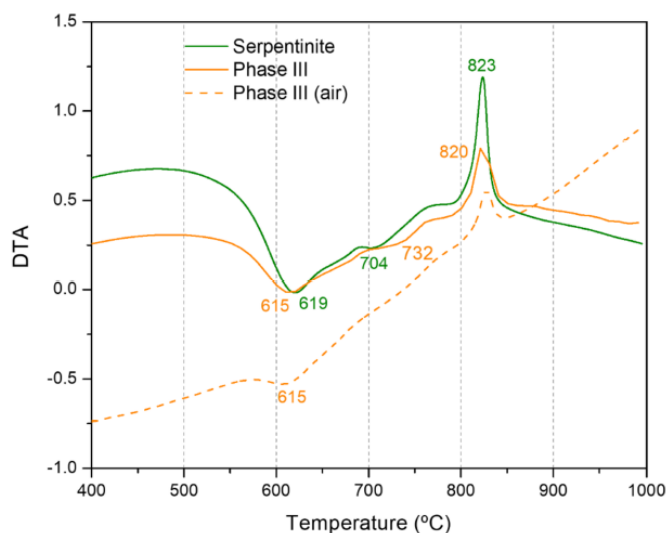


Figure 5. DTA analysis of serpentinite, phase III and phase III (air).

As with the FT-IR analysis, the thermal analysis does not show appreciable differences between the Phase III and serpentinite (Figure 4A,C,E and Figure 5; Table 1). There was a mass loss of only ~2% during the last thermal stage (> 450 °C) (Figure 4A). This suggests that there was not a significant amount of polymer covering the mineral surface, and, in consequence, the thermal profile obtained was dominated by the thermal behavior of serpentinite. However, for the Phase III, the total weight loss was 10.8%, an amount lower than the weight loss for the control sample, the clean serpentinite. Since dehydration is the unique thermal degradation processes for the serpentinite, it seems that the polymeric

coating might partially prevent the release of water. This also would influence the phase change, because a reduction in the exothermicity of the forsterite formation was observed (Figures 4E and 5). In addition, no thermal degradation of the coating was observed in the thermal curves herein considered. The next section discusses that this thermal decomposition seems to be minor. Furthermore, the thermal degradation of the Phase III in the presence of air led to an additional weight loss of 0.6 % compared to the weight loss obtained by heating under Ar atmosphere (Figure 4A). This result can be related to the total degradation of the polymeric coating, indicating a very low organic contribution (relative percentage in weight) from the film covering the mineral.

On the other hand, the presence of air did not affect the thermal behavior of the serpentinite, since there are not great differences between the thermal curves recorded in the presence of air (previously reported) with those recorded using an inert atmosphere of Ar. Nevertheless, the changes observed in the shapes of the DSC and DTA curves of the Phase III registered in the presence of air seem to be due to the polymeric coating, although without highly significant variations with respect to the clean control serpentinite. These results might indicate a physical (physisorption) interaction between the polymeric coating and the mineral surface instead of a strong chemical interaction (chemisorption). This fact is important to elucidate the possible role of the mineral in the full process of the cyanide polymerization and to understand the interaction between the mineral and the organic polymer. To the best of our knowledge, this is the first time that the thermal analysis of a covered mineral by a HCN-derived polymer has been described.

In regard to the Phase II, a mass loss of around 10 wt% was observed during the drying stage (<150 °C), which is a consequence of the release of volatile compounds retained in the polymer, predominantly H₂O. This value is consistent with previous reports [46,68,69,72]. In the second stage, the pyrolysis stage (150–450 °C), the mass loss was also 10 wt%. This value is considerably lower than those previously reported (approx. 25 wt%) [46,68,69,72]. This suggests that, as the second thermal stage has been associated with the decomposition of the side groups on the main chain, the polymer has no highly stable side structures. Two clear DTG peaks appear at 174 and 290 °C. Similar peaks also appear in the DTG curve for HCN-DTP (Figure 4B) [46]. In addition, a shoulder around ~135 °C is detected. The third step, the carbonization stage (>450 °C), showed the most significant differences between the Phase II and the HCN-DTP previously synthesized [46]. The sample yield was approximately ~63 wt% of char residues at the end of the ramp temperature. This is unexpectedly high, which is because of the fact that HCN-DTP yields around 15 wt%, while other HCN-derived polymers have 20 wt% [46,68,69,72]. In addition, this value represents almost the double percentage of the original weight reported (i.e., 36.4%) for the black polymer formed by the thermal decomposition of formamide [76]. It seems, as is the case for the coating film (Phase III), that this Phase II is highly thermally stable. Three signals are evident in the DTG curve: first a slight shoulder around 550 °C and then two predominant peaks at 654 and 691 °C. These peaks match with the signals detected in HCN-derived polymers synthesized from NH₄CN and DAMN [72]; however, this does not mean that identical structures are present. For instance, although there is no clear signal after 800 °C, as in other experiments performed at high temperatures (>80 °C) and high concentrations (>0.1 M) [46,72], there is a change in slope that starts at ~800 °C in the sample synthesized in presence of the mineral (Phase II). Finally, the DSC curve of the Phase II shows only three clear endothermic events at 71, 164, and 649 °C (Table 1). These signals correspond to evaporation of the absorbed water and the two main decomposition processes of the polymer [46,72]. Although the FT-IR spectra of the Phase II and the HCN-DTP previously synthesized are essentially alike, the thermal analysis shows important specific thermal fingerprints for each sample. The main difference is shown in the comparison of the DTG curve from Phase II and the HCN-DTP [46], where there is a peak after 900 °C in the control sample. Likewise, the Phase II shows a higher release of volatile species (e.g., H₂O) in the first thermal step (i.e., <70 °C). This considerable difference might be associated with an increment of hydroxyl groups in the polymer as a consequence of interactions with the

serpentine structure. Also, the high amount of char for the Phase II could be related with a higher degree of oxidation, in agreement with the FT-IR spectra. It has been proposed that an increase in the thermal stability of the HCN-derived polymers is related to a higher content of oxidizing groups in the macrostructures, which eventually leads to an increase in cross-linking [69]. On the other hand, the residual amount of serpentine in the Phase II may be very small, because its characteristic thermal peaks are not identified in any of the thermal curves (TGA, DTG, or DSC) of the Phase II (Figure 4B,D,F).

3.3. Mass Spectroscopy Thermal Analysis

Serpentine control, Phase II, and Phase III were analyzed by in situ mass spectrometry (Figure 6) to gain more information about the chemical species released in each thermal step shown in the DTG curves. We considered the same three thermal stages to compare the thermal behavior. The serpentine control shows only signals associated to OH^- ($m/z = 17$) and H_2O ($m/z = 18$) at 621 and 700 °C, which signals are consistent with the predominant peaks related to the release of hydroxyl groups from serpentine as is confirmed by the DTG curve (figure not shown) and is in agreement with previous results [73]. Comparatively, the Phase III shows four clear signals. Three of them coincide around ~620 and ~700 °C and could be associated with NH_2 ($m/z = 16$); OH^- , NH_3 ($m/z = 17$); and H_2O , NH_4^+ ($m/z = 18$). In addition, an appreciable signal at 214 °C is related to HCN ($m/z = 27$) (Figure 6A). Since the serpentine control does not show peaks below 600 °C, the peak at 214 °C can be directly related to the thermal decomposition of the organic coating (Figure 6A). Considering the intensity of these TG-MS data, the amount of coating on the serpentine is small, though it seems to partially protect the mineral of dehydration. Further works are needed to determine the thickness and the nature of these films synthesized under hydrothermal conditions. Only one previous paper has reported the kinetics of the deposition of AMN-derived polymers, but it did so at room temperature [59] and did not focus on the thermal stability of this new series of coatings.

Table 2. Summary of detected volatile species in Phase II. The MS peaks are associated with each thermal stage. Orange = Stage I. Evaporation (25–150 °C); Blue = Stage II. Low thermal decomposition (150–450 °C); Green = Stage III. High thermal decomposition (450–1000 °C).

Probable Species	MS Peaks (m/z)	TG-MS Peaks for Phase II				
		62	174	285	550	654
C+	12					
?	13					
N,CH_2^+	14					
NH	15					
NH_2	16					
OH^-/NH_3	17					
$\text{H}_2\text{O}/\text{NH}_4^+$	18					
?	22					
-CN	26					
HCN	27					
CO,N_2	28					
$\text{N}_2\text{H,HCO}$	29					
NO	30					
NCO	42					
HNCO/HOCN	43					
$\text{CO}_2/$	44					
HC(=NH)NH_2						
HCONH_2	45					
?	46					
Stage		I	II		III	

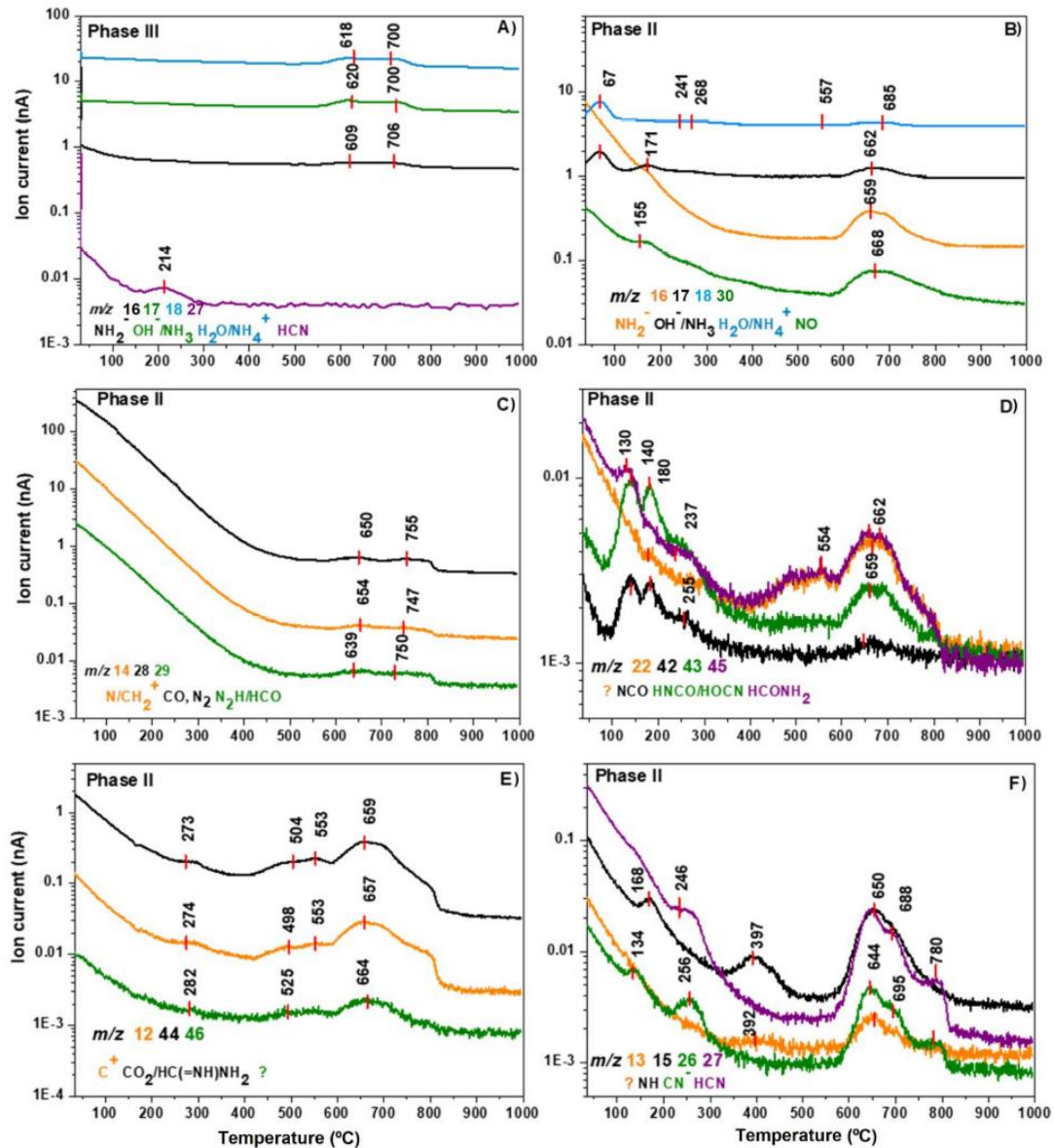


Figure 6. Ion intensity curves: (A) for Phase III; (B–F) for the Phase II. All signals are indicated in Table 2 with their correspondent DTG peaks. The predominant peaks on the third stage are the result of the contribution of several carbon and/or nitrogen species.

Phase II shows several changes related to the signals observed in the HCN-DTP control sample [46]. Figure 6B displays the predominant signals linked to NH_2 ($m/z = 16$; $T = 659$ °C); OH^- , NH_3 ($m/z = 17$; $T = 67, 171,$ and 662 °C); H_2O , NH_4^+ ($m/z = 18$; $T = 67,$

241, 268, 557, and 685 °C); and NO ($m/z = 30$; T = 155 and 668 °C). Though these species and peaks were also present in the HCN-DTP, the Phase II has new, well-defined signals associated with NH_2 , OH^-/NH_3 , and NO around ~660 °C. In addition, the $m/z = 30$ profile does not have the same broad peak around ~160 °C as the control sample (Figure 6B). Two clear peaks are shown for the profiles associated with N/CH_2 ($m/z = 14$); CO, N_2 ($m/z = 28$); and $\text{N}_2\text{H}/\text{HCO}$ ($m/z = 29$) at ~650 and 750 °C (Figure 6C). These signals contribute to the broad peak shown in the DTG curve at the third stage (>450 °C). The thermal profile is totally different, even though these species are released in the HCN-DTP. First, the ion current is considerably higher, and it is thus impossible to identify peaks before 600 °C as is possible in the control sample (e.g., 172 and 283 °C). Moreover, the Phase II does not present peaks after 900 °C as is evident in the HCN-DTP.

In general, the signals in the pyrolysis (150–450 °C) and carbonization stages (>450 °C) are considerably different to the thermal profile of the polymer synthesized in the absence of mineral. The main differences are the predominant peaks around ~660 °C and the absence of peaks after ~900 °C (Figure 6D,E,F). The peaks around ~660 °C are the result of the contribution of several carbon and/or nitrogen species, e.g., C^+ ($m/z = 12$), NH ($m/z = 15$), NCO ($m/z = 42$), HNCO/HOCN ($m/z = 43$), $\text{CO}_2/\text{HC}(=\text{NH})\text{NH}_2$ ($m/z = 44$), and HCONH_2 ($m/z = 45$), which suggest the dominance of decarboxylation and/or deamination mechanisms. Other peaks displayed in the same species profiles below 300 °C (e.g., 130, 180, 255, 282) are present in the polymer synthesized without mineral. However, the peaks at 392, 500, and 550 °C are only present for the CH , NH , NCO , $\text{CO}_2/\text{HC}(=\text{NH})\text{NH}_2$, and HCONH_2 species in the Phase II (Figure 6E,F). New signals without clear assignments are present in the polymer synthesized in the presence of mineral (e.g., $m/z = 13$ and $m/z = 46$). Interesting, the profiles associated to cyanide species, CN^- ($m/z = 26$) and HCN ($m/z = 27$), are totally different from the control HCN-DTP sample. For instance, the profile of the sample without mineral shows a broad peak that starts at 423 °C and disappears after 900 °C. Instead, in the presence of serpentinite, cyanide species profiles only show three peaks between 640 and 780 °C (Figure 6F). These profiles resemble the general pattern of the DTG curve from the Phase II. Hence, decyanogenation of the polymer takes place mainly at 650 °C. In general, the thermal profile of Phase II shows that decarboxylation, deamination, and/or decyanogenation mechanisms occur mainly around ~660 °C. The absence of this thermal step and the predominant peak after 900 °C in the polymer synthesized without mineral suggest that the presence of serpentinite considerably affects the thermal and structural properties of the HCN-derived thermal polymers. In addition, the possible decyanogenation and degradation process of the Phase III is centered at 214 °C, suggesting a higher thermal lability of the coating than the insoluble black solid, Phase II; this implies that the coating and the insoluble black solid have different structural natures.

Table 2 shows a review of each volatile species contribution related to the thermal stages previously described. In summary, the peak at 124 °C and the two signals after 900 °C do not appear on the DTG curve of the polymer synthesized in the presence of serpentinite. In addition, the serpentinite contributes with an important amount of hydroxyl groups released in the first thermal step (i.e., 62 °C). Finally, the peak around 550 °C is unique in this sample.

3.4. XPS Analysis

The general thermal analysis suggested important physicochemical differences between the HCN-DTP synthesized with and without serpentinite, so X-ray photoelectron spectroscopy analysis was carried out to elucidate the interactions between the organic coating and the mineral surface. Figure 7A shows the photoemission spectra of both the clean serpentinite and the Phase III. The data were registered by using pellets from both samples. The serpentinite control shows clear signals related to its atomic composition (Mg, Si, and O) in strong agreement with previous reports [77]. In this case, the spectra of the clean serpentinite and the Phase III do not show significant chemical changes (Figure 7A). This could be a result of the low amount of organic polymer deposited onto the mineral

surface and diluted in the bulk of the pellet, which may have been insufficient to obtain characteristic or specific signals from the organic film. Some previous studies by our group, where the characterization HCN-derived polymers and *tholins* was performed, reported that ~25% in weight of organic material by total mass of sample (mineral + organic) is necessary [71,78,79] to identify the chemical features of that material without doubt.

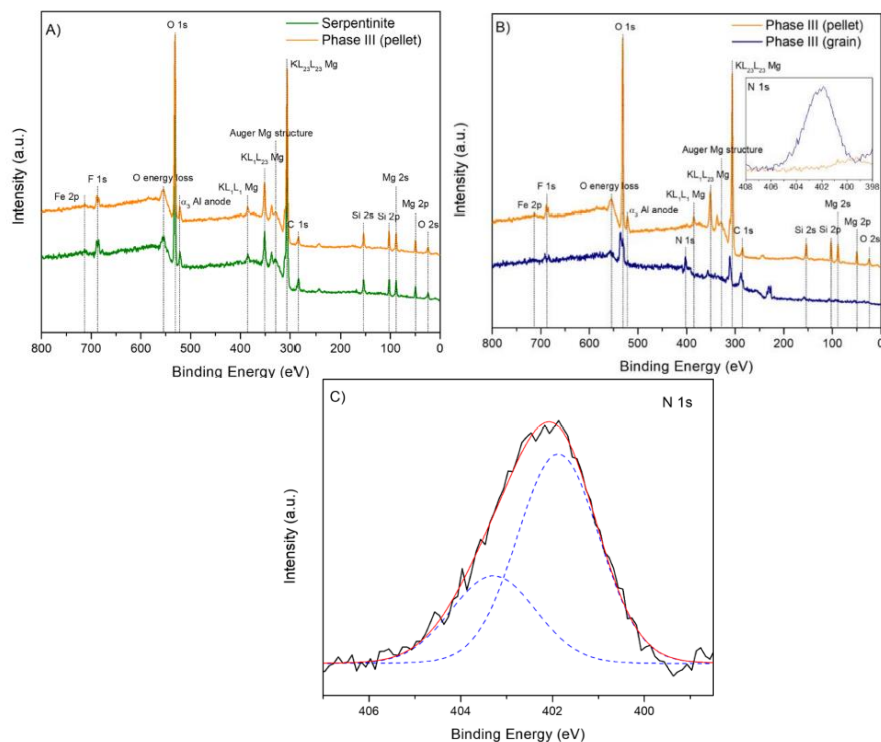


Figure 7. Photoemission spectra of samples. (A) XPS overview photoemission spectra of serpentinite control and Phase III (pellet); (B) XPS overview photoemission spectra of Phase III (pellet and grain); and (C) XPS spectra of N 1s core level peak of Phase III (grain sample), recognized as the fingerprint of the polymeric film.

However, when the XPS spectrum of the Phase III was performed using a coated serpentinite grain, the differences were remarkable (Figure 7B). The main difference among the samples containing an organic coating on the surface is that the mineral signals are attenuated. This can be explained by one main reason: the XPS technique is mainly sensible to the first surface layers of the sample; therefore, once the polymer covers the mineral surface forming a film, the mineral surface stays hidden underneath the organic material. Because of this phenomenon, a signal assigned to N 1s, the fingerprint of the polymeric film, is observed in the Phase III (inset plot in Figure 7B,C). The first component (at 401.8 eV) can be assigned to ammonium cations, and the second one (at 403.3 eV) to azide groups (R-N=N=N-) or nitrites (Figure 7B). The assignment of these components is

different to those of others coatings obtained from AMN at room temperature (although the N 1s signal is significant, Thissen et al. performed deep analysis of C 1s spectra and the binding energies were referenced to aliphatic hydrocarbons peak at 285.0 eV [80] or insoluble cyanide polymers (397.6 eV to imine and/or heterocyclic groups and 398.7 eV to amides [71]). This result is consistent with the fact that the structural nature of the HCN polymers is directly dependent on the experimental synthetic conditions, as well as the chosen monomers used in their syntheses [72]. In the present case, the nature of the mineral substrate could also be considered to explain these differences. Recent works have suggested that the presence of inorganic surfaces (i.e., silica) can affect the properties (e.g., morphology and change of composition film) of AMN-based films [59]. Likewise, Ball [81] reported that AMN-based films deposited on amorphous carbon can affect its electrochemical activity as a consequence of the change in the composition, morphology, and thickness of the film. In addition, he suggested that long deposition times (21 h) produce thicker films. Because our experiments were performing using 50 h of reaction time at a higher temperature, the attenuated XPS signals from the mineral (Figure 7B) may be the consequence of a thick coating that covers the mineral surface. Nevertheless, we cannot discard molecular interactions and/or chemical reactions catalyzed by the mineral between the HCN-DTP and serpentinite once the polymer was formed (e.g., effects of the hydroxyl groups and/or Fe/Mg atoms during polymerization reaction). Additional systematic experiments are needed to understand the real interactions between the HCN polymers and inorganic surfaces. As a result, it seems that there is a physical adsorption of the polymeric coating on the serpentinite mineral, but chemisorption cannot be ruled out. Under the point of view of origin of life studies, these considerations about coating mineral superficies are of interest because they have not been previously taken into account and may increase the chemical space of prebiotic chemistry due to the potential redox properties of these coatings.

3.5. GC-MS Analysis of Hydrolyzed Samples

The dynamism of hydrothermal systems offers important temperature (25–400 °C) and pH gradients (pH = 2–11) along the hydrothermal fields [29,46,82–84]. Hence, the polymers formed in these environments are probably continuously exposed to thermolysis and hydrolysis reactions. Because hydrolysis conditions (i.e., heating time and pH value) are directly related to the amount of organic molecules released [7,66,85], we carried out a hydrolysis procedure (both alkaline and acid hydrolysis at 100–110 °C) for each phase to identify some polar organic compounds associated with each sample. In addition, we compared the detected molecules with those found in the HCN-DTP synthesized in the control experiment (in the absence of serpentinite). Figure 8 summarizes all the organic compounds identified in this work.

The predominant species, both in acidic and basic hydrolysis, are glycerol, glycolic acid, succinic acid, orotic acid, stearic acid, and palmitic acid (Figure 9). However, some trends can be distinguished among phases and hydrolysis conditions. For instance, after acidic hydrolysis, carboxylic acids predominated, such as lactic, glycolic, and succinic acid (Figure 9A,C) and only after acid hydrolysis was 2, 5-dihydroxy pyrazine was present. Interestingly, some fatty acids were detected after the basic hydrolysis of the Phase I and II (Figure 9B,D). Related to this, Takahashi and coworkers [86] described the synthesis of fatty acids from HCN using organic solvents and high temperatures (>100 °C). Likewise, Eschenmoser [87] proposed a hypothetical pathway based on the hydrolysis of diamino-maleonitrile (DAMN) and other intermediates previously detected [46] to explain the formation of fatty acids.

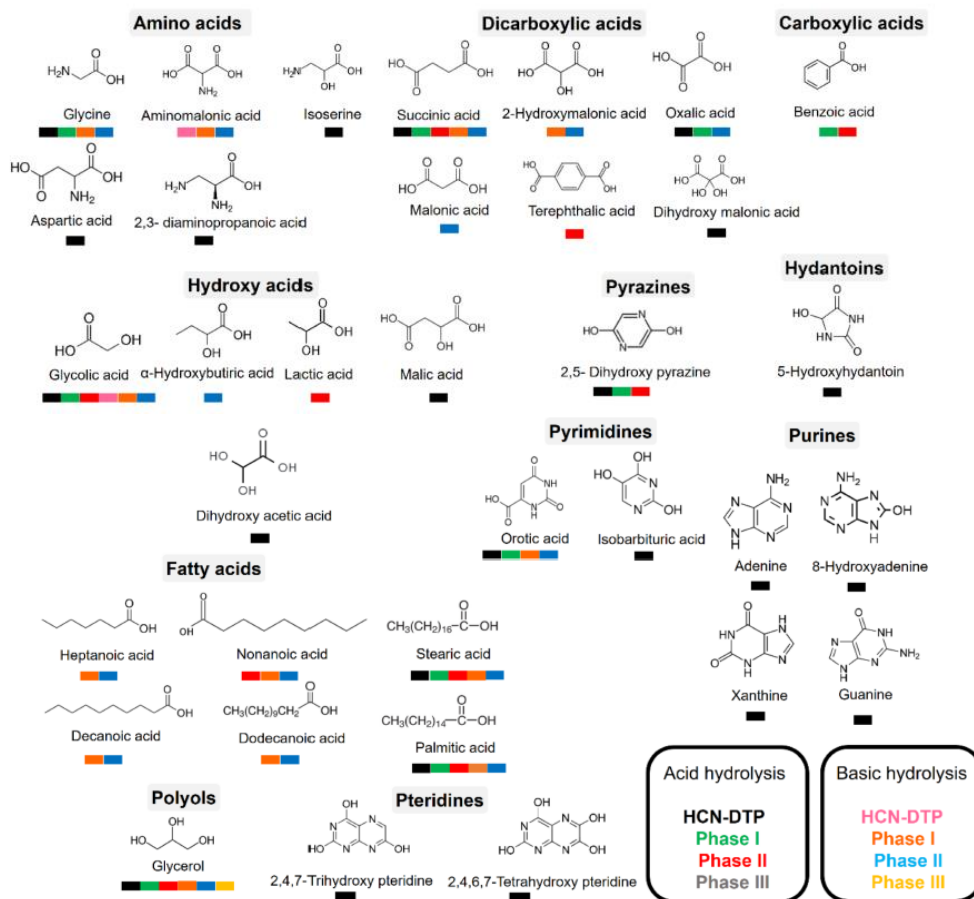


Figure 8. Organic compounds identified in samples after hydrolysis treatments. The colors indicate the sample from which the organic compounds were released.

In basic hydrolysis there was a broader spectrum of hydroxylated species in addition to the species detected by the acid hydrolysis, such as α -hydroxybutyric acid, oxalic acid, malonic acid, hydroxymalonic acid, aminomalonic acid, and other fatty acids (heptanoic acid, decanoic acid, and dodecanoic acid). Carbamate, glycine, orotic acid, and urea were also detected. Notably, in all cases, glycerol was present.

Regarding the Phase III, even using a higher amount of sample (50 mg), there were no clear signals associated with important organic compounds. As mentioned before, this could be a result of the low amount of polymer deposited onto mineral. Only carbamate and glycerol were identified after basic hydrolysis. Thissen et al. [88], in analogous deposition experiments performed on gold substrates, proposed that hydrolysis of imine groups promotes the formation of carbonyl compounds. In our case, the hydrolysis reactions could also lead to the formation of these compounds. Some uncertain signals, probably attributed to alkanes, could be distinguished after acid hydrolysis.

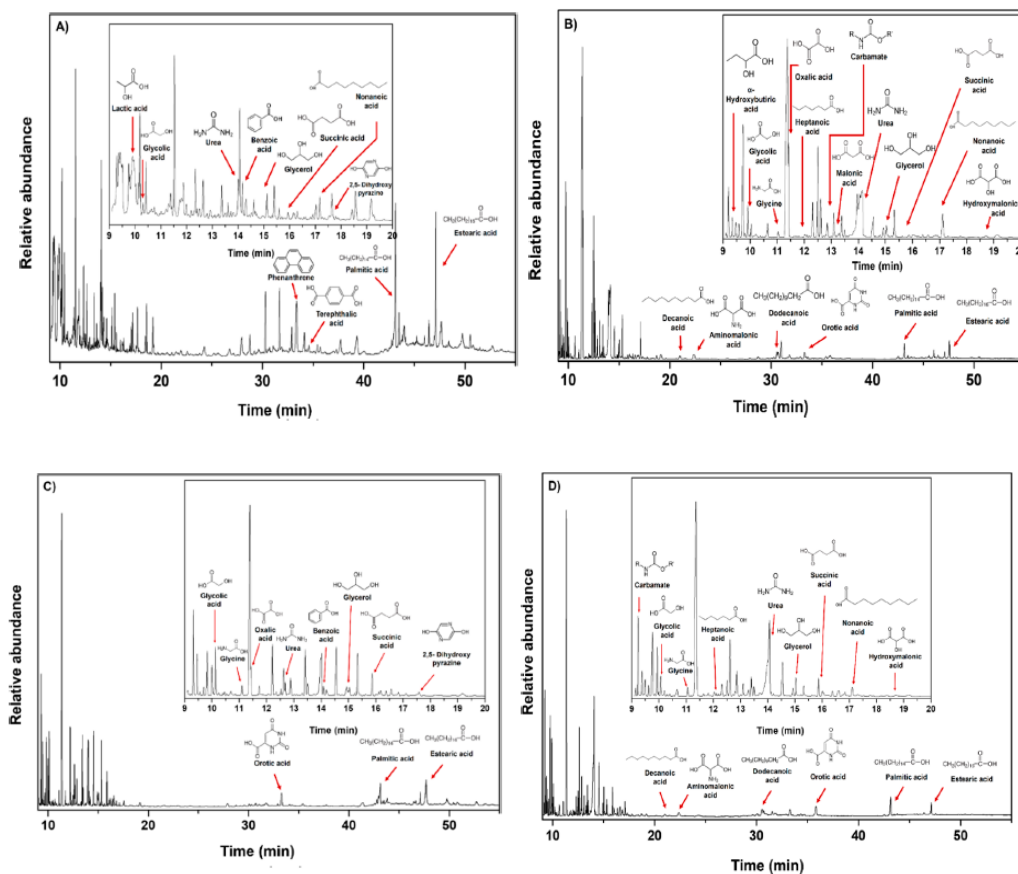


Figure 9. Organic compounds identified in samples after hydrolysis treatments: (A) acid hydrolysis for Phase II; (B) basic hydrolysis for Phase II; (C) acid hydrolysis for Phase I; and (D) basic hydrolysis for Phase I. The predominant species, both for acidic and basic hydrolysis, were glycerol, glycolic acid, succinic acid, orotic acid, stearic acid, and palmitic acid.

Minerals could affect the nature of the formed product, even if the exact mechanisms for this are not fully understood. For example, González-López and coworkers [89] found that olivine biases the products formed by thermolysis of acetic acid and formic acid. In our experiments, the presence of serpentinite had interesting repercussions in the diversity of organic molecules detected after hydrolysis treatment (Figures 8 and 9). On the one hand, after acid hydrolysis in presence of mineral, some carboxylic acids, fatty acids, and pyrazine in the Phase I and Phase II were identified. The presence of mineral seems to inhibit the formation of N-heterocyclic compounds, as is evident in the control experiment (HCN-DTP). On the other hand, after basic hydrolysis of samples synthesized in the presence of inorganic surfaces, some amino acids and predominantly fatty acids were released from Phase I and II. Orotic acid was the only cyclic compound detected after both hydrolysis treatments for the samples synthesized in the presence of mineral.

4. Outlook on Studies about Prebiotic Molecular Complexity

The current knowledge about the formation of HCN-derived polymers shows that their features depend on synthesis conditions, including concentration, temperature, presence of oxygen, time of reaction, and raw material [11,46,48,53–55,69,72]. Alkaline hydrothermal systems have been pointed out as very versatile and crucial environments for chemical evolution and, eventually, for origin of life scenarios [38–40,45,90–95]. Con-

sidering the new perspectives of prebiotic chemistry (that suggest to take into account the dynamism of environments, as well as the interactions among their geochemical variables; [29,46,96]), we tested the role of serpentinite during the polymerization of HCN as a first approximation of a simple simulation of an alkaline hydrothermal system. The results suggest that the presence of this mineral affects the thermal properties of HCN-DTP. For instance, the release of volatile species as a function of temperature increment having a maximum peak around ~ 660 °C is considerably different from the control sample. In addition, some interesting carbon and/or nitrogen volatile species are associated with specific thermal events.

Although the synthesis of organic compounds from serpentinization fluids in ultramafic systems has been reported [97,98], our results suggest that the presence of serpentinite could affect the chemical structure of the formed polymer (in this case HCN-DTP). Hence, it could decrease the diversity of organic molecules released after hydrolysis treatment. Markedly, this inorganic surface inhibited the formation of polar organic compounds and mainly N-heterocyclic compounds, unlike the control experiment (HCN-DTP) [46]. These results raise interesting questions: Is molecular complexity, considering the polymerization of HCN as a prebiotic pathway, reduced in mineral-rich environments? How can the addition of more geochemical variables affect the reactivity of the system? What is the potentiality of these coatings?

Considering the role of minerals in HCN polymerization, previous reports have suggested that montmorillonite inhibits the formation of oligomers [47,56] and reduces the amount of carboxylic acids formed [58]. However, this does not mean that all mineral surfaces may have the same effect. Related to the second question, an interesting study showed that the addition of salts during the HCN polymerization process reduced the diversity of organic molecules, and ammonia had the opposite effect [9]. Compared with similar experiments that simulated alkaline hydrothermal environments using NH_4CN as initial reagent and microwave conditions as energy source, the polar organic compounds identified by the same GC-MS method were considerably lower in our case [48].

On the other hand, the considerable thermal stability of HCN-DTP suggests that its persistence under hydrothermal conditions as well as the presence of coated mineral surfaces could establish new steps in chemical evolution, e.g., acting as semiconductors and catalysts, which are phenomena with important repercussions in the development of new chemical pathways [72] such as photocatalyst reactions [99]. In this way, understanding the properties and roles of these complex materials can shed light about specific catalytic reactions and the formation of some constituents of primitive chemical cycles that were necessary in the first steps of the origin of life [100].

These results indicate that the contribution of different geochemical variables in the same experiment, which tried to simulate the dynamism in these primitive environments, could modify the production of organic compounds. This does not mean a “knock-out” for these systems and their role in chemical evolution. For example, after basic hydrolysis of samples synthesized in presence of serpentinite, the release of some fatty acids is possible. The availability of these molecules and their eventual concentration in microporous matrices of alkaline vents can be enough to precipitate into vesicles [101]. Likewise, depending of pH conditions and salt concentrations, some fatty acid membranes resist extreme environments [102]. On the other hand, even though purines were not synthesized in the presence of mineral, orotic acid was released after hydrolysis treatment (acid and basic). Recently, the importance of orotic acid as a starting point in chemical pathways to RNA has been pointed out [103–105]. Orotic acid can form metal complexes with common ions in hydrothermal conditions (e.g., Cu^{2+} , Mn^{2+} , Zn^{2+}) [106], which complexes could establish new chemical interactions with other organic molecules or surfaces.

5. Conclusions

New perspectives in prebiotic chemistry suggest the necessity of considering the dynamism of primitive environments. Since minerals and organic molecules should have

interacted continuously during early Earth, important phenomena could have developed. Common environments like alkaline hydrothermal systems could have important repercussions in the synthesis and evolution of complex materials such as HCN-DTP and coatings of mineral surfaces. The results suggest that the presence of serpentinite affects the thermal properties of the formed polymer as well the carbon and/or nitrogen volatile species released in specific thermal events. After hydrolysis treatment, several organic molecules with interesting importance in pre-RNA scenarios were identified. Although the effect of mineral surfaces in chemical evolution process has been widely investigated, the focus on coating mineral surfaces is recent. The effect of the presence of mineral surfaces in polymerization reactions and their repercussions in the physicochemical nature of the polymers formed is a new area that introduces a novel vision in prebiotic chemistry.

Author Contributions: Conceptualization, M.R.-B. and M.C.-G.; methodology M.R.-B.; validation, S.A.V.-B., P.R.-P., M.R.-B., and E.M.-M.; formal analysis, S.A.V.-B., P.R.-P., and S.G.-M.; investigation, S.A.V.-B. and S.G.-M.; resources, M.R.-B. and E.M.-M.; writing—original draft preparation, S.A.V.-B., M.R.-B., and M.C.-G.; writing—review and editing, M.C.-G.; supervision, M.R.-B. and M.C.-G.; funding acquisition, M.R.-B., M.C.-G., and E.M.-M. All authors have read and agreed to the published version of the manuscript.

Funding: This research was funded by the projects PID2019-104205GB-C21 and PID2019-107442RB-C32 from the Spanish Ministerio de Ciencia, Innovación y Universidades, and by the Spanish State Research Agency, project MDM-2017-0737 Centro de Astrobiología (CSIC-INTA), Unidad de Excelencia María de Maeztu.

Institutional Review Board Statement: No applicable

Informed Consent Statement: Not applicable

Data Availability Statement: Not applicable

Acknowledgments: S.A.V.-B. acknowledges Posgrado en Ciencias de la Tierra (UNAM), Instituto de Ciencias Nucleares (UNAM), CONACyT (Ph. D. grant 697442 and the financial support for a research stay grant), and the technical assistance of Claudia Camargo and Alicia Negrón-Mendoza. The Instituto de Ciencias Nucleares (UNAM) and Centro de Astrobiología (CAB) are acknowledged for the use of their facilities. M.R.-B., P.R.-P., S.G.-M. and E.M.-M. used the research facilities of the Centro de Astrobiología (CAB) and were supported by the Instituto Nacional de Técnica Aeroespacial “Esteban Terradas” (INTA). Additionally, the authors are grateful to M^a Teresa Fernández, for performing the FT-IR spectra, and to the “Servicio de Análisis Térmico” of ICMN (CSIC, Spain).

Conflicts of Interest: The authors declare no conflict of interest. The funders had no role in the design of the study; in the collection, analyses, or interpretation of data; in the writing of the manuscript, or in the decision to publish the results.

References

1. Ruiz-Bermejo, M.; Zorzano, M.-P.; Osuna-Esteban, S. Simple Organics and Biomonomers Identified in HCN Polymers: An Overview. *Life* **2013**, *3*, 421–448. [[CrossRef](#)]
2. Sutherland, J.D. The Origin of Life—Out of the Blue. *Angew. Chem. Int. Ed.* **2016**, *55*, 104–121. [[CrossRef](#)]
3. Islam, S.; Powner, M.W. Prebiotic Systems Chemistry: Complexity Overcoming Clutter. *Chem* **2017**, *2*, 470–501. [[CrossRef](#)]
4. Powner, M.W.; Gerland, B.; Sutherland, J.D. Synthesis of Activated Pyrimidine Ribonucleotides in Prebiotically Plausible Conditions. *Nature* **2009**, *459*, 239. [[CrossRef](#)] [[PubMed](#)]
5. Ritson, D.; Sutherland, J.D. Prebiotic Synthesis of Simple Sugars by Photoredox Systems Chemistry. *Nat. Chem.* **2012**, *4*, 895–899. [[CrossRef](#)] [[PubMed](#)]
6. Ritson, D.J.; Sutherland, J.D. Synthesis of Aldehydic Ribonucleotide and Amino Acid Precursors by Photoredox Chemistry. *Angew. Chem. Int. Ed.* **2013**, *52*, 5845–5847. [[CrossRef](#)]
7. Marín-Yaseli, M.R.; Mompeán, C.; Ruiz-Bermejo, M. A Prebiotic Synthesis of Pterins. *Chem. Eur. J.* **2015**, *21*, 13531–13534. [[CrossRef](#)] [[PubMed](#)]
8. Patel, B.H.; Percivalle, C.; Ritson, D.J.; Duffy, C.D.; Sutherland, J.D. Common Origins of RNA, Protein and Lipid Precursors in a Cyanosulfidic Protometabolism. *Nat. Chem.* **2015**, *7*, 301–307. [[CrossRef](#)] [[PubMed](#)]
9. Marín-Yaseli, M.R.; González-Toril, E.; Mompeán, C.; Ruiz-Bermejo, M. The Role of Aqueous Aerosols in the “Glyoxylate Scenario”: An Experimental Approach. *Chem. Eur. J.* **2016**, *22*, 12785–12799. [[CrossRef](#)] [[PubMed](#)]

10. Xu, J.; Ritson, D.J.; Ranjan, S.; Todd, Z.R.; Sasselov, D.D.; Sutherland, J.D. Photochemical Reductive Homologation of Hydrogen Cyanide Using Sulfite and Ferrocyanide. *Chem. Commun.* **2018**, *54*, 5566–5569. [\[CrossRef\]](#)
11. Mompeán, C.; Marin-Yaseli, M.R.; Espigares, P.; González-Toril, E.; Zorzano, M.-P.; Ruiz-Bermejo, M. Prebiotic Chemistry in Neutral/Reduced-Alkaline Gas-Liquid Interfaces. *Sci. Rep.* **2019**, *9*, 1–12.
12. Das, T.; Ghule, S.; Vanka, K. Insights into the Origin of Life: Did It Begin from HCN and H₂O? *ACS Cent. Sci.* **2019**, *5*, 1532–1540. [\[CrossRef\]](#)
13. Liu, Z.; Wu, L.-F.; Bond, A.D.; Sutherland, J.D. Photoredox Chemistry in the Synthesis of 2-Aminoazoles Implicated in Prebiotic Nucleic Acid Synthesis. *Chem. Commun.* **2020**, *56*, 13563–13566. [\[CrossRef\]](#) [\[PubMed\]](#)
14. Burcar, B.; Castañeda, A.; Lago, J.; Daniel, M.; Pasek, M.A.; Hud, N.V.; Orlando, T.M.; Menor-Salván, C. A Stark Contrast to Modern Earth: Phosphate Mineral Transformation and Nucleoside Phosphorylation in an Iron- and Cyanide-Rich Early Earth Scenario. *Angew. Chem. Int. Ed.* **2019**, *58*, 16981–16987. [\[CrossRef\]](#) [\[PubMed\]](#)
15. Mukhin, L.E.V. Evolution of Organic Compounds in Volcanic Regions. *Nature* **1974**, *251*, 50–51. [\[CrossRef\]](#)
16. Mukhin, L. Volcanic Processes and Synthesis of Simple Organic Compounds on Primitive Earth. *Orig. Life* **1976**, *7*, 355–368. [\[CrossRef\]](#) [\[PubMed\]](#)
17. Dowler, M.J.; Ingmanson, D.E. Thiocyanate in Red Sea Brine and Its Implications. *Nature* **1979**, *279*, 51–52. [\[CrossRef\]](#)
18. Arrhenius, T.; Arrhenius, G.; Paplawsky, W. Archean Geochemistry of Formaldehyde and Cyanide and the Oligomerization of Cyanohydrin. *Orig. Life Evol. Biosph.* **1994**, *24*, 1–17. [\[CrossRef\]](#)
19. Keefe, A.D.; Miller, S.L. Was Ferrocyanide a Prebiotic Reagent? *Orig. Life Evol. Biosph.* **1996**, *26*, 111–129. [\[CrossRef\]](#)
20. Dzombak, D.A.; Ghosh, R.S.; Wong-Chong, G.M. *Cyanide in Water and Soil: Chemistry, Risk, and Management*; CRC/Taylor & Francis: Boca Raton, FL, USA, 2006.
21. Martin, W.; Baross, J.; Kelley, D.; Russell, M.J. Hydrothermal Vents and the Origin of Life. *Nat. Rev. Microbiol.* **2008**, *11*, 805–814. [\[CrossRef\]](#)
22. Colin-García, M.; Ortega-Gutiérrez, F.; Heredia, A.; Negrón-Mendoza, A.; Ramos-Bernal, S.; Cordero, G.; Camprubi, A.; Beraldi, H. Hydrothermal Vents and Prebiotic Chemistry: A Review. *Boletín Soc. Geológica* **2016**, *68*, 599–620. [\[CrossRef\]](#)
23. Colin-García, M.; Villafañe-Barajas, S.; Camprubi, A.; Ortega-Gutiérrez, F.; Colás, V.; Negrón-Mendoza, A. Prebiotic Chemistry in Hydrothermal Vent Systems. In *Handbook of Astrobiology*, 1st ed.; CRC Press: Boca Raton, FL, USA, 2018; pp. 297–329.
24. Schulte, M.; Blake, D.; Hoehler, T.; McCollom, T. Serpentinization and Its Implications for Life on the Early Earth and Mars. *Astrobiology* **2006**, *6*, 364–376. [\[CrossRef\]](#)
25. Sleep, N.H.; Bird, D.K.; Pope, E.C. Serpentinite and the Dawn of Life. *Philos. Trans. R. Soc. B* **2011**, *366*, 2857–2869. [\[CrossRef\]](#)
26. McCollom, T.M.; Seewald, J.S. Serpentinites, Hydrogen, and Life. *Elements* **2013**, *9*, 129–134. [\[CrossRef\]](#)
27. Müntener, O. Serpentine and Serpentinization: A Link between Planet Formation and Life. *Geology* **2010**, *38*, 959–960. [\[CrossRef\]](#)
28. Arndt, N.T.; Nisbet, E.G. Processes on the Young Earth and the Habitats of Early Life. *Annu. Rev. Earth Planet Sci.* **2012**, *40*, 521–549. [\[CrossRef\]](#)
29. Stüeken, E.E.; Anderson, R.E.; Bowman, J.S.; Brazelton, W.J.; Colangelo-Lillis, J.; Goldman, A.D.; Som, S.M.; Baross, J.A. Did Life Originate from a Global Chemical Reactor? *Geobiology* **2013**, *11*, 101–126. [\[CrossRef\]](#) [\[PubMed\]](#)
30. Schrenk, M.O.; Brazelton, W.J.; Lang, S.Q. Serpentinization, Carbon, and Deep Life. *Rev. Miner. Geochem.* **2013**, *75*, 575–606. [\[CrossRef\]](#)
31. Evans, B.W.; Hattori, K.; Baronnet, A. Serpentinite: What, Why, Where? *Elements* **2013**, *9*, 99–106. [\[CrossRef\]](#)
32. Kelley, D.S. A Serpentinite-Hosted Ecosystem: The Lost City Hydrothermal Field. *Science* **2005**, *307*, 1428–1434. [\[CrossRef\]](#)
33. Shibuya, T.; Komiya, T.; Nakamura, K.; Takai, K.; Maruyama, S. Highly Alkaline, High-Temperature Hydrothermal Fluids in the Early Archean Ocean. *Precambrian Res.* **2010**, *182*, 230–238. [\[CrossRef\]](#)
34. Golding, S.D.; Duck, L.J.; Young, E.; Baublys, K.A.; Glikson, M.; Kamber, B.S. Earliest Seafloor Hydrothermal Systems on Earth: Comparison with Modern Analogues. In *Earliest Life on Earth: Habitats, Environments and Methods of Detection*; Golding, S.D., Glikson, M., Eds.; Springer Netherlands: Dordrecht, The Netherlands, 2011; pp. 15–49.
35. Shibuya, T.; Yoshizaki, M.; Sato, M.; Shimizu, K.; Nakamura, K.; Omori, S.; Suzuki, K.; Takai, K.; Tsunakawa, H.; Maruyama, S. Hydrogen-Rich Hydrothermal Environments in the Hadean Ocean Inferred from Serpentinization of Komatiites at 300 °C and 500 Bar. *Prog. Earth Planet. Sci.* **2015**, *2*, 46. [\[CrossRef\]](#)
36. Corliss, J.B.; Baross, J.A.; Hoffman, S.E. An Hypothesis Concerning the Relationships between Submarine Hot Springs and the Origin of Life on Earth. *Oceanol. Acta Spec. Issue* **1981**.
37. Baross, J.A.; Hoffman, S.E. Submarine Hydrothermal Vents and Associated Gradient Environments as Sites for the Origin and Evolution of Life. *Orig. Life Evol. Biosph.* **1985**, *15*, 327–345. [\[CrossRef\]](#)
38. Holm, N.G.; Dumont, M.; Ivarsson, M.; Konn, C. Alkaline Fluid Circulation in Ultramafic Rocks and Formation of Nucleotide Constituents: A Hypothesis. *Geochem. Trans.* **2006**, *7*, 1–7. [\[CrossRef\]](#)
39. Holm, N.G.; Neubeck, A. Reduction of Nitrogen Compounds in Oceanic Basement and Its Implications for HCN Formation and Abiotic Organic Synthesis. *Geochem. Trans.* **2009**, *10*, 1–11. [\[CrossRef\]](#) [\[PubMed\]](#)
40. Rimmer, P.B.; Shorttle, O. Origin of Life's Building Blocks in Carbon- and Nitrogen-Rich Surface Hydrothermal Vents. *Life* **2019**, *9*, 12. [\[CrossRef\]](#)
41. Toner, J.D.; Catling, D.C. Alkaline Lake Settings for Concentrated Prebiotic Cyanide and the Origin of Life. *Geochim. Cosmochim. Acta* **2019**, *260*, 124–132. [\[CrossRef\]](#)

42. Milesi, V.; McCollom, T.M.; Guyot, F. Thermodynamic Constraints on the Formation of Condensed Carbon from Serpentinization Fluids. *Geochim. Cosmochim. Acta* **2016**, *189*, 391–403. [[CrossRef](#)]
43. Milesi, V.; Guyot, F.; Brunet, F.; Richard, L.; Recham, N.; Benedetti, M.; Dairou, J.; Prinzhofer, A. Formation of CO₂, H₂ and Condensed Carbon from Siderite Dissolution in the 200–300°C Range and at 50MPa. *Geochim. Cosmochim. Acta* **2015**, *154*, 201–211. [[CrossRef](#)]
44. Sforza, M.C.; Brunelli, D.; Pisapia, C.; Pasini, V.; Malferrari, D.; Ménez, B. Abiotic Formation of Condensed Carbonaceous Matter in the Hydrating Oceanic Crust. *Nat. Commun.* **2018**, *9*, 1–8. [[CrossRef](#)]
45. Burcar, B.T.; Barge, L.M.; Trail, D.; Watson, E.B.; Russell, M.J.; McGown, L.B. RNA Oligomerization in Laboratory Analogues of Alkaline Hydrothermal Vent Systems. *Astrobiology* **2015**, *15*, 509–522. [[CrossRef](#)]
46. Villafañe-Barajas, S.A.; Ruiz-Bermejo, M.; Rayo-Pizarroso, P.; Colín-García, M. Characterization of HCN-Derived Thermal Polymer: Implications for Chemical Evolution. *Processes* **2020**, *8*, 968. [[CrossRef](#)]
47. Villafañe-Barajas, S.A.; Colín-García, M.; Negrón-Mendoza, A.; Ruiz-Bermejo, M. An Experimental Study of the Thermolysis of Hydrogen Cyanide: The Role of Hydrothermal Systems in Chemical Evolution. *Int. J. Astrobiol.* **2020**, 1–10. [[CrossRef](#)]
48. Hortal, L.; Pérez-Fernández, C.; de la Fuente, J.L.; Valles, P.; Mateo-Martí, E.; Ruiz-Bermejo, M. A Dual Perspective on the Microwave-Assisted Synthesis of HCN Polymers towards the Chemical Evolution and Design of Functional Materials. *Sci. Rep.* **2020**, *10*, 1–14. [[CrossRef](#)]
49. Sanchez, R.A.; Ferris, J.P.; Orgel, L.E. Studies in Prebiotic Synthesis. II. Synthesis of Purine Precursors and Amino Acids from Aqueous Hydrogen Cyanide. *J. Mol. Biol.* **1967**, *30*, 223–253. [[PubMed](#)]
50. Ferris, J.P.; Donner, D.B.; Lotz, W. Chemical Evolution. IX. Mechanism of the Oligomerization of Hydrogen Cyanide and Its Possible Role in the Origins of Life. *J. Am. Chem. Soc.* **1972**, *94*, 6968–6974. [[CrossRef](#)] [[PubMed](#)]
51. Ferris, J.P.; Edelson, E.H. Chemical Evolution. 31. Mechanism of the Condensation of Cyanide to Hydrogen Cyanide Oligomers. *J. Org. Chem.* **1978**, *43*, 3989–3995. [[CrossRef](#)]
52. Miyakawa, S.; Cleaves, H.J.; Miller, S.L. The Cold Origin of Life: A. Implications Based on the Hydrolytic Stabilities of Hydrogen Cyanide and Formamide. *Orig. Life Evol. Biosph.* **2002**, *32*, 195–208. [[CrossRef](#)]
53. Marin-Yaseli, M.R.; Moreno, M.; de la Fuente, J.L.; Briones, C.; Ruiz-Bermejo, M. Experimental Conditions Affecting the Kinetics of Aqueous HCN Polymerization as Revealed by UV-Vis Spectroscopy. *Spectrochim. Acta A* **2018**, *191*, 389–397. [[CrossRef](#)] [[PubMed](#)]
54. Fernández, A.; Ruiz-Bermejo, M.; José, L. Modelling the Kinetics and Structural Property Evolution of a Versatile Reaction: Aqueous HCN Polymerization. *Phys. Chem. Chem. Phys.* **2018**, *20*, 17353–17366. [[CrossRef](#)]
55. Mas, I.; de la Fuente, J.L.; Ruiz-Bermejo, M. Temperature Effect on Aqueous NH₄CN Polymerization: Relationship between Kinetic Behaviour and Structural Properties. *Eur. Polym. J.* **2020**, *132*, 109719. [[CrossRef](#)]
56. Ferris, J.P.; Edelson, E.H.; Mount, N.M.; Sullivan, A.E. The Effect of Clays on the Oligomerization of HCN. *J. Mol. Biol.* **1979**, *13*, 317–330. [[CrossRef](#)] [[PubMed](#)]
57. Boclair, J.W.; Braterman, P.S.; Brister, B.D.; Jiang, J.; Lou, S.; Wang, Z.; Yarberr, F. Cyanide self-addition, controlled adsorption, and other processes at layered double hydroxides. *Orig. Life Evol. Biosph.* **2001**, *31*, 53–69. [[CrossRef](#)] [[PubMed](#)]
58. Negrón-Mendoza, A.; Ramos-Bernal, S.; Cruz, E.; Juárez, J.M. Radiolysis of HCN in Heterogeneous Phase. *Radiat. Phys. Chem.* **2001**, *61*, 771–772. [[CrossRef](#)]
59. Toh, R.J.; Evans, R.; Thissen, H.; Voelcker, N.H.; d’Ischia, M.; Ball, V. Deposition of Aminomalononitrile-Based Films: Kinetics, Chemistry, and Morphology. *Langmuir* **2019**, *35*, 9896–9903. [[CrossRef](#)] [[PubMed](#)]
60. González-Mancera, G.; Ortega-Gutiérrez, F.; Proenza, J.A.; Atudorei, V. Petrology and Geochemistry of Tehuiztzingo Serpentinites (Acatlán Complex, SW Mexico). *Bol. Soc. Geol. Mex.* **2009**, *61*, 419–435. [[CrossRef](#)]
61. Rucklidge, J.C.; Zussman, J. The Crystal Structure of the Serpentine Mineral, Lizardite Mg₃Si₂O₅(OH)₄. *Acta Cryst.* **1965**, *19*, 381–389. [[CrossRef](#)]
62. Mellini, M. Crystal Structure of Lizardite 1T. *Acta Cryst. Sect. A Found. Crystallogr.* **1981**, *37*, C189. [[CrossRef](#)]
63. Zheng, S.M.; Wang, K.M. Preparation and Characterization of Lizardite. *AMM* **2014**, *556–562*, 109–112. [[CrossRef](#)]
64. Carmignano, O.R.D.; Vieira, S.S.; Brandão, P.R.G.; Bertoli, A.C.; Lago, R.M. Serpentinites: Mineral Structure, Properties and Technological Applications. *J. Braz. Chem. Soc.* **2020**, *31*, 2–14. [[CrossRef](#)]
65. Chastain, J.; King, R.C., Jr. Handbook of X-Ray Photoelectron Spectroscopy. *Perkin-Elmer Corp.* **1992**, *40*, 221.
66. Ferris, J.P.; Wos, J.D.; Nooner, D.W.; Oró, J. Chemical Evolution: XXI. The Amino Acids Released on Hydrolysis of HCN Oligomers. *J. Mol. Evol.* **1974**, *3*, 225–231. [[CrossRef](#)]
67. Rivero Crespo, M.A.; Pereira Gómez, D.; Villa García, M.V.; Gallardo Amores, J.M.; Sánchez Escribano, V. Characterization of Serpentinites from Different Regions by Transmission Electron Microscopy, X-ray Diffraction, BET Specific Surface Area and Vibrational and Electronic Spectroscopy. *Fibers* **2019**, *7*, 47. [[CrossRef](#)]
68. de la Fuente, J.L.; Ruiz-Bermejo, M.; Nna-Mvondo, D.; Minard, R.D. Further Progress into the Thermal Characterization of HCN Polymers. *Polym. Degrad. Stab.* **2014**, *110*, 241–251. [[CrossRef](#)]
69. Ruiz-Bermejo, M.; José, L.; Marin-Yaseli, M.R. The Influence of Reaction Conditions in Aqueous HCN Polymerization on the Polymer Thermal Degradation Properties. *J. Anal. Appl. Pyrolysis.* **2017**, *124*, 103–112. [[CrossRef](#)]
70. de la Fuente, J.L.; Ruiz-Bermejo, M.; Menor-Salván, C.; Osuna-Esteban, S. Thermal Characterization of HCN Polymers by TG-MS, TG, DTA and DSC Methods. *Polym. Degrad. Stab.* **2011**, *96*, 943–948. [[CrossRef](#)]

71. Ruiz-Bermejo, M.; de la Fuente, J.L.; Rogero, C.; Menor-Salván, C.; Osuna-Esteban, S.; Martín-Gago, J.A. New Insights into the Characterization of ‘Insoluble Black HCN Polymers. *Chem. Biodivers.* **2012**, *9*, 25–40. [[CrossRef](#)] [[PubMed](#)]
72. Ruiz-Bermejo, M.; José, L.; Carretero-González, J.; García-Fernández, L.; Aguilar, M.R. A Comparative Study on HCN Polymers Synthesized by Polymerization of NH_4CN or Diaminomaleonitrile in Aqueous Media: New Perspectives for Prebiotic Chemistry and Materials Science. *Chem. Eur. J.* **2019**, *25*, 11437–11455. [[CrossRef](#)]
73. Viti, C. Serpentine Minerals Discrimination by Thermal Analysis. *Am. Min.* **2010**, *95*, 631–638. [[CrossRef](#)]
74. Dlugogorski, B.Z.; Balucan, R.D. Dehydroxylation of Serpentine Minerals: Implications for Mineral Carbonation. *Renew. Sustain. Energy Rev.* **2014**, *31*, 353–367. [[CrossRef](#)]
75. Hršak, D.; Sučik, G.; Lazić, L. The Thermophysical Properties of Serpentinite. *Metalurgija* **2008**, *47*, 29–31.
76. Cataldo, F.; Lilla, E.; Ursini, O.; Angelini, G. TGA–FT-IR Study of Pyrolysis of Poly (Hydrogen Cyanide) Synthesized from Thermal Decomposition of Formamide. Implications in Cometary Emissions. *J. Anal. Appl. Pyrol.* **2010**, *87*, 34–44. [[CrossRef](#)]
77. Schulze, R.K.; Hill, M.A.; Field, R.D.; Papin, P.A.; Hanrahan, R.J.; Byler, D.D. Characterization of Carbonated Serpentine Using XPS and TEM. *Energ. Convers. Manag.* **2004**, *45*, 3169–3179. [[CrossRef](#)]
78. Ruiz-Bermejo, M.; Menor-Salván, C.; Mateo-Martí, E.; Osuna-Esteban, S.; Martín-Gago, J.Á.; Veintemillas-Verdaguer, S. $\text{CH}_4/\text{N}_2/\text{H}_2$ Spark Hydrophilic Tholins: A Systematic Approach to the Characterization of Tholins. *Icarus* **2008**, *198*, 232–241. [[CrossRef](#)]
79. Ruiz-Bermejo, M.; Menor-Salván, C.; de la Fuente, J.L.; Mateo-Martí, E.; Osuna-Esteban, S.; Martín-Gago, J.Á.; Veintemillas-Verdaguer, S. $\text{CH}_4/\text{N}_2/\text{H}_2$ -Spark Hydrophobic Tholins: A Systematic Approach to the Characterisation of Tholins. Part II. *Icarus* **2009**, *204*, 672–680. [[CrossRef](#)]
80. Thissen, H.; Koegler, A.; Salwiczek, M.; Easton, C.D.; Qu, Y.; Lithgow, T.; Evans, R.A. Prebiotic-Chemistry Inspired Polymer Coatings for Biomedical and Material Science Applications. *NPG Asia Mater.* **2015**, *7*, e225. [[CrossRef](#)]
81. Ball, V. Antioxidant Activity of Films Inspired by Prebiotic Chemistry. *Mater. Lett.* **2021**, *285*, 129050. [[CrossRef](#)]
82. Little, S.A.; Stolzenbach, K.D.; Von Herzen, R.P. Measurements of Plume Flow from a Hydrothermal Vent Field. *J. Geophys. Res.* **1987**, *92*, 2587–2596. [[CrossRef](#)]
83. Holm, N.G.; Hennes, R.J.-C. Hydrothermal systems: their varieties, dynamics, and suitability for prebiotic chemistry. In *Marine Hydrothermal Systems and the Origin of Life*; Springer: Berlin, Germany, 1992; pp. 15–31.
84. Bemis, K.; Lowell, R.; Farrow, A. Diffuse Flow On and Around Hydrothermal Vents at Mid-Ocean Ridges. *Oceanog* **2012**, *25*, 182–191. [[CrossRef](#)]
85. Borquez, E.; Cleaves, H.J.; Lazcano, A.; Miller, S.L. An Investigation of Prebiotic Purine Synthesis from the Hydrolysis of HCN Polymers. *Orig. Life Evol. Biosph.* **2005**, *35*, 79–90. [[CrossRef](#)]
86. Takahashi, T.; Ido, T.; Hatano, K.; Iwata, R.; Nakanishi, H. Synthesis of 1- ^{11}C -Labeled Fatty Acid from [^{11}C]HCN. *Int. J. Rad. Appl. Instr. A* **1990**, *41*, 649–654. [[CrossRef](#)]
87. Eschenmoser, A. On a Hypothetical Generational Relationship between HCN and Constituents of the Reductive Citric Acid Cycle. *Chem. Biodivers.* **2007**, *4*, 554–573. [[CrossRef](#)]
88. Thissen, H.; Evans, R.A.; Ball, V. Films and Materials Derived from Aminomalononitrile. *Processes* **2021**, *9*, 82. [[CrossRef](#)]
89. González-López, L.A.; Colín-García, M.; Meléndez-López, A.; Cruz-Castañeda, J.; Negrón-Mendoza, A. Prebiotic Experi-Ments Simulating Hydrothermal Vents: Influence of Olivine in the Decomposition of Simple Carboxylic Acids. *Bol. Soc. Geol. Mex* **2021**, in press. [[CrossRef](#)]
90. Herschy, B.; Whicher, A.; Camprubi, E.; Watson, C.; Dartnell, L.; Ward, J.; Evans, J.R.G.; Lane, N. An Origin-of-Life Reactor to Simulate Alkaline Hydrothermal Vents. *J. Mol. Evol.* **2014**, *79*, 213–227. [[CrossRef](#)]
91. Sojo, V.; Herschy, B.; Whicher, A.; Camprubi, E.; Lane, N. The Origin of Life in Alkaline Hydrothermal Vents. *Astrobiology* **2016**, *16*, 181–197. [[CrossRef](#)] [[PubMed](#)]
92. Camprubi, E.; de Leeuw, J.W.; House, C.H.; Raulin, F.; Russell, M.J.; Spang, A.; Tirumalai, M.R.; Westall, F. The Emergence of Life. *Space Sci. Rev.* **2019**, *215*, 56. [[CrossRef](#)]
93. Damer, B.; Deamer, D. The Hot Spring Hypothesis for an Origin of Life. *Astrobiology* **2020**, *20*, 429–452. [[CrossRef](#)]
94. Duval, S.; Branscomb, E.; Trolard, F.; Bourrié, G.; Grauby, O.; Heresanu, V.; Schoepp-Cothenet, B.; Zuchan, K.; Russell, M.J.; Nitschke, W. On the Why’s and How’s of Clay Minerals’ Importance in Life’s Emergence. *Appl. Clay Sci.* **2020**, *195*, 105737. [[CrossRef](#)]
95. Deamer, D. Where Did Life Begin? Testing Ideas in Prebiotic Analogue Conditions. *Life* **2021**, *11*, 134. [[CrossRef](#)]
96. Dass, A.V.; Hickman-Lewis, K.; Brack, A.; Kee, T.P.; Westall, F. Stochastic Prebiotic Chemistry within Realistic Geological Systems. *Chem. Sel.* **2016**, *1*, 4906–4926. [[CrossRef](#)]
97. Konn, C.; Charlou, J.L.; Holm, N.G.; Mousis, O. The Production of Methane, Hydrogen, and Organic Compounds in Ultramafic-Hosted Hydrothermal Vents of the Mid-Atlantic Ridge. *Astrobiology* **2015**, *15*, 381–399. [[CrossRef](#)]
98. McDermott, J.M.; Seewald, J.S.; German, C.R.; Sylva, S.P. Pathways for Abiotic Organic Synthesis at Submarine Hydrothermal Fields. *Proc. Natl. Acad. Sci. USA* **2015**, *112*, 7668–7672. [[CrossRef](#)] [[PubMed](#)]
99. Yang, Q.; Peng, P.; Xiang, Z. Covalent Organic Polymer Modified TiO_2 Nanosheets as Highly Efficient Photocatalysts for Hydrogen Generation. *Chem. Eng. Sci.* **2017**, *162*, 33–40. [[CrossRef](#)]
100. Eschenmoser, A. The Search for the Chemistry of Life’s Origin. *Tetrahedron* **2007**, *63*, 12821–12844. [[CrossRef](#)]

101. Budin, I.; Bruckner, R.J.; Szostak, J.W. Formation of protocell-like vesicles in a thermal diffusion column. *J. Am. Chem. Soc.* **2009**, *131*, 9628–9629. [[CrossRef](#)]
102. Namani, T.; Deamer, D.W. Stability of model membranes in extreme environments. *Orig. Life Evol. Biosph.* **2008**, *38*, 329–341. [[CrossRef](#)]
103. Kim, E.-K.; Martin, V.; Krishnamurthy, R. Orotidine-containing RNA: Implications for the hierarchical selection (systems chemistry emergence) of RNA. *Chem. Eur. J.* **2017**, *23*, 12668–12675. [[CrossRef](#)]
104. Krishnamurthy, R. Life's biological chemistry: A destiny or destination starting from prebiotic chemistry? *Chem. Eur. J.* **2018**, *24*, 16708–16715. [[CrossRef](#)] [[PubMed](#)]
105. Yadav, M.; Kumar, R.; Krishnamurthy, R. Chemistry of abiotic nucleotide synthesis. *Chem. Rev.* **2020**, *120*, 4766–4805. [[CrossRef](#)] [[PubMed](#)]
106. Maistralis, G.; Koutsodimou, A.; Katsaros, N. Transition metal orotic acid complexes. *Transit. Met. Chem.* **2000**, *25*, 166–173. [[CrossRef](#)]

Estabilidad y reactividad de las moléculas orgánicas

Polimerización de aminoácidos en sistemas hidrotermales

Ensayos de Química Prebiótica IV

Resumen Aunque varios experimentos han demostrado que la formación de oligopéptidos es posible en entornos primitivos, existen dudas sobre la selectividad en la sorción y polimerización de aminoácidos. En el presente estudio, reportamos la evolución del sistema (Ala + Glu) / SiO₂ en condiciones hidrotermales submarinas (*HT, por sus siglas en inglés*) y subaéreas (*DA, por sus siglas en inglés*). Después de los tratamientos en altas presiones y temperaturas así como por activación seca, es posible una serie de condensaciones peptídicas entre los AAs. El análisis de XRD y TG permitió entender la interacción de los AAs con la superficie mineral. El análisis ESI-MS muestra la formación de algunos oligómeros después de los tratamientos térmicos secos e hidrotermales. Los resultados sugieren que los sistemas hidrotermales, tanto submarinos como subaéreos, tendrían un papel importante en la formación de precursores de oligopéptidos.

Polimerización de aminoácidos en escenarios hidrotermales: Ensayos de química prebiótica

Estancia de Investigación

Study of amino acids polymerization under HV conditions scenario: A prebiotic chemistry experiment. Asesor, Dr. Jean-François Lambert. Sorbonne Universités, UPMC Univ Paris 2018-2020.

Introducción

Diversos experimentos han demostrado que existe una gran diversidad de mecanismos que pueden participar en la síntesis de aminoácidos (AAs) bajo posibles condiciones primitivas (Miller 1953; Rode 1999; Muñoz Caro *et al.* 2002; Huber y Wachtershauser 2006; Aubrey *et al.* 2009; Burton *et al.* 2012; Ruiz-Bermejo *et al.* 2013). Sin embargo, aún no es claro cómo estas moléculas orgánicas podrían interactuar entre ellas y, bajo qué condiciones podrían dar lugar a la formación de largos oligopéptidos lineales y, eventualmente, a un "Mundo de péptidos/proteínas" (Wieland y Bodanszky 1991; Plankensteiner *et al.* 2005). Por lo tanto, la síntesis de oligopéptidos es uno de los grandes retos de la química prebiótica (Danger *et al.* 2012). Por ello, es necesario proponer escenarios primitivos complejos en donde este tipo de reacciones se favorezcan (Hazen y Sverjensky 2010).

Sistemas hidrotermales

Los sistemas hidrotermales, tanto subaéreos como submarinos, brindan un amplio espectro de variables geoquímicas (*e.g.*, gradientes térmicos y de pH, fluidos, sales disueltas, varias fuentes de energía, disponibilidad de elementos y minerales, así como estructuras porosas; Cleaves 2013; Deamer y Georgiou 2015; Colín-García *et al.* 2016, 2018; Van Kranendonk *et al.* 2017; Westall *et al.* 2018) que pueden favorecer la elongación de aminoácidos (Tabla 6.1). Sin embargo, aunque la formación del enlace peptídico se favorece a altas temperaturas, las reacciones de dimerización, ciclación y descomposición no deben ser subestimadas (Cleaves *et al.* 2009). En consecuencia, es necesario estudiar a detalle cada ambiente hidrotermal para definir cuáles son las condiciones favorables para las reacciones de polimerización (Deamer y Georgiou 2015; Omran y Pasek 2020).

Polimerización de aminoácidos en condiciones hidrotermales

La formación de enlaces peptídicos a partir de α -aminoácidos no activados no es espontánea en disolución acuosa y al equilibrio; la reacción de hidrólisis se ve favorecida, sobre la de síntesis de oligómeros (Benoiton 2016). Se han propuesto al menos tres escenarios de reacciones de condensación para resolver este problema: I) condensación a partir de calentamiento directo de

aminoácidos; II) la existencia de sistemas heterogéneos, considerando minerales; y III) la presencia de agentes de condensación en disolución homogénea (Rode 1999; Cleaves *et al.* 2009). A excepción de los experimentos que consideran los agentes de condensación, la mayoría de las simulaciones utilizan condiciones de deshidratación (Pascal *et al.* 2005; Danger *et al.* 2012). Por otro lado, algunos experimentos han destacado el papel de las superficies minerales en la formación del enlace peptídico. Los minerales pueden proporcionar condiciones de deshidratación al secarse, resolviendo el problema termodinámico; también pueden actuar como catalizadores en la formación del enlace amida (Bujdák *et al.* 1996; Lambert 2008; Shanker *et al.* 2012; Iqbal *et al.* 2017; Rimola *et al.* 2018).

Aunque se han considerado algunas secuencias de aminoácidos preferenciales en sistemas binarios (*e.g.*, Glu-Gly) (Harada y Fox 1958; Fox *et al.* 1959; Fox y Harada 1960; Rode 1999; Higgs y Pudritz 2009), solo unos pocos experimentos han utilizado mezclas de AAs para examinar la selectividad de dichas combinaciones en los procesos de sorción y polimerización (Hartmann *et al.* 1981; Jaber *et al.* 2014; Sakhno *et al.* 2018, Bedoin *et al.* 2020). En esta serie de experimentos, consideramos el sistema binario alanina (Ala, A) + ácido glutámico (Glu, E) debido a que estos aminoácidos tienen una relevancia significativa en estudios de química prebiótica. Por ejemplo, el Glu puede tener un papel crucial en la copolimerización de aminoácidos mixtos en la síntesis de péptidos lineales (*i.e.*, presencia de ácido piroglutámico (PyroGlu) en la posición N-terminal en poliaminoácidos). Además, ambos aminoácidos son de los productos más comunes en experimentos prebióticos (Harada y Fox, 1958; Fox y Harada, 1960; Harada y Fox 1965; Melius y Hubbard, 1987; Zaia *et al.* 2008; Higgs y Pudritz, 2009).

Diversos experimentos han demostrado que la Ala y el Glu, se descomponen en condiciones hidrotermales por medio de mecanismos de descarboxilación, desaminación, transaminación y en el caso del Glu por la apertura del anillo para generar productos no-proteicos (Bada *et al.* 1995; Andersson y Holm, 2000; Islam *et al.* 2003; Abdelmoez *et al.* 2007; Klingler *et al.* 2007; Kibet *et al.* 2013) (Tabla 6.1). Sin embargo, otros mecanismos, como la dimerización de aminoácidos, la formación de un anhídrido cíclico y el alargamiento de la cadena peptídica son posibles (Faisal *et al.* 2005). De acuerdo con esto, algunos experimentos han evidenciado que es posible formar oligómeros lineales a partir de aminoácidos simples (*e.g.*, decámeros), aunque la formación de dicetopiperazinas (DKP), por dimerización y posterior ciclación, es la vía preferencial (Bujdák *et al.* 1996; Alargov *et al.* 2002; Islam *et al.* 2003; Cox y Seward 2007; Lemke *et al.* 2009; Cleaves *et al.* 2009; Sakata *et al.* 2010; Otake *et al.* 2011).

Tabla 6.1. Resumen de estudios experimentales en condiciones hidrotermales submarinas (HT) y subaéreas (DA) que incluyen a los aminoácidos alanina y ácido glutámico.

Aminoácido	Condiciones	Oligómeros formados	Notas	Referencia
AAs con Glu	DA. Tubo calentado en baño de aceite a 175-180 °C.	Glu se co-polimeriza en DKP o en forma lineal con otros AAs.	La propiedad ácida de Glu puede ser importante en la polimerización (<i>i.e.</i> , formación de enlaces amida catalizada por protones).	Harada y Fox 1958
Ala-Glu con mezclas de AAs	DA. En ausencia de H ₂ O a 180-190 °C por varias horas. Matraz en baño de aceite. Atmósfera libre de O ₂ .	Formación de oligómeros.	Pyro Glu podría estar presente en las posiciones N-terminales. Enlaces por puente de H en el producto Glu-Pyro Glu.	Phillips y Melius 1974
Glu mezclado con AAs (Gly y Tyr)	DA. Baño de aceite bajo corriente de nitrógeno a 180 °C durante 24 h.	Formación de trímeros and DKP.	Formación de tripéptidos (<i>i.e.</i> Pyro Glu-Tyr-Gly) y péptidos de mayor peso molecular no identificados. Formación preferencial de compuestos heterocíclicos (<i>i.e.</i> piroglutamidipéptidos).	Hartmann <i>et al.</i> 1981
Ala	HT. 90-250°C Buffer de fosfatos pH 7.	---	La descarboxilación de Ala produce etilamina. Ala es destruida irreversiblemente.	Bada <i>et al.</i> 1995
Glu/Ala	HT. Tubo de vidrio Pyrex en autoclave a 80 atm 200-350 °C 2 h. Atmósfera de H ₂ .	Formación de compuestos resistentes al calor (DKP y / o polímeros más complicados).	Los AAs se descomponen pero es posible la formación de compuestos resistentes al calor. PyroGlu es la especie más predominante. Glu se descompone en Gly y Ala. La descomposición es menor en un atm de H ₂ .	Kohara <i>et al.</i> 1997
Ala	HT. 200 °C y 50 bar en autoclave recubierta de teflón (48 h). Minerales sintéticos.	---	Descomposición de Ala por medio de la reacción de descarboxilación y liberación de CO ₂ y etilamina.	Andersson y Holm 2000
Glu-AAs	HT. Soluciones acuosas de AAs a 200–350 °C por 2 minutos a 25 MPa. Reactor de flujo (agua supercrítica).	---	El ácido glutámico es más estable que otros AA debido a la formación de PyroGlu.	Islam <i>et al.</i> 2003
Ala	HT. Reactor tubular de flujo continuo a 300 °C y 20 MPa.	---	Ala es descompuesta principalmente en ácidos orgánicos (<i>e.g.</i> , ácido láctico , ácido pirúvico) Glu es el AAs más estable.	Sato <i>et al.</i> 2004
Ala, Glu	HT. 230-290°C, 2.8-7.4 MPa. 40 min de calentamiento. 35 mM de K ⁺ a pH 6.2. Reactor discontinuo.	---	La mayoría de los aminoácidos son lábiles a pH ácido y natural. Son más estables a pH muy básico debido que están en su forma ionizada.	Abdelmoez <i>et al.</i> 2007
Ala	HT. Reactor continuo de alta presión con una disolución de alimentación de 1.0 y 2.0% (gg ⁻¹) de AAs a 250–450 °C, 24–34 MPa y tiempos de exposición de 2.5–35 s.	---	Descomposición térmica de Ala a 300–450°C y 34 MPa, 2.5–35 s. Formación de una mezcla de ácido láctico y etilamina.	Klingler <i>et al.</i> 2007
Ala	HT. 120-165°C y 20 bar en un reactor inerte.	Dimerización y posterior ciclización.	α -alanina y la β -alanina preferentemente se dimerizan y posteriormente se ciclan.	Cox y Seward 2007
Ala	DA. Muestra sólida de AAs calentada a 180–400°C en altas	Oligómeros largos (<i>i.e.</i> , decámeros) a	A temperaturas moderadas (<i>e.g.</i> , 100-150 °C) es posible la producción de	Otake <i>et al.</i> , 2011

	presiones (1.0–5.5 GPa). Prensa hidráulica.	temperaturas baja y con tiempos de reacción prolongados (<i>i.e.</i> , 32 días).	péptidos más largos cuando se prolonga el tiempo de reacción. Los péptidos de Ala se descomponen más lentamente que los péptidos de Gly a 250 °C. La desaminación y las altas presiones aplicadas podrían ser el proceso clave que determina la estabilidad de aminoácidos y péptidos.	
Ala	HT. Los óxidos se impregnaron con una solución acuosa de AA 0.01-0.1 M. Las muestras se calentaron a tres temperaturas (<i>i.e.</i> , 50 °C, 90 °C y 120 °C) durante 1-35 días.	Ciclo (Ala) ₂ y Ala ₍₂₎ lineal.	A 120 °C, la ciclación de Ala ₍₂₎ en DKP es mucho más favorable que el alargamiento de la cadena peptídica. La superficie de los óxidos de hierro (<i>i.e.</i> , la acidez de los grupos hidroxilo de la superficie) puede promover la formación de oligopéptidos.	Shanker <i>et al.</i> 2012
Glu-Arg	DA. 2 h a 200 °C. Montmorillonita.	Formación de DKP o especies cíclicas (<i>e.g.</i> ciclo (Arg-Arg-Glu).	Formación de oligopéptidos (condensación heterogénea entre Glu y Arg).	Jaber <i>et al.</i> 2014
Ala	HT. Soluciones saturadas de Ala a 25 °C, 5-11GPa. Prensa toroidal.	Oligómeros.	La presión puede inducir la formación de péptidos al reducir la distancia intermolecular de las moléculas de Ala vecinas. La oligomerización de Ala ocurrió a > 5 Pa incluso a 25 °C.	Fujimoto <i>et al.</i> 2015
Glu-Leu	DA. Las muestras fueron sorbidas en sílice y activadas en un horno tubular (rampa lineal de temperatura 5 °C min ⁻¹).	Alta rendimiento en la formación de oligómeros lineales.	El producto principal es el dímero cíclico DKP. Sin embargo, el sistema Glu + Leu/SiO ₂ produce oligómeros lineales, al menos hasta hexámeros. El PyroGlu puede ser un paso crucial para iniciar la formación de cadenas lineales.	Sakhno <i>et al.</i> 2018
Ala/Glu	HT. P3m con AAs en solución acuosa a a 35 °C por 7 días.	Dipéptidos lineales.	El trimetafosfato (P _{3m}) puede favorecer la formación de dipéptidos y no favorece las formas heterocíclicas.	Ying <i>et al.</i> 2018

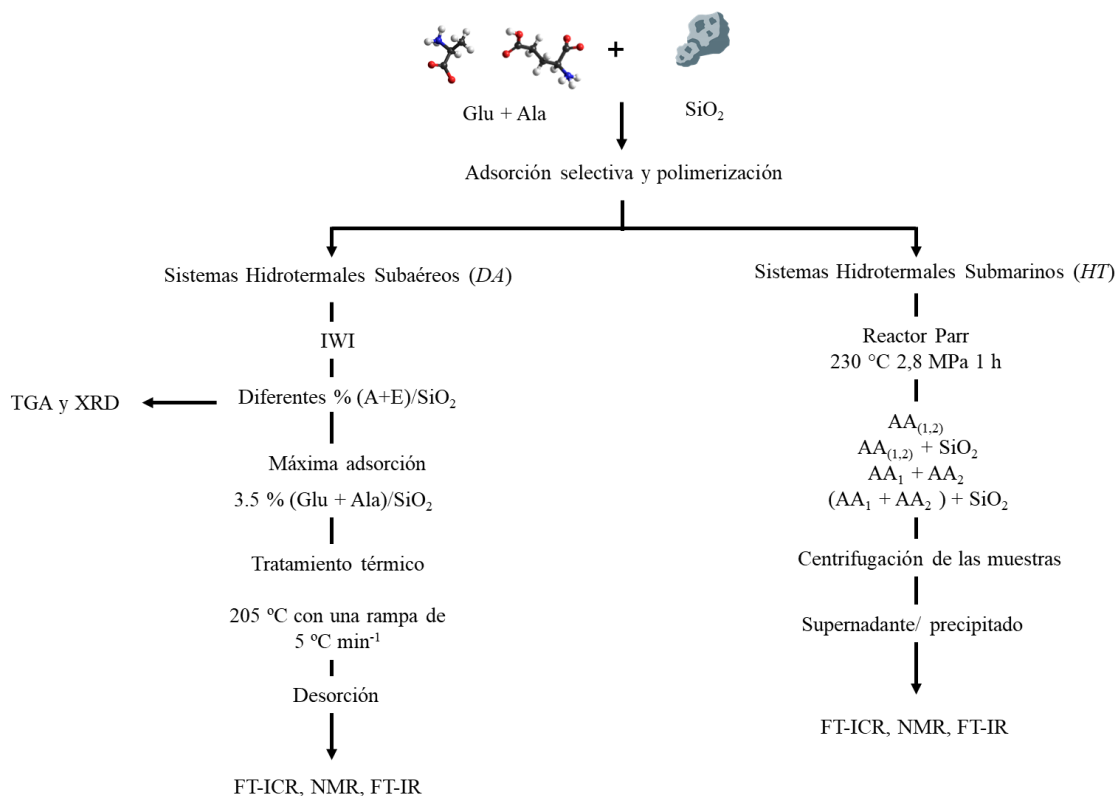
Nota: **Ala** Alanina **Glu** Ácido glutámico **Gly** Glicina **Tyr** Tirosina **Leu** Leucina **DKP** Dicetopiperazinas. Tratamiento por activación seca (*DA*, por sus siglas en inglés), tratamiento hidrotermal submarino (*HT*, por sus siglas en inglés).

El estudiar las condiciones que permiten la interacción entre superficies inorgánicas y moléculas orgánicas considerando escenarios hidrotermales puede ser un punto de partida para entender con mayor profundidad el papel de estos ambientes en la evolución química. De hecho, los escenarios que implican el secado de los aminoácidos adsorbidos, por un lado, y la activación hidrotermal, por el otro, pueden representar dos escenarios posibles en donde se llevaron a cabo reacciones prebióticas, es decir, los sistemas subaéreos y submarinos. Estos entornos pueden considerarse adecuados para el surgimiento de los componentes fundamentales de la vida (*e.g.*, membranas, material genético y metabolismo) porque albergan muchas condiciones interesantes: gradientes térmicos y de pH, fluidos dinámicos, sales disueltas, varias fuentes de energía, disponibilidad de elementos y minerales disueltos, incluidas las estructuras porosas (Cleaves 2013; Deamer y Georgiou 2015; Colín-García *et al.* 2016, 2018; Van Kranendonk *et al.* 2017; Westall *et al.* 2018).

En el presente estudio, se consideró la evolución del sistema (Ala + Glu)/SiO₂, abreviado como (A + E)/SiO₂, en condiciones hidrotermales subaéreas y submarinas, con el fin de determinar algunos signos de selectividad en la sorción y/o en polimerización. Se reporta la formación de algunos oligómeros lineales largos después del tratamiento térmico seco (de ahora en adelante llamado DA por “dry activation”) y tratamiento hidrotermal submarino (llamado HT por “hydrothermal treatment”). En general, nuestros resultados sugieren que las superficies minerales pueden tener un papel importante en la sorción y polimerización de AAs tanto en condiciones secas como acuosas. Discutimos las implicaciones y el posible papel de los ambientes hidrotermales y sus consecuencias para la evolución química.

Procedimiento experimental

Los materiales así como las distintas técnicas de caracterización son descritos en el Capítulo III. La Figura 6.1 muestra el procedimiento experimental general para la elaboración de estos experimentos.



Nota: **IWI** Método de impregnación húmeda incipiente (*Incipient wetness impregnation*), **A₁** Alanina, **A₂** Ácido glutámico, **TGA** Análisis termogravimétrico, **XRD** Difracción de Rayos X, **FT-ICR** Espectrometría de masas por resonancia ion-ciclotrón con transformada de Fourier, **NMR** Resonancia Magnética Nuclear, **FT-IR** Espectroscopía infrarroja por transformada de Fourier.

Figura 6.1. Procedimiento experimental general para estudiar la polimerización de AAs en escenarios hidrotermales. **DA** Tratamiento por activación seca (*DA, por sus siglas en inglés*), **HT** tratamiento hidrotermal submarino (*HT, por sus siglas en inglés*).

Resultados y discusión

Difracción de Rayos X. Con el fin de estimar la cobertura de saturación de la mezcla de aminoácidos en sílice, se prepararon una serie de muestras con cargas crecientes de AAs a partir de disoluciones acuosas a su pH natural (pH ~ 4.8). La Figura 6.2 muestra los difractogramas de las muestras (A + E)/SiO₂ con diferente porcentaje de carga. A partir de una carga del 5 %, es posible identificar algunos picos de Bragg asociados a la Ala y el Glu, significando que a este porcentaje de carga se supera la capacidad de adsorción del SiO₂ (*i.e.*, cobertura de saturación). Es posible asignar los picos visibles a la fase β-ácido glutámico. Esto está en consonancia con la observación de que el ácido glutámico a granel precipita a cargas bastante bajas en sílice, ya sea solo o coadsorbido con otro aminoácido hidrófobo (Tesis Hagop Abadian, Ph.D. Sorbonne Université). Dado que las cargas de hasta el 4 % no muestran picos de los AAs a granel, utilizamos la muestra de 3.5% (A + E)/SiO₂ para llevar a cabo los experimentos de activación térmica. De esta manera, el comportamiento observado se puede asignar a los aminoácidos adsorbidos sin interferencia de las fases a granel. Determinar la concentración máxima de AAs que se puede adsorber en el mineral es crucial para establecer la cantidad de AAs que están directamente interaccionando con la superficie de sílice, o bien cristalizan como cristales a granel (Bouchoucha *et al.* 2011). Sakhno y colaboradores (2018) mostraron que en algunos sistemas de AAs mixtos (*i.e.*, L + E/SiO₂) adsorbidos en sílice, el Glu puede permitir una mejor dispersión de Leu en la superficie a altos porcentajes de carga, mientras que en otros sistemas mixtos (*i.e.*, D + V/SiO₂) mejora la cobertura de saturación en comparación con un sistema de un solo AA.

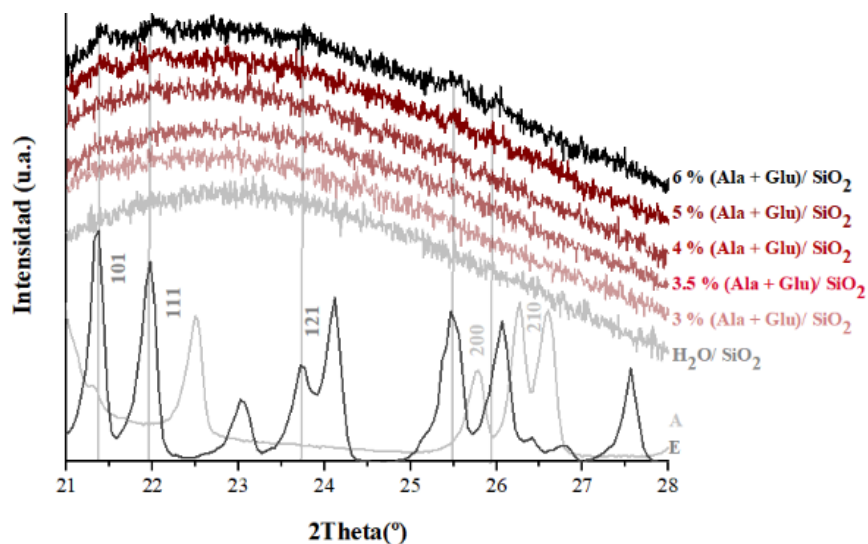


Figura 6.2. Difractogramas de diferentes porcentajes de cargas de (Ala + Glu)/SiO₂. *Nota:* Asignaciones basadas en Moshe *et al.* 2013; Sakhno *et al.* 2018; Vijayan *et al.* 2006.

Análisis térmico. El análisis termogravimétrico es una herramienta valiosa para analizar la activación térmica y la transformación de aminoácidos en péptidos (Bouchoucha *et al.* 2011; Jaber *et al.* 2014; Sakhno *et al.* 2018). Los resultados de la primera derivada de las curvas termogravimétricas (DTG) de las muestras con diferentes cargas de A + E/SiO₂ se muestran en la Figura 6.3. Todos los termogramas exhiben picos bien definidos en tres regiones diferentes: I) < 100 °C; II) 120 - 200 °C; y III) > 200 °C. Como se ha sugerido en otros trabajos, el pico principal a T < 100 °C corresponde a la emisión de agua fisisorbida en el mineral. La señal mal definida en la muestra control del sílice, alrededor de 200 °C, está asociada al proceso progresivo de deshidroxilación (Zhuravlev 2000; Sakhno *et al.* 2018). En las muestras que contienen AAs, se aprecia un pico bien definido a 287 °C que corresponde a la degradación térmica de los aminoácidos y / o péptidos (picos similares se reportaron a 210 °C para el Glu y a 295 °C para la Ala) (Bouchoucha *et al.* 2011; Sakhno *et al.* 2018). Debido a que el Aerosil 380 no exhibe picos entre 100 - 200 °C, los eventos térmicos observados en esta región para las muestras de sorción pueden estar asociados con eventos térmicos de los AAs, es decir, condensación peptídica y la eliminación de moléculas de agua. La señal en este intervalo parece ser compuesta, pero sus componentes no se resolvieron bien en las condiciones elegidas inicialmente.

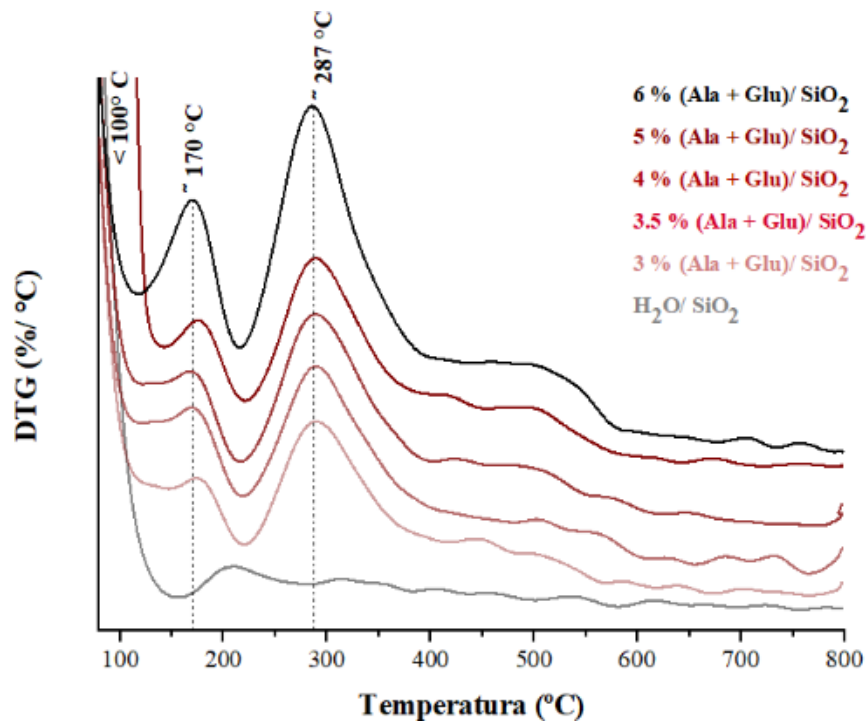


Figura 6.3. Termogramas (DTG) de diferentes porcentajes de cargas de aminoácidos (Ala + Glu)/SiO₂.

Para determinar con mayor precisión los fenómenos asociados a los picos entre los 100-200 °C, realizamos un análisis detallado de la muestra 3.5 % (A + E)/SiO₂ y su respectivo sistema de un solo aminoácido considerando una rampa de temperatura de 1 °C min⁻¹ (Fig. 6.4). Los termogramas muestran una forma global similar a la reportada en trabajos anteriores (Bouchoucha *et al.* 2011; Lambert *et al.* 2013; Jaber *et al.* 2014). Sin embargo, existen diferencias importantes que pueden asociarse con el sistema (A + E)/SiO₂.

El sistema A/SiO₂ exhibe en este intervalo un solo pico a 177 °C. De acuerdo con Lambert *et al.* (2013), este evento térmico puede deberse a la formación del dímero cíclico de la alanina (vía B en la Figura 6.5, segunda línea) El sistema E/SiO₂ tiene un comportamiento más complejo con dos eventos térmicos bien definidos (*i.e.*, 98 °C y otro a 135 °C, Fig. 6.4). El termograma es esencialmente el mismo reportado por Bouchoucha *et al.* (2011). El primer pico puede corresponder a la formación del PyroGlu (anteriormente observado a 110 - 120 °C, pero para una rampa de calentamiento más rápida que debería desplazar los eventos térmicos a temperaturas más altas). Aunque la ciclación interna de Glu a granel a PyroGlu ocurre a temperaturas más altas, como 197 °C (Melius y Yon-Ping Sheng 1975; Nunes y Cavalheiro 2007; Bouchoucha *et al.* 2011), la presencia de sílice puede tener un efecto cinético en la condensación de ácido glutámico (Lambert *et al.* 2009; Rimola *et al.* 2013).

El segundo pico (alrededor de 160 °C en Bouchoucha *et al.* 2011) puede estar relacionado con la formación de PyroGluDKP (Figura 6.5 línea A). Cada uno de estos dos pasos resultaría en la eliminación de un molécula de agua por cada Glu, *i.e.*, una pérdida de peso correspondiente al 24.4 % respecto al peso inicial del ácido glutámico. Experimentalmente, la integración de los dos eventos y la corrección de la contribución de sílice producen una pérdida de peso del 28.8% de Glu inicial; sin embargo, la contribución del primer pico parece ser significativamente menor a la mitad.

El termograma del sistema mixto muestra dos eventos térmicos principales en la región de 100 – 200 °C (Fig. 6.4), con máximos a 103 y 137 °C. El segundo pico es más amplio que el de los aminoácidos individuales, y el patrón global no es demasiado diferente de lo que se esperaría al sumar los termogramas de los aminoácidos adsorbidos individualmente. Sin embargo, la pérdida de peso en esta región es más alta de lo esperado para una pérdida total de dos moléculas de H₂O por AA, en casi la mitad; esto podría significar que la condensación peptídica va acompañada de una sublimación, como se observó para el sistema Gly/SiO₂ (Lambert *et al.* 2013). En particular, el primer pico es casi dos veces más grande de lo que cabría esperar para la transformación Glu → PyroGlu (pérdida de un H₂O por Glu), lo que posiblemente indica que en el sistema mixto la ciclación de Glu es seguida inmediatamente por otras condensaciones.

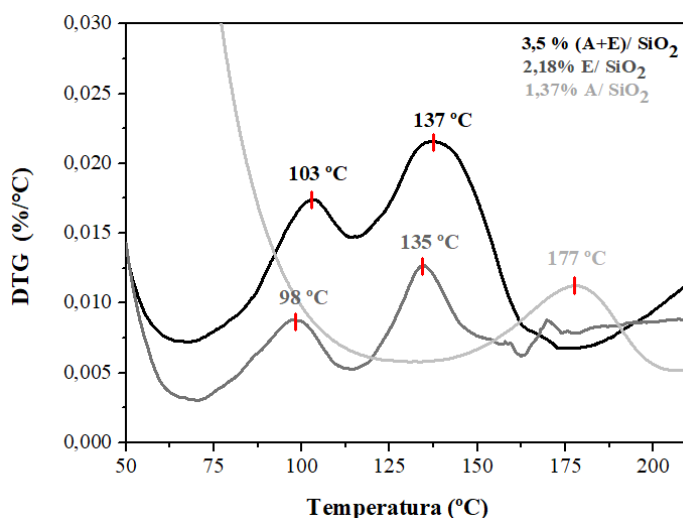


Figura 6.4. Termogramas (DTG) de sistema mixto y sistema con un solo AA.

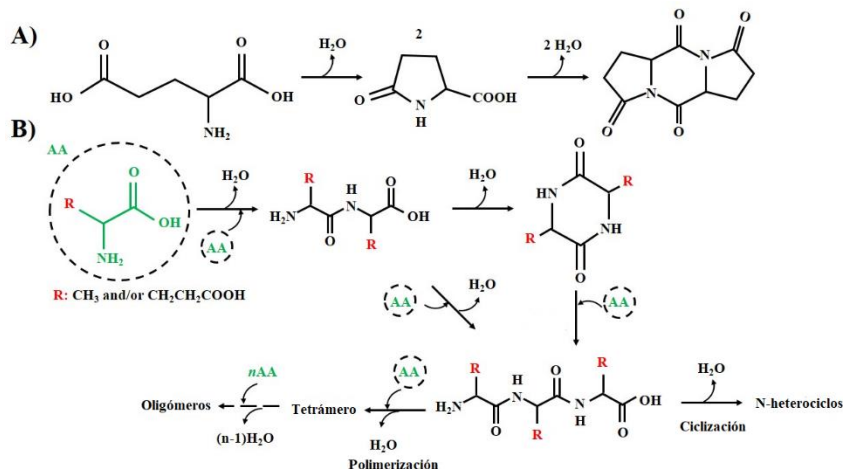


Figura 6.5. Probables reacciones de condensación para la formación de oligómeros y compuestos cíclicos.

Resonancia Magnética Nuclear (NMR, por sus siglas en inglés). La Figura 6.6 muestra la ¹³C NMR de la disolución de alanina después del tratamiento hidrotermal (A HT), comparado con los espectros de varios compuestos de referencia: Ala (A), dímero lineal (A₂) y dímero cíclico (ciclo A₂).

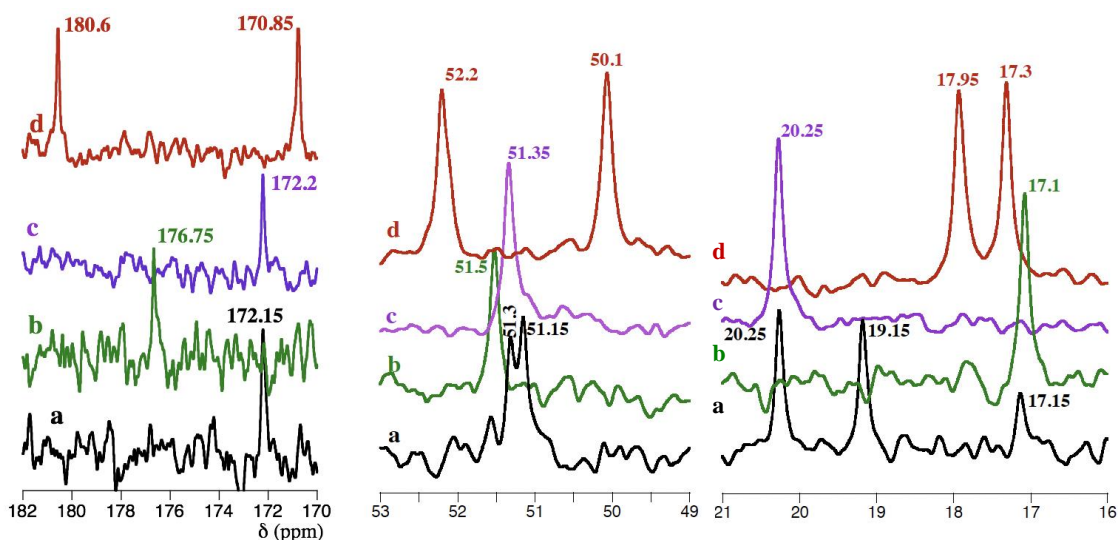


Figura 6.6. Espectro de ¹³C NMR de la disolución A HT (a), comparado con los de los compuestos de referencia (b: alanina, c: ciclo A₂, d: dímero lineal A₂), en las regiones del carbonilo (izquierda), metano (centro) y metilo (derecha).

La muestra A HT solo contiene señales en regiones compatibles con péptidos derivados de alanina (*i.e.*, grupos carbonilo, metino y metilo), lo que indica que el tratamiento hidrotermal puede causar la formación de enlaces peptídicos, pero no reacciones de degradación más profundas. Las señales en las tres regiones muestran que la disolución problema contiene una cantidad significativa de ciclo A₂. En la región del metilo, una cantidad menor (< 25%) de Ala monomérica parece estar todavía presente; la señal correspondiente en el grupo carbonilo no está presente (quizás no es apreciable por el ruido). Las señales características del dímero lineal no se observan en ninguna de las tres regiones, lo que significa que el dímero lineal A₂ no se encuentra entre las especies formadas más importantes. Finalmente, en la región de metilo, no se puede asignar una señal fuerte a +19.15 ppm a ninguna de las tres referencias.

Los espectros de ¹H NMR de la misma muestra y referencias se muestran en la Figura 6.7.

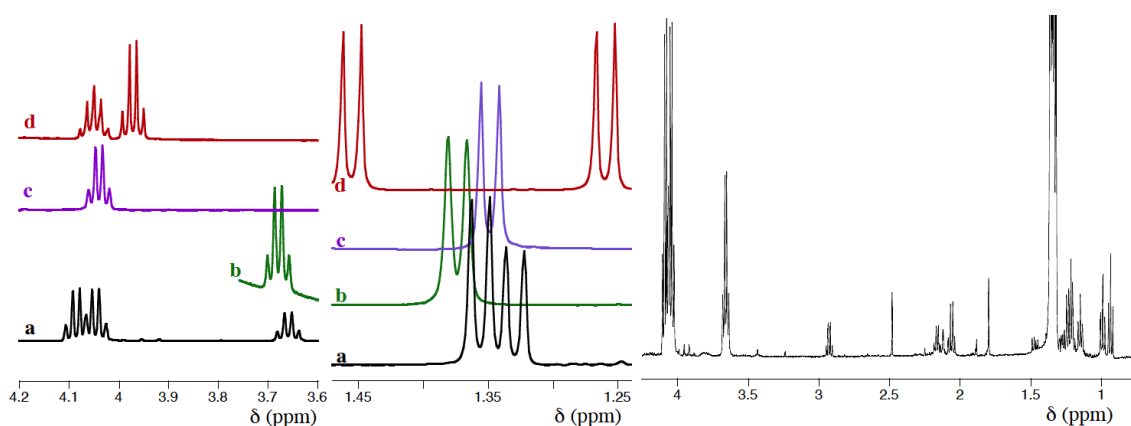


Figura 6.7. Espectro de ¹H NMR de la disolución A HT (a), comparado con los de los compuestos de referencia (b: alanina, c: ciclo A₂, d: dímero lineal A₂), en las regiones CH (izquierda), CH₃ (centro), y zoom vertical en la región de 1-4 ppm (derecha).

Las señales más intensas son dos dobletes alrededor de 1.35 ppm, atribuibles a protones de metilo acoplados a CH, y tres señales cuádruples en la región de 3.7 a 4.1 ppm, atribuibles a protones de metano acoplados a CH₃. Una vez más, estas son las señales de los oligopéptidos. La comparación con los espectros de referencia coincide con los datos de ¹³C: el dímero lineal A₂ no parece estar presente en cantidades importantes, ya que no se observan sus dos dobletes de CH₃ no equivalentes y las otras señales son compatibles con el monómero (especie minoritaria) y ciclo A₂. Sin embargo, en la última región se observan dos señales cuádruples distintas. Proponemos que estas señales

podrían indicar un grado de racemización que conduce a dos diastereoisómeros para el ciclo A₂, esto también puede explicar la señal adicional de ¹³C a +19.15 ppm.

Además, debido a que la resonancia magnética de protón es mucho más sensible que la resonancia magnética de carbono, se pueden observar muchas señales adicionales de menor intensidad, como se muestra en la vista ampliada a la derecha de la Figura 6.7. Las señales individuales no se pueden identificar debido a la superposición. De hecho, los polipéptidos superiores pueden estar presentes en proporciones no despreciables, ya que todos los núcleos de un polipéptido lineal pequeño pueden producir señales diferentes, lo que conduce a la dispersión de la intensidad de la señal en muchos componentes. La resonancia magnética nuclear no es un método ideal para detectar oligopéptidos minoritarios en una mezcla heterogénea; una técnica diferente, la espectrometría de masas, es más adecuada para este propósito.

Si se considera el tratamiento hidrotermal en presencia de sílice (muestra A/SiO₂ HT) no muestran cambios significativos respecto a la apariencia del espectro de ¹³C (Figura 6.1 IC). Una señal a 51.6 ppm ahora es claramente evidente en la región CH, mientras que no emergió del ruido en el caso de la muestra A HT. Además, la cantidad relativa de monómero (A) sin reaccionar es algo mayor que en ausencia de sílice. El aspecto general del espectro ¹H tampoco es muy diferente en la región de los protones de metino. Probablemente, en la región de metilo, las señales más importantes todavía corresponden a la misma especie, pero al menos una sufre una división adicional inexplicable, y las especies menores parecen haber aumentado en importancia.

De la misma forma, se estudió la evolución de ácido glutámico en tratamiento con HT. Cuando se activó una disolución de Glu sola (disolución E HT), los únicos picos que pudieron identificarse claramente en el espectro de ¹³C fueron los de la forma lactama, es decir, del PyroGlu que se forma por una ciclación interna de la molécula de Glu. En particular, el monómero ya no era detectable. La activación del ácido glutámico en presencia de sílice (E/SiO₂ HT) no cambió esta conclusión. La ¹H NMR del Glu solo es bastante compleja, pero un enfoque de huellas dactilares indica que la disolución activada E HT es muy similar a la disolución de referencia de PyroGlu. En el caso de E, como en el caso de A, la adición de sílice a la mezcla de activación térmica no cambió el resultado.

A continuación, estudiamos la evolución de mezclas equimolares de (Ala + Glu) o (A + E). Los espectros de NMR se muestran en la Figura 6.8 para las muestras (A + E) HT, (A + E)/SiO₂ HT y (A + E)/SiO₂ DA. Se comparan con algunas referencias relevantes, incluido un dímero mixto, A-E lineal (H-Ala-Glu-OH).

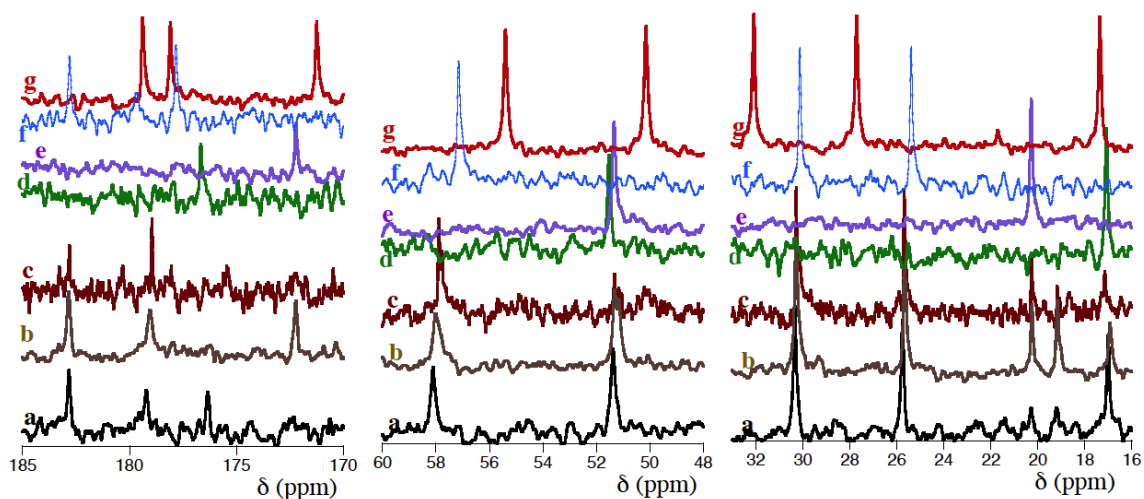


Figura 6.8. Espectros de ^{13}C NMR de las disoluciones A +E HT (a), (A +E)/SiO₂ HT (b), y de (A +E)/SiO₂ DA (c), comparados con los de los compuestos de referencia (d: alanina, e: ciclo A₂, f: PyroGlu, g: dímero lineal A-E), en las regiones carbonilo (izquierda), metino (centro), y metilo (derecha).

Si bien algunas características aún indican la presencia de PyroGlu y ciclo A₂, estas mezclas son obviamente menos simples y más variables que los sistemas de un solo aminoácido. Por ejemplo, en la región metilo de (A + E)/SiO₂ DA (espectro c), las señales identificables son débiles y no representan el total de monómeros Ala introducidos. Posiblemente, la existencia de varios oligómeros que contienen alanina da como resultado una distribución de la intensidad de NMR en muchas señales, cada una de las cuales es demasiado débil para emerger del ruido en el tiempo de análisis. Además, en la región del carbonilo, la señal aproximadamente a 179 ppm parece la más cercana, entre las referencias, al dímero lineal A-E; pero no se observa la otra señal esperada de este dímero. La NMR alcanza aquí sus límites de sensibilidad.

La ^1H NMR de estas muestras es muy compleja, lo que compromete una comprensión detallada. Una excepción es la región protónica de amida (-CO-NH-), que se presenta en la Figura 6.9. Se compara con los espectros de referencias que contienen amida (sin incluir los monómeros originales). Se puede concluir que contiene una pequeña cantidad de ciclo A₂, probablemente algo de PyroGlu (ambas interpretaciones de acuerdo con los datos de ^{13}C NMR), pero también otros péptidos, incluidos algunos que resuenan en posiciones cercanas al dímero lineal mixto A-E de referencia a aproximadamente +8.35 ppm.

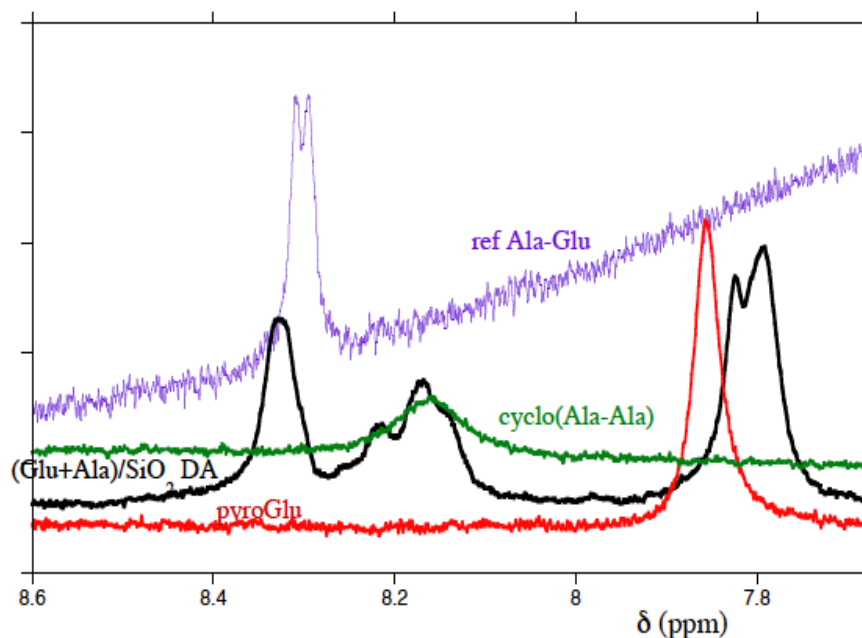


Figura 6.9. Espectro de ^1H NMR de la muestra (A + E)/SiO₂ DA en la región de protones de amida, comparado con los compuestos de referencia.

Estudios de espectrometría de masas FT-ICR.

La espectrometría de masas es una técnica muy poderosa para la caracterización de mezclas de péptidos, pero sólo se puede aplicar a disoluciones, y no directamente a la fase sólida. Así, fue posible estudiar directamente la fase acuosa obtenida en los experimentos de HT (única fase en experimentos llevados a cabo en disoluciones homogéneas), y la fase que era fácilmente separable de los sólidos en experimentos de sistemas heterogéneos (disoluciones de AAs + sílice). Por otro lado, para los experimentos de activación de DA, primero se desorbieron las moléculas orgánicas de la superficie de la sílice. En el sistema (E + L) /SiO₂, Sakhno *et al.* (2018) determinó que los productos de activación térmica fueron desorbidos cuantitativamente por simple contacto con agua desmineralizada, y se espera que también sea el caso para el sistema químicamente similar (E + A)/SiO₂.

La interpretación de los espectros de MS es complicada por varios factores. Primero, aunque la mayoría de los picos corresponden a moléculas protonadas, también se pueden detectar algunas formas cationizadas (*i.e.*, complejadas) por sodio. Por ejemplo, el dímero A-A puede aparecer tanto como la forma protonada (fórmula $\text{C}_6\text{H}_{13}\text{N}_2\text{O}_3^+$, masa exacta 161.0921 uma) o como el complejo de sodio (fórmula $\text{C}_6\text{H}_{12}\text{N}_2\text{O}_3\text{Na}^+$, masa exacta 183.0740 uma). Ocasionalmente también se observa cationización de K^+ .

En segundo lugar, las especies formadas en las cámaras de ionización no son solo iones moleculares. Pueden incluir algunos productos de descomposición de los iones moleculares. La causa más probable de error es la posible existencia de "complejos no covalentes" entre un ion H^+

y dos o más moléculas. Por ejemplo, la masa (exacta) 232,1292 una corresponde a la estequiometría $C_9H_{17}N_3O_4^+$ que puede corresponder al trímero lineal protonado H-Ala-Ala-Ala-OH (o A_3), pero también al aducto no covalente entre un dímero cíclico y un monómero, (ciclo A_2 , A) H^+ . Para poder discriminar entre estas dos contribuciones se requiere hacer una comparación entre análisis a diferentes diluciones de la disolución de desorción.

Finalmente, la cuantificación de datos espectroscópicos de masas, aunque no es estrictamente imposible, es difícil y requiere mucho tiempo. Cada ion molecular detectado tendrá su propio factor de respuesta, y en el caso de los péptidos pueden diferir hasta en un orden de magnitud. Además, la configuración del experimento FT-ICR determinará un intervalo óptimo de masa molecular para la detección de iones: el método que usamos había sido optimizado para la detección de oligómeros de longitud media (hasta los decámeros) y probablemente subestima la contribución de los monómeros. Como consecuencia, no se pueden tomar las proporciones de intensidad para representar las proporciones de concentración; pero aún pueden utilizarse como índices que permitan determinar tendencias generales en una serie de muestras, siempre que se analicen en las mismas condiciones.

Los espectros ESI-MS de las muestras mostraron un gran número de señales de alto peso molecular (Fig. 6.10.). Estos incluyen el monómero inicial, Glu, su producto de ciclización, PyroGlu, así como péptidos lineales y cíclicos. Estos últimos incluyen: Glu-Glu (E_2), E_3 y E_6 , A_2 , Ciclo A_2 , A_3 , A_4 y A_5 , y productos mixtos EA, EA_2 , E_2A , EA_3 , E_2A_2 , E_3A , EA_4 , E_2A_3 , E_3A_2 , E_3A_3 y E_2A_5 . Para la mayoría de estas composiciones son posibles varias secuencias. No se pueden distinguir sobre la base de un único espectro de masas. Pueden ser discriminados por métodos en tándem como MS/MS (Bedoin *et al.* 2020) pero esto requiere mucho más trabajo. Una primera observación es que los oligómeros hasta los heptámeros, a veces incluso más largos, son detectables, lo que hasta ahora solo se había informado en un estudio sobre el sistema mixto (E + L)/SiO₂ (Sakhno *et al.* 2018).

Un resultado interesante es que fue posible identificar el dímero lineal mixto Glu-Ala o Ala-Glu en $m/z = 219.09748 \pm 0.00001$. Además, los productos de las sucesivas deshidrataciones de este péptido se caracterizaron a $m/z = 183.07623 \pm 0.00006$ ($EA - 2H_2O$) H^+ , 223.06884 ± 0.00003 ($EA - H_2O$) Na^+ y 239.04283 ± 0.00003 ($EA - H_2O$) K^+ (Fig. 6.2-6.6 IC). Además, un oligómero determinado puede aparecer con diferentes grados de deshidratación (*e.g.*, ($E_2A_3 - H_2O$) H^+ , ($E_2A_3 - H_2O$) Na^+ y ($E_2A_3 - 2H_2O$) H^+). La pérdida de moléculas de agua adicionales puede deberse a la formación de un péptido cíclico y / o a la ciclación del residuo interno de un Glu a un PyroGlu (Fig. 6.5). En general, detectamos aproximadamente las mismas especies de péptidos poliméricos para las muestras (A + E)/SiO₂ después de DA y HT. La detección de octámeros en la muestra (A + E)/SiO₂ HT sugiere que el mineral podría favorecer las reacciones de polimerización en estas condiciones (la muestra sin mineral sólo produce hexámeros). Adicionalmente, fue posible identificar algunas estequiometrías asociadas con oligómeros más grandes con una intensidad y una asignación confiable: E_3A_6 , E_2A_7 y E_4A_5 para la muestra después de la activación en seco, mientras que para las muestras después del tratamiento hidrotermal en presencia de sílice se detectó hasta octámeros (*i.e.*, E_3A_5 , E_2A_6). Asimismo, otros picos identificados corresponden a degradaciones parciales, sucesivas deshidrataciones, o a complejaciones iónicas de estas especies (Fig. 6.5 y 6.6 IC).

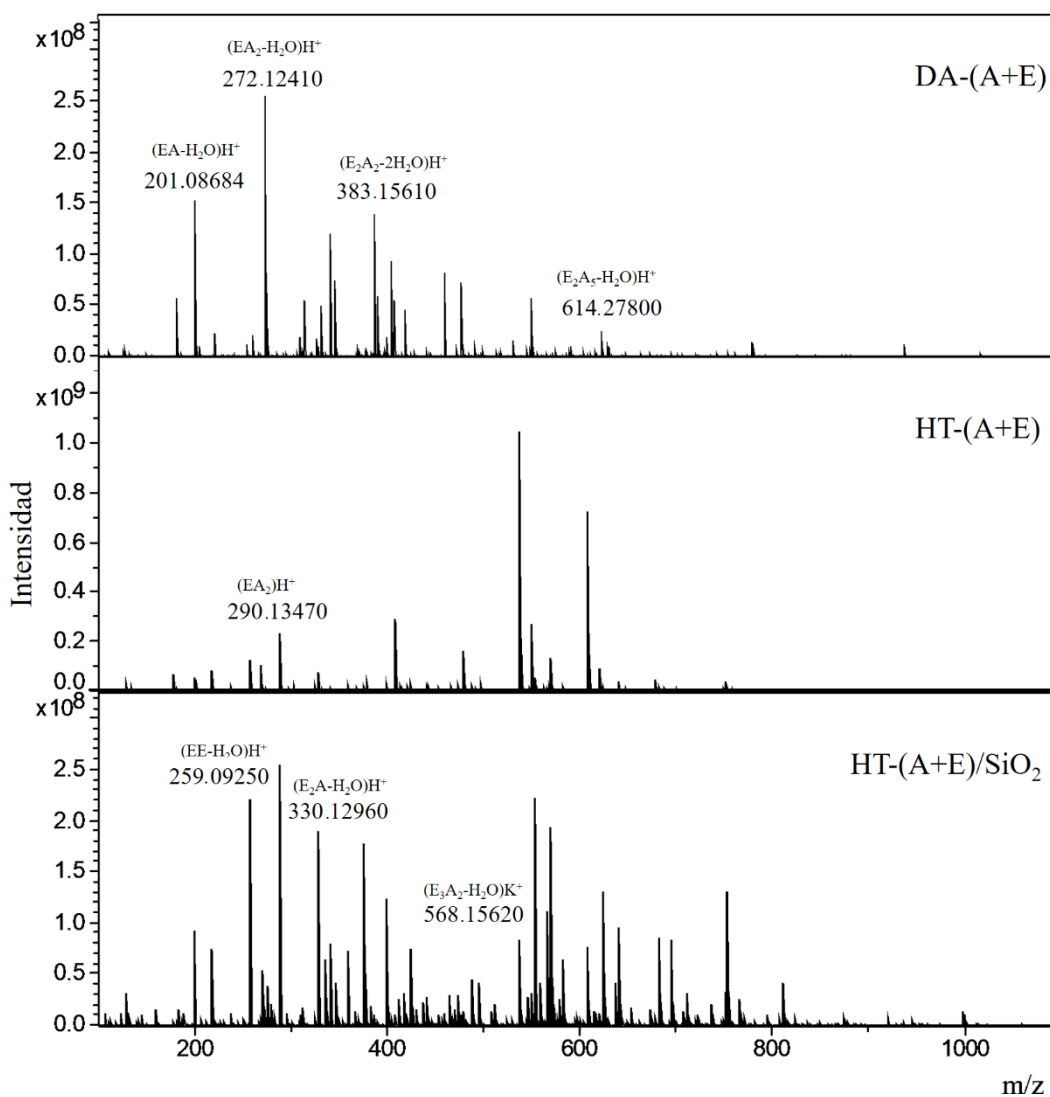


Figura 6.10. Muestra de espectros FT-ICR de los productos formados después de los tratamientos DA y HT.

Las señales de ESI-MS sugieren que la presencia de un segundo aminoácido puede afectar las vías de oligomerización favoreciendo la formación de oligómeros lineales en comparación con los sistemas individuales (*i.e.*, (A + E)/SiO₂ vs. E/SiO₂) aunque el producto más predominante sigue siendo la forma cíclica. La Figura 6.11 resume el número de oligómeros detectados para cada experimento. Los experimentos, tanto en condiciones HT como DA, que utilizan aminoácidos individuales solo producen, en el mejor de los casos, hexámeros (Fig. 6.2-6.6 IC). Además, los resultados sugieren que el ácido glutámico (cuando se encuentra solo) tiene una mejor capacidad de polimerización que la alanina. Por ejemplo, es posible sintetizar hasta hexámeros de ácido glutámico bajo DA mientras que la alanina solo produce tetrámeros. En general, las condiciones hidrotermales permiten la síntesis de hexámeros y no hay un efecto apreciable de la presencia de

sílice en la polimerización de aminoácidos individuales (Fig. 6.3-6.4 IC). El sistema mixto produce una mayor variedad de especies químicas (Fig. 6.6 IC).

Relacionado con el tratamiento hidrotermal, la presencia de sílice parece permitir la formación de oligómeros más largos (*i.e.*, octámeros) en comparación con la muestra sin mineral (*i.e.*, hexámeros). Por otro lado, las condiciones secas e hidrotermales, mostraron resultados similares. En ambos sistemas, fue posible detectar oligómeros más largos (nonámeros para DA y octámeros para HT). Esto sugiere que, aunque la polimerización de aminoácidos libera una molécula de agua en cada paso, el uso de alta presión y alta temperatura en estos experimentos permite la reacción de polimerización incluso en medio acuoso.

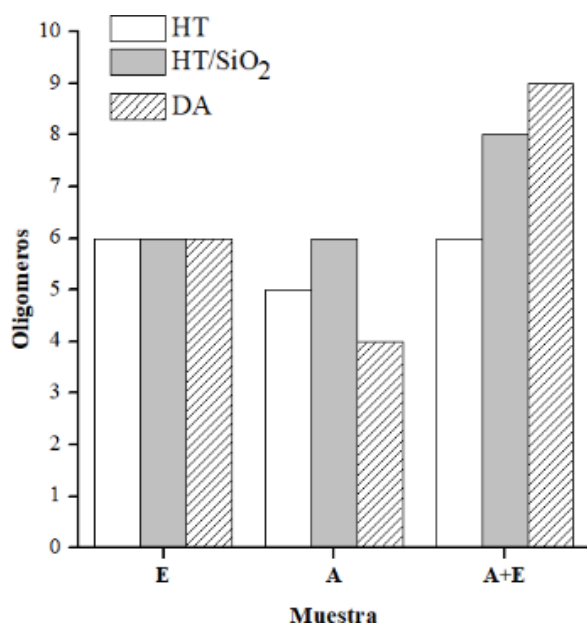


Figura 6.11. Oligómeros detectados para tratamientos hidrotermales y de activación seca. En el mejor caso, usando el tratamiento DA, es posible la formación de nonámeros.

La naturaleza de los productos de condensación depende en gran medida de las condiciones de reacción (*i.e.*, cantidad de agua, temperatura, tiempo de reacción, estructura química del adsorbato y adsorbente; Meng *et al.* 2004). Se ha reportado que una de las limitaciones de los sistemas hidrotermales, tanto submarinos como sub-aéreos, respecto a las reacciones de polimerización son: I) la dificultad de llevar a cabo reacciones de polimerización por reacciones de condensación en un ambiente acuoso; II) la hidrólisis de los enlaces peptídicos; y III) la aminólisis interna a altas temperaturas que conlleva a la formación de DKP a partir de la descomposición de péptidos (Steinberg y Bada 1983; Lambert *et al.* 2013; Deamer y Georgiou 2015; Benoiton 2016).

Sin embargo, algunos experimentos han sugerido que las altas presiones y altas temperaturas pueden favorecer algunas vías de polimerización (*i.e.*, dimerización y la formación de DKP) sobre las reacciones de descarboxilación e hidrólisis de aminoácidos (Shiota y Nakashima 2005; Cox y Seward 2007; Otake *et al.* 2011). Asimismo, algunos modelos teóricos han sugerido que las altas temperaturas (Shock 1993) y la presencia de gases disueltos (*e.g.*, CO₂, H₂) (Kitadai 2015) pueden producir condiciones termodinámicas favorables para la polimerización. Cabe destacar que, aunque el producto principal, después de ambos tratamientos, es la forma cíclica, algunos experimentos han demostrado que es posible obtener oligómeros lineales largos en condiciones acuosas (Kawamura *et al.* 2005; Cox y Seward 2007; Futamura *et al.* 2008; Cleaves *et al.* 2009; Shanker *et al.* 2012; Ying *et al.* 2018) o condiciones secas (Harada y Fox, 1958; Phillips y Melius, 1974; Hartmann *et al.* 1981; Otake *et al.* 2011; Sakhno *et al.* 2018). Se ha propuesto que la apertura del anillo y el reordenamiento molecular del anhídrido cíclico (Bujdák y Rode 1997) o la reacción entre DKP con monómeros (Lambert *et al.* 2009) son mecanismos plausibles para el alargamiento de la cadena peptídica. Asimismo, la polimerización puede ser mediada por DKP en un amplio intervalo de temperaturas (*i.e.*, 90-200 °C) (Mitsuzawa y Yukawa 2004) y la DKP puede ser el bloque de construcción para la formación de péptidos (Nagayama *et al.* 1990).

Por otro lado, la presencia de minerales puede tener diferentes roles. Pueden promover la descomposición de aminoácidos (McCullom 2013) o bien, favorecer la dimerización lineal sobre la forma cíclica (Pedreira-Segade *et al.* 2019). Asimismo, la presencia de superficies inorgánicas puede facilitar la apertura adicional del anillo cíclico de piperazinadiona para formar los dipéptidos lineales (Zamaraev *et al.* 1997). Otros experimentos con nano partículas de goetita o de ferrita metálica confirman que, en un amplio intervalo de temperaturas (~ 50 a 120 °C), la ciclación es mucho más favorable que el alargamiento de la cadena peptídica debido a la energía de activación de la formación de DKP a partir de H-Ala-Ala-OH es menor en comparación con la formación de H-Ala-Ala-OH a partir de la condensación de dos moléculas individuales (Shanker *et al.* 2012; Iqbal *et al.* 2017)

Nuestros resultados sugieren que la presencia de sílice tiene un papel interesante. Con respecto a las condiciones secas, se ha estudiado ampliamente que los grupos silanol en la superficie de la sílice pueden actuar como sitios de condensación activadores, favoreciendo el paso de deshidratación necesario en la formación del enlace amida a través del grupo amino (Lambert *et al.* 2013; Rimola *et al.* 2018). En condiciones hidrotermales, la presencia de sílice aumenta la formación de especies más largas para el ácido glutámico y marcadamente para el sistema mixto. La mayor formación de oligómeros más largos en presencia de sílice puede estar asociada con mecanismos de activación de aminoácidos como resultado de la formación de enlaces éster entre los grupos silanol en la superficie de la sílice (Si-OH) y el grupo carboxílico del aminoácido (Bujdák y Rode 1997; Meng *et al.* 2004; Rimola *et al.* 2009). Debido a que el ácido glutámico tiene dos grupos carboxílicos, la formación de enlaces éster con la sílice es mayor que la de la alanina y, por tanto, se podría favorecer la formación de oligómeros. Otro mecanismo puede estar asociado con una reacción especial con sitios activados, como los ciclos de siloxano (Lambert *et al.* 2009). Además, la formación de oligómeros más largos en los sistemas mixtos puede resultar de reacciones competitivas donde hay una formación preferencial de un polímero sobre el anhídrido cíclico como ocurre en otros sistemas (*e.g.*, A + G /SiO₂) (Bujdák y Rode 1997).

Conclusiones

En el presente estudio, se consideró la evolución del sistema (Ala + Glu) / SiO₂ en condiciones hidrotermales subaéreas y submarinas con el objetivo de determinar algunos signos de selectividad en los proceso de sorción y/o polimerización. Los resultados preliminares sugieren la formación de algunos oligómeros lineales largos después del tratamiento térmico seco (activación seca; *DA*, por sus siglas en inglés) y tratamiento hidrotermal submarino (*HT*, por sus siglas en inglés). En general, nuestros resultados sugieren que las superficies minerales pueden tener un papel importante en la sorción y polimerización de AAs tanto en condiciones secas como acuosas y se engloban en las siguientes conclusiones generales:

1. La producción de compuestos cíclicos (*e.g.*, ciclo A₂, PyroGlu) predomina sobre la formación de oligómeros lineales después de los ambos tratamientos.
2. La presencia de la silica parece tener un efecto cinético en las reacciones de condensación implicadas en la formación de oligómeros lineales largos considerando ambos sistemas. Notablemente, la presencia del mineral en los experimentos HT podría favorecer la elongación de oligómeros más largos.
3. La diversidad de oligómeros formados es considerablemente mayor en el sistema mixto (*e.g.*, (Ala + Glu)/SiO₂) respecto al sistema con aminoácidos individuales (*e.g.*, Ala/SiO₂). Esto sugiere que en un ambiente primitivo, la diversidad de moléculas favorecería la formación de moléculas más complejas (*i.e.*, oligómeros heterogéneos).

Referencias

- Abadian, H. (2021) Adsorption of biomolecules on minerals surfaces and Activation under ambient pressure and controlled water activity *Ph.D. Thesis*, Sorbonne Université.
- Abdelmoez W, Nakahasi T, Yoshida H (2007) Amino Acid Transformation and Decomposition in Saturated Subcritical Water Conditions. *Industrial & Engineering Chemistry Research* 46:5286–5294. <https://doi.org/10.1021/ie070151b>
- Alargov DK, Deguchi S, Tsujii K, Horikoshi K (2002) Reaction behaviors of glycine under super- and subcritical water conditions. *Orig Life Evol Biosph* 32:1–12
- Andersson E, Holm NG (2000) The stability of some selected amino acids under attempted redox constrained hydrothermal conditions. *Orig Life Evol Biosph* 30:9–23
- Aubrey AD, Cleaves HJ, Bada JL (2009) The Role of Submarine Hydrothermal Systems in the Synthesis of Amino Acids. *Origins of Life and Evolution of Biospheres* 39:91–108. <https://doi.org/10.1007/s11084-008-9153-2>
- Bada JL, Miller SL, Zhao M (1995) The stability of amino acids at submarine hydrothermal vent temperatures. *Origins of Life and Evolution of the Biosphere* 25:111–118. <https://doi.org/10.1007/BF01581577>

- Bedoin L, (2018) Emergence de biopolymères "prometteurs" dans les scénarios d'origine de la vie *MSc Thesis*, Sorbonne Université
- Bedoin L, Alves S, Lambert J-F (2020) Origins of Life and Molecular Information: Selectivity in Mineral Surface-Induced Prebiotic Amino Acid Polymerization. *ACS Earth and Space Chemistry* 4:1802–1812
- Benoiton NL (2016) Chemistry of peptide synthesis
- Bouchoucha M, Jaber M, Onfroy T, et al (2011) Glutamic Acid Adsorption and Transformations on Silica. *The Journal of Physical Chemistry C* 115:21813–21825. <https://doi.org/10.1021/jp206967b>
- Bujdák J, Le Son H, Rode BM (1996) Montmorillonite catalyzed peptide bond formation: The effect of exchangeable cations. *Journal of Inorganic Biochemistry* 63:119–124. [https://doi.org/10.1016/0162-0134\(95\)00186-7](https://doi.org/10.1016/0162-0134(95)00186-7)
- Bujdák J, Rode BM (1997) Silica, Alumina, and Clay-Catalyzed Alanine Peptide Bond Formation. *Journal of Molecular Evolution* 45:457–466. <https://doi.org/10.1007/PL00006250>
- Burton AS, Stern JC, Elsilá JE, et al (2012) Understanding prebiotic chemistry through the analysis of extraterrestrial amino acids and nucleobases in meteorites. *Chemical Society Reviews* 41:5459. <https://doi.org/10.1039/c2cs35109a>
- Cleaves H (2013) Prebiotic Chemistry: Geochemical Context and Reaction Screening. *Life* 3:331–345. <https://doi.org/10.3390/life3020331>
- Cleaves HJ, Aubrey AD, Bada JL (2009) An Evaluation of the Critical Parameters for Abiotic Peptide Synthesis in Submarine Hydrothermal Systems. *Origins of Life and Evolution of Biospheres* 39:109–126. <https://doi.org/10.1007/s11084-008-9154-1>
- Colín-García M, Heredia A, Cordero G, et al (2016) Hydrothermal vents and prebiotic chemistry: a review. *Boletín de la Sociedad Geológica Mexicana* 68:599–620
- Colín-García M, Villafañe-Barajas S, Camprubí A, et al (2018) 5.4 Prebiotic Chemistry in Hydrothermal Vent Systems. *Handbook of Astrobiology* 297
- Cox JS, Seward TM (2007) The reaction kinetics of alanine and glycine under hydrothermal conditions. *Geochimica et Cosmochimica Acta* 71:2264–2284. <https://doi.org/10.1016/j.gca.2007.01.020>
- Danger G, Plasson R, Pascal R (2012) Pathways for the formation and evolution of peptides in prebiotic environments. *Chemical Society Reviews* 41:5416. <https://doi.org/10.1039/c2cs35064e>
- Deamer DW, Georgiou CD (2015) Hydrothermal conditions and the origin of cellular life. *Astrobiology* 15:1091–1095
- Faisal M, Sato N, Quitain AT, et al (2005) Hydrolysis and Cyclodehydration of Dipeptide under Hydrothermal Conditions. *Industrial & Engineering Chemistry Research* 44:5472–5477. <https://doi.org/10.1021/ie0500568>
- Fox SW, Harada K (1960) The Thermal Copolymerization of Amino Acids Common to Protein¹. *Journal of the American Chemical Society* 82:3745–3751. <https://doi.org/10.1021/ja01499a069>

- Fox SW, Harada K, Vegotsky A (1959) Thermal polymerization of amino acids and a theory of biochemical origins. *Experientia* 15:81–84. <https://doi.org/10.1007/BF02301336>
- Fujimoto C, Shinozaki A, Mimura K, et al (2015) Pressure-induced oligomerization of alanine at 25 °C. *Chemical Communications* 51:13358–13361. <https://doi.org/10.1039/C5CC03665H>
- Futamura Y, Fujioka K, Yamamoto K (2008) Hydrothermal treatment of glycine and adiabatic expansion cooling: implications for prebiotic synthesis of biopolymers. *Journal of materials science* 43:2442–2446
- Harada K, Fox SW (1958) The Thermal Condensation of Glutamic Acid and Glycine to Linear Peptides ¹. *Journal of the American Chemical Society* 80:2694–2697. <https://doi.org/10.1021/ja01544a027>
- Harada K, Fox SW (1965) Characterization of thermal polymers of neutral α -amino acids with dicarboxylic amino acids or lysine. *Archives of Biochemistry and Biophysics* 109:49–56. [https://doi.org/10.1016/0003-9861\(65\)90285-7](https://doi.org/10.1016/0003-9861(65)90285-7)
- Hartmann J, Christel Brand M, Dose K (1981) Formation of specific amino acid sequences during thermal polymerization of amino acids. *Biosystems* 13:141–147. [https://doi.org/10.1016/0303-2647\(81\)90055-1](https://doi.org/10.1016/0303-2647(81)90055-1)
- Hazen RM, Sverjensky DA (2010) Mineral Surfaces, Geochemical Complexities, and the Origins of Life. *Cold Spring Harbor Perspectives in Biology* 2:a002162–a002162. <https://doi.org/10.1101/cshperspect.a002162>
- Higgs PG, Pudritz RE (2009) A Thermodynamic Basis for Prebiotic Amino Acid Synthesis and the Nature of the First Genetic Code. *Astrobiology* 9:483–490. <https://doi.org/10.1089/ast.2008.0280>
- Huber C, Wachtershauser G (2006) -Hydroxy and -Amino Acids Under Possible Hadean, Volcanic Origin-of-Life Conditions. *Science* 314:630–632. <https://doi.org/10.1126/science.1130895>
- Iqbal Md, Sharma R, Jheeta S, Kamaluddin (2017) Thermal Condensation of Glycine and Alanine on Metal Ferrite Surface: Primitive Peptide Bond Formation Scenario. *Life* 7:15. <https://doi.org/10.3390/life7020015>
- Islam MdN, Kaneko T, Kobayashi K (2003) Reaction of Amino Acids in a Supercritical Water-Flow Reactor Simulating Submarine Hydrothermal Systems. *Bulletin of the Chemical Society of Japan* 76:1171–1178. <https://doi.org/10.1246/bcsj.76.1171>
- Jaber M, Georgelin T, Bazzi H, et al (2014a) Selectivities in Adsorption and Peptidic Condensation in the (Arginine and Glutamic Acid)/Montmorillonite Clay System. *The Journal of Physical Chemistry C* 118:25447–25455. <https://doi.org/10.1021/jp507335e>
- Jaber M, Georgelin T, Bazzi H, et al (2014b) Selectivities in Adsorption and Peptidic Condensation in the (Arginine and Glutamic Acid)/Montmorillonite Clay System. *The Journal of Physical Chemistry C* 118:25447–25455. <https://doi.org/10.1021/jp507335e>
- Kawamura K, Nishi T, Sakiyama T (2005) Consecutive Elongation of Alanine Oligopeptides at the Second Time Range under Hydrothermal Conditions Using a Microflow Reactor System. *Journal of the American Chemical Society* 127:522–523. <https://doi.org/10.1021/ja0447917>

- Kibet JK, Khachatryan L, Dellinger B (2013) Molecular Products from the Thermal Degradation of Glutamic Acid. *Journal of Agricultural and Food Chemistry* 61:7696–7704. <https://doi.org/10.1021/jf401846t>
- Kitadai N (2015) Energetics of amino acid synthesis in alkaline hydrothermal environments. *Origins of Life and Evolution of Biospheres* 45:377–409
- Klingler D, Berg J, Vogel H (2007) Hydrothermal reactions of alanine and glycine in sub- and supercritical water. *The Journal of Supercritical Fluids* 43:112–119. <https://doi.org/10.1016/j.supflu.2007.04.008>
- Kohara M, Gamo T, Yanagawa H, Kobayashi K (1997) Stability of Amino Acids in Simulated Hydrothermal Vent Environments. *Chemistry Letters* 26:1053–1054. <https://doi.org/10.1246/cl.1997.1053>
- Lambert J-F (2008) Adsorption and Polymerization of Amino Acids on Mineral Surfaces: A Review. *Origins of Life and Evolution of Biospheres* 38:211–242. <https://doi.org/10.1007/s11084-008-9128-3>
- Lambert J-F, Jaber M, Georgelin T, Stievano L (2013) A comparative study of the catalysis of peptide bond formation by oxide surfaces. *Physical Chemistry Chemical Physics* 15:13371. <https://doi.org/10.1039/c3cp51282g>
- Lambert J-F, Stievano L, Lopes I, et al (2009) The fate of amino acids adsorbed on mineral matter. *Planetary and Space Science* 57:460–467. <https://doi.org/10.1016/j.pss.2009.01.012>
- Lemke KH, Rosenbauer RJ, Bird DK (2009) Peptide Synthesis in Early Earth Hydrothermal Systems. *Astrobiology* 9:141–146. <https://doi.org/10.1089/ast.2008.0166>
- McCullom TM (2013) The influence of minerals on decomposition of the n-alkyl- α -amino acid norvaline under hydrothermal conditions. *Geochimica et Cosmochimica Acta* 104:330–357. <https://doi.org/10.1016/j.gca.2012.11.008>
- Melius P, Hubbard W-L (1987) Pyroglutamyl N-termini of thermal polyamino acids. *Biosystems* 20:213–217. [https://doi.org/10.1016/0303-2647\(87\)90027-X](https://doi.org/10.1016/0303-2647(87)90027-X)
- Melius P, Yon-Ping Sheng J (1975) Thermal condensation of a mixture of six amino acids. *Bioorganic Chemistry* 4:385–391. [https://doi.org/10.1016/0045-2068\(75\)90049-8](https://doi.org/10.1016/0045-2068(75)90049-8)
- Meng M, Stievano L, Lambert J-F (2004) Adsorption and Thermal Condensation Mechanisms of Amino Acids on Oxide Supports. 1. Glycine on Silica. *Langmuir* 20:914–923. <https://doi.org/10.1021/la035336b>
- Miller SL (1953) A Production of Amino Acids Under Possible Primitive Earth Conditions. *Science* 117:528–529. <https://doi.org/10.1126/science.117.3046.528>
- Mitsuzawa S, Yukawa T (2004) A reaction network for triglycine synthesis under hydrothermal conditions. *Bulletin of the Chemical Society of Japan* 77:965–973
- Moshe H, Levi G, Mastai Y (2013) Polymorphism stabilization by crystal adsorption on a self-assembled monolayer. *CrystEngComm* 15:9203. <https://doi.org/10.1039/c3ce41237g>

- Muñoz Caro GM, Meierhenrich UJ, Schutte WA, et al (2002) Amino acids from ultraviolet irradiation of interstellar ice analogues. *Nature* 416:403–406. <https://doi.org/10.1038/416403a>
- Nagayama M, Takaoka O, Inomata K, Yamagata Y (1990) Diketopiperazine-mediated peptide formation in aqueous solution. *Origins of Life and Evolution of the Biosphere* 20:249–257
- Nunes RS, Cavaleiro ÉTG (2007) Thermal behavior of glutamic acid and its sodium, lithium and ammonium salts. *Journal of Thermal Analysis and Calorimetry* 87:627–630. <https://doi.org/10.1007/s10973-006-7788-7>
- Olafsson PG, Bryan AM (1970) Evaluation of thermal decomposition temperatures of amino acids by differential enthalpic analysis. *Mikrochimica Acta* 58:871–878. <https://doi.org/10.1007/BF01225712>
- Omran A, Pasek M (2020) A Constructive Way to Think about Different Hydrothermal Environments for the Origins of Life. *Life* 10:36. <https://doi.org/10.3390/life10040036>
- Otake T, Taniguchi T, Furukawa Y, et al (2011) Stability of Amino Acids and Their Oligomerization Under High-Pressure Conditions: Implications for Prebiotic Chemistry. *Astrobiology* 11:799–813. <https://doi.org/10.1089/ast.2011.0637>
- Pascal R, Boiteau L, Commeyras A (2005) From the Prebiotic Synthesis of α -Amino Acids Towards a Primitive Translation Apparatus for the Synthesis of Peptides. In: Walde P (ed) *Prebiotic Chemistry*. Springer-Verlag, Berlin/Heidelberg, pp 69–122
- Pedreira-Segade U, Hao J, Montagnac G, et al (2019) Spontaneous polymerization of glycine under hydrothermal conditions. *ACS Earth and Space Chemistry* 3:1669–1677
- Phillips RD, Melius P (1974) THE THERMAL POLYMERIZATION OF AMINO ACIDS: The Role and Fate of the Reactants. *International Journal of Peptide and Protein Research* 6:309–319. <https://doi.org/10.1111/j.1399-3011.1974.tb02390.x>
- Plankensteiner K, Reiner H, Rode B (2005) Prebiotic Chemistry: The Amino Acid and Peptide World. *Current Organic Chemistry* 9:1107–1114. <https://doi.org/10.2174/1385272054553640>
- Rimola A, Costa D, Sodupe M, et al (2013) Silica Surface Features and Their Role in the Adsorption of Biomolecules: Computational Modeling and Experiments. *Chemical Reviews* 113:4216–4313. <https://doi.org/10.1021/cr3003054>
- Rimola A, Fabbiani M, Sodupe M, et al (2018a) How Does Silica Catalyze the Amide Bond Formation under Dry Conditions? Role of Specific Surface Silanol Pairs. *ACS Catalysis* 8:4558–4568. <https://doi.org/10.1021/acscatal.7b03961>
- Rimola A, Fabbiani M, Sodupe M, et al (2018b) How Does Silica Catalyze the Amide Bond Formation under Dry Conditions? Role of Specific Surface Silanol Pairs. *ACS Catalysis* 8:4558–4568. <https://doi.org/10.1021/acscatal.7b03961>
- Rimola A, Sodupe M, Ugliengo P (2009) Affinity Scale for the Interaction of Amino Acids with Silica Surfaces. *The Journal of Physical Chemistry C* 113:5741–5750. <https://doi.org/10.1021/jp811193f>
- Rode BM (1999) Peptides and the origin of life. *Peptides* 20:773–786. [https://doi.org/10.1016/S0196-9781\(99\)00062-5](https://doi.org/10.1016/S0196-9781(99)00062-5)

- Ruiz-Bermejo M, Zorzano M-P, Osuna-Esteban S (2013) Simple Organics and Biomonomers Identified in HCN Polymers: An Overview. *Life* 3:421–448. <https://doi.org/10.3390/life3030421>
- Sakata K, Kitadai N, Yokoyama T (2010) Effects of pH and temperature on dimerization rate of glycine: Evaluation of favorable environmental conditions for chemical evolution of life. *Geochimica et Cosmochimica Acta* 74:6841–6851. <https://doi.org/10.1016/j.gca.2010.08.032>
- sakhno yuriy, Battistella A, Mezzetti A, et al (2018) One step up the ladder of prebiotic complexity: Formation of non-random linear polypeptides from binary systems of amino acids on silica. *Chemistry - A European Journal*. <https://doi.org/10.1002/chem.201803845>
- Sakhno Y, Battistella A, Mezzetti A, et al (2019) One Step up the Ladder of Prebiotic Complexity: Formation of Nonrandom Linear Polypeptides from Binary Systems of Amino Acids on Silica. *Chemistry - A European Journal* 25:1275–1285. <https://doi.org/10.1002/chem.201803845>
- Sato N, Quitain AT, Kang K, et al (2004) Reaction Kinetics of Amino Acid Decomposition in High-Temperature and High-Pressure Water. *Industrial & Engineering Chemistry Research* 43:3217–3222. <https://doi.org/10.1021/ie020733n>
- Shanker U, Bhushan B, Bhattacharjee G, Kamaluddin (2012) Oligomerization of Glycine and Alanine Catalyzed by Iron Oxides: Implications for Prebiotic Chemistry. *Origins of Life and Evolution of Biospheres* 42:31–45. <https://doi.org/10.1007/s11084-012-9266-5>
- Shiota D, Nakashima S (2005) Threonine transformation under hydrothermal conditions. *Chemistry letters* 34:158–159
- Shock EL (1993) Hydrothermal dehydration of aqueous organic compounds. *Geochimica et Cosmochimica Acta* 57:3341–3349
- Steinberg SM, Bada JL (1983) Peptide decomposition in the neutral pH region via the formation of diketopiperazines. *The Journal of Organic Chemistry* 48:2295–2298. <https://doi.org/10.1021/jo00161a036>
- Van Kranendonk MJ, Deamer DW, Djokic T (2017) Life Springs. *Scientific American* 317:28–35. <https://doi.org/10.1038/scientificamerican0817-28>
- Vijayan N, Rajasekaran S, Bhagavannarayana G, et al (2006) Growth and Characterization of Nonlinear Optical Amino Acid Single Crystal: L -Alanine. *Crystal Growth & Design* 6:2441–2445. <https://doi.org/10.1021/cg049594y>
- Westall F, Hickman-Lewis K, Hinman N, et al (2018) A Hydrothermal-Sedimentary Context for the Origin of Life. *Astrobiology* 18:259–293. <https://doi.org/10.1089/ast.2017.1680>
- Wieland T, Bodanszky M (1991) *The World of Peptides: a Brief History of Peptide Chemistry*. Springer Berlin Heidelberg, Berlin, Heidelberg
- Ying J, Lin R, Xu P, et al (2018) Prebiotic formation of cyclic dipeptides under potentially early Earth conditions. *Scientific Reports* 8:. <https://doi.org/10.1038/s41598-018-19335-9>
- Zaia DAM, Zaia CTBV, De Santana H (2008) Which Amino Acids Should Be Used in Prebiotic Chemistry Studies? *Origins of Life and Evolution of Biospheres* 38:469–488. <https://doi.org/10.1007/s11084-008-9150-5>

- Zamaraev KI, Romannikov VN, Salganik RI, et al (1997) Modelling of the prebiotic synthesis of oligopeptides: silicate catalysts help to overcome the critical stage. *Orig Life Evol Biosph* 27:325–337
- Zhuravlev LT (2000) The surface chemistry of amorphous silica. Zhuravlev model. *Colloids and Surfaces A: Physicochemical and Engineering Aspects* 173:1–38. [https://doi.org/10.1016/S0927-7757\(00\)00556-2](https://doi.org/10.1016/S0927-7757(00)00556-2)

Información Complementaria

Figura 6.1. IC. Espectro de ^{13}C NMR de la disolución A/SiO₂ HT (b) comparado con el de A HT (a).

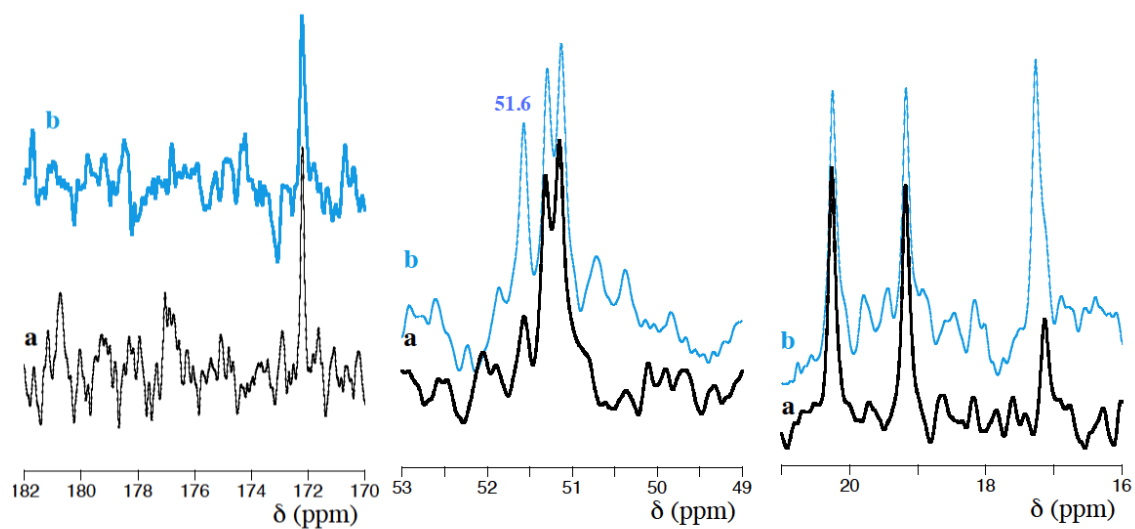


Figura 6.2. IC. Resumen de especies detectadas por ESI-MS de las muestras para un único aminoácido después del tratamiento por activación en seco.

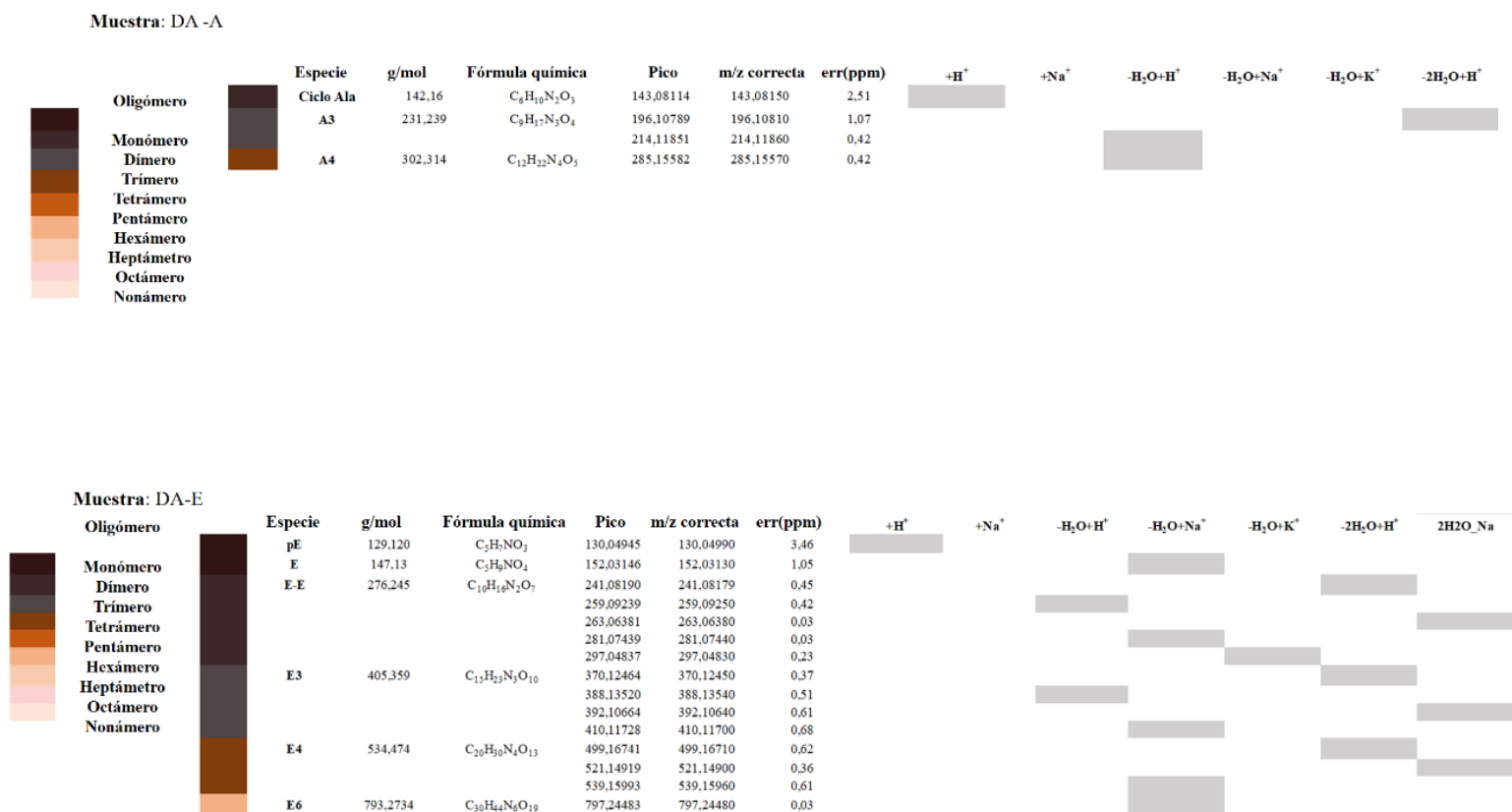
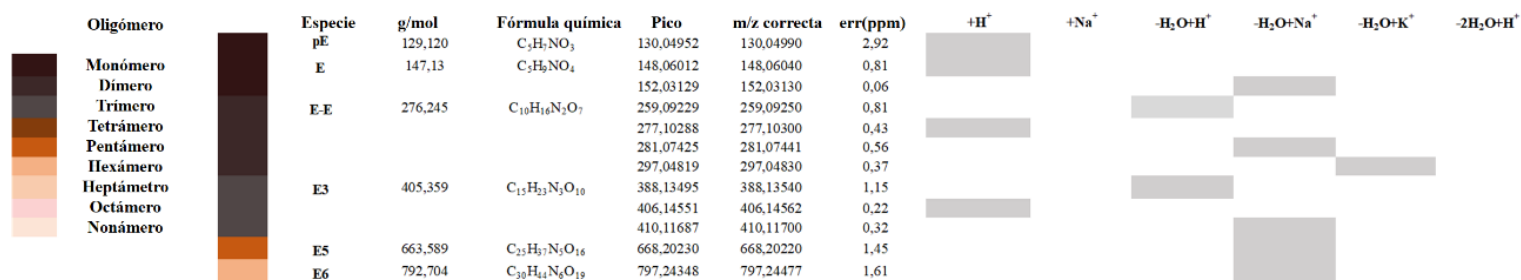


Figura 6.3. IC. Resumen de especies detectadas por ESI-MS de las muestras para un único aminoácido después del tratamiento hidrotérmal sin mineral.

Muestra: HT-E



Muestra: HT-A

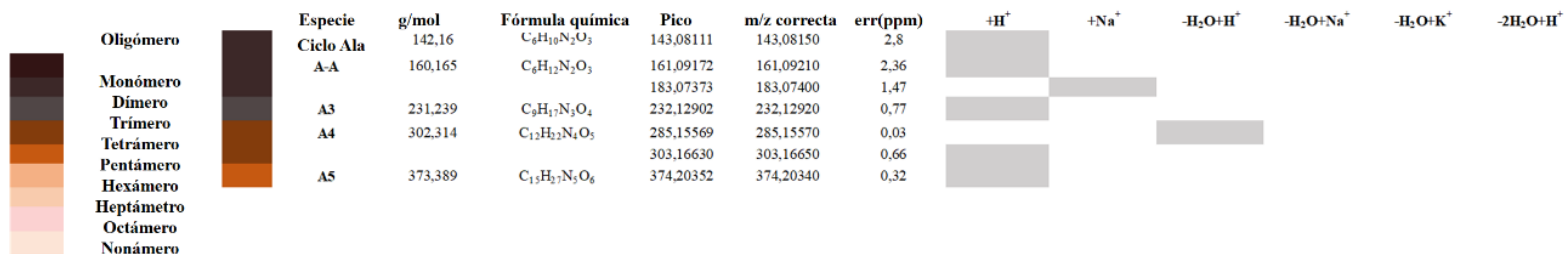
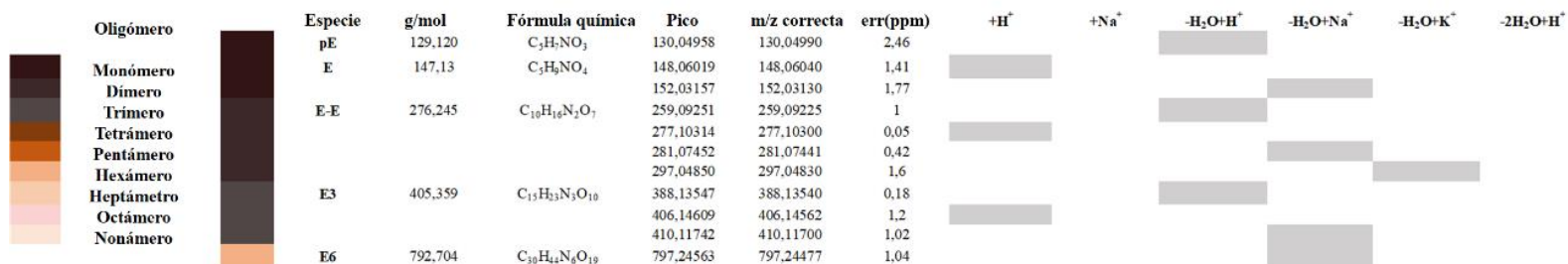


Figura 6.4. IC. Resumen de especies detectadas por ESI-MS de las muestras para un único aminoácido después del tratamiento hidrotérmal con mineral.

Muestra: IIT-E/SiO₂



Muestra: IIT-A/SiO₂

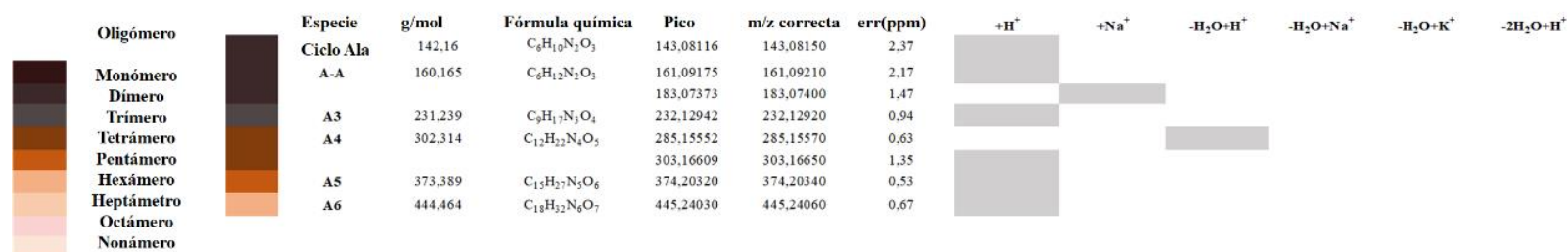


Figura 6.5. IC. Resumen de especies detectadas por ESI-MS de las muestras para los sistemas de aminoácidos mixtos después del tratamiento por activación en seco.

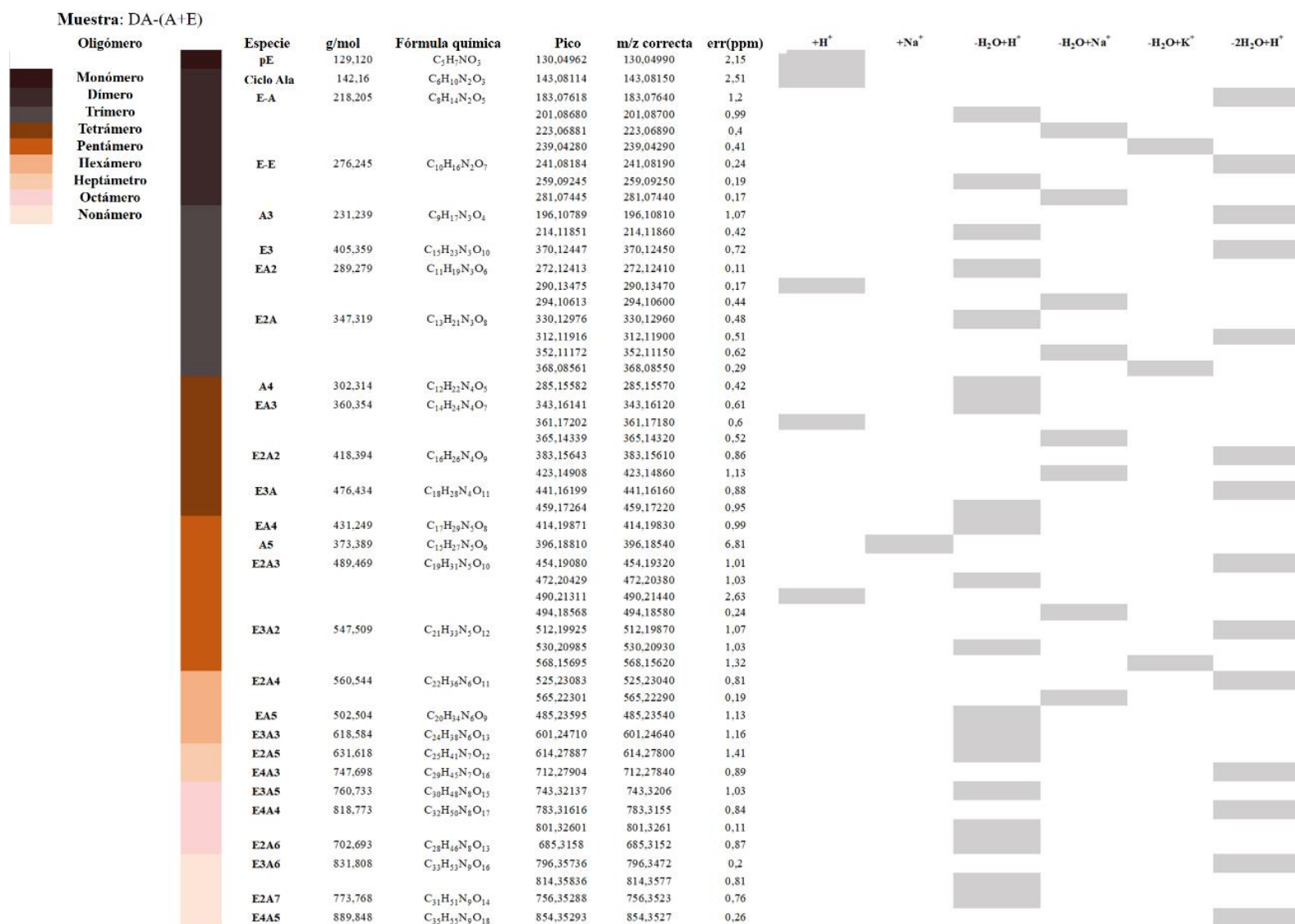
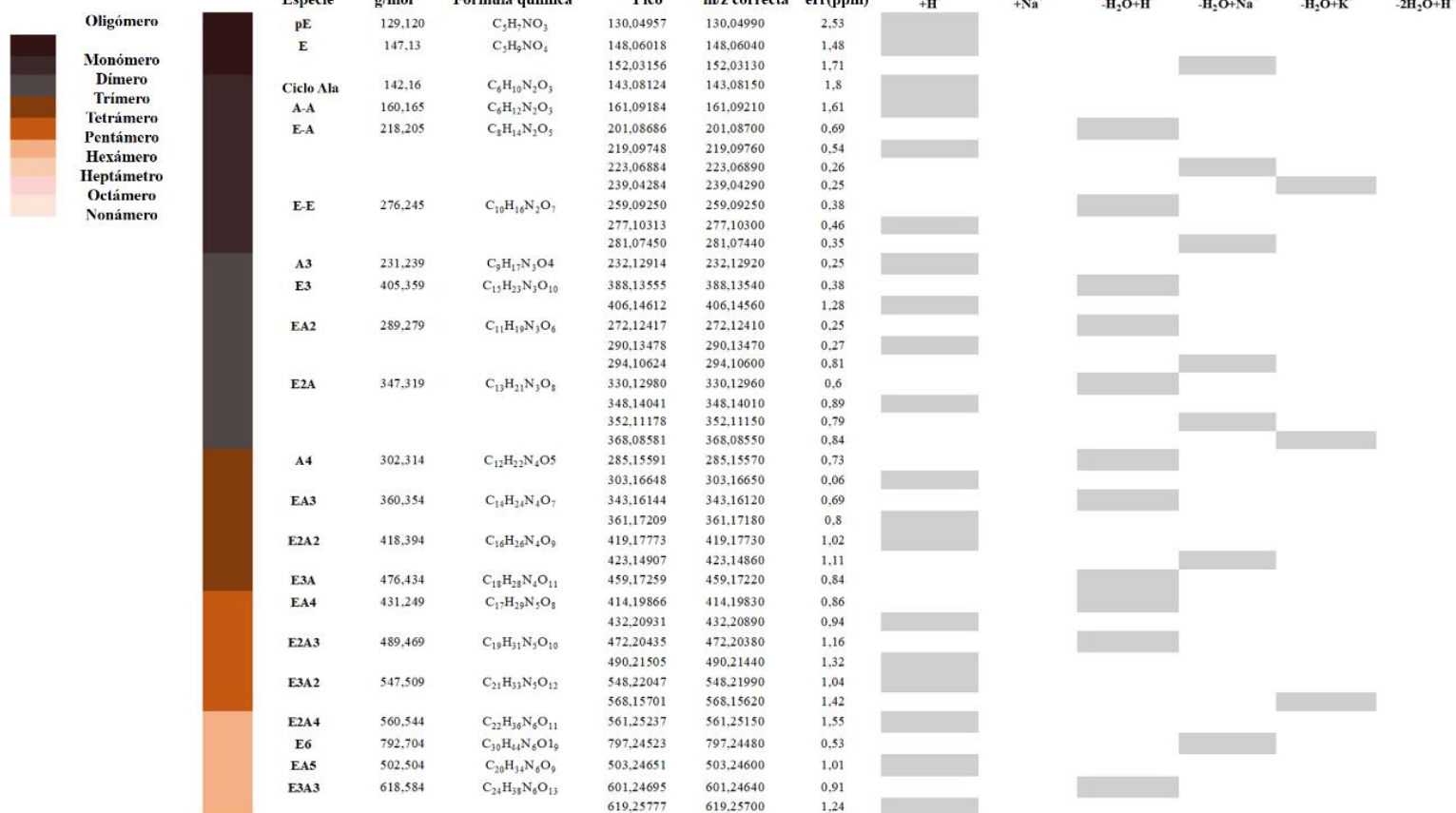


Figura 6.6. IC. Resumen de especies detectadas por ESI-MS de las muestras para los sistemas de aminoácidos mixtos después del tratamiento hidrotermal.

Muestra: HT-(A+E)



Muestra: HT-(A+E)/SiO₂



Especie	g/mol	Fórmula química	Pico	m/z correcta	err(ppm)	+H ⁺	+Na ⁺	-H ₂ O+H ⁺	-H ₂ O+Na ⁺	-H ₂ O+K ⁺	-2H ₂ O+H ⁺
pE	129,120	C ₅ H ₇ N ₃ O ₃	130,04958	130,04990	2,46						
	E	C ₅ H ₅ N ₃ O ₄	148,06019	148,06040	1,41						
			152,03158	152,03130	1,84						
Ciclo Ala	142,16	C ₆ H ₁₀ N ₂ O ₃	143,08125	143,08150	1,74						
	A-A	C ₆ H ₁₂ N ₂ O ₃	161,09185	161,09210	1,55						
			183,07627	183,07640	0,71						
E-A	218,205	C ₈ H ₁₄ N ₂ O ₅	201,08687	201,08700	0,64						
			219,09747	219,09760	0,5						
			239,04286	239,04290	0,16						
E-E	276,245	C ₁₀ H ₁₆ N ₂ O ₇	223,06887	223,06890	0,13						
			259,09252	259,09250	0,77						
			277,10314	277,10300	0,5						
A3	231,239	C ₉ H ₁₇ N ₇ O ₄	281,07452	281,07440	0,42						
			297,04851	297,04830	0,7						
			232,12917	232,12920	0,12						
E3	405,359	C ₁₃ H ₃₃ N ₃ O ₁₀	388,13549	388,13540	0,23						
			406,14610	406,14560	1,23						
			410,11746	410,11700	1,12						
EA2	289,279	C ₁₁ H ₁₉ N ₃ O ₆	272,12419	272,12410	0,33						
			290,13480	290,13470	0,34						
			294,10623	294,10600	0,78						
E2A	347,319	C ₁₃ H ₂₁ N ₃ O ₈	330,12983	330,12960	0,69						
			348,14045	348,14010	1						
			352,11183	352,11150	0,93						
A4	302,314	C ₁₂ H ₂₂ N ₄ O ₅	368,08584	368,08550	0,92						
			285,15588	285,15570	0,63						
			303,16649	303,16650	0,03						
EA3	360,354	C ₁₄ H ₂₄ N ₄ O ₇	343,16148	343,16120	0,76						
			361,17180	361,17180	0,88						
			365,14356	365,14320	0,98						
E2A2	418,394	C ₁₆ H ₂₆ N ₄ O ₉	419,17779	419,17730	1,16						
			423,14917	423,14860	1,34						
			459,17271	459,17220	1,11						
E3A	476,434	C ₁₈ H ₃₂ N ₄ O ₁₁	432,20940	432,20890	1,15						
			414,19877	414,19830	1,13						
			374,20378	374,20340	1,01						
E2A3	489,469	C ₁₉ H ₃₁ N ₅ O ₁₀	472,20442	472,20380	1,31						
			490,21512	490,21440	1,46						
			494,18640	494,18580	1,21						
E3A2	547,509	C ₂₁ H ₃₁ N ₅ O ₁₂	548,22059	548,21990	1,25						
			568,15714	568,15620	1,65						
			530,21008	530,20930	1,47						
E2A4	560,544	C ₂₂ H ₃₅ N ₆ O ₁₁	561,25247	561,25150	1,72						
			792,704	792,70480	1,26						
			797,24581	797,24480	1,26						
EA5	502,504	C ₂₀ H ₃₄ N ₆ O ₉	503,24670	503,24600	1,39						
			485,23664	485,23540	2,55						
			601,24743	601,24640	1,71						
E3A3	618,584	C ₂₄ H ₃₁ N ₆ O ₁₃	619,25789	619,25700	1,43						
			623,22917	623,22880	0,59						
			632,28964	632,28860	1,64						
E2A5	631,618	C ₂₅ H ₄₁ N ₇ O ₁₂	614,27880	614,27800	1,3						
			761,33226	761,3312	1,39						
E3A5	760,733	C ₁₆ H ₄₈ N ₈ O ₁₃	761,33226	761,3312	1,39						
E2A6	702,693	C ₂₈ H ₄₆ N ₈ O ₁₃	703,32682	703,3257	1,59						

Destino de las moléculas orgánicas

Sorción de aminoácidos

Ensayos de Química Prebiótica V

Resumen El proceso de sorción de moléculas orgánicas es fundamental para comprender los mecanismos que pudieron preceder los procesos de polimerización durante la evolución química. Aunque varios experimentos han demostrado la capacidad de sorción de diferentes minerales, la mayoría de esas simulaciones se han realizado utilizando agua destilada y/o modelos simples de agua de mar como entornos de reacción. De esta manera, el realizar experimentos que tengan en cuenta algunas de las variables geoquímicas, que pudieron estar presentes en algunos ambientes primitivos permite comprender de mejor manera los procesos de sorción que pudieron llevar a una mayor complejidad molecular. En este trabajo se realizó la sorción de glicina (Gly), alanina (Ala), ácido glutámico (Glu) y ácido aspártico (Asp) en serpentinita considerando un modelo de agua hidrotermal (HWM), enriquecida en iones Na^+ , Cl^- y Ca^{2+} . Los resultados sugieren que los iones disueltos mejoran la sorción de aminoácidos. Esto puede ser el resultado de la formación de puentes cationes entre los grupos COO^- de los aminoácidos y la carga superficial negativa de la serpentinita. Además, la formación de enlaces de hidrógeno y otro tipo de interacciones pueden contribuir en la interacción entre aminoácidos y minerales a diferentes valores de pH.

Papel de los iones en la sorción de aminoácidos en serpentinita: Ensayos de química prebiótica

Introducción

Varios experimentos han demostrado que es posible sintetizar una gran diversidad de aminoácidos (AAs) en diversos escenarios primitivos (*e.g.*, sistemas hidrotermales, interacciones superficie-atmósfera y/o meteoritos / cometas) (Miller 1953; Rode 1999; Muñoz Caro *et al.* 2002; Huber y Wachtershauser 2006; Aubrey *et al.* 2009; Burton *et al.* 2012). Sin embargo, se ha propuesto que la concentración de AAs en los océanos primitivos probablemente fue muy baja, del orden de 10^{-4} a 10^{-7} mol L⁻¹ (Stribling y Miller 1987; Zaia *et al.* 2008). En consecuencia, se necesitan mecanismos que favorezcan la concentración de estas moléculas orgánicas para llevar a cabo futuras reacciones de polimerización (*i.e.*, formación de oligopéptidos).

Minerales como agentes concentradores de moléculas orgánicas

Dependiendo de las condiciones fisicoquímicas del medio, las superficies minerales pueden concentrar diversas moléculas orgánicas a partir de disoluciones diluidas (Zaia 2004, 2012; Schoonen *et al.* 2004; Lambert 2008; Cleaves *et al.* 2012). No obstante, independientemente del escenario primitivo, estas disoluciones diluidas son más que la suma de un medio acuoso y compuestos orgánicos. Pocos experimentos han tomado en cuenta diversas variables geoquímicas acopladas (*i.e.*, iones, temperatura y diferentes valores de pH) en los fenómenos de sorción (Tessis *et al.* 1999; Franchi *et al.* 2003; Zaia 2012; Wei *et al.* 2012; Farias *et al.* 2014, 2016; Sebben y Pendleton 2015; Pandey *et al.* 2015; Pedreira-Segade *et al.* 2018; Villafaña-Barajas *et al.* 2018; Hao *et al.* 2019); y solo algunos de ellos han considerado un modelo de agua de mar representativo.

Sistemas hidrotermales y aminoácidos

Los sistemas hidrotermales, tanto subaéreos como submarinos, son considerados como entornos ideales para permitir el proceso de evolución química (Martin *et al.* 2008; Colín-García, *et al.* 2016, 2018). En particular, se ha propuesto que los sistemas hidrotermales con basamento de serpentina y los fluidos hidrotermales alcalinos liberados a partir del proceso de serpentización (ver Anexo) pudieron ofrecer condiciones favorables para el desarrollo de vías metabólicas primitivas debido a la disponibilidad de diferentes variables geoquímicas (*e.g.*, alta [Ca], [K], [Na], baja [Mg], pH > 9, alta [H₂]) y su amplia distribución durante los primeros 500 Ma en la historia de la Tierra (Schulte *et al.* 2006; Martin *et al.* 2008; Sleep *et al.* 2011; McCollom y Seewald 2013).

Las serpentinitas son rocas formadas principalmente por minerales del grupo de las serpentinas que se derivan del metamorfismo de rocas máficas-ultramáficas, las cuales fueron abundantes durante el Hadeano-Arqueano (Müntener 2010). En general, estos silicatos de magnesio se forman durante la hidratación a baja temperatura (*i.e.*, < 400 °C) de minerales ferromagnesianos o

magnesianos (*e.g.*, olivina, ortopiroxeno) presentes en rocas básicas y ultra básicas (Evans *et al.* 2013).

Los aminoácidos son esencialmente inestables a altas presiones y altas temperaturas (White 1984; Bernhardt *et al.* 1984; Bada *et al.* 1995). Sin embargo, nuevos experimentos que han considerado otras variables geoquímicas (*e.g.*, gradientes de temperatura y pH, iones y gases disueltos, minerales y estados redox) muestran que la estabilidad y el destino de estas moléculas orgánicas dependen de las condiciones ambientales. La glicina (Gly), la alanina (Ala), el ácido glutámico (Glu) y el ácido aspártico (Asp) se han sintetizado en condiciones hidrotermales y son los aminoácidos más abundantes recolectados *in situ* en sistemas hidrotermales submarinos (Yuasa *et al.* 1984). ; Horiuchi *et al.* 2004; Aubrey *et al.* 2009; Fuchida *et al.* 2014). Además, estas moléculas orgánicas se han identificado en fluidos hidrotermales reducidos y alcalinos (Lang *et al.* 2013), aunque se ha mencionado que su presencia podría estar asociada con la producción biológica local.

Fluidos hidrotermales y modelo de agua hidrotermal

La composición de los fluidos hidrotermales es el resultado de un continuo intercambio químico entre el agua oceánica y la litósfera. Varios procesos geoquímicos están involucrados en la formación de estos fluidos, tales como: reacciones entre agua-roca, la composición de la cámara magmática debajo de los campos hidrotermales, desgasificación magmática y/o la entrada de volátiles, separación de fases durante el enfriamiento, así como las diferencias en las condiciones hidrológicas en la zona de reacción (James *et al.* 2014). Por lo tanto, no es trivial generalizar su composición. Aun así, algunos investigadores han sugerido que los iones Na^+ , Ca^{2+} , Mg^{2+} y Fe^{2+} eran los predominantes en el agua oceánica y/o en los fluidos hidrotermales durante el Hadeano-Arqueano temprano (De Ronde *et al.* 1997; Zaia 2012; Hao *et al.* 2019).

A pesar de que se han realizado algunos experimentos de sorción utilizando serpentinita (Hashizume, H. 2007; Fornaro *et al.* 2018), ninguno de ellos ha considerado el papel de los iones disueltos en la sorción de aminoácidos en este mineral.

Por ello, se estudió la sorción de Gly, Ala, Glu y Asp (Fig.7.1) en serpentinita considerando un modelo de agua hidrotermal (*Hydrothermal Water Model, HWM*), con el fin de analizar el papel de los iones en el proceso de sorción de aminoácidos. Asimismo, se evaluaron diferentes condiciones de pH para estudiar las interacciones entre las moléculas orgánicas y la superficie mineral.

	Glicina (Gly)	Alanina (Ala)	Ácido glutámico (Glu)	Ácido aspártico (Asp)
	$\begin{array}{c} \text{O} \\ \parallel \\ \text{H}_2\text{N}-\text{CH}-\text{C}-\text{OH} \\ \\ \text{H} \end{array}$	$\begin{array}{c} \text{O} \\ \parallel \\ \text{H}_2\text{N}-\text{CH}-\text{C}-\text{OH} \\ \\ \text{CH}_3 \end{array}$	$\begin{array}{c} \text{O} \\ \parallel \\ \text{H}_2\text{N}-\text{CH}-\text{C}-\text{OH} \\ \\ \text{CH}_2-\text{CH}_2-\text{COOH} \end{array}$	$\begin{array}{c} \text{O} \\ \parallel \\ \text{H}_2\text{N}-\text{CH}-\text{C}-\text{OH} \\ \\ \text{CH}_2-\text{COOH} \end{array}$
pKa ₁ α-grupo carboxilo	2.34	2.34	2.19	1.88
pKa ₂ α-ion amonio	9.60	9.69	9.67	9.60
pKa ₃ α-grupo cadena lateral			4.25	3.65

Figura 7.1. Estructura química y valores de constantes de disociación de los aminoácidos utilizados en este trabajo.

Procedimiento Experimental

Los materiales así como las distintas técnicas de caracterización son descritos en el Capítulo III. La Figura 7.2 muestra el procedimiento experimental general para la elaboración de estos experimentos.

Modelo de agua hidrotermal. El modelo de agua hidrotermal, HWM, se preparó de acuerdo con Zaia (2012) (Tabla 7.1). Sin embargo, con base en el modelo original de Ronde (De Ronde *et al.* 1997), decidimos eliminar el aporte de NH_4^+ porque está asociado con la descomposición de materia orgánica o un subproducto de microorganismos, lo cual no es consistente con un modelo prebiótico. Aunque existen diferencias importantes entre la composición del modelo HWM y los fluidos hidrotermales actuales medidos *in situ* (James *et al.* 2014; Seyfried *et al.* 2015) (Tabla 7.1), en todos los casos predominan los iones $\text{Cl}^- \sim \text{Na}^+ \gg \text{Ca}^{2+} \sim \text{K}^+$.

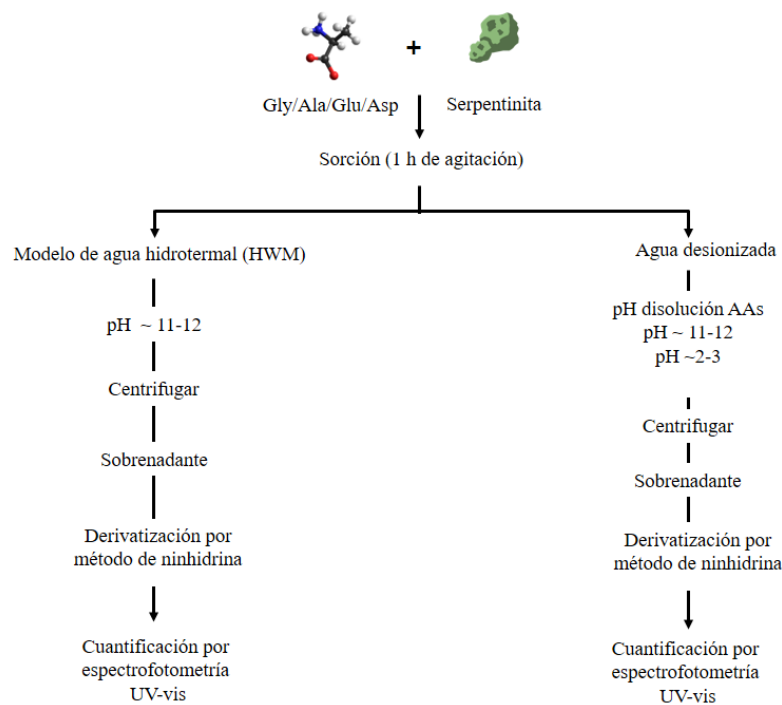


Figura 7.2. Procedimiento experimental para realizar la sorción de AAs en serpentinita

Resultados y discusión

La Figura 7.3 muestra los resultados de la sorción de los cuatro aminoácidos en serpentinita usando el HWM. El pH de las muestras de AAs/serpentinita en HWM tuvo valores entre $\text{pH} = 11 - 12$. El porcentaje de sorción para todos los aminoácidos utilizando el modelo hidrotermal es de alrededor del 50 %. En este intervalo de pH, como se muestra en la Figura 7.3, los aminoácidos están predominantemente en su forma aniónica (*i.e.*, $\geq 96\%$ Gly⁻, $\geq 95\%$ Ala⁻, $\geq 95\%$ Glu⁻², $\geq 95\%$ Asp⁻²). El punto de carga cero, a estos valores de pH, de la muestra de serpentinita es $\text{pH}_{\text{PZC}} \sim 8.5$ y, por lo tanto, en estas condiciones, la superficie mineral está cargada negativamente. En consecuencia, la simple interacción electrostática entre la superficie del mineral y los aminoácidos cargados negativamente no puede ser el mecanismo de sorción predominante (ver abajo).

Por otro lado, los experimentos realizados en agua destilada a pH básico mostraron que el porcentaje de sorción no supera el 20 % (Fig. 7.3). La diferencia de porcentaje de sorción entre los experimentos con el modelo de agua hidrotermal respecto a los realizados con agua destilada a pH básico, puede estar asociada con la presencia de los iones disueltos en el HWM. En contraste con estos resultados, algunos autores han demostrado que la alta concentración de sales reduce la sorción de AAs en algunos minerales (*e.g.*, arcillas, goethita, sílice; Farias *et al.* 2014, 2016;

Sebben y Pendleton 2015) y que el grupo R cargado de los AAs podría tener un papel crucial en el mecanismo de sorción (Benetoli *et al.* 2007). Sin embargo, cabe mencionar que ninguno de estos informes utiliza el mismo modelo de agua y la relación de cargas entre los AAs y los minerales no es completamente negativa.

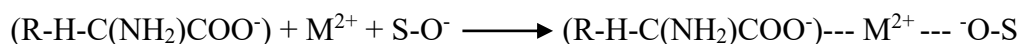
Tabla 7.1. Composición del modelo de agua hidrotermal (HWM) y de los fluidos hidrotermales naturales.

Iones (mmol L ⁻¹)	Composición de fluidos hidrotermales			
	Zaia (2012)	De Ronde <i>et al.</i> (1997)	James <i>et al.</i> (2014)	Seyfried <i>et al.</i> (2015)
Cl ⁻	688	920	552	542
Na ⁺	638	789	406	491
Br ⁻	2.6	2.25	---	0.844
SO ₄ ⁻²	---	2.3	---	4.12
I ⁻	6.02*10 ⁻⁵	0.037	---	---
NH ₄ ⁺	11.42	5.1	---	---
K ⁺	21.6	18.9	72.5	10.5
Mg ⁺²	---	50.9	---	1.9
Ca ⁺²	42.56	232	20	26.5
Sr ⁺²	0.04	4.52	69.5	0.101
Ambiente geológico				
	Composición sugerida de agua hidrotermal artificial 3.2 Ga pH ~12.	Fluidos ubicados en las dorsales oceánicas y en el ambiente tectónico tras-arco. Barbeton 3.2 Ga, Depósito de Hierro.	Composición de los fluidos terminales de las cuencas tras-arco. Basamento con [K ⁺] baja a media basalto/andesita basáltica (T ~310 °C and pH ~4.8). Cuenca tras-arco. «Trough, Iheya North Knoll »	Fluidos hidrotermales provenientes del campo hidrotermal Lost City. T ~116 °C and pH ~10.4. “BH, J2-360IGT2”.

Nota: El modelo de agua hidrotermal utilizado en este estudio fue básicamente el propuesto por Zaia (2012), excepto que no se utilizó amoniaco. Los reactivos se disolvieron en 1,0 litro de agua MiliQ.

La baja cantidad de aminoácidos sorbidos a pH básico en agua destilada (< 20 %) (Fig. 7.3) se puede explicar por diferentes mecanismos. De acuerdo con el diagrama de distribución de especies (Fig. 7.4), a los valores de pH experimentales, ~ 15 % de Gly y Ala están en su forma de zwitterion. Por tanto, los aminoácidos cargados en su grupo amino protonado pueden tener una

atracción electrostática hacia la superficie mineral que está cargada de manera opuesta. Otras opciones pueden ser mediante mecanismos no electrostáticos en ambiente acuosos, tales como: I) la formación de enlaces entre el grupo carboxilo del aminoácido y un átomo de la superficie mineral (*i.e.*, Si); II) formando un enlace coordinado del carboxilato (R-COO⁻) con los átomos de oxígeno de la superficie; III) a través de enlaces coordinados entre el AA y los iones divalentes en la superficie del oxihidróxido (*e.g.*, Fe²⁺, Mg²⁺); y/o por IV) la formación de complejos de esfera externa con aductos unidos por hidrógeno (Lambert 2008). Además, la posibilidad de formar "puentes catiónicos" entre el grupo carboxilato (R-H-C(NH₂)COO⁻) y el catión K⁺ disuelto (proveniente de la solución de KOH utilizada para preparar la muestra control a pH básico, ver métodos) con la superficie mineral con carga neta negativa. Dado que el Glu y el Asp tienen cargas negativas a pH básico, la sorción mediada por interacciones de "puente catiónico" podría ser el mecanismo de sorción predominante. Benetoli *et al.* (2007) reportaron una mayor sorción de Asp que Ala en caolinita (Al₂Si₂O₅(OH)₄) (con estructura similar a la serpentinita; polimorfo lizardita, Mg₃Si₂O₅(OH)₄) a pH = 8 y sugirieron que esta diferencia podría estar asociada con el grupo R cargado del Asp. Hashizume (2007) mostró que la capacidad de sorción de Asp y Glu por crisotilo, Mg₃(Si₂O₅)(OH)₄, a pH = 8 - 9, es mayor para los aminoácidos Gly y Ala; el autor asocia este resultado con las interacciones entre las cargas negativas de los AAs y los grupos silanol (S-OH₂⁺) en el borde del crisotilo así como a la baja solubilidad de Glu y Asp. Por lo tanto, la capacidad de sorción de los aminoácidos en la serpentinita, a pH básico, puede ser el resultado de mecanismos no electrostáticos y la probable formación de puentes catiónicos entre el grupo carboxilato y el K⁺ disuelto. Experimentos recientes muestran que la presencia de cationes divalentes (*e.g.*, Ca²⁺, Mg²⁺; M²⁺) y metales de transición (*e.g.*, Zn, Ni) pueden mejorar la sorción de oligonucleótidos porque pueden actuar como mediadores de unión entre ácidos nucleicos y superficies de arcilla debido a la capacidad de interactuar con el fosfato cargado negativamente del esqueleto del ácido nucleico (modelo de puente catiónico; Franchi *et al.* 2003; Pedreira-Segade *et al.* 2018; Hao *et al.* 2019). Mecanismos similares pueden ocurrir entre los aminoácidos y los grupos anfóteros de la serpentinita (S-OH, donde S es un átomo de superficie) a través del grupo carboxilo cargado negativamente, en los valores de pH del HWM:



Considerando el error experimental, el orden de sorción fue: Asp ~ Ala ~ Gly > Glu usando HWM (Fig. 7.3). Debido a que los aminoácidos tienen esencialmente la misma estructura química, estas diferencias podrían atribuirse a la cadena lateral (Fig. 7.1). Aunque el ácido glutámico y el ácido aspártico tienen doble carga negativa a pH básico, la sorción de Asp es mayor que el Glu (Fig. 7.3). La sorción de Ala y Gly es esencialmente la misma que el Asp. Se ha propuesto que la glicina y la alanina pueden formar complejos débiles con Na⁺ y especies estables con Ca²⁺ y Mg²⁺. El ácido glutámico y aspártico forman especies relativamente débiles con los cationes Na⁺, Ca²⁺ y Mg²⁺ (Bottari y Porto 1982; De Stefano *et al.* 1995). Además, el grupo carboxilo interactúa débilmente con Na⁺ y fuertemente con cationes divalentes (*i.e.*, Ca²⁺ y Mg²⁺) y los grupos amino no protonados interactúan débilmente con Ca²⁺ y Mg²⁺ (De Stefano *et al.* 2000). Rundberg *et al.*

(1994) demostraron que los cationes, como el Na^+ , pueden ser sorbidos en goethita formando un complejo de esfera externa a valores de pH por encima del punto de carga cero del mineral (superficie con carga negativa). Asimismo, la leucina, en su forma zwitteriónica, puede interactuar con los metales divalentes (*i.e.*, Cu^{2+} y Mg^{2+}) de las arcillas (Pandey *et al.* 2015). Otra posibilidad es la unión de grupos negativos (*i.e.*, COO^-) con sitios metálicos ubicados en el borde de los minerales (Hao *et al.* 2019). En consecuencia, se podría favorecer la formación de puentes catiónicos, mediados por los cationes disueltos en el agua hidrotermal, entre el grupo carboxilato y/o los grupos amino no protonados en los aminoácidos y la superficie serpentina. Esto podría explicar la mayor absorción de aminoácidos en entornos ricos en cationes en comparación con los experimentos realizados con agua destilada.

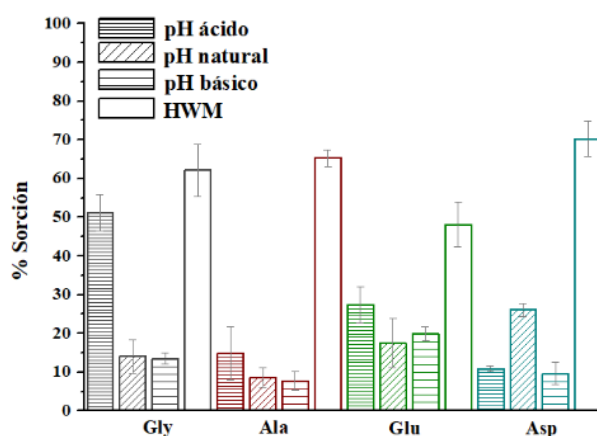


Figura 7.3. Porcentaje de sorción de aminoácidos a pH ácido, natural, básico y en presencia de iones disueltos, HWM. pH básico = 10-12, natural (pH natural de la solución de AA en agua desionizada) y pH ácido = 2-3, pH HWM = 11-12.

Para obtener más información sobre la función de los iones divalentes, se realizó la sorción de los AAs a pH básico (pH = 10 - 11) usando CaCl_2 (Fig. 7.5). Las diferencias del porcentaje de sorción muestran que el calcio tiene un efecto apreciable sobre la sorción de Gly y Ala, lo cual es consistente con la posibilidad de formar complejos estables entre estos aminoácidos con un catión divalente (Bottari y Porto 1982; De Stefano *et al.* 1995, 2000). Además, la cantidad sorbida de Gly es más alta que Ala. Debido a que la única diferencia entre estos aminoácidos es un grupo metilo, el impedimento estérico podría afectar el mecanismo de sorción a través de interacciones de puente catiónico. No hay diferencia entre la sorción de Glu y Asp en presencia de CaCl_2 en comparación con la solución de KOH (Fig. 7.5). Sin embargo, el Glu se absorbe un poco más que el Asp en ambos sistemas. Los resultados (Fig. 7.5) mostraron que el catión divalente (*i.e.*, Ca^{2+}) favorece la sorción hasta un 30 % en el caso de la glicina, pero es inferior al 20 % para el resto de aminoácidos. Por lo tanto, la gran capacidad de sorción de aminoácidos en la serpentinita,

utilizando el HWM, podría ser resultado de la contribución de todas las especies de cationes (*i.e.*, Na^+ (el catión predominante), Sr^{+2}) que componen el modelo de agua hidrotermal.

Las sorciones a pH natural muestran que Glu y Asp se sorben ligeramente más (~ 20 %) que Gly y Ala (Fig. 7.3). En estas condiciones, Gly y Ala están en su forma zwitterion. El Asp está esencialmente en su forma negativa y Glu está alrededor del 50:50% en su forma zwitteriónica y negativa. La superficie de la serpentinita está débilmente positiva en el valor de pH de las disoluciones de Gly, Ala y Asp; mientras que es predominantemente positiva en la disolución de Glu (Fig. 7.4). Hedges y Hare (1987) mostraron una tendencia similar usando caolinita a pH = 6 - 8. Estos autores sugirieron que una carga positiva apreciable en los bordes de los cristales de caolinita puede favorecer la mayor absorción de Asp.

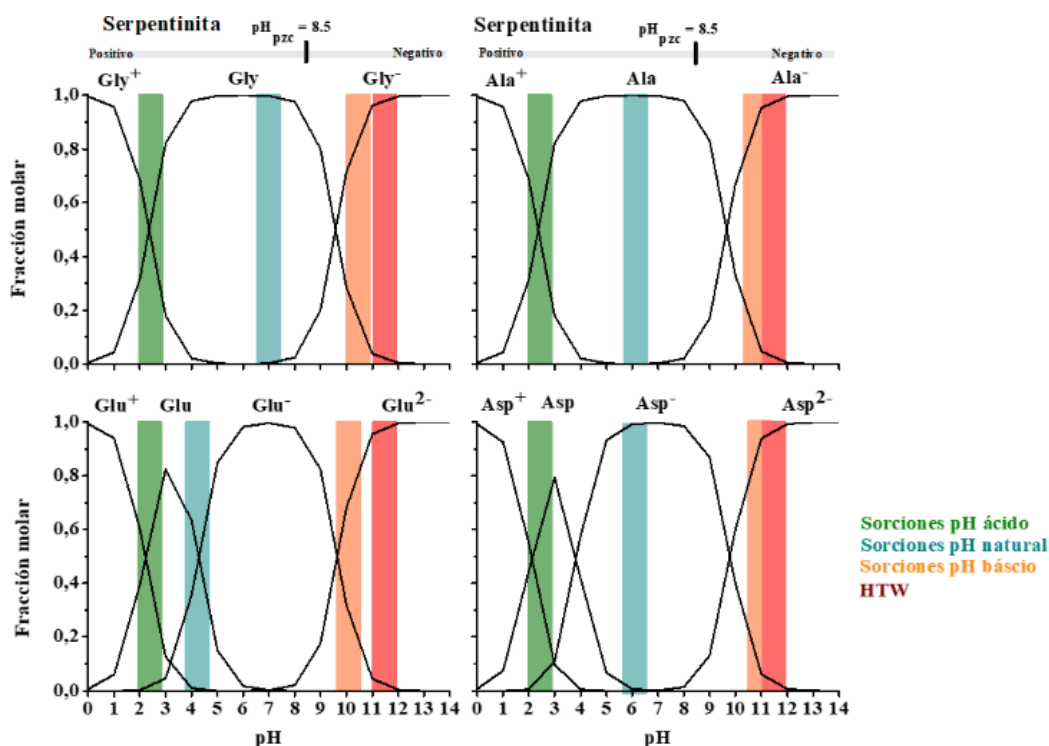


Figura 7.4. Diagrama de distribución de especies de los AAs usados respecto a la carga superficial de la serpentinita. El intervalo de pH de la solución de AA se muestra para cada experimento.

Finalmente, las sorciones a pH ácido muestran un comportamiento diferente (Fig. 7.3). El orden de sorción fue: Gly > Glu > Ala > Asp. En este intervalo de pH, todos los aminoácidos están en su forma zwitteriónica y protonada (~ 50:50 %) y la superficie mineral es predominantemente positiva. Aunque se ha demostrado que algunos minerales adsorben más aminoácidos con grupos R cargados (Zaia 2004), en nuestro caso, el sistema Gly/serpentinita mostró la mayor sorción a pH ácido.

Para obtener información sobre los mecanismos físico-químicos que podrían estar involucrados en la capacidad de sorción de la serpentinita, se realizó un análisis XRD para determinar el polimorfo de la serpentina. El patrón de difracción muestra picos de difracción distintivos de lizardita (91 %), antigorita (5 %) e impurezas típicas como magnetita y brucita (≈ 4 %) (Fig. 7.6). De esta manera, en nuestra muestra de serpentinita predomina el polimorfo de lizardita.

La lizardita tiene una fórmula estructural $M_3T_2O_5(OH)_4$, con capas planas 1:1 de láminas de tetraedro de SiO_4 y láminas de octaedro de $MgO_2(OH)_4$ unidas por enlaces de hidrógeno. M es principalmente Mg y T es Si, aunque varios elementos comunes pueden estar presentes en la estructura como $Fe^{2+,3+}$, Al^{3+} , Ni, Mn^{2+} , Zn^{2+} (Rucklidge y Zussman 1965; Mellini 1981; Zheng y Wang 2014). El politipo más común es el apilamiento de tres capas sin ningún desplazamiento lateral (Carmignano *et al.* 2020), en tanto que la disolución de los grupos hidroxilo de la superficie y los bordes deja una carga positiva en un amplio rango de pH (Feng *et al.* 2013). El agua en las estructuras cristalinas puede actuar como ácido de Lewis moderado o base de Lewis y puede controlar la polimerización dimensional de las unidades estructurales (*e.g.*, moderador de carga). En otras palabras, los enlaces de hidrógeno en la lizardita pueden impartir carácter catiónico en el lado (OH) y un carácter aniónico en el lado silicato (Hawthorne, 2015).

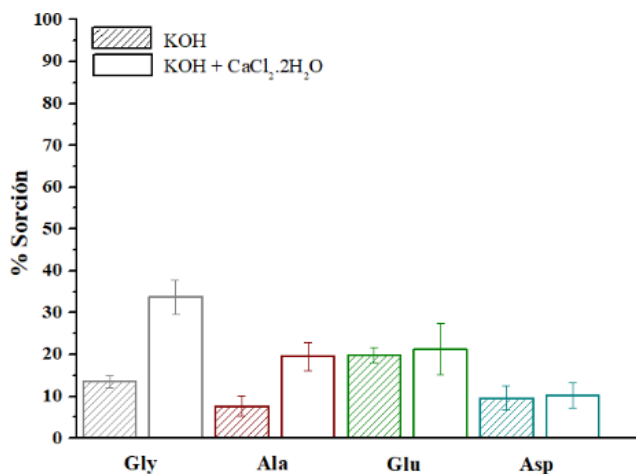


Figura 7.5. Porcentaje de sorción de aminoácidos a pH básico y usando $CaCl_2$. El catión Ca^{2+} parece favorecer la sorción de aminoácidos.

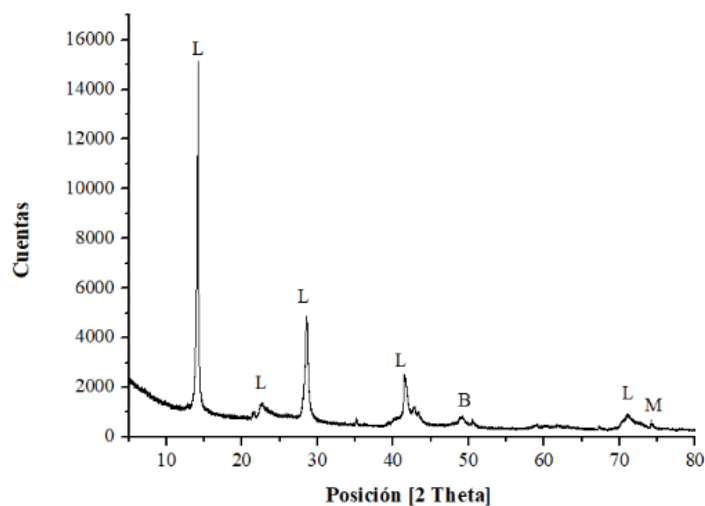


Figura 7.6. Patrón de difracción de rayos X de la muestra de serpentinita. Los picos de difracción se asignaron según Rucklidge y Zussman (1965) y Zheng y Wang (2014). Leyenda: (L) lizardita $\text{Mg}_3\text{Si}_2\text{O}_5(\text{OH})_4$, (M) magnetita (Fe_3O_4) y (B) brucita ($\text{Mg}(\text{OH})_2$).

El pH_{pzc} del mineral es crucial en el proceso de sorción, disolución, precipitación y formación de coloides durante la interface mineral-agua. La capacidad de formar capas de agua superficial en el material hidróxido conduce a sitios reactivos que pueden establecer especies superficiales cargadas (S-OH_2^+ y S-O^-) (Churchill *et al.* 2004). Además, otros iones adsorbentes, además del H^+ , pueden dar como resultado la configuración de otros complejos superficiales de aniones o cationes. Por lo tanto, la capacidad de formar enlaces de hidrógeno entre la superficie hidratada expuesta y los bordes protonados de la lizardita, a valores de pH por debajo de su pH_{pzc} , podrían ser los mecanismos que expliquen la capacidad de sorción $< 20\%$.

Otro experimento usando minerales de silicato, mostró que el ácido aspártico se sorbe débilmente en la caolinita a través de la complejación de iones aspartato de esfera externa en sitios de superficie de carga variable [las especies adsorbentes cargadas negativamente están unidas electrostáticamente a un grupo hidroxilo de superficie cargado positivamente (protonado)] (Ikhsan *et al.* 2004). El grupo carboxilo ionizado del ion aspartato se mantiene adyacente a la superficie. La capacidad de sorción (hasta un 20 %) varió ligeramente con el pH (Ikhsan *et al.* 2004). Además, algunos experimentos han informado que ciertos aminoácidos comunes se absorben en aproximadamente un 10 % en caolinita (Hedges y Hare 1987). Por otro lado, se ha demostrado que los aminoácidos básicos se sorben más que los aminoácidos neutros o ácidos debido a las reacciones de intercambio iónico con la superficie de la arcilla, cargada negativamente (Ramos y Huertas 2013). Ikhsan *et al.* (2004) informaron que el Asp se sorbe alrededor del 10 % a un pH = 3.5 y un 18 % a un pH = 8.5 a través de la formación de complejos de esfera externa de los iones de aspartato en sitios de superficie de carga variable. En otras palabras, cada especie cargada

negativamente se absorbe electrostáticamente a un grupo hidroxilo superficial cargado positivamente ($\text{SOH}_2^+ \text{-Asp}^-$).

En nuestro caso, en condiciones ácidas, la glicina podría ser absorbida a través del grupo R-COO^- del ion híbrido y los grupos S-OH_2^+ en la superficie del mineral, por la formación de complejos de esfera externa en los bordes de lizardita y/o mediante la formación de puentes de hidrógeno con la forma iónica híbrida. Las interacciones electrostáticas, la formación de puentes de hidrógeno, el intercambio de ligandos, las reacciones de intercambio iónico, las fuerzas de van der Waals y las interacciones específicas de los grupos carboxilo y amino, son mecanismos probables que explicarían el proceso de sorción de AA en minerales. Dado que la lizardita es un mineral que no se expande, las reacciones de intercambio entre capas no son posibles.

Conclusiones

En resumen, los fenómenos de sorción son más que una atracción electrostática. Los enlaces de hidrógeno, los enlaces coordinados y las interacciones de London/van der Waals pueden contribuir a la sorción de las moléculas orgánicas. Asimismo, fenómenos como la dependencia del pH de la superficie hidroxilada, la presencia de impurezas iónicas, que pueden cambiar el valor pH_{PZC} del mineral, la capacidad de sorber iones en óxidos por intercambio iónico con el catión estructural y/o por la formación de enlaces con los grupos hidroxilo de superficie (carga dependiente del pH) y la posibilidad de formar un puente catiónico entre el grupo carboxilato ($\text{R-H-C(NH}_2\text{)COO}^-$) y los cationes disueltos, deben ser considerado.

El proceso de sorción de las moléculas orgánicas es fundamental para comprender los mecanismos de polimerización que pudieron haber ocurrido durante las primeras etapas en la Tierra primitiva. Aunque varios experimentos han demostrado la capacidad de sorción de diferentes minerales, la mayoría de esas simulaciones se han realizado utilizando agua destilada o modelos simples de agua oceánica. De esta manera, es necesario realizar experimentos que tengan en cuenta algunas de las variables geoquímicas que probablemente estaban presentes en los ambientes primitivos. Esto permitirá tener un mejor entendimiento de los procesos de sorción que pudieron llevar a una mayor complejidad molecular. En este trabajo, se analizó la sorción de Gly, Ala, Glu y Asp en serpentinita considerando un modelo de agua hidrotermal (HWM), enriquecida en iones Na^+ , Cl^- y Ca^{2+} . Los resultados preliminares sugirieron que los iones disueltos aumentan la sorción de aminoácidos. Esto puede ser el resultado de la formación de puentes, mediados por los cationes presentes en solución, entre el grupo COO^- de los aminoácidos y la carga superficial negativa de la serpentinita. Además, la formación de puentes de hidrógeno y otro tipo de interacciones pueden ser relevantes en las interacciones entre aminoácidos y minerales a diferentes valores de pH.

Referencias

Aubrey AD, Cleaves HJ, Bada JL (2009) The Role of Submarine Hydrothermal Systems in the Synthesis of Amino Acids. *Origins of Life and Evolution of Biospheres* 39:91–108. <https://doi.org/10.1007/s11084-008-9153-2>

- Bada JL, Miller SL, Zhao M (1995) The stability of amino acids at submarine hydrothermal vent temperatures. *Origins of Life and Evolution of the Biosphere* 25:111–118. <https://doi.org/10.1007/BF01581577>
- Benetoli LOB, de Souza CMD, da Silva KL, et al (2007) Amino Acid Interaction with and Adsorption on Clays: FT-IR and Mössbauer Spectroscopy and X-ray Diffractometry Investigations. *Orig Life Evol Biosph* 37:479–493. <https://doi.org/10.1007/s11084-007-9072-7>
- Bernhardt G, Luedemann H-D, Jaenicke R, et al (1984) Biomolecules are unstable under 'black smoker' conditions. *Naturwissenschaften* 71:583–586. <https://doi.org/10.1007/BF01189186>
- Bottari E, Porto R (1982) Complex formation between glycine and magnesium (II), calcium(II), and iron(II) at 25 °C in 3.00M NaClO₄. *Monatsh Chem* 113:1245–1252. <https://doi.org/10.1007/BF00808739>
- Burton AS, Stern JC, Elsilá JE, et al (2012) Understanding prebiotic chemistry through the analysis of extraterrestrial amino acids and nucleobases in meteorites. *Chemical Society Reviews* 41:5459. <https://doi.org/10.1039/c2cs35109a>
- Carmignano ORD, Vieira SS, Brandão PRG, et al (2020) Serpentinites: Mineral Structure, Properties and Technological Applications. *Journal of the Brazilian Chemical Society* 31:2–14
- Churchill H, Teng H, Hazen RM (2004) Correlation of pH-dependent surface interaction forces to amino acid adsorption: Implications for the origin of life. *American Mineralogist* 89:1048–1055. <https://doi.org/10.2138/am-2004-0716>
- Colín-García, M., & Ortega-Gutiérrez, F., & Heredia, A., & Negrón-Mendoza, A., & Ramos-Bernal, S., & Cordero, G., & Camprubí, A., & Beraldi, H. (2016) Hydrothermal vents and prebiotic chemistry: a review. *Boletín de la Sociedad Geológica Mexicana* 68 (3):599–620
- Colín-García M, Villafañe-Barajas S, Camprubí A, et al (2018) 5.4 Prebiotic Chemistry in Hydrothermal Vent Systems. *Handbook of Astrobiology* 297
- De Ronde CEJ, Channer DM deR., Faure K, et al (1997) Fluid chemistry of Archean seafloor hydrothermal vents: Implications for the composition of circa 3.2 Ga seawater. *Geochimica et Cosmochimica Acta* 61:4025–4042. [https://doi.org/10.1016/S0016-7037\(97\)00205-6](https://doi.org/10.1016/S0016-7037(97)00205-6)
- De Stefano C, Foti C, Gianguzza A, et al (1995) Chemical speciation of amino acids in electrolyte solutions containing major components of natural fluids. *Chemical Speciation & Bioavailability* 7:1–8. <https://doi.org/10.1080/09542299.1995.11083234>
- De Stefano C, Foti C, Gianguzza A, Sammartano S (2000) The interaction of amino acids with the major constituents of natural waters at different ionic strengths. *Marine Chemistry* 72:61–76. [https://doi.org/10.1016/S0304-4203\(00\)00067-0](https://doi.org/10.1016/S0304-4203(00)00067-0)
- Evans BW, Hattori K, Baronnet A (2013) Serpentinite: What, Why, Where? *Elements* 9:99–106. <https://doi.org/10.2113/gselements.9.2.99>
- Farias APSF, Carneiro CEA, de Batista Fonseca IC, et al (2016) The adsorption of amino acids and cations onto goethite: a prebiotic chemistry experiment. *Amino Acids* 48:1401–1412. <https://doi.org/10.1007/s00726-016-2191-6>

- Farias APSF, Tadayozzi YS, Carneiro CEA, Zaia DAM (2014) Salinity and pH affect Na⁺ - montmorillonite dissolution and amino acid adsorption: a prebiotic chemistry study. *International Journal of Astrobiology* 13:259–270. <https://doi.org/10.1017/S1473550414000044>
- Feng B, Lu Y, Feng Q, et al (2013) Mechanisms of surface charge development of serpentine mineral. *Transactions of Nonferrous Metals Society of China* 23:1123–1128. [https://doi.org/10.1016/S1003-6326\(13\)62574-1](https://doi.org/10.1016/S1003-6326(13)62574-1)
- Fornaro T, Brucato JR, Feuillie C, et al (2018) Binding of Nucleic Acid Components to the Serpentinite-Hosted Hydrothermal Mineral Brucite. *Astrobiology* 18:989–1007. <https://doi.org/10.1089/ast.2017.1784>
- Franchi M, Ferris JP, Gallori E (2003) Cations as mediators of the adsorption of nucleic acids on clay surfaces in prebiotic environments. *Orig Life Evol Biosph* 33:1–16
- Fuchida S, Mizuno Y, Masuda H, et al (2014) Concentrations and distributions of amino acids in black and white smoker fluids at temperatures over 200°C. *Organic Geochemistry* 66:98–106. <https://doi.org/10.1016/j.orggeochem.2013.11.008>
- González-Mancera G, Ortega-Gutiérrez F, Proenza JA, Atudorei V (2009) Petrology and geochemistry of Tehuizingo serpentinites (Acatlán Complex, SW Mexico). *Boletín de la Sociedad Geológica Mexicana* 61:419–435
- Hao J, Mokhtari M, Pedreira-Segade U, et al (2019) Transition Metals Enhance the Adsorption of Nucleotides onto Clays: Implications for the Origin of Life. *ACS Earth Space Chem* 3:109–119. <https://doi.org/10.1021/acsearthspacechem.8b00145>
- Hashizume, H. (2007) Adsorption of Some Amino Acids by Chrysotile. *Viva Origino* 35, 60–65:
- Hawthorne FC (2015) Toward theoretical mineralogy: A bond-topological approach. *American Mineralogist* 100:696–713. <https://doi.org/10.2138/am-2015-5114>
- Hedges JJ, Hare PE (1987) Amino acid adsorption by clay minerals in distilled water. *Geochimica et Cosmochimica Acta* 51:255–259. [https://doi.org/10.1016/0016-7037\(87\)90237-7](https://doi.org/10.1016/0016-7037(87)90237-7)
- Horiuchi T, Takano Y, Ishibashi J, et al (2004) Amino acids in water samples from deep sea hydrothermal vents at Suiyo Seamount, Izu-Bonin Arc, Pacific Ocean. *Organic Geochemistry* 35:1121–1128. <https://doi.org/10.1016/j.orggeochem.2004.06.006>
- Huber C, Wachtershauser G (2006) -Hydroxy and -Amino Acids Under Possible Hadean, Volcanic Origin-of-Life Conditions. *Science* 314:630–632. <https://doi.org/10.1126/science.1130895>
- Ibanez JG, Hernandez-Esparza M, Doria-Serrano C, et al (2008) The Point of Zero Charge of Oxides. In: *Environmental Chemistry*. Springer New York, New York, NY, pp 70–78
- Ikhsan J, Johnson BB, Wells JD, Angove MJ (2004) Adsorption of aspartic acid on kaolinite. *Journal of Colloid and Interface Science* 273:1–5. <https://doi.org/10.1016/j.jcis.2004.01.061>
- James Cleaves II H, Michalkova Scott A, Hill FC, et al (2012) Mineral–organic interfacial processes: potential roles in the origins of life. *Chem Soc Rev* 41:5502. <https://doi.org/10.1039/c2cs35112a>

- James RH, Green DRH, Stock MJ, et al (2014) Composition of hydrothermal fluids and mineralogy of associated chimney material on the East Scotia Ridge back-arc spreading centre. *Geochimica et Cosmochimica Acta* 139:47–71. <https://doi.org/10.1016/j.gca.2014.04.024>
- Lambert J-F (2008) Adsorption and Polymerization of Amino Acids on Mineral Surfaces: A Review. *Origins of Life and Evolution of Biospheres* 38:211–242. <https://doi.org/10.1007/s11084-008-9128-3>
- Lang SQ, Früh-Green GL, Bernasconi SM, Butterfield DA (2013) Sources of organic nitrogen at the serpentinite-hosted Lost City hydrothermal field. *Geobiology* 11:154–169. <https://doi.org/10.1111/gbi.12026>
- Martin W, Baross J, Kelley D, Russell MJ (2008) Hydrothermal vents and the origin of life. *Nature Reviews Microbiology*. <https://doi.org/10.1038/nrmicro1991>
- McCullom TM, Seewald JS (2013) Serpentinites, Hydrogen, and Life. *Elements* 9:129–134. <https://doi.org/10.2113/gselements.9.2.129>
- Mellini M (1981) Crystal structure of lizardite 1T. *Acta Crystallogr A Found Crystallogr* 37:C189–C189. <https://doi.org/10.1107/S0108767381093902>
- Miller SL (1953) A Production of Amino Acids Under Possible Primitive Earth Conditions. *Science* 117:528–529. <https://doi.org/10.1126/science.117.3046.528>
- Mundo, B., Cruz, A. y Colin M (2017) Cuantificación de aminoácidos libres por reacción con ninhidrina
- Muñoz Caro GM, Meierhenrich UJ, Schutte WA, et al (2002) Amino acids from ultraviolet irradiation of interstellar ice analogues. *Nature* 416:403–406. <https://doi.org/10.1038/416403a>
- Müntener O (2010) Serpentine and serpentization: A link between planet formation and life. *Geology* 38:959–960
- Pandey P, Pant CK, Gururani K, et al (2015) Affinity of Smectite and Divalent Metal Ions (Mg²⁺, Ca²⁺, Cu²⁺) with L-leucine: An Experimental and Theoretical Approach Relevant to Astrobiology. *Orig Life Evol Biosph* 45:411–426. <https://doi.org/10.1007/s11084-015-9437-2>
- Pedreira-Segade U, Michot LJ, Daniel I (2018) Effects of salinity on the adsorption of nucleotides onto phyllosilicates. *Phys Chem Chem Phys* 20:1938–1952. <https://doi.org/10.1039/C7CP07004G>
- Ramos ME, Huertas FJ (2013) Adsorption of glycine on montmorillonite in aqueous solutions. *Applied Clay Science* 80–81:10–17. <https://doi.org/10.1016/j.clay.2013.05.007>
- Rode BM (1999) Peptides and the origin of life¹. *Peptides* 20:773–786. [https://doi.org/10.1016/S0196-9781\(99\)00062-5](https://doi.org/10.1016/S0196-9781(99)00062-5)
- Rucklidge JC, Zussman J (1965) The crystal structure of the serpentine mineral, lizardite Mg₃Si₂O₅(OH)₄. *Acta Cryst* 19:381–389. <https://doi.org/10.1107/S0365110X65003493>
- Rundberg RS, Albinsson Y, Vannerberg K (1994) Sodium Adsorption onto Goethite as a Function of pH and Ionic Strength. *Radiochimica Acta* 66–67:. <https://doi.org/10.1524/ract.1994.6667.special-issue.333>

- Schoonen M, Smirnov A, Cohn C (2004) A Perspective on the Role of Minerals in Prebiotic Synthesis. *AMBIO: A Journal of the Human Environment* 33:539–551. <https://doi.org/10.1579/0044-7447-33.8.539>
- Schulte M, Blake D, Hoehler T, McCollom T (2006) Serpentinization and Its Implications for Life on the Early Earth and Mars. *Astrobiology* 6:364–376. <https://doi.org/10.1089/ast.2006.6.364>
- Sebben D, Pendleton P (2015) Analysis of ionic strength effects on the adsorption of simple amino acids. *Journal of Colloid and Interface Science* 443:153–161. <https://doi.org/10.1016/j.jcis.2014.12.016>
- Seyfried WE, Pester NJ, Tutolo BM, Ding K (2015) The Lost City hydrothermal system: Constraints imposed by vent fluid chemistry and reaction path models on seafloor heat and mass transfer processes. *Geochimica et Cosmochimica Acta* 163:59–79. <https://doi.org/10.1016/j.gca.2015.04.040>
- Sleep NH, Bird DK, Pope EC (2011) Serpentinite and the dawn of life. *Phil Trans R Soc B* 366:2857–2869. <https://doi.org/10.1098/rstb.2011.0129>
- Stribling R, Miller SL (1987) Energy yields for hydrogen cyanide and formaldehyde syntheses: The hcn and amino acid concentrations in the primitive ocean. *Origins of Life and Evolution of the Biosphere* 17:261–273. <https://doi.org/10.1007/BF02386466>
- Tessis AC, Penteadó-Fava A, Pontes-Buarque M, et al (1999) [No title found]. *Origins of Life and Evolution of the Biosphere* 29:361–374. <https://doi.org/10.1023/A:1006535029107>
- Villafañe-Barajas SA, Baú JPT, Colín-García M, et al (2018) Salinity Effects on the Adsorption of Nucleic Acid Compounds on Na-Montmorillonite: a Prebiotic Chemistry Experiment. *Origins of Life and Evolution of Biospheres* 48:181–200. <https://doi.org/10.1007/s11084-018-9554-9>
- Wei Y, Thyparambil AA, Latour RA (2012) Peptide-Surface Adsorption Free Energy Comparing Solution Conditions Ranging from Low to Medium Salt Concentrations. *ChemPhysChem* 13:3782–3785. <https://doi.org/10.1002/cphc.201200527>
- White RH (1984) Hydrolytic stability of biomolecules at high temperatures and its implication for life at 250 °C. *Nature* 310:430–432. <https://doi.org/10.1038/310430a0>
- Yuasa S, Flory D, Basile B, Oró J (1984) On the abiotic formation of amino acids I. HCN as a precursor of amino acids detected in extracts of lunar samples II. Formation of HCN and amino acids from simulated mixtures of gases released from lunar samples. *Journal of Molecular Evolution* 20:52–58. <https://doi.org/10.1007/BF02101985>
- Zaia DAM (2004) A review of adsorption of amino acids on minerals: Was it important for origin of life? *Amino Acids* 27:1–10. <https://doi.org/10.1007/s00726-004-0106-4>
- Zaia DAM (2012) Adsorption of amino acids and nucleic acid bases onto minerals: a few suggestions for prebiotic chemistry experiments. *International Journal of Astrobiology* 11:229–234. <https://doi.org/10.1017/S1473550412000195>
- Zaia DAM, Zaia CTBV, De Santana H (2008) Which Amino Acids Should Be Used in Prebiotic Chemistry Studies? *Origins of Life and Evolution of Biospheres* 38:469–488. <https://doi.org/10.1007/s11084-008-9150-5>

Zheng SM, Wang KM (2014) Preparation and Characterization of Lizardite. AMM 556–562:109–112.
<https://doi.org/10.4028/www.scientific.net/AMM.556-562.109>

Conclusiones generales

Los experimentos que tratan de entender el papel que pudieron tener los sistemas hidrotermales, tanto submarinos como subaéreos, en los procesos de evolución química y en las etapas previas al surgimiento de las componentes básicas de la vida se han modificado en los últimos años. Actualmente, sabemos que algunas de las condiciones que imperan en estos ambientes favorecen la generación y evolución de moléculas orgánicas. Debido a que los sistemas hidrotermales son ambientes muy dinámicos y con numerosas variables geoquímicas, es necesario realizar experimentos que consideren la mayor cantidad de ellas con el objetivo de desarrollar una química prebiótica con modelos más consistentes y robustos.

En este trabajo se realizó un estudio sistemático partiendo de la justificación de un escenario geoquímico consistente con las probables condiciones en la Tierra primitiva, esto es, el destino del ácido cianhídrico en sistemas hidrotermales. Después, se identificaron las condiciones fisicoquímicas que favorecen la transformación del HCN en moléculas más complejas, es decir, polímeros térmicos de HCN. Así mismo, se realizó un estudio detallado de las propiedades térmicas y estructurales de estos materiales así como el efecto de la presencia de superficies minerales durante su síntesis. Se identificaron las condiciones fisicoquímicas que favorecen la liberación de una amplia diversidad de moléculas orgánicas a partir de la hidrólisis de estos materiales. Finalmente, se realizaron simulaciones experimentales enfocadas en el destino de algunas de las moléculas orgánicas obtenidas a partir de la hidrólisis de los polímeros de HCN. En este caso, los aminoácidos. Por un lado, se estudió la oligomerización del sistema Ala + Glu en presencia de sílica, SiO₂, tanto en condiciones hidrotermales submarinas (*e.g.*, altas presiones y temperaturas) y subaeras (*e.g.*, ciclos mojado-secado). Por otro lado, se estudió el efecto de iones disueltos en la sorción de aminoácidos en serpentinita considerando un modelo de agua hidrotermal. Los resultados obtenidos se engloban en el estudio del efecto de diversas variables geoquímicas, presentes en escenarios hidrotermales, tanto en la estabilidad, la reactividad y el destino de diversas moléculas orgánicas desde el punto de vista de la química prebiótica. Considerando lo anterior, el carácter sistemático de los experimentos realizados se puede concluir de la siguiente manera:

1) *Relevancia del escenario geoquímico.* Hasta ahora, no existe una propuesta única de un entorno primitivo que pueda contribuir con todas las condiciones para el desarrollo de una estructura orgánica compleja. Sin embargo, el dinamismo que presentan los sistemas hidrotermales parece ser un buen punto de partida. Sin embargo, debe tenerse en cuenta que cualquier experimento que simule algunas de las condiciones presentes en estos sistemas debe ser claro en la escala que simula, y por lo tanto, ser consistente con las condiciones fisicoquímicas que prevalecen en esas escalas. Asimismo, es necesario ser cauteloso y coherente con el alcance de los resultados para

evitar sobreestimaciones sobre el papel de estos sistemas en la evolución química y eventualmente, en el origen de la vida. En nuestro caso, un escenario hidrotermal con la continua aportación de materia prima (*e.g.*, CH₄, NH₃, CO₂) pudo llevar a la formación de HCN. Una vez disponible esa molécula orgánica y en concentraciones > 0.1 mol L⁻¹, un ambiente alcalino (pH > 8.5) favorecería su polimerización. Además, las altas temperaturas (≈ 100 °C) podrían favorecer su polimerización. Finalmente, la presencia de superficies minerales podrían afectar las propiedades térmicas y estructurales de estos materiales.

2) Disponibilidad de materia prima para llevar a cabo reacciones químicas y estudio de las condiciones de síntesis, la estabilidad y reactividad de compuestos orgánicos. La síntesis de un polímero térmico de HCN, simulando algunas de las condiciones presentes en sistemas hidrotermales alcalinos, refuerzan las hipótesis sobre la relevancia de estos entornos para la síntesis orgánica durante la Tierra primitiva. Actualmente, es claro que los polímeros de HCN son un grupo enorme de macromoléculas y su estudio requiere el uso de diferentes técnicas analíticas. El polímero sintetizado en este experimento es muy complejo y presenta propiedades químicas diferentes a las de los polímeros caracterizados considerando otras condiciones de síntesis. Después de su hidrólisis (*i.e.*, a pH ácidos y básicos), fue posible caracterizar un amplio espectro de moléculas orgánicas que podrían estar disponibles en los alrededores de los sistemas hidrotermales (*e.g.*, aminoácidos, ácidos carboxílicos, N-heterociclos) y en consecuencia, ser nichos ideales para la evolución química. Estos resultados respaldan propuestas como los mundos de pre-RNA.

3) Destino de las moléculas orgánicas en sistemas hidrotermales alcalinos. Una vez que el medio circundante al sistema hidrotermal se enriquezca en material orgánico, las moléculas orgánicas podrán experimentar diversos fenómenos. En particular, durante este trabajo nos centramos en el fenómeno de polimerización de una mezcla de aminoácidos en presencia de minerales (Ala + Glu/SiO₂). Notablemente, tanto en condiciones acuosas como secas, es posible sintetizar oligómeros heterogéneos largos (*i.e.*, nonameros). Estos resultados contribuyen a un mejor entendimiento del efecto de la presencia de minerales así como de las condiciones de reacción en la formación de oligopéptidos sencillos. Por otro lado, se estudió el efecto de iones disueltos en la sorción de aminoácidos en serpentinita considerando un modelo de agua hidrotermal. Este modelo es consistente con la composición de fluidos hidrotermales alcalinos y se toma como punto de partida para entender los procesos de sorción de moléculas orgánicas en minerales. Los resultados preliminares sugieren que la presencia de cationes podría favorecer la formación de puentes entre orgánico-mineral, actuado como anclajes y favoreciendo su concentración.

Los experimentos realizados en este trabajo son una primera aproximación para entender el dinamismo de los sistemas hidrotermales, así como su papel de modelos de ambientes primitivos. Particularmente, se desarrolló un camino de evidencias experimentales que sostienen que a partir de una molécula relativamente sencilla como es el ácido cianhídrico y en un entorno geoquímico consistente con la Tierra primitiva, es posible alcanzar cierta complejidad química. En otras palabras, obtener oligopéptidos lineales a partir del HCN. Los resultados sugieren que el desarrollo de experimentos que combinen diversas variables geoquímicas tiene repercusiones importantes en el comportamiento del sistema. En consecuencia, este trabajo contribuye en un mejor entendimiento de los procesos que pudieron tener lugar en el desarrollo de la complejidad química

en los sistemas hidrotermales. Si bien esta investigación se centra en estudiar el destino del HCN en los sistemas hidrotermales alcalinos y su impacto en la evolución química, las condiciones para su síntesis se aplican fácilmente a la ciencia de materiales. Asimismo, caracterizar sus propiedades fisicoquímicas puede ser útil para otros enfoques y expandirse a otras áreas de investigación.

ANEXO I

Sistemas Hidrotermales Submarinos: La relevancia de los sistemas dinámicos en la Evolución Química y sus consecuencias en la Química Prebiótica

Artículo de revisión

Villafañe-Barajas, S. A. y Colin-García M. Submarine Hydrothermal Vents Systems: The relevance of dynamic systems in chemical evolution, and aftermath in prebiotic chemistry
(Enviado *IJA*)

Resumen Desde su descubrimiento, los sistemas hidrotermales submarinos han sido señalados como sitios importantes para el desarrollo de diversos procesos durante la evolución química así como su probable papel en escenarios de origen de la vida. Sin embargo, las simulaciones experimentales que consideran las condiciones geoquímicas presentes en estos entornos se han enfocado en una parte muy específica de estos sistemas. Si bien el dinamismo de estos ambientes es evidente, es necesario tener claridad en la escala del sistema así como el alcance de los resultados experimentales para no sobrestimar las hipótesis sobre el papel de estos escenarios en cuestiones de origen de la vida. En esta revisión intentamos comunicar cómo se puede interpretar este dinamismo y su importancia en los experimentos de química prebiótica

Submarine Hydrothermal Vents Systems: The relevance of dynamic systems in chemical evolution, and aftermath in prebiotic chemistry

Saúl A. Villafañe-Barajas^{1*}, María Colín-García²

¹Posgrado en Ciencias de la Tierra, Universidad Nacional Autónoma de México, Ciudad Universitaria, 04510 Cd. Mx, Mexico.

²Instituto de Geología, Universidad Nacional Autónoma de México, Ciudad Universitaria, 04510 Cd. Mx, Mexico.

***Corresponding author information:** saulvillafanephd@gmail.com

Saúl Alberto Villafañe-Barajas

Adress: Investigación Científica, Copilco Universidad, Coyoacán, 04510, Ciudad Universitaria, Ciudad de México, México

Telephone: +52 55 7878 5536

e-mail:saulvillafanephd@gmail.com

Abstract: Since their discovery, the submarine hydrothermal vents systems have been pointed out as important sites for the development of several processes during chemical evolution and their probable role related with origin of life scenarios. However, the experimental simulations that consider the geochemical conditions present in these environments have been focused in a specific part of these systems. Although the dynamism of these environments is evident, it is necessary to be clear in the scale of the venting as well as in the scope of the experimental results in order not to overestimate the results and hypothesis. In this review, we try to communicate how this dynamism can be interpreted as well their importance on prebiotic chemistry experiments.

Keywords: submarine hydrothermal vents systems; chemical evolution niches; early earth; dynamic systems; prebiotic chemistry

Introduction

Before the discovery of submarine hydrothermal vents systems (**SHVS**) (Corliss et al. 1979), some scientists pointed out the importance of high temperatures in the first steps along the formation of life. Markedly, R. B. Harvey suggested the thermal spring environments as probable scenarios for the emergence of life (Harvey 1924). On the other hand, S. Fox (1967), D. E. Ingmanson and M. J. Dowler (1977) suggested that temperature gradients would be important for the generation and evolution of organic compounds under high temperature environments (*e.g.*, brine pools associated with the axes of plate spreading, and hot springs associated with submarine volcanism). A few years after, J. B. Corliss, J. A. Baross and S. E. Hoffman (1981; 1985) suggested that these environments “provide all conditions necessary for the creation of life on Earth” as consequence of the discovery of the first SHVS, the “Clambake 1” (Ballard 1977) . These authors proposed the possibility that life could have originated in a Precambrian hydrothermal oceanic system, based on chemosynthesis processes, as result of reactions through gradients of temperature, pH, and chemical composition.

As soon as these proposals permeated the scientific community, several scientists tried to test them experimentally. The first approximations showed that the organic molecules (*e.g.*, amino acids, carboxylic acids, and nitrogen bases) are mainly decomposed at high temperatures (> 100 °C) (Vallentyne 1964; Povoledo and Vallentyne 1964; White 1984; Bernhardt et al. 1984; Miller and Bada 1988; Qian et al. 1993; Bell et al. 1994; Bada et al. 1995; Larralde et al. 1995; Kohara et al. 1997; Levy and Miller 1998). Hence, S. Miller, J. Bada and A. Lazcano (Miller and Bada 1988; Bada et al. 1995; Miller and Lazcano 1995; Bada and Lazcano 2002) argued that submarine

hydrothermal conditions, still at some stage in the thermal gradient (*i.e.*, even considering low temperatures, > 25 °C), are hostile environments because the organic molecules are essentially decomposed after their synthesis. In addition, these authors considered that the most probable contribution of those environments was rather the chemical regulation of the ocean-atmosphere system during the early Earth (*e.g.*, contribution of metals and dissolved ions). However, they did not discard that “some protective mechanisms” may have been available in hydrothermal systems and they could have improved the stability of the organic molecules.

Nowadays, several researchers have taken into account some of previous ideas and they have proposed interesting hypothesis about the steps that could led to the formation of the first living organisms in this kind of environments (Wächtershäuser 2006; Martin et al. 2008; Lane and Martin 2012; Herschy et al. 2014; Sojo et al. 2016; Barge and White 2017). However, although these environments harbor the basic requirements for life (*i.e.* energy, water, and organic molecules; Omran and Pasek 2020), there are several questions that still need to be resolved. For example, the decomposition of biomolecules *vs* their polymerization in aqueous medium, and the formation of lipid-membranes under high salt concentration (Cleaves et al. 2009; Deamer and Georgiou 2015).

In consequence, whether or not life originated in environments like SHVS, a possibility so far unproven, it is necessary to constrain the most feasible submarine hydrothermal vent scenario for chemical evolution to accomplish. In this sense, our goal in this paper is not to justify the emergence of life in these environments. The idea is to describe, according to our experience, what could be the physic-chemical scenario in primitive submarine hydrothermal vents systems that could have allowed the chemical evolution.

Early Earth environment

The Earth was and still remains as a dynamic system. New evidence, supported by detrital zircons, suggest: 1) the probable presence of liquid water on planet surface along the first 1000 Ma of the Earth's history, 2) a proto-continental crust composed by granitic rocks (TTG), 3) the presence of fluvial erosion processes, and 4) continental crust recycling during subduction events (Cavosie et al. 2007; Harrison 2009; Sleep 2010; Kemp et al. 2010; Arndt and Nisbet 2012; Trail et al. 2013; Boehnke et al. 2018). In consequence, probably, an intense hydrothermal activity was present during the Hadean and the early Archean. This could have allowed the transport of organic compounds, gases, ions, metals and minerals on these environments (Kelley 2005; Golding et al. 2011; Stüeken et al. 2013). This intense hydrothermal activity led to great changes on the geochemical processes on Primitive Earth, such as: 1) a great hydrothermal mineral deposits formation, 2) the synthesis of organic molecules, 3) an enrichment of gases and dissolved ions in a neutral-alkaline ocean, and 4) the formation of oligomers and polymers as a prelude to biomolecules (Sleep et al. 2004; Schulte et al. 2006; Hazen et al. 2008; Novoselov and Silantyev 2010; Papineau 2010; Schrenk et al. 2013; Wang et al. 2014; Shibuya et al. 2015; Morrison et al. 2018; Villafañe-Barajas et al. 2020a, b). Therefore, it is very likely that SHVS were present and were abundant on early Earth, so they could have acted as niches of chemical evolution to accomplish.

Submarine hydrothermal vents systems: dynamic systems

The complexity of SHVS is intrinsically linked to a highly dynamic environment. The convection processes in SHVS can be separated into three spatial scales of venting: I) the flow coming from a single hydrothermal chimney (smokers) (10 m^2), II) the vent field that includes all active hydrothermal fluids (both at low, $< 100 \text{ }^\circ\text{C}$, and high temperatures, $< 400 \text{ }^\circ\text{C}$) (100 m^2), and III) the active ridge segment (10 km^2) that include hydrothermal deposits and venting sites (Little et al.

1987). Thence, it is possible to consider these hydrothermal fields, in an overall way, as a dynamic system resulted of a constant interaction among the hydrothermal fluids coming from several sources (*e.g.*, rich array of plumes, poly-metallic mounds, chimneys, buoyancy fluxes and currents along topography). The hydrothermal field can be dominated by one single vents, several vents with enough separation or by clustering vents that can interact with each other (Lupton et al. 1985; Tao et al. 2013) (Fig. 1).

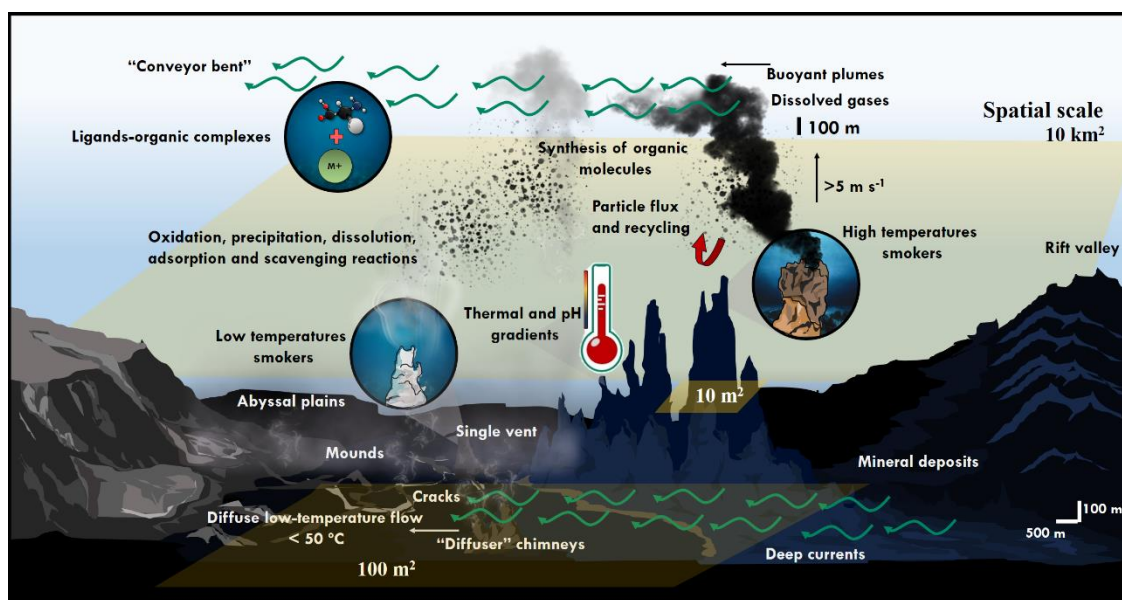


Figure 1. Submarine hydrothermal vents systems are highly dynamic environments. Any experiment that simulate some of the conditions present on these systems should be clear in the scale of the venting (*e.g.*, smokers, diffuse and low temperature vents or the active ridge segment) as well as in the scope of their results. Figure is detailed described on the text.

A significant number of prebiotic experiments, simulating submarine hydrothermal vents conditions, only focus on the stability and decomposition of organic molecules at high temperatures and high pressures (*i.e.*, >100 °C and >10 bar). Other few experiments have studied

the role of minerals, dissolved ions and gases, the quenching effect (350 °C - 2 °C), the pH effect and the redox state on the behavior of different organic molecules and the synthesis of oligomers (for a detailed revision, please review Colín-García et al. 2016, 2018). Despite these experiments have improved the understanding of the role of physicochemical variables (coupled or individually) on the fate of organic molecules in these environments, most of the experiments just represent a small portion of the submarine hydrothermal vents systems. In other words, they are focused in the first scale of the venting (see above), and they do not consider the nature of the environment, the dynamism. As we will explain later, the process of chemical evolution must have been presented in a wide space throughout these systems; although the high temperatures and pressures are the most evident parameters on SHVS, they do not fully represent all the conditions found on these systems. There are other variables that strongly influence the system, such as salinity, minerals, and pH gradients. In consequence, in order to “simulate” the submarine hydrothermal vents conditions, the scale and the scope of simulation must be specified.

Flow and spread

Because SHVS are very dynamic, the water flow is highly variable in space, time, and temperature as well as the topography (Stein et al. 2013).

The hydrothermal fluids can be released and transported by several ways: either by localized hot vents (up to 400 °C, 22-119 cm s⁻¹ for fluid temperatures between 200 - 300 °C), or by diffuse flow warm plumes (< 100 °C) from other discharge sites (*e.g.*, cracks in lava flows and seafloor around vent field, breccia, collapse pits, lava rubble, mineral deposits, and faults) at low flow rates (*e.g.*, vertical velocities of diffuse effluent range between 0.9-11.1 cm s⁻¹ for fluids temperatures between 3 - 33.5 °C) (Lupton et al. 1985; Little et al. 1987; Bemis et al. 2012; Mittelstaedt et al. 2012). This warm diffuse flow could represent the most important part of SHVS from a chemical evolution

point of view (Fig. 1). In other words, these surroundings can extend for kilometers, and represent a continuous heat output fraction. Some authors have reported that these diffuse flow warm plumes can represent up to 90 % of the total heat fraction of the system (Ramondenc et al. 2006; Bemis et al. 2012).

The simplest model about the dynamic flux from hydrothermal fluid is the buoyant flow. Depending of the variables used (*e.g.*, ambient sea water buoyancy frequencies, source diameters, source velocities, dissolved ions, density gradient, hydrographic conditions, convection and conduction of heat and sea water stratification) the vertical thermal diffusion can be different (Wilcock 1998; Coumou et al. 2006; Tao et al. 2013; Kadko et al. 2013). Some models suggest that the maximum plume rising height can be ~ 300 m (Tao et al. 2013) and that it can spread laterally through diffusion and advection mechanism (Thomson 2005). These models match the measured values height of the plume TAG hydrothermal site (German and Sparks 1993).

When the vent water and sea water reach an equilibrium density, they form a plume named conveyor belt. This plume can spread laterally up to 100 kilometers along basement relief through and driven by abyssal currents (Dymond and Roth 1988; Khripounoff et al. 2001). In this way, several reactions among plume constituents and seawater can accomplished at different time scales (*e.g.*, oxidation, precipitation, dissolution, sorption and scavenging reactions; Kadko et al. 1990) (see below).

Bottom currents

Other factor that should not be underestimate is the bottom currents. They influence the turbulent mixing and venting activity, and result in environmental thermal gradients ($5- 10$ °C cm^{-1} at timescales of hours and days). Bottom currents, also contribute to the lateral transport of the fluids

over a large region (kilometers) (Bates et al. 2010; Mittelstaedt et al. 2012). These low temperatures could induce the precipitation of minerals from the suspended particles in hydrothermal clouds at distances until 100 km from the ridge crest (Baker et al. 1985; Hannington et al. 2001).

Thermal gradients

On the other hand, the variations of temperature can be associated with several phenomena. For instance, it could be the result of changes in the porous diffusive system in the chimney, tidal cycles, hydrothermal fluid discharge or the turbulent mixing with the environment (Chevaldonné et al. 1991; Khripounoff et al. 2001). Other phenomena such as thermophoresis, at the micro scale, can result in the accumulation of organic molecules on the convection chamber (Braun and Libchaber 2004; Mast et al. 2013). It has been reported that fluids, associated with turbulences and that were mixed between sources, exhibit high temperature differences (*e.g.* 50 °C) at the centimeter scale (Fornari et al. 1998). Some models suggest that the rise of a plume until maximum height of rise is reached in ~ 1 h and that quenching is about of 30 seconds (Mcduff 2013). Other models suggest important thermal gradients along the chimney wall (McCollom and Shock 1997).

Chemical interactions along plume and sea water

Hydrothermal fluids can be considered as multicomponent electrolytes with high metal concentrations, and an important amount of organic and volatile components (Lemke 2013). The ability to form ligands, among metal and organic matter, can have important repercussions on the fate of molecules. For instance, the interaction of organic compounds with dissolved metals forms very high stable complexes, they can be widely distributed along hydrothermal systems (Sander and Koschinsky 2011). It has been reported that 90 % of metals in hydrothermal fluids can be

present as metal-organic molecules (*e.g.*, amino acids) complexes. The turbulent mixing may result in different thermal stabilities of amino acids and, hence the distribution and absolute concentrations of those complexes vary in each hydrothermal site (Klevenz et al. 2010). These complexes eventually precipitate, enriching the amino acids concentration in the low temperature (5 -100 °C) hydrothermal sedimentary environments, compared to the high temperature vent fluid habitats ($T > 150$ °C).

In present day systems, the concentration reported can be affected by *in situ* production of microbial biomass in the sediment (Haberstroh and Karl 1989). On the other hand, the complexation reactions in hydrothermal brines (*i.e.*, rich in Na^+ , Ca^{2+} , Cl^-) suggest that they depend of the solubility of organic salts, their concentration, and the pH conditions (Hennet *et al.* 1988). On the other hand, it has been showed that supercritical water enhance the solubility of organic compounds and reduces solvation properties for ionic species due to its loss of aqueous hydrogen bonding (Simoneit 1992). The ability of hydrothermal fluids to transport ions and other aqueous species, into and away from alteration zones, is strongly correlated to changes in the electrostatic properties of the fluid. In consequence, it is possible that H_2O -organic compound reactions occur at hydrothermal conditions (Shock 1992).

Another fundamental aspect to consider is the chemical reactions along the plume. For example, some oxidation/reduction reactions can be some kinetically slow in some cases (*e.g.*, Fe and Mn) (McCollom 2000). Dissolved Mn (II) has residence times close to one month; although, it is highly dependent of precipitation mechanisms (*e.g.*, coordination polymers with sodium azide) (Mandernack and Tebo 1993). Some species (*e.g.* H_2S) can be removed by their precipitation as oxides (Mottl and McConachy 1990; Gartman et al. 2011). Other chemical species, such as

methane, remain in dissolution for one week before their complete oxidation. This can represent an important carbon source to the surroundings of the vent field (10 km) (De Angelis et al. 1993).

One of the most discussed problems in chemical evolution is the concentration and the availability of organic molecules. Since the SHVS are open systems, it seems extremely difficult to reach high organic concentrations in them. On the one hand, to delimitate the amount of organic carbon along the hydrothermal plumes is very difficult, due to the biological production and consumption. Some differences among the dissolved organic carbon (DOC) and the POC (particulate organic carbon) concentrations (DOC; 38-47 μM and POC; 0.16-3.81 μM), in the mid-ocean ridge hydrothermal systems, have been reported. These differences are associated with the heterogeneous physical conditions of the system (*i.e.*, subsurface biological production, sorption onto mineral surfaces, thermal decomposition, etc.). Essentially, DOC is depleted both at high-temperature ridge-axis vents as in warm off-axis vents ($< 10 \mu\text{M}$). (Lang et al. 2006; Bennett et al. 2011). On the other hand, the distribution of organic species can be controlled by the seawater mixing, temperature and cooling effects and the $\text{CO}_2\text{-CO-H}_2$ thermodynamic equilibria (Foustoukos et al. 2009). Although some amino acids have been detected in hydrothermal fluids (directly collected from deep-sea hydrothermal systems), it is necessary to consider several things. First of all, it not easy to distinguish between the contribution of organism (direct biological origin), and those produced by hydrolysis of polymeric forms (*i.e.*, derived from organism and bio-debris) (Horiuchi et al. 2004). Likewise, it is not clear which part of hydrothermal area (*i.e.*, chimney (hot spots) or in low temperature hydrothermal fluids) is the most important source for amino acids (Fuchida et al. 2014). Nonetheless, it has been suggested that low temperature hydrothermal fluids can be an important source of amino acids and not the hydrothermal plume *per se* (Svensson et al. 2004; Lang et al. 2013).

Finally, it is necessary to consider the gas and particle distribution. As we can expect, gas diffusion should be very quickly. For instance, hydrogen (H_2) is removed from the plume within hours while manganese (Mn) is removed after two-weeks (Kadko et al. 1990). The particle distribution will depend of mineral phase and solubility (sulfate and sulfite particles have a slower process of dissolution than hydrous iron) (Lilley et al. 2013). Likewise, some data suggest that the particle recycling and re-entrainment in the plume can occur over a length of 1-10 km (German and Sparks 1993). Besides, this dissipation of material could be replaced by a continuous input from low-temperature water-rock reactions (Mayhew et al. 2013). In addition, the scavenging processes could impact these processes and affect the ocean geochemical cycles (German et al. 2002).

Conclusions

A consistent submarine hydrothermal vent scenario?

As we can deduct from the previous arguments; a more consistent submarine hydrothermal scenario includes not only high pressures and high temperatures as main conditions. The fluids discharged by different sources from hydrothermal systems experiment a chemical evolution as they interacts with seawater (Kadko et al. 1990) and hardly remain at high temperatures (> 100 °C).

Although the properties of water and chemical species are clearly affected by physicochemical gradients through the circulation in hydrothermal systems, that are often ignored in the prebiotic chemistry and the origin of life experiments (Holm and Hennes 1992). Recently, the scientific community has noticed these ideas and developed more consistent experiments.

For example, some experiments suggest that abiotic reactions from dissolved gases, at $T > 150$ °C and 350 bar, form carbon compounds in just few days (Seewald et al. 2006). Additionally,

theoretical models suggest that is thermodynamically possible, considering temperature gradients and oxidation-reduction reactions, to synthesize organic molecules from some common gases (*e.g.*, CO₂, H₂) (Shock 1993; Shock and Schulte 1998; Shock and Canovas 2010; McDermott et al. 2015). These experiments seem to be consistent with the availability of organic compounds in SHVS. For instance, Lang *et al.* (2010) reported, based in isotopic evidence, the abiotic production of organic molecules (*i.e.*, formate, 158 μmol kg⁻¹; acetate, 35 μmol kg⁻¹) from alkaline hydrothermal vents (*i.e.*, Lost City hydrothermal field). A recent experimental results suggested that HCO₃/CO₂ can be reduced to formate and trace amounts of acetate, using metal sulphides as catalysts, and H₂S as a reductant at hydrothermal conditions (300 °C, 3 h, basic pH) (He et al. 2019). On the other hand, Ying et al. (2019) showed that the formation of dipeptides increase with rising pressure (300 bar, T < 50 °C, amino acid, P3M, pH 10.7) because the high hydrostatic pressure increases the equilibrium constant of the reaction. Also, the interaction among minerals (olivine and orthopyroxene) with amino acids during several days (147 days) at 200 bar with periodic thermal cycling (30-100 °C) leads to the synthesis of dipeptide species and their chemisorption (Takahagi et al. 2019). Other researchers have focused on the thermolysis and polymerization reactions of hydrogen cyanide under simple hydrothermal conditions (Das et al. 2019; Villafañe-Barajas et al. 2020a, b) and showed the formation of several organic compounds, suggesting that this kind of reactions can occur in the vicinity of hydrothermal vents. Moreover, other studies suggest that ferrocyanide solutions are stables at lower pCO₂, temperature < 25 °C, and higher pH (6.9-9.3); for example, in environments saturated in carbonate or bicarbonate brines (Toner and Catling 2019). As we can see, there are many gaps in prebiotic chemistry studies and there is no clear knowledge about the role of geochemical variables present in SHVS. Therefore, it is necessary to develop more experiments with a clearer idea about the conditions and variables simulated (Holm and Andersson 2005).

Even though there are several proposals about submarine environments and their role in chemical evolution and origin of life, it is necessary to have an epistemic modesty. For example, some of these ideas can be overviewed in the suggestions that some protometabolic pathway raised from the result of the interaction of hydrothermal fluids (considering redox and pH disequilibria) with mineral in an ancient submarine hydrothermal vent (Wächtershäuser 1988a, b, 2006; Cartwright and Russell 2019). While these ideas have stimulated the thinking of the scientific community about the role of these scenarios, according to our point of view, they are far from the scope of the experimental approaches about origin of life. However, the importance of these ideas is that the authors considered the dynamism of hydrothermal systems as the main argument related to the interaction of minerals with organic molecules where the pH has a dramatic role.

Until now, there is no a unique proposal of a primitive environment that could have contributed to fulfill all the conditions for the development of a complex organic structure. Nevertheless, the dynamism presented in submarine hydrothermal systems seems to be a good starting point. However, it should be kept in mind that any experiment that simulates some of the conditions present on SHVS must be clear in the scale it simulates (*e.g.*, smokers, diffuse and low temperature vents or the active ridge segment), and thus, be consistent with the conditions prevailing on those scales. Also, it is necessary to it be cautious and consistent with the scope of its results, to avoid overestimations about the role of these systems on chemical evolution and eventually, in origin of life.

Acknowledgments

This research is part of SVB Ph.D. dissertation. He acknowledges the CONACyT (697442) for a scientific grant and the Posgrado en Ciencias de la Tierra. MCG acknowledges CONACyT for the financial support (A1-S-25341).

References

- Arndt NT, Nisbet EG (2012) Processes on the young Earth and the habitats of early life. *Annual Review of Earth and Planetary Sciences* 40:521–549
- Bada JL, Lazcano A (2002) Some like it hot, but not the first biomolecules. *Science* 296:1982–1983
- Bada JL, Miller SL, Zhao M (1995) The stability of amino acids at submarine hydrothermal vent temperatures. *Origins of Life and Evolution of the Biosphere* 25:111–118. <https://doi.org/10.1007/BF01581577>
- Baker ET, Lavelle JW, Massoth GJ (1985) Hydrothermal particle plumes over the southern Juan de Fuca Ridge. *Nature* 316:342–344. <https://doi.org/10.1038/316342a0>
- Ballard RD (1977) Notes on a major oceanographic find (marine animals near hot-water vents at ocean bottom). *Oceanus* 20:35–44
- Barge LM, White LM (2017) Experimentally testing hydrothermal vent origin of life on Enceladus and other icy/ocean worlds. *Astrobiology* 17:820–833
- Baross JA, Hoffman SE (1985) Submarine hydrothermal vents and associated gradient environments as sites for the origin and evolution of life. *Origins of Life and Evolution of the Biosphere* 15:327–345. <https://doi.org/10.1007/BF01808177>
- Bates AE, Lee RW, Tunnicliffe V, Lamare MD (2010) Deep-sea hydrothermal vent animals seek cool fluids in a highly variable thermal environment. *Nat Commun* 1:14. <https://doi.org/10.1038/ncomms1014>
- Bell JLS, Palmer DA, Barnes HL, Drummond SE (1994) Thermal decomposition of acetate: III. Catalysis by mineral surfaces. *Geochimica et Cosmochimica Acta* 58:4155–4177. [https://doi.org/10.1016/0016-7037\(94\)90271-2](https://doi.org/10.1016/0016-7037(94)90271-2)
- Bemis K, Lowell R, Farough A (2012) Diffuse Flow On and Around Hydrothermal Vents at Mid-Ocean Ridges. *oceanog* 25:182–191. <https://doi.org/10.5670/oceanog.2012.16>
- Bennett SA, Statham PJ, Green DRH, et al (2011) Dissolved and particulate organic carbon in hydrothermal plumes from the East Pacific Rise, 9°50'N. *Deep Sea Research Part I: Oceanographic Research Papers* 58:922–931. <https://doi.org/10.1016/j.dsr.2011.06.010>
- Bernhardt G, Lüdemann H-D, Jaenicke R, et al (1984) Biomolecules are unstable under black smoker conditions. *Naturwissenschaften* 71:583–586. <https://doi.org/10.1007/BF01189186>
- Boehnke P, Bell EA, Stephan T, et al (2018) Potassic, high-silica Hadean crust. *Proc Natl Acad Sci USA* 115:6353–6356. <https://doi.org/10.1073/pnas.1720880115>
- Braun D, Libchaber A (2004) Thermal force approach to molecular evolution. *Phys Biol* 1:P1–P8. <https://doi.org/10.1088/1478-3967/1/1/P01>
- Cartwright JH, Russell MJ (2019) The origin of life: the submarine alkaline vent theory at 30. *The Royal Society*

- Cavosie AJ, Valley JW, Wilde SA (2007) .5 The Oldest Terrestrial Mineral Record: A Review of 4400 to 4000 Ma Detrital Zircons from Jack Hills, Western Australia. *Developments in Precambrian Geology* 15:91–111
- Chevaldonné P, Desbruyères D, Haître ML (1991) Time-series of temperature from three deep-sea hydrothermal vent sites. *Deep Sea Research Part A Oceanographic Research Papers* 38:1417–1430. [https://doi.org/10.1016/0198-0149\(91\)90014-7](https://doi.org/10.1016/0198-0149(91)90014-7)
- Cleaves HJ, Aubrey AD, Bada JL (2009) An Evaluation of the Critical Parameters for Abiotic Peptide Synthesis in Submarine Hydrothermal Systems. *Origins of Life and Evolution of Biospheres* 39:109–126. <https://doi.org/10.1007/s11084-008-9154-1>
- Colín-García M, Heredia A, Cordero G, et al (2016) Hydrothermal vents and prebiotic chemistry: a review. *Boletín de la Sociedad Geológica Mexicana* 68:599–620
- Colín-García M, Villafañe-Barajas S, Camprubí A, et al (2018) 5.4 Prebiotic Chemistry in Hydrothermal Vent Systems. *Handbook of Astrobiology* 297
- Corliss, J. B., Baross, J. A., & Hoffman, S. E (1981) An hypothesis concerning the relationships between submarine hot springs and the origin of life on earth. *Oceanologica Acta*, Special issue
- Corliss JB, Dymond J, Gordon LI, et al (1979) Submarine Thermal Springs on the Galápagos Rift. *Science* 203:1073–1083. <https://doi.org/10.1126/science.203.4385.1073>
- Coumou D, Driesner T, Geiger S, et al (2006) The dynamics of mid-ocean ridge hydrothermal systems: Splitting plumes and fluctuating vent temperatures. *Earth and Planetary Science Letters* 245:218–231. <https://doi.org/10.1016/j.epsl.2006.02.044>
- Das T, Ghule S, Vanka K (2019) Insights into the origin of life: Did it begin from HCN and H₂O? *ACS central science* 5:1532–1540
- De Angelis M, Lilley M, Baross J (1993) Methane oxidation in deep-sea hydrothermal plumes of the Endeavour Segment of the Juan de Fuca Ridge. *Deep Sea Research Part I: Oceanographic Research Papers* 40:1169–1186
- Deamer DW, Georgiou CD (2015) Hydrothermal conditions and the origin of cellular life. *Astrobiology* 15:1091–1095
- Dymond J, Roth S (1988) Plume dispersed hydrothermal particles: A time-series record of settling flux from the Endeavour Ridge using moored sensors. *Geochimica et Cosmochimica Acta* 52:2525–2536. [https://doi.org/10.1016/0016-7037\(88\)90310-9](https://doi.org/10.1016/0016-7037(88)90310-9)
- Fornari DJ, Shank T, Von Damm KL, et al (1998) Time-series temperature measurements at high-temperature hydrothermal vents, East Pacific Rise 9°49'–51'N: evidence for monitoring a crustal cracking event. *Earth and Planetary Science Letters* 160:419–431. [https://doi.org/10.1016/S0012-821X\(98\)00101-0](https://doi.org/10.1016/S0012-821X(98)00101-0)
- Foustoukos DI, Pester NJ, Ding K, Seyfried WE (2009) Dissolved carbon species in associated diffuse and focused flow hydrothermal vents at the Main Endeavour Field, Juan de Fuca Ridge: Phase equilibria and kinetic constraints: CARBON SPECIES IN MEF VENT FLUIDS. *Geochem Geophys Geosyst* 10:n/a-n/a. <https://doi.org/10.1029/2009GC002472>

- Fox SW (1967) Self-assembly of the protocell from a self-ordered polymer
- Fuchida S, Mizuno Y, Masuda H, et al (2014) Concentrations and distributions of amino acids in black and white smoker fluids at temperatures over 200°C. *Organic Geochemistry* 66:98–106. <https://doi.org/10.1016/j.orggeochem.2013.11.008>
- Gartman A, Yücel M, Madison AS, et al (2011) Sulfide oxidation across diffuse flow zones of hydrothermal vents. *Aquatic Geochemistry* 17:583–601
- German CR, Colley S, Palmer MR, et al (2002) Hydrothermal plume-particle fluxes at 13°N on the East Pacific Rise. *Deep Sea Research Part I: Oceanographic Research Papers* 49:1921–1940. [https://doi.org/10.1016/S0967-0637\(02\)00086-9](https://doi.org/10.1016/S0967-0637(02)00086-9)
- German CR, Sparks RSJ (1993) Particle recycling in the TAG hydrothermal plume. *Earth and Planetary Science Letters* 116:129–134. [https://doi.org/10.1016/0012-821X\(93\)90049-F](https://doi.org/10.1016/0012-821X(93)90049-F)
- Golding SD, Duck LJ, Young E, et al (2011) Earliest Seafloor Hydrothermal Systems on Earth: Comparison with Modern Analogues. In: Golding SD, Glikson M (eds) *Earliest Life on Earth: Habitats, Environments and Methods of Detection*. Springer Netherlands, Dordrecht, pp 15–49
- Haberstroh PR, Karl DM (1989) Dissolved free amino acids in hydrothermal vent habitats of the Guaymas Basin. *Geochimica et Cosmochimica Acta* 53:2937–2945. [https://doi.org/10.1016/0016-7037\(89\)90170-1](https://doi.org/10.1016/0016-7037(89)90170-1)
- Hannington M, Herzig P, Stoffers P, et al (2001) First observations of high-temperature submarine hydrothermal vents and massive anhydrite deposits off the north coast of Iceland. *Marine Geology* 177:199–220. [https://doi.org/10.1016/S0025-3227\(01\)00172-4](https://doi.org/10.1016/S0025-3227(01)00172-4)
- Harrison TM (2009) The Hadean crust: evidence from > 4 Ga zircons. *Annual Review of Earth and Planetary Sciences* 37:479–505
- Harvey RB (1924) Enzymes of thermal algae. *Science* 60:481–482. <https://doi.org/10.1126/science.60.1560.481>
- Hazen RM, Papineau D, Bleeker W, et al (2008) Mineral evolution. *American Mineralogist* 93:1693–1720
- He R, Hu B, Zhong H, et al (2019) Reduction of CO₂ with H₂S in a simulated deep-sea hydrothermal vent system. *Chem Commun* 55:1056–1059. <https://doi.org/10.1039/C8CC08075E>
- Hennet RJC, Crerar DA, Schwartz J (1988) Organic complexes in hydrothermal systems. *Economic Geology* 83:742–764. <https://doi.org/10.2113/gsecongeo.83.4.742>
- Herschy B, Whicher A, Camprubi E, et al (2014) An Origin-of-Life Reactor to Simulate Alkaline Hydrothermal Vents. *Journal of Molecular Evolution* 79:213–227. <https://doi.org/10.1007/s00239-014-9658-4>
- Holm NG, Andersson E (2005) Hydrothermal Simulation Experiments as a Tool for Studies of the Origin of Life on Earth and Other Terrestrial Planets: A Review. *Astrobiology* 5:444–460. <https://doi.org/10.1089/ast.2005.5.444>
- Holm NG, Hennet RJ-C (1992) Hydrothermal systems: their varieties, dynamics, and suitability for prebiotic chemistry. In: *Marine Hydrothermal Systems and the Origin of Life*. Springer, pp 15–31

- Horiuchi T, Takano Y, Ishibashi J, et al (2004) Amino acids in water samples from deep sea hydrothermal vents at Suiyo Seamount, Izu-Bonin Arc, Pacific Ocean. *Organic Geochemistry* 35:1121–1128. <https://doi.org/10.1016/j.orggeochem.2004.06.006>
- Ingmanson DE, Dowler MJ (1977) Chemical evolution and the evolution of the Earth's crust. *Origins Life Evol Biosphere* 8:221–224. <https://doi.org/10.1007/BF00930683>
- Kadko D, Baross J, Alt J (2013) The Magnitude and Global Implications of Hydrothermal Flux. In: Humphris SE, Zierenberg RA, Mullineaux LS, Thomson RE (eds) *Geophysical Monograph Series*. American Geophysical Union, Washington, D. C., pp 446–466
- Kadko DC, Rosenberg ND, Lupton JE, et al (1990) Chemical reaction rates and entrainment within the Endeavour Ridge hydrothermal plume. *Earth and Planetary Science Letters* 99:315–335. [https://doi.org/10.1016/0012-821X\(90\)90137-M](https://doi.org/10.1016/0012-821X(90)90137-M)
- Kelley DS (2005) A Serpentinite-Hosted Ecosystem: The Lost City Hydrothermal Field. *Science* 307:1428–1434. <https://doi.org/10.1126/science.1102556>
- Kemp AIS, Wilde SA, Hawkesworth CJ, et al (2010) Hadean crustal evolution revisited: New constraints from Pb–Hf isotope systematics of the Jack Hills zircons. *Earth and Planetary Science Letters* 296:45–56. <https://doi.org/10.1016/j.epsl.2010.04.043>
- Khripounoff A, Vangriesheim A, Crassous P, et al (2001) Particle flux in the Rainbow hydrothermal vent field (Mid-Atlantic Ridge): Dynamics, mineral and biological composition. *Journal of Marine Research* 59:633–656. <https://doi.org/10.1357/002224001762842217>
- Klevenz V, Sumoondur A, Ostertag-Henning C, Koschinsky A (2010) Concentrations and distributions of dissolved amino acids in fluids from Mid-Atlantic Ridge hydrothermal vents. *Geochem J* 44:387–397. <https://doi.org/10.2343/geochemj.1.0081>
- Kohara M, Gamo T, Yanagawa H, Kobayashi K (1997) Stability of Amino Acids in Simulated Hydrothermal Vent Environments. *Chemistry Letters* 26:1053–1054. <https://doi.org/10.1246/cl.1997.1053>
- Lane N, Martin WF (2012) The origin of membrane bioenergetics. *Cell* 151:1406–1416
- Lang SQ, Butterfield DA, Lilley MD, et al (2006) Dissolved organic carbon in ridge-axis and ridge-flank hydrothermal systems. *Geochimica et Cosmochimica Acta* 70:3830–3842. <https://doi.org/10.1016/j.gca.2006.04.031>
- Lang SQ, Butterfield DA, Schulte M, et al (2010) Elevated concentrations of formate, acetate and dissolved organic carbon found at the Lost City hydrothermal field. *Geochimica et Cosmochimica Acta* 74:941–952. <https://doi.org/10.1016/j.gca.2009.10.045>
- Lang SQ, Früh-Green GL, Bernasconi SM, Butterfield DA (2013) Sources of organic nitrogen at the serpentinite-hosted Lost City hydrothermal field. *Geobiology* 11:154–169. <https://doi.org/10.1111/gbi.12026>
- Larralde R, Robertson MP, Miller SL (1995) Rates of decomposition of ribose and other sugars: implications for chemical evolution. *Proceedings of the National Academy of Sciences* 92:8158–8160. <https://doi.org/10.1073/pnas.92.18.8158>

- Lemke K (2013) The Stability of Biomolecules in Hydrothermal Fluids. *COC* 17:1724–1731. <https://doi.org/10.2174/13852728113179990079>
- Levy M, Miller SL (1998) The stability of the RNA bases: Implications for the origin of life. *Proceedings of the National Academy of Sciences* 95:7933–7938. <https://doi.org/10.1073/pnas.95.14.7933>
- Lilley MD, Feely RA, Trefry JH (2013) Chemical and Biochemical Transformations in Hydrothermal Plumes. In: Humphris SE, Zierenberg RA, Mullineaux LS, Thomson RE (eds) *Geophysical Monograph Series*. American Geophysical Union, Washington, D. C., pp 369–391
- Little SA, Stolzenbach KD, Von Herzen RP (1987) Measurements of plume flow from a hydrothermal vent field. *J Geophys Res* 92:2587–2596. <https://doi.org/10.1029/JB092iB03p02587>
- Lupton JE, Delaney JR, Johnson HP, Tivey MK (1985) Entrainment and vertical transport of deep-ocean water by buoyant hydrothermal plumes. *Nature* 316:621–623. <https://doi.org/10.1038/316621a0>
- Mandernack KW, Tebo BM (1993) Manganese scavenging and oxidation at hydrothermal vents and in vent plumes. *Geochimica et Cosmochimica Acta* 57:3907–3923. [https://doi.org/10.1016/0016-7037\(93\)90343-U](https://doi.org/10.1016/0016-7037(93)90343-U)
- Martin W, Baross J, Kelley D, Russell MJ (2008) Hydrothermal vents and the origin of life. *Nature Reviews Microbiology*. <https://doi.org/10.1038/nrmicro1991>
- Mast C, Osterman N, Braun D (2013) Could Thermal Gradients Drive Molecular Evolution? *COC* 17:1732–1737. <https://doi.org/10.2174/13852728113179990080>
- Mayhew LE, Ellison ET, McCollom TM, et al (2013) Hydrogen generation from low-temperature water–rock reactions. *Nature Geosci* 6:478–484. <https://doi.org/10.1038/ngeo1825>
- McCollom TM (2000) Geochemical constraints on primary productivity in submarine hydrothermal vent plumes. *Deep Sea Research Part I: Oceanographic Research Papers* 47:85–101. [https://doi.org/10.1016/S0967-0637\(99\)00048-5](https://doi.org/10.1016/S0967-0637(99)00048-5)
- McCollom TM, Shock EL (1997) Geochemical constraints on chemolithoautotrophic metabolism by microorganisms in seafloor hydrothermal systems. *Geochimica et cosmochimica acta* 61:4375–4391
- McDermott JM, Seewald JS, German CR, Sylva SP (2015) Pathways for abiotic organic synthesis at submarine hydrothermal fields. *Proceedings of the National Academy of Sciences* 112:7668–7672. <https://doi.org/10.1073/pnas.1506295112>
- Mcduff RE (2013) Physical Dynamics of Deep-Sea Hydrothermal Plumes. In: Humphris SE, Zierenberg RA, Mullineaux LS, Thomson RE (eds) *Geophysical Monograph Series*. American Geophysical Union, Washington, D. C., pp 357–368
- Miller SL, Bada JL (1988) Submarine hot springs and the origin of life. *Nature* 334:609–611. <https://doi.org/10.1038/334609a0>
- Miller StanleyL, Lazcano A (1995) The origin of life?did it occur at high temperatures? *Journal of Molecular Evolution* 41:. <https://doi.org/10.1007/BF00173146>

- Mittelstaedt E, Escartín J, Gracias N, et al (2012) Quantifying diffuse and discrete venting at the Tour Eiffel vent site, Lucky Strike hydrothermal field: HEAT FLUX TOUR EIFFEL. *Geochem Geophys Geosyst* 13:n/a-n/a. <https://doi.org/10.1029/2011GC003991>
- Morrison S, Runyon S, Hazen R (2018) The Paleomineralogy of the Hadean Eon Revisited. *Life* 8:64. <https://doi.org/10.3390/life8040064>
- Mottl MJ, McConachy TF (1990) Chemical processes in buoyant hydrothermal plumes on the East Pacific Rise near 21 N. *Geochim Cosmochim Acta* 54:1911–1927
- Novoselov AA, Silantyev SA (2010) Hydrothermal systems of the hadean ocean and their influence on the matter balance in the crust-hydrosphere-atmosphere system of the early earth. *Geochemistry International* 48:643–654
- Omran A, Pasek M (2020) A Constructive Way to Think about Different Hydrothermal Environments for the Origins of Life. *Life* 10:36. <https://doi.org/10.3390/life10040036>
- Papineau D (2010) Mineral Environments on the Earliest Earth. *Elements* 6:25–30. <https://doi.org/10.2113/gselements.6.1.25>
- Povoleto D, Vallentyne JR (1964) Thermal reaction kinetics of the glutamic acid-pyroglutamic acid system in water. *Geochimica et Cosmochimica Acta* 28:731–734. [https://doi.org/10.1016/0016-7037\(64\)90089-4](https://doi.org/10.1016/0016-7037(64)90089-4)
- Qian Y, Engel MH, Macko SA, et al (1993) Kinetics of peptide hydrolysis and amino acid decomposition at high temperature. *Geochimica et Cosmochimica Acta* 57:3281–3293. [https://doi.org/10.1016/0016-7037\(93\)90540-D](https://doi.org/10.1016/0016-7037(93)90540-D)
- Ramondenc P, Germanovich LN, Von Damm KL, Lowell RP (2006) The first measurements of hydrothermal heat output at 9°50'N, East Pacific Rise. *Earth and Planetary Science Letters* 245:487–497. <https://doi.org/10.1016/j.epsl.2006.03.023>
- Sander SG, Koschinsky A (2011) Metal flux from hydrothermal vents increased by organic complexation. *Nature Geosci* 4:145–150. <https://doi.org/10.1038/ngeo1088>
- Schrenk MO, Brazelton WJ, Lang SQ (2013) Serpentinization, carbon, and deep life. *Reviews in Mineralogy and Geochemistry* 75:575–606
- Schulte M, Blake D, Hoehler T, McCollom T (2006) Serpentinization and Its Implications for Life on the Early Earth and Mars. *Astrobiology* 6:364–376. <https://doi.org/10.1089/ast.2006.6.364>
- Seewald JS, Zolotov MYu, McCollom T (2006) Experimental investigation of single carbon compounds under hydrothermal conditions. *Geochimica et Cosmochimica Acta* 70:446–460. <https://doi.org/10.1016/j.gca.2005.09.002>
- Shibuya T, Yoshizaki M, Sato M, et al (2015) Hydrogen-rich hydrothermal environments in the Hadean ocean inferred from serpentinization of komatiites at 300 C and 500 bar. *Progress in Earth and Planetary Science* 2:46
- Shock E, Canovas P (2010) The potential for abiotic organic synthesis and biosynthesis at seafloor hydrothermal systems. *Geofluids*. <https://doi.org/10.1111/j.1468-8123.2010.00277.x>

- Shock EL (1992) Chemical Environments of Submarine Hydrothermal Systems. In: Holm NG (ed) *Marine Hydrothermal Systems and the Origin of Life*. Springer Netherlands, Dordrecht, pp 67–107
- Shock EL (1993) Hydrothermal dehydration of aqueous organic compounds. *Geochimica et Cosmochimica Acta* 57:3341–3349
- Shock EL, Schulte MD (1998) Organic synthesis during fluid mixing in hydrothermal systems. *Journal of Geophysical Research: Planets* 103:28513–28527
- Simoneit BRT (1992) Aqueous Organic Geochemistry at High Temperature/High Pressure. In: Holm NG (ed) *Marine Hydrothermal Systems and the Origin of Life*. Springer Netherlands, Dordrecht, pp 43–65
- Sleep NH (2010) The hadean-archaeon environment. *Cold spring harbor perspectives in biology* 2:a002527
- Sleep NH, Meibom A, Fridriksson T, et al (2004) H₂-rich fluids from serpentinization: geochemical and biotic implications. *Proceedings of the National Academy of Sciences* 101:12818–12823
- Sojo V, Herschy B, Whicher A, et al (2016) The origin of life in alkaline hydrothermal vents. *Astrobiology* 16:181–197
- Stein CA, Stein S, Pelayo AM (2013) Heat Flow and Hydrothermal Circulation. In: Humphris SE, Zierenberg RA, Mullineaux LS, Thomson RE (eds) *Geophysical Monograph Series*. American Geophysical Union, Washington, D. C., pp 425–445
- Stüeken EE, Anderson RE, Bowman JS, et al (2013) Did life originate from a global chemical reactor? *Geobiology* 11:101–126. <https://doi.org/10.1111/gbi.12025>
- Svensson E, Skoog A, Amend JP (2004) Concentration and distribution of dissolved amino acids in a shallow hydrothermal system, Vulcano Island (Italy). *Organic Geochemistry* 35:1001–1014. <https://doi.org/10.1016/j.orggeochem.2004.05.005>
- Takahagi W, Seo K, Shibuya T, et al (2019) Peptide Synthesis under the Alkaline Hydrothermal Conditions on Enceladus. *ACS Earth Space Chem* 3:2559–2568. <https://doi.org/10.1021/acsearthspacechem.9b00108>
- Tao Y, Rosswog S, Brüggem M (2013) A simulation modeling approach to hydrothermal plumes and its comparison to analytical models. *Ocean Modelling* 61:68–80. <https://doi.org/10.1016/j.ocemod.2012.10.001>
- Thomson RE (2005) Numerical simulation of hydrothermal vent-induced circulation at Endeavour Ridge. *J Geophys Res* 110:C01004. <https://doi.org/10.1029/2004JC002337>
- Toner JD, Catling DC (2019) Alkaline lake settings for concentrated prebiotic cyanide and the origin of life. *Geochimica et Cosmochimica Acta* 260:124–132
- Trail D, Watson EB, Tailby ND (2013) Insights into the Hadean Earth from experimental studies of zircon. *Journal of the Geological Society of India* 81:605–636
- Vallentyne JR (1964) Biogeochemistry of organic matter—II Thermal reaction kinetics and transformation products of amino compounds. *Geochimica et Cosmochimica Acta* 28:157–188. [https://doi.org/10.1016/0016-7037\(64\)90147-4](https://doi.org/10.1016/0016-7037(64)90147-4)

- Villafañe-Barajas SA, Colín-García M, Negrón-Mendoza A, Ruiz-Bermejo M (2020a) An experimental study of the thermolysis of hydrogen cyanide: the role of hydrothermal systems in chemical evolution. *International Journal of Astrobiology* 1–10. <https://doi.org/10.1017/S1473550420000142>
- Villafañe-Barajas SA, Ruiz-Bermejo M, Rayo-Pizarroso P, Colín-García M (2020b) Characterization of HCN-Derived Thermal Polymer: Implications for Chemical Evolution. *Processes* 8:968
- Wächtershäuser G (2006) From volcanic origins of chemoautotrophic life to Bacteria, Archaea and Eukarya. *Phil Trans R Soc B* 361:1787–1808. <https://doi.org/10.1098/rstb.2006.1904>
- Wächtershäuser G (1988a) Pyrite formation, the first energy source for life: a hypothesis. *Systematic and Applied Microbiology* 10:207–210
- Wächtershäuser G (1988b) Before enzymes and templates: theory of surface metabolism. *Microbiological reviews* 52:452
- Wang X, Ouyang Z, Zhuo S, et al (2014) Serpentinization, abiogenic organic compounds, and deep life. *Science China Earth Sciences* 57:878–887
- White RH (1984) Hydrolytic stability of biomolecules at high temperatures and its implication for life at 250 °C. *Nature* 310:430–432. <https://doi.org/10.1038/310430a0>
- Wilcock WS (1998) Cellular convection models of mid-ocean ridge hydrothermal circulation and the temperatures of black smoker fluids. *Journal of Geophysical Research: Solid Earth* 103:2585–2596
- Ying J, Chen P, Wu Y, et al (2019) Effect of high hydrostatic pressure on prebiotic peptide synthesis. *Chinese Chemical Letters* 30:367–370. <https://doi.org/10.1016/j.ccllet.2018.06.015>

ANEXO II

Anortosita. Roca plutónica compuesta casi enteramente por Ca-plagioclasa-feldespato (> 90 %) y menores cantidades de piroxeno y olivina.

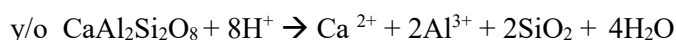
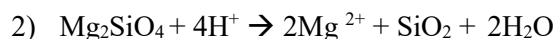
Arcillas. Grupo de minerales aluminosilicatos hidratados con estructura laminar de dos a tres capas tetraédricas (SiO₄) unidas a capas de Al-O o (Mg,Fe)-O. Tamaño de partícula <2 μm.

Basalto. Roca ígnea de grano fino formada a partir de la fusión parcial de un magma peridotítico (ultramáfico; compuesto predominantemente por olivina, piroxeno y plagioclasa). Los basaltos proceden de un magma básico (45-52 % SiO₂), y generalmente son formados en dorsales oceánicas o en *hot spots* (magma extrusivo).

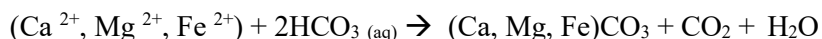
Carbonatos. Rocas sedimentarias compuestas principalmente (> 95 %) por minerales que contienen el ion carbonato (CO₃²⁻) (*e.g.*, calcita, CaCO₃)

Ciclo del CO₂. Una vez que se estableció el equilibrio océano-atmosfera (producto de los volátiles liberados, el desgasamiento del manto, la alteración de la capa más superficial de la corteza, la radiación solar, presión atmosférica, la formación y reciclamiento de rocas en el interior de la Tierra) el CO₂ guó la dinámica terrestre.

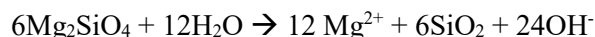
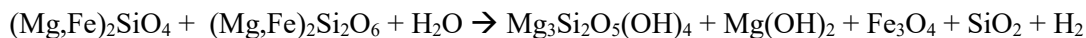
Las primeras rocas ígneas reaccionantes (basalto y rocas ultramáficas con composición similar a la del manto) se formaron en un ambiente similar a lo que vemos en dorsales oceánicas modernas. En presencia de una atmósfera masiva de CO₂, su interacción con las rocas y el océano dio paso a la formación de carbonatos. Estas rocas fueron recicladas liberando de nuevo CO₂ a la atmosfera junto con otros elementos (*e.g.*, Ca, Mg, Fe). La continua repetición de este ciclo condujo al enriquecimiento de CO₂ en el interior de la Tierra y la posibilidad de formar arcos de islas de corteza continental carbonatada. Aunado a lo anterior, la continua actividad hidrotermal estableció un equilibrio entre carbonatos y basaltos dejando un pH relativamente alcalino. De igual modo, procesos de serpentinización pudieron contribuir con un océano más alcalino (Sleep, 2010). Las siguientes reacciones químicas engloban el proceso:

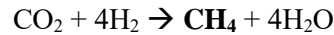
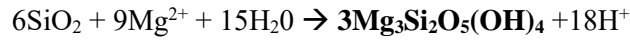


Los cationes divalentes liberados reaccionan con el CO₂ disuelto y precipita en carbonatos,



Serpentinización y producción de metano





Esquisto (*shale*). Rocas sedimentarias de grano fino laminadas con alto contenido limo-arcilloso. Generalmente consisten en >30 % SiO₂ y el resto es material variado (*e.g.*, carbonatos, ferróxidos, feldespatos y materia orgánica).

Granitoides. Rocas compuestas por cuarzo, feldespato, micas, minerales ferromagnesianos y difieren en su abundancia de plagioclasa/feldespato (*e.g.*, granitos, granodioritas, tonalitas, trondhjemitas). Principal componente de la corteza continental. Estas rocas son generadas a través de fusión parcial a altas presiones a partir de un basalto hidratado.

Komatiita. Roca volcánica derivado de una fuente ultramáfica con alto contenido en magnesio, principalmente en su forma de óxido (*i.e.*, MgO). La roca *peridotita* es su equivalente intrusivo.

Magmas félsicos. Alto contenido en SiO₂ (> 60 %) y iones Na⁺ y K⁺. Consolida en rocas graníticas y/o riolíticas (equivalente extrusiva). Se asocian a zonas de subducción. Las rocas ácidas son rocas ígneas que contienen más de 66 % de SiO₂.

Magmas básicos. Bajo contenido en sílice (< 50 %) y alto en iones Ca²⁺, Fe^{2+,3+} y Mg²⁺. Consolida en rocas como el basalto y/o gabro (equivalente intrusivo). Ricas en minerales ferromagnesianos como olivina, piroxenos y anfíboles. Ultramáfico <45 % SiO₂ es su composición química bruta.

Actividad hidrotermal. Los sistemas hidrotermales se pueden definir como sistemas geológicos que son productos de la circulación de fluidos calientes (T > 25 °C).

Cualquier proceso asociado a la actividad ígnea que involucra la acción de agua caliente. Esta agua puede derivar directamente de intrusiones ígneas así como fluidos residuales formados durante los últimos estados de cristalización de cuerpo magmático, o agua externa (meteórica). Los fluidos hidrotermales pueden reaccionar con las rocas y pueden depositar minerales. Algunas reacciones hidrotermales son la serpentización, la cloritización, sausrización y propilitización.

Una alteración hidrotermal en rocas o minerales es causada por la interacción de fluidos hidrotermales (fluido residual caliente derivado de magmas durante los últimos estados de cristalización y comúnmente contienen grandes cantidades de metales disueltos los cuales son depositados como vetas minerales).

Tabla 1. Principales restos corticales más antiguos conocidos.

Complejo	Lugar	Origen	Edad	Referencias
Acasta gneiss	Canada	TTG	4.031 ± 0.003	(Iizuka <i>et al.</i> , 2007a, 2007b)
Nuvvuagittuq	Canada	sedimentario y/o volcánico	>3.825 ± 0.016	(Adam <i>et al.</i> , 2012; O'Neil <i>et al.</i> , 2012)

Akilia BIF and Isua gneisses	Groelandia	BIF	>3.872 +0.010	(Rizo <i>et al.</i> , 2016; Nutman <i>et al.</i> , 2019)
Amitsoq gneiss	Groelandia	TTG	3.872+0.010	(Nutman & Bridgwater, 1986)
Uivak gneiss	Canada	TTG	3.863+0.012	(Safacińska <i>et al.</i> , 2019)

Tabla modificada a partir de Gargaud *et al.*, 2013. **Nota:** Las rocas más antiguas son remanentes metamorfisados y deformados de corteza formada a partir de rocas graníticas sódicas de tonalita-trondhjemita, granodiorita (TTG), mientras que la BIF (Formación de hierro con bandas) y los gneises de Nuvvuagittuq son de origen sedimentario y volcán-sedimentario.

Tabla 2. Minerales relevantes en los primeros 1000 Ma de años en la historia de la Tierra.

Mineral	Formula Química
Anfibol	$AX_2Z_5((Si,Al,Ti)_8O_{22})(OH,F,Cl,O)_2$ A =Na, K, Ca, Pb ²⁺ ; X =Li, Na, Mg, Fe ²⁺ , Mn ²⁺ , Ca; Z = Li, Na, Mg, Fe ²⁺ , Mn ²⁺ , Zn, Co, Ni, Al, Fe ³⁺ , Cr ³⁺ , Mn ³⁺ , V ³⁺ , Ti, Zr
Cuarzo	SiO ₂
Muscovita	KAl ₂ (AlSi ₃ O ₁₀)(OH) ₂
Olivina	(Fe, Mg) ₂ SiO ₄
Ortoclasa	K(AlSi ₃ O ₈)
Piroxeno	(Ca _x Mg _y Fe _z)(Mg _{y1} Fe _{z1})Si ₂ O ₆
Plagioclasa	Na(AlSi ₃ O ₈) y/o Ca(Al ₂ Si ₂ O ₈)
Serpentinita	D ₃ [Si ₂ O ₅](OH) ₄ D = Mg, Fe, Ni, Mn, Al, Zn
Talco	Mg ₃ Si ₄ O ₁₀ (OH) ₂
Zircon	ZrSiO ₄

Referencias

- Adam J, Rushmer T, O'Neil J, Francis D (2012) Hadean greenstones from the Nuvvuagittuq fold belt and the origin of the Earth's early continental crust. *Geology* **40**, 363–366.
- Gargaud M, Martin H, López-García P, Montmerle T, Pascal R (2013) *Young sun, early earth and the origins of life: lessons for astrobiology*. Springer Science & Business Media.
- Iizuka T, Komiya T, Maruyama S (2007a) Chapter 3.1 The Early Archean Acasta Gneiss Complex: Geological, Geochronological and Isotopic Studies and Implications for Early Crustal Evolution. In: *Developments in Precambrian Geology*. Elsevier, pp. 127–147.
- Iizuka T, Komiya T, Ueno Y, Katayama I, Uehara Y, Maruyama S, Hirata T, Johnson SP, Dunkley DJ (2007b) Geology and zircon geochronology of the Acasta Gneiss Complex, northwestern Canada: New constraints on its tectonothermal history. *Precambrian Research* **153**, 179–208.

- Nutman AP, Bridgwater D (1986) Early Archaean Amitsoq tonalites and granites of the Isukasia area, southern West Greenland: development of the oldest-known sial. *Contributions to Mineralogy and Petrology* **94**, 137–148.
- Nutman AP, Friend CRL, Bennett VC, Van Kranendonk M, Chivas AR (2019) Reconstruction of a 3700 Ma transgressive marine environment from Isua (Greenland): Sedimentology, stratigraphy and geochemical signatures. *Lithos* **346–347**, 105164.
- O’Neil J, Carlson RW, Paquette J-L, Francis D (2012) Formation age and metamorphic history of the Nuvvuagittuq Greenstone Belt. *Precambrian Research* **220–221**, 23–44.
- Rizo H, Walker RJ, Carlson RW, Touboul M, Horan MF, Puchtel IS, Boyet M, Rosing MT (2016) Early Earth differentiation investigated through ¹⁴²Nd, ¹⁸²W, and highly siderophile element abundances in samples from Isua, Greenland. *Geochimica et Cosmochimica Acta* **175**, 319–336.
- Sałacińska A, Kusiak MA, Whitehouse MJ, Dunkley DJ, Wilde SA, Kielman R, Król P (2019) Gneiss-forming events in the Saglek Block, Labrador; a reappraisal of the Uivak gneiss. *International Journal of Earth Sciences* **108**, 753–778.
- Sleep NH (2010) The hadean-archaeon environment. *Cold spring harbor perspectives in biology* **2**, a002527.